

SKB

**TECHNICAL
REPORT**

91-22

**Äspö Hard Rock Laboratory.
Evaluation and conceptual modelling
based on the pre-investigations
1986-1990**

P Wikberg (ed), G Gustafson, I Rhén, R Stanfors

June 1991

SVENSK KÄRNBRÄNSLEHANTERING AB

SWEDISH NUCLEAR FUEL AND WASTE MANAGEMENT CO

BOX 5864 S-102 48 STOCKHOLM

TEL 08-665 28 00 TELEX 13108 SKB S

TELEFAX 08-661 57 19

ÄSPÖ HARD ROCK LABORATORY.
EVALUATION AND CONCEPTUAL MODELLING BASED ON THE
PRE-INVESTIGATIONS 1986-1990

P Wikberg (ed), G Gustafson, I Rhén, R Stanfors

June 1991

**Äspö Hard Rock Laboratory.
Evaluation and conceptual modelling based on
the pre-investigations 1986–1990.**

**Peter Wikberg (ed)
Gunnar Gustafson
Ingvar Rhén
Roy Stanfors**

June 1991

INTRODUCTORY COMMENT

This report is No III, of four summarizing the pre-investigation phase of the Äspö Hard Rock Laboratory.

The reports are:

- I Stanfors R, Erlström M, Markström I.
 Äspö Hard Rock Laboratory
 Overview of the investigations 1986-1990.
 SKB TR 91-20.

- II Almén K-E, Zellman O.
 Äspö Hard Rock Laboratory
 Field investigation methodology and instruments used in the pre-
 investigation phase, 1986-1990.
 SKB TR 91-21.

- III Wikberg P, Gustafson G, Rhén I, Stanfors R.
 Äspö Hard Rock Laboratory
 Evaluation and conceptual modelling based on the pre-investigations
 1986-1990.
 SKB TR 91-22.

- IV Gustafson G, Liedholm M, Rhén I, Stanfors R, Wikberg P.
 Äspö Hard Rock Laboratory
 Predictions prior to excavation and the process of their validation.
 SKB TR 91-23.

The background and objectives of the project are presented in a background report to SKB R&D programme 1989 (Hard Rock Laboratory) where a detailed description of the HRL project can be found.

ACKNOWLEDGEMENTS

The authors are grateful to the members of the Äspö HRL advisory committee for the constructive discussion on the contents of this report. In preparing the report, planning and conducting the investigations the cooperation with Tommy Hedman, Göran Bäckblom, Olle Zellman, Karl-Erik Almén and Olle Broman is highly appreciated.

We are also grateful to all the contractors, see list of progress reports, who have been involved in the investigations and thus contributed to this report.

We wish to extend special thanks to Ingemar Markström, Magnus Liedholm, Urban Svensson and Marcus Laaksoharju for their specific contribution to this report and to Pär Olsson and Håkan Stille for preparing the rock mechanics section.

Finally, we wish to express our gratitude to our colleagues for the interest they have shown regarding this work.

ABSTRACT

In order to prepare for the siting and licensing of a spent fuel repository SKB has decided to construct a new underground research laboratory.

The pre-investigations for the Äspö Hard Rock Laboratory started late in 1986. Intermediate reports on the investigations were published in 1988 and 1989.

The investigations have been grouped to several geometric scales under the disciplines of geology, geohydrology and groundwater chemistry, transport of solutes and mechanical stability.

Geological mapping and geophysical measurements have been made both on a regional and on a site scale. On the site scale additional surface measurements, drilling of 35 percussion boreholes and 19 cored boreholes was made. The results of the geological investigations show that the Äspö bedrock is a complex mixture between Småland granite, Äspö diorite and fine grained granite. The island is divided into a southern and a northern block by a shear zone, with a strike to the NE.

Hydraulic and chemical data was collected from existing well records within the Kalmar County. Hydraulic conductivity measurements and interference pumping tests were made in the core drilled holes and to some extent in the percussion holes. The hydraulic conductors are basically the fracture zones, but one of the most important is a NNW striking system of single fractures which is difficult to distinguish geologically.

The chemical conditions of the groundwater and the fracture minerals from water-bearing sections of the core drilled holes have been examined. Water samples were collected from percussion boreholes. The groundwater can be divided into three categories. Fresh water down to approximately 50 m depth. Mixed fresh and seawater 50-100 m, present and/or relict seawater 100-500 m and old (relict) seawater below a depth of 500 m.

An important task in the evaluations is to set up "conceptual models" These models are the basis for calculations of the ambient groundwater situation and the way in which the hydrological regime will change during the excavation of the laboratory.

In order to allow for different levels of detail the conceptual models are established on different scales. The geometrical scales chosen are 500 m, 50 m and 5 m. For every scale a lithological-structural model is presented. This basic model is supplemented with hydraulic properties and data on groundwater chemistry. Depending on the scale, deterministic or stochastic methods have been used to facilitate interpretation.

CONTENTS

1	INTRODUCTION	
1.1	Background	1
1.2	Objectives of the Äspö HRL project	1
1.3	Overview of the Pre-investigation Phase	2
1.4	Overview of this report	5
2	PURPOSE OF THE PRE-INVESTIGATIONS FOR THE ÄSPÖ HARD ROCK LABORATORY	
2.1	Goals	7
2.2	Approach to investigation and evaluation of the Äspö HRL	7
2.3	Investigation scales and their rationale	7
2.4	Investigation stages	8
3	ANALYSIS OF FIELD DATA AND RESULTS FROM THE INVESTIGATION	
3.1	Geology	9
3.1.1	Purpose of the investigation	9
3.1.2	Overview of the geological investigations	9
3.1.3	REGIONAL SCALE: Summarized presentation of main geological data - interpretation and analysis	11
3.1.4	REGIONAL SCALE: Geological - tectonic model of the Simpevarp area	19

3.1.5	REGIONAL SCALE: Correlation between geological data and the water-bearing ability of different rocks and fracture zones	20
3.1.6	REGIONAL SCALE: Evaluation of the methods of investigation	21
3.1.7	SITE SCALE: Summarized presentation of main geological investigation data, interpretation and analyses	22
3.1.8	SITE SCALE: Correlation to geohydrology and ground-water chemistry	49
3.1.9	SITE SCALE: Evaluation of the methods of investigation	50
3.2	Geohydrology	53
3.2.1	Purpose of the investigation	53
3.2.2	An overview of the geohydrological investigation	53
3.2.3	REGIONAL SCALE: Summarized presentation of main geohydrological data - Interpretation and analysis	55
3.2.4	Generic modelling	60
3.2.5	REGIONAL SCALE: Evaluation of the methods of investigation	68
3.2.6	SITE SCALE: Summarized presentation of main geohydrological data - Interpretation and analysis	70
3.2.7	SITE SCALE: Numerical modelling	111
3.2.8	SITE SCALE: Evaluation of methods of investigation	115
3.3	Chemistry	119
3.3.1	Purpose of the investigation	119
3.3.2	REGIONAL SCALE: Overview of the groundwater and geochemical investigations	119
3.3.3	REGIONAL SCALE: Interpretation and evaluation of the results	123
3.3.4	SITE SCALE: Overview of groundwater and geochemical investigations	123
3.3.5	SITE SCALE: Interpretation and evaluation of the results	130
3.3.6	Fracture mineral chemistry on Äspö	136
3.3.7	Chemical conditions of the Äspö groundwater	137
3.3.8	Correlation to other methods and parameters	145
3.3.9	Evaluation of the methods of investigation	145

3.4	Transport of solutes	146
3.4.1	Purpose of the investigations	146
3.4.2	Dilution and tracer tests	146
3.5	Mechanical stability	147
3.5.1	Purpose of the investigation	147
3.5.2	Rock stress measurements	149
3.5.3	Laboratory tests on rock samples	152
3.5.4	Classification of the rock mass	153
3.5.5	Stability	154
3.5.6	Failure of intact rock	155
3.5.7	Structural conditions and future loads	156
3.5.8	Potential movements	157
4	CONCEPTUAL MODELS	
4.1	Major fracture zones - Site scale	159
4.1.1	Fracture zone EW-1	164
4.1.2	Fracture zone NE-2	166
4.1.3	Fracture zone EW-3	168
4.1.4	Fracture zones NE-1 and EW-5	170
4.1.5	The fracture zone system EW-7, NE-3 and NE-4	174
4.1.6	The fracture zone system NNW	176
4.1.7	The fracture zone system NW-1	179
4.2	<u>Rock Mass Units</u> - Site scale	180
4.2.1	RMU-0	181
4.2.2	RMU-1	181
4.2.3	RMU-2	182
4.2.4	RMU-3	183
4.2.5	RMU-4	183
4.3	<u>Geological Units</u> - Block scale, <u>50 m</u>	184
4.3.1	GU 50 - 01	185
4.3.2	GU 50 - 02	186
4.3.3	GU 50 - 03	187
4.3.4	GU 50 - 04	188
4.3.5	GU 50 - 05	189

4.3.6	GU 50 - 06	190
4.3.7	GU 50 - 07	191
4.3.8	GU 50 - 08	192
4.3.9	GU 50 - 09	193
4.3.10	GU 50 - 10	194
4.4	<u>Geological Units</u> - Detailed scale, <u>5</u> m	195
4.4.1	GU 5 - 01	195
4.4.2	GU 5 - 02	196
4.4.3	GU 5 - 03	197
4.4.4	GU 5 - 04	198
5	GROUNDWATER FLOW MODEL OF SOUTHERN ÄSPÖ	
5.1	The transformation of the conceptual model to the numerical model	199
5.2	Calibration exercises	201
5.2.1	Calibration of the HRL model	201
5.3	Model for predictions of the HRL	206
	References	207

1 INTRODUCTION

1.1 BACKGROUND

Since the end of the 1970s, SKB has carried out extensive studies of the geological conditions at many different sites in Sweden. Investigations have been carried out from the surface and in boreholes down to a depth of 1000 metres on eight so-called study sites. Furthermore, a great deal of work has been done at the Stripa Mine within the framework of the international Stripa Project. Special research projects focussing on the properties of fracture zones have been carried out at the Finnsjön study site, at the Saltsjö Tunnel, on a tunnel construction site at the hydropower station in Hylte and within the Lansjärv Project. For an account of the results of these studies, the reader is referred to R&D-programme 89 and to SKB's Technical Reports. In summary, these studies show that good geological conditions exist for siting a final repository at many locations in Sweden.

Investigations of conceivable final repository sites carried out so far have only involved measurements on the surface and in boreholes. Investigations have also been carried out in and from tunnels at Stripa and in connection with certain construction work for other purposes. There is a need to directly verify the results of surface and borehole investigations with systematic observations from shafts and tunnels down to the depth of a future repository. The construction of the Äspö Hard Rock Laboratory provides excellent opportunities for such verification. This verification will permit greater confidence in our ability to judge the suitability of future candidate sites for a final repository even before detailed investigations of these sites have been made. This can facilitate the decision-making process that will lead to technical-scientific acceptance for the proposed candidates.

The goals and objectives of the Äspö HRL are discussed in more detail in SKB's R&D- programme 89/SKB, 1989/.

1.2 OBJECTIVES OF THE ÄSPÖ HRL PROJECT

The main goals of the R&D work in the Hard Rock Laboratory are to:

- Test the quality and appropriateness of different methods for characterizing the bedrock with respect to conditions of importance for a final repository.
- Refine and demonstrate methods for adapting a final repository to the local properties of the rock in connection with planning and construction.
- Collect material and data of importance for the safety of the final repository and for confidence in the quality of the safety assessments.

To meet the overall timetable for SKB's research work, the following stage goals have been set up for the activities at the Äspö Hard Rock Laboratory. The goals are commented in SKB's R&D programme. Prior to the siting of the final repository for spent fuel in the mid-1990s, the activities at the Hard Rock Laboratory shall serve to:

- **Verify pre-investigation methodology**
Demonstrate that the investigations on the ground surface and in boreholes provide sufficient data on essential safety-related properties of the rock at repository level, and
- **Finalize detailed investigation methodology**
Refine and verify the methods and the technology needed for characterization of the rock in the detailed site investigations.

As a basis for optimization of the final repository system and for a safety assessment as a basis for the siting application, which is planned to be submitted a couple of years after 2000, it is necessary to:

- **Test models for groundwater flow and transport of solutes**
Refine and test on large scale at repository depth, methods and models for determination of ground water flow and transport of solutes in rock.

In preparation for the construction of the final repository, which is planned to begin in 2010, the following shall be done at the planned repository depth and under representative conditions:

- **Demonstrate construction and handling methods**
Provide access to rock where methods and technology can be refined and tested so that high quality can be guaranteed in the construction, design and operation of the final repository, and
- **Test important parts of the repository system**
On full scale, test, investigate and demonstrate different components that are of importance for the long-term safety of the final repository system.

1.3

OVERVIEW OF THE PRE-INVESTIGATION PHASE

Like SKB's other R&D work, the R&D activities at HRL are mainly contracted to universities, institutes of technology, research institutions, consultants, industrial companies and other Swedish and foreign experts. The project is headed by SKB, which has assigned a project group responsible for the planning and execution of the work. The authors of this report are the principal investigators for geology, geohydrology and groundwater chemistry.

The work of the Äspö HRL project has basically been divided into three major phases. The first phase includes the pre-investigations before excavation. The second phase is the construction of the laboratory and the third the operating phase, see R&D programme 89/SKB, 1989/.

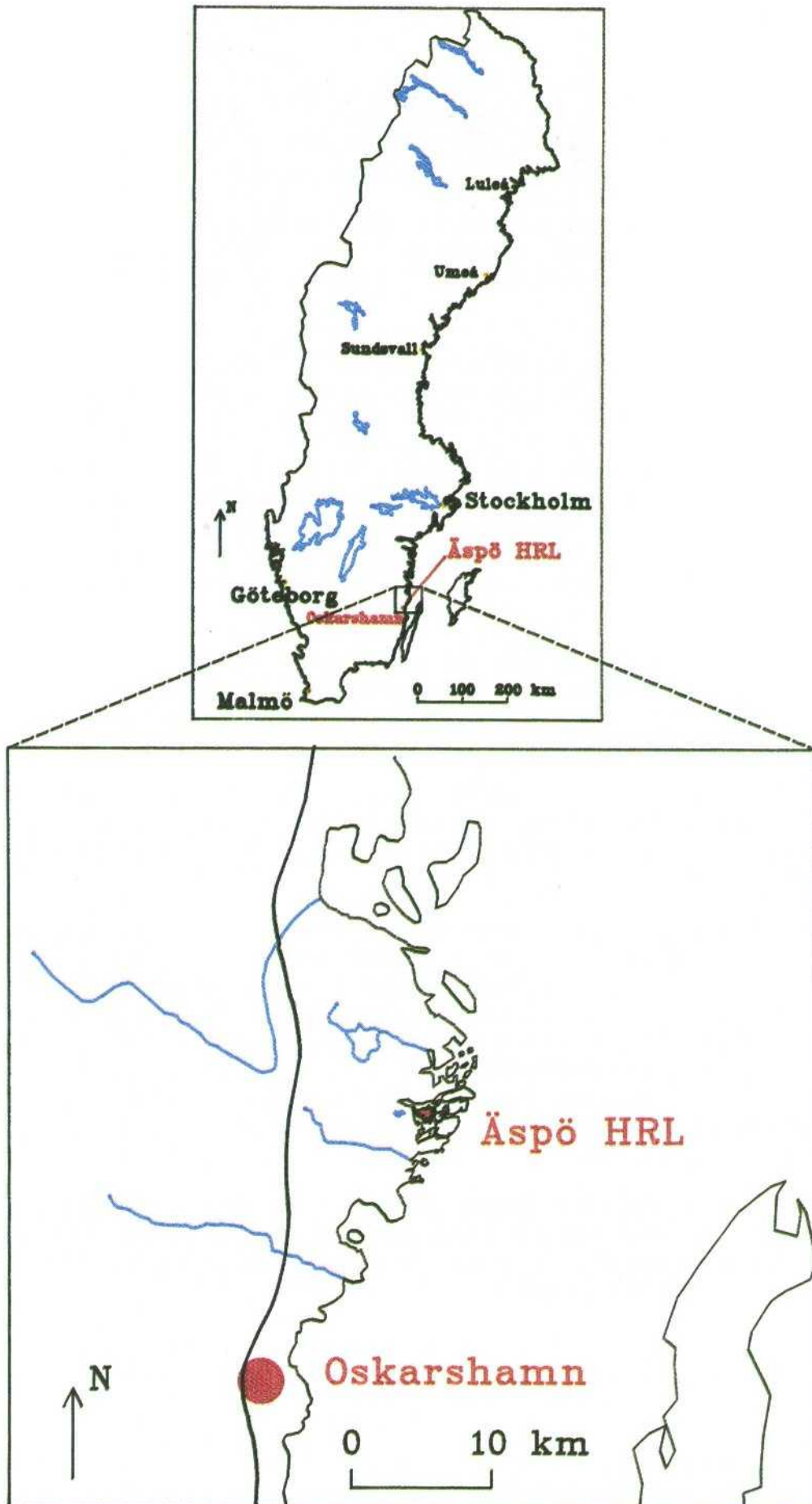


Figure 1.1 Location of the Äspö HRL.

The first evaluation /Gustafson et al, 1988/ presented the outcome of the regional investigations of geology, geohydrology and groundwater chemistry and a preliminary evaluation of several target areas. An important part of the report is the geological prediction of the situation on Äspö prior to any deep drillings.

The second evaluation /Gustafson et al, 1989/ used the regional conceptual model in the above report in order to develop the first site specific groundwater models. The report also presents the results of the first deep drillings and conceptual models based on the data.

In parallel with the evaluation, the second and third drilling programmes were started with the aim of increasing confidence in the existence and extent of indicated fracture zones. However, this investigation stage was extended much further than was initially intended. This extension was required by the regulatory authorities for permits and to change the layout of the laboratory. The government decided that the project should be reviewed under the Act on the Conservation of Natural Resources. In connection herewith, SKB decided to reduce the environmental impact at Äspö by starting the entrance tunnel from Simpevarp, see Figure 1.2. The extended target area required further drillings and evaluations. The results of these investigations are included in this report.

Site characterization is a multi- and interdisciplinary task that necessitates integration during data acquisition, evaluation and presentation. In order to facilitate such integration three basic decisions were made for the site characterization of the Äspö HRL /Bäckblom et al, 1990/.

The first decision was to divide the investigations to stages. Evaluations were made and reported after each stage. This offered an opportunity to document what was achieved in each stage and an opportunity for the investigators to jointly interpret all data simultaneously.

The second decision was to conceptualize¹ the investigations on different geometrical scales, appropriate for the planning of a real repository. The regional scale >> 1000 m forms a basis for later detailed investigations and for selection of suitable rock bodies for a repository. The site scale 100 - 1000 m will be used for the layout of a repository and for the far field evaluations in a siting application. The 10 - 100 m block scale will be used for selection of canister positions and for near field performance assessment. The very near field 0 - 10 m defines the near field to the buffer and canister. It also includes the so called "disturbed zone" that develops close to the excavated rock.

The third decision was to designate five key issues of relevance for design, and/or performance assessment and/or safety assessment. The designated key issues are the geological-structural model, groundwater flow, groundwater chemistry, transport of solutes and mechanical stability.

¹ A conceptual model is a qualitative description of a system or a sub-system and its representation judged to describe aspects of its representation, relevant to the intended usage of the model.

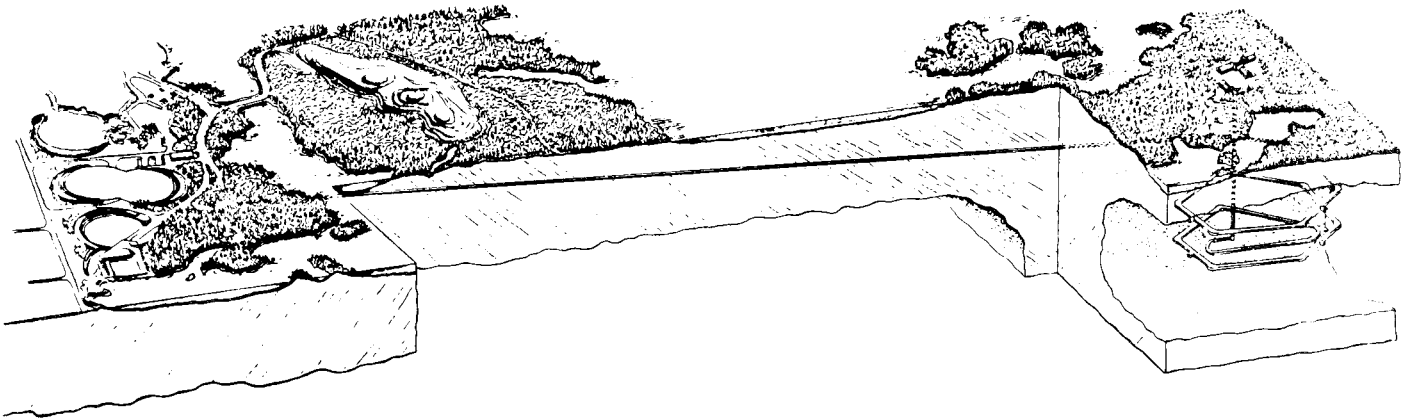


Figure 1.2 Schematic design of the Äspö Hard Rock Laboratory.

1.4

OVERVIEW OF THIS REPORT

This report is the third evaluation during the pre-investigation phase and is intended to provide the basis for all predictions prior to excavation of the ramp. It is not the final evaluation of the pre-investigation phase. It should instead be treated as the very first summarized report of the pre-investigation phase. The predictions, which are based on the conceptual models presented in this report, will be checked during the excavation of the laboratory and evaluated. This means that the final report on the pre-investigations will probably be published during 1995.

Chapter 2 presents the goals, the approach and rationale behind the investigations.

Chapter 3 presents an overview of the different investigations and the analyses and evaluations of the geological, geohydrological and the groundwater chemical data.

Chapter 4 presents the conceptual models on the different scales. It describes the fracture zones and rock mass units on the site scale and the properties with respect to the designated key issues. The major structures are defined as either certain, probable or possible.

Chapter 5 gives a more detailed presentation of the groundwater flow modelling and how the models have been calibrated to the existing data and used for predictive modelling.

2 PURPOSE OF THE PRE-INVESTIGATIONS FOR THE ÄSPÖ HARD ROCK LABORATORY

2.1 GOALS

The pre-investigation phase has been conducted with the following stage goals:

- Collect the geoscientific data required to evaluate whether it is possible to locate the Hard Rock Laboratory around Simpevarp and to evaluate the need for detailed investigations for the siting of it.
- Establish the basic data required for the preliminary facility layout of the Hard Rock Laboratory.
- Establish programmes for shaft sinking/tunnelling and monitoring.
- Make a prediction for the geological conditions and for the geohydrological and geochemical changes that will occur in connection with construction of the research laboratory.

2.2 APPROACH TO INVESTIGATION AND EVALUATION OF THE ÄSPÖ HRL

As mentioned in the introduction, the investigations were performed on different scales. The reason for such a division is simply that different types of knowledge are needed to answer the key questions. It is for instance necessary to know how the structural and lithological pattern of the HRL site resembles the corresponding pattern in the region. It is also necessary to know how large a variation there is in hydraulic properties and chemical characteristics on the site scale compared to the regional scale.

The investigations were therefore focussed on somewhat different goals on the regional and site scales. On the regional scale the emphasis was to select a site which from the geological, geohydrological and geochemical standpoints was representative of the region. The emphasis of the site scale investigations was to yield detailed knowledge of the site on which the predictions prior to the excavation could be based.

2.3 INVESTIGATION SCALES AND THEIR RATIONALE

Characterization on a regional scale $\gg 1000$ m forms the basis for more detailed investigations. Areas of recharge and discharge can be defined, as well as variations in the rock mass composition and chemical composition of the groundwater. The regional assessment will also form the basis for long term descriptions of possible future discharge areas and potential zones of movement.

The site scale characterization, 100 - 1000 m, locates major fracture zones and/or major flow paths. These investigations are essential as they provide guidance on the design of the laboratory as well as important information to define the geological structure pattern. Characterization on this scale also defines the far field groundwater flow.

Block scale assessment 10 - 100 m, is used mainly to investigate and define the occurrence and frequency of geological and lithological features.

The detailed scale, 0 - 10 m, may be the most important scale as the properties on this scale define the geohydrological, chemical and mechanical near field to the laboratory tunnel. Many of these features are easy to check in the tunnel although the tunnel effects may obscure some of the true properties.

2.4

INVESTIGATION STAGES

The pre-investigation phase is divided into the following stages:

- siting,
- site description and
- prediction.

An overview of the investigations in the different stages is given in Stanfors et al /1991/.

The siting stage investigations involved mostly geophysical measurements, geological mapping and a percussion drilling programme at Äspö, Ävrö and Laxemar.

The site description stage included detailed ground geophysical mapping on Äspö, fracture mapping on outcrops and drilling programme including cored holes and percussion holes on Äspö. Two of the three holes reached a depth of 1000 m.

Core mapping, geophysical logging, single and cross-hole hydraulic testing and groundwater chemical characterization were made in the boreholes to characterize the bedrock of Äspö.

The prediction stage involved two more drilling campaigns on the southern part of Äspö. The emphasis was to characterize geologically indicated fracture zones. The evaluation of these investigations necessitated the third drilling campaign.

3**ANALYSIS OF FIELD DATA AND RESULTS
FROM THE INVESTIGATION**

The main purpose of this part of the report is to give an overview of the pre-investigations set-up and present the most important results, especially with respect to the interpretation and analyses of the data which formed the basis for the conceptual models presented in Chapter 4. Correlation of the results from different investigation methods and the relevance of methods are also discussed.

3.1**GEOLOGY****3.1.1****Purpose of the investigation**

The main aim of the geological pre-investigations at the initial stage was to give a brief description on a regional scale of the rock distribution and the structural pattern in the Simpevarp area. At a later stage, further investigations were performed in steps to characterize the rock mass in the Äspö - Hälö area on a site scale.

The goal is to describe the composition and heterogeneity of a given selected rock volume. This includes a precise description of the special distribution of rock types, large and small fracture zones and the fracture geometry and minerals of the rock mass.

3.1.2**Overview of the geological investigations**

The geological pre-investigations for the Äspö HRL, which were started in 1986, were performed on different scales.

Tables 3.1.1 and 3.1.2 present an overview of the geological pre-investigations. The specific objectives of the different investigation methods are presented briefly by Stanfors et al /1991/. For a more detailed description the reader is recommended to consult the specific progress reports. Results and discussion on the results are shortly reviewed in sections 3.1, 3.2 and 3.3, but for more detailed discussion of the topics the reader is referred to the progress reports.

**Table 3.1 Overview of geological investigations in the Simpevarp area.
Regional scale
(approx. 25 x 35 km)**

Airborne geophysical survey (magnetic, EM,VLF, radiometric)
Gravity measurements (one station per square kilometre)
Petrophysical measurements (density, magnetic susceptibility, IP)
Interpretation of lineaments (Landsat, digital terrain models)
Mapping of solid rocks
Mapping and analyses of main structures and fracture pattern

Table 3.2 Overview of geological investigations on the Äspö - Hålö scale

Detailed mapping of solid rocks and petrographic studies along cleaned trenches across the island of Äspö
Detailed ground geophysical measurements (VLF, resistivity, magnetic, radiometric, seismic refraction/reflection)
Detailed study and analyses of ductile and brittle structures
Borehole investigations (20 percussion boreholes, total length: 2200 m and 14 cored boreholes, total length: 6600 m)
- Lithology (detailed petrographic mapping, studies of thin sections, modal and chemical analyses)
- Fractures (frequency, RQD, mineral filling, relative and absolute orientation)
- Geophysics (10-13 different logs)
- Rock stress measurements (hydraulic fracturing and overcoring in two boreholes).

3.1.3

REGIONAL SCALE: Summarized presentation of main geological data - interpretation and analysis

Geophysical surveys

The initial airborne geophysical survey, combined with gravity measurements and petrophysical measurements on typical rock samples, was performed in the Simpevarp area mainly to locate and characterize big rock bodies and, possible, fracture zones on a regional scale.

Aerogeophysical results revealed some magnetic, almost circular, granitic structures which coincide with two especially distinct negative Bouguer anomalies /Nylund, 1987/. Gravity and magnetic modelling of these granites (the Götemar and Uthammar massifs /Figure 3.1/) strongly suggest an outward dip, that is, the body of the granites becomes larger with depth. The estimated depth of these granites is about five kilometres and they are interpreted as true diapirs. /Nisca, 1987, a/ /Figure 3.2/.

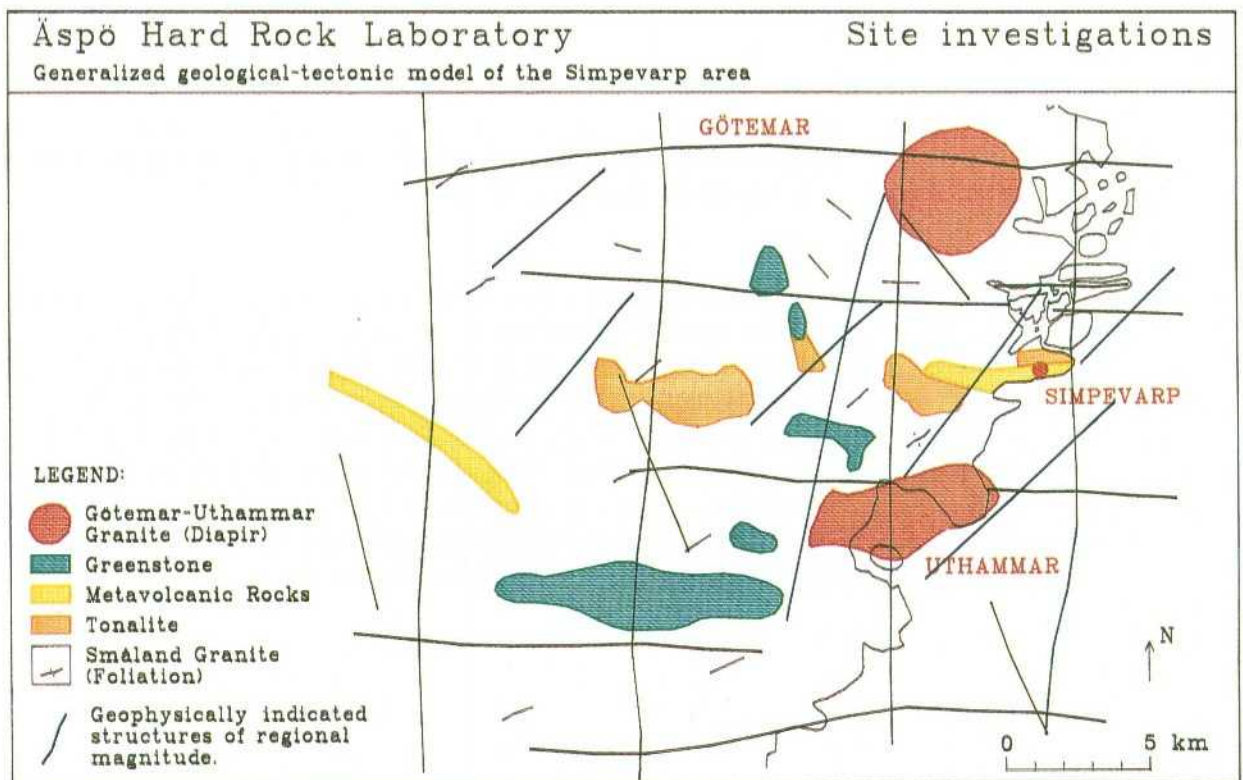


Figure 3.1 Regional model of the distribution of major bedrock units and geophysically indicated structures of the Simpevarp area.

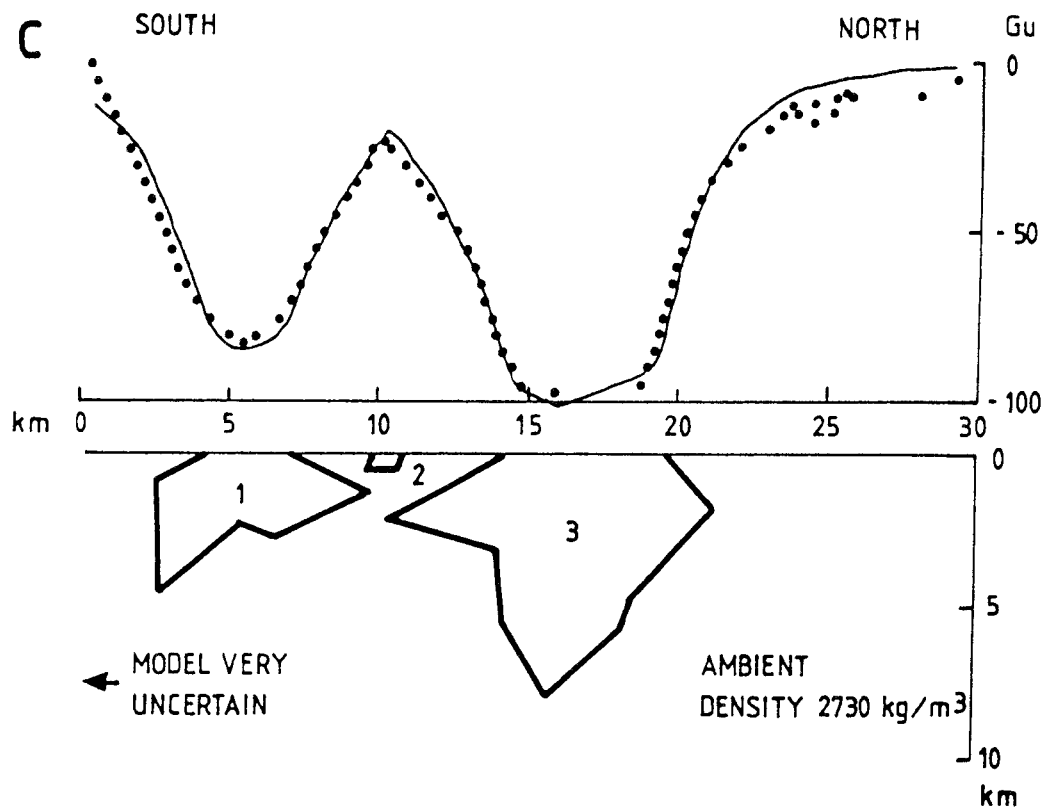


Figure 3.2 Gravity modelling of the Götemar and Uthammar granites /Nisca, 1988/ Some east-west, elongated, positive gravity anomalies consist of diorite - gabbro massifs with very high magnetic susceptibility and are estimated to be about two kilometres thick.

Geophysical data obtained by aerial survey were also used to interpret the location and character of supposed regional fracture zones. An orthogonal regional pattern consisting of geophysical features trending N-S and E-W dominates. The aeromagnetic anomalies are often about 100-200 metres wide, and dipping vertically-subvertically. Ground geophysical profiling over some of these zones confirmed that in general the width of the zones of low magnetic intensity due to oxidation is between 100 and 200 metres. VLF and seismic refraction measurements showed, however, very narrow indications less than 10 metres wide at most, associated with increased fracturing and depressions in the topography /Stenberg and Sehlstedt, 1989/ Figure 3.3.

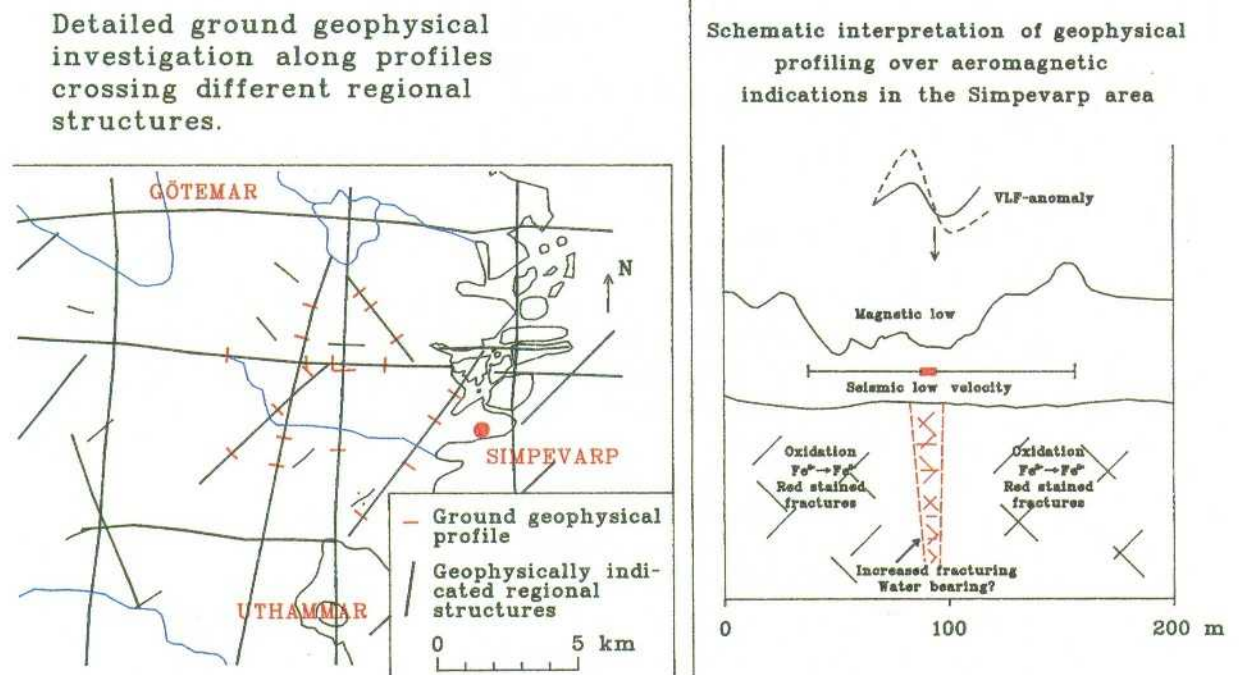


Figure 3.3 Schematic interpretation of ground geophysical profiling over some aeromagnetic indications in the Simpevarp area

E-W trending zones were presumed to have low dips, often to the north. VLF-anomalies indicated that the N-S trending zones were more likely to be waterbearing than the E-W ones. Indications trending NE and NW were interpreted as representing an older orthogonal system of presumed fracture zones /Nisca, 1987a/.

Interpretation of lineaments

Lineaments in the Simpevarp area have been interpreted from four different digital terrain models processed using EBBA II image analysis techniques.

The aerogeophysical results - which also were processed using the EBBA image system - have been compared with the results from the digital terrain models.

Lineament interpretation shows four main lineament sets, representing presumed fracture zones in the area. Their orientations are NW-SE, E-W (oldest), N-S and NE-SW (established later). All four sets occur all over the area but lineaments trending NW-SE are expressed in the northern part and lineaments trending NE-SW in the southern part of the area /Tirén et al, 1987/.

NW-WNW trending lineaments from the inland area west of Simpevarp have been described by Nordenskjöld /1944/ as gently dipping thrusts. According to Palmqvist /1991/ thrusts of this kind must be regarded as very important in the eastern coastal area as well, where they are more difficult to observe due to the lower relief.

Mapping of solid rocks

The dominant rocks in the Simpevarp area - Småland granites - are normally porphyritic and comprise very different types. In mineralogical composition these rocks vary from granite-granodiorite-monzodiorite to diorite. The greyish-red granite on the island of Ävrö is an example of a more acid variety with rather small potash megacrysts (Ävrö granite).

These granites belonging to the Småland-Värmland batholith predominate the older Svecokarelian metavolcanics and gneiss-granite. The Småland-Värmland intrusions are post-orogenic in relation to the Svecokarelian folding /Kornfält and Wikman, 1987a/ Figure 3.1/.

The Småland granite within the area is often intruded by fine-grained, greyish-red granite, presumably representing a later differentiation phase of the post-orogenic magma. An anorogenic origin, however, cannot be ruled out. The fine-grained granite occurs both in smaller massifs and in dikes, usually 0.5-5 metres thick in older rock.

Metavolcanic rocks occur as minor inclusions in the granite mass, especially on the Simpevarp peninsula and the island of Ävrö. These fine-grained, grey to dark grey rocks are often penetrated and in part brecciated by granites. Compared with the intrusive rocks, the metavolcanics exhibit more intense and closely spaced fracturing. /Ericsson, 1987/. Greenstone occurs both as large massifs-especially in the southern part of the investigated area - and as small irregular lenses and sheets in the granite mass. The larger massifs - of diorite-gabbroid composition - can be related to east-west, elongated, positive-gravity and magnetic anomalies. /Nisca, 1987a/.

The fine-grained rather homogeneous greenstone is probably a metabasalt. The greenstone has often been intruded by the fine-grained granite. The designation "tonalite" has often been used for a group of grey, generally medium-grained rocks which, according to macroscopic assessments, were supposed to be more basic than the common Småland granites but not as basic as the greenstones.

The tonalite is as a rule massive and relatively homogeneous. It often has xenoliths of metavolcanics and is intruded by the porphyritic Småland granite, which is therefore younger.

The red-coloured coarse-grained granites which are present as separate, almost circular (Götemar, Uthammar) massifs are estimated to be anorogenic in relation to the Svecokarelian folding.

As can be seen in Figure 3.1, the lithology of the Simpevarp area exhibit a very pronounced ENE-WSW elongation. This direction is parallel to the foliation, which is often very weak but still evident and appears to dip steeply to the north in the granitic rocks.

Fracture mapping

A fracture mapping programme was carried out in the Simpevarp area. /Ericsson, 1987/. The mapping was done on outcrops and road cuts. Fractures exceeding 0.5 metres were measured on outcrops which have surface areas from about 30 to 200 square metres. About 9 600 of the 10 400 outcrop fractures were mapped as steep, with dips of 70° to 90° /Figure 3.4/.

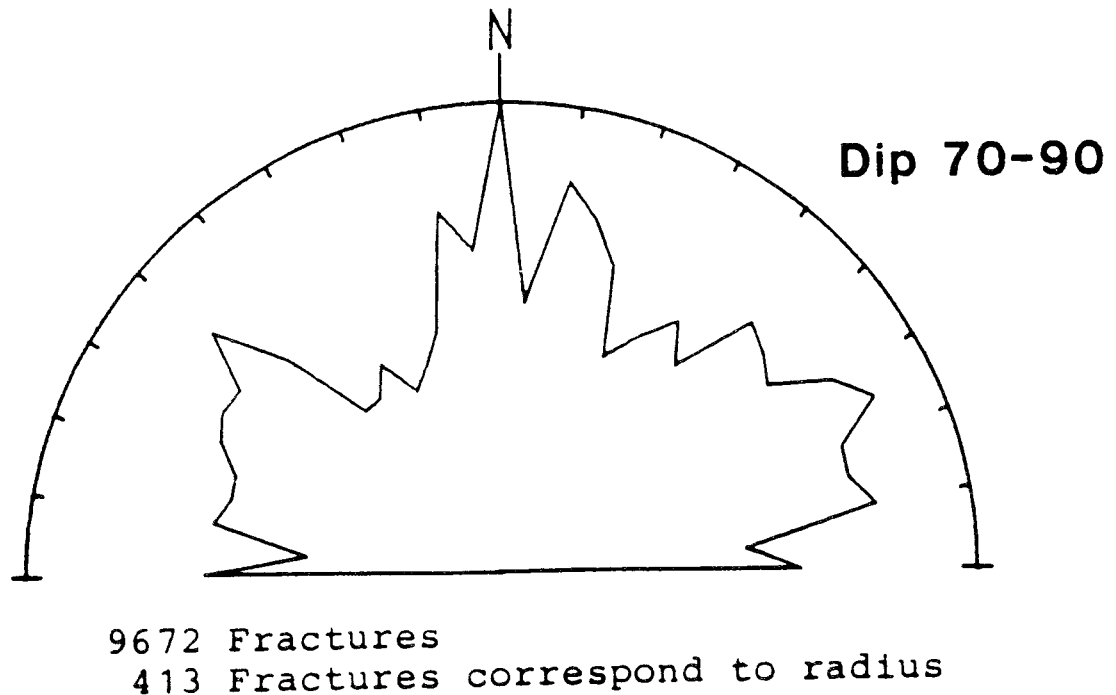


Figure 3.4 Rosette diagram for all outcrop fractures in the Simpevarp region with dips of 70° to 90° /Ericsson, 1987/.

The fracture sets mainly coincide with the most conspicuous lineament directions (valleys) in the region. The general pattern shows evident strike directions around N-S and N50°W. A tendency of a predominant fracture set also strikes in an E-W direction. In the sector between N40°W and N80°E there appears a fracture set with a somewhat less predominant peak in the direction N65°E. This sector coincides with the most common foliation strikes in the region. Even if gentle fracture dips may have been underestimated during the road-cut mapping a summarized interpretation also shows that predominant dips are vertical or almost vertical.

The most predominant peaks of the fracture sets for the different bedrock types in the region have been evaluated. The most common Småland granite has predominant fracture sets in the directions E-W, N60°W, N5°E and N75°E, and the fine-grained granite N45°W, N10°W, N25°E and N75°E. The foliation influences the fracture sets, especially in the sector N45°E to E-W. E-W sets occur but are not so frequent. The fractures of the red Götemar-Uthammar granite are relatively less influenced by any foliation.

The fracture lengths in different rock types are presented. The geometric mean value (median) varies from about 0.6 to 1.2 m. The lengths in the greenstone are

significantly shorter than those of all other bedrock types. The tonalite and porphyritic granite exhibit the longest fractures. There is a similar deviation in length among the different rocks, with a possibly somewhat larger spread in the fine-medium-grained granite and the gneissic granodiorite.

The fracture density distribution was found to be log-normal and the median values were almost equal. The Småland granite and granodiorite dominate the region. The confidence interval (95%) for the mean (median) value of the fracture density in this rock type is 1.4 to 1.7 fractures per square metre.

Concerning fracture filling, epidote and quartz have been formed in deeper processes in connection with some kind of regional metamorphism close to the plastic or semi-plastic crust. Calcite and red stains tend to be more superficial processes within a brittle environment. Calcite may be precipitated under hydrothermal as well as low-temperature conditions. Thus, the distribution of calcite-filled fractures may be used as an indicator of previous and present water paths in the rock. Strong alteration of a rock often implies a colouring around the fractures. For example, red hematite staining of the wall rock may be used as an indicator of hydrothermal activity. Referring to the above, calcite-filled fractures and fractures with red stains may constitute relatively young discontinuities that are able to transport water. Calcite and red-stained fractures have predominant N-S strikes. The altered fractures in wall rock also occur relatively frequently in the E-W direction. This result indicates that fractures in the N-S and E-W directions could be the ones that conduct most water.

The most conspicuous structures in the region are some N-S and E-W valleys. These lineaments have been interpreted as being block boundaries, i.e. fracture zones in the macroscopic regional scale. A special correlation study was made on the outcrops that surround one N-S lineament and one NE lineament. Furthermore, one E-W lineament was evaluated. Within a distance of 2.5 kilometres the correlation between the lineament direction and the dominant fracture sets is evident.

The results are used in a fracture network model, see section 3.2.

Main structures and outline of the tectonic history on a regional scale.

The pattern of fractures and fracture zones in the Simpevarp area seem to be very much influenced by the precursory ductile strains /Talbot et. al., 1988/. The oldest sign of ductile deformation is a penetrating planar foliation trending NE to ENE - often diffuse - marked by the orientation of feldspar phenocrysts in the Småland granite and enclaves of mafic sheets or swarms of enclaves ranging in the thickness from less than a metre to tens of metres.

In subsequent ductile-semiductile deformation phases, the segmentation of the region began with the development of gneissic zones trending ENE and dipping 20-80° to the NNW. Between 1700-1400 Ma the old gneissic zones became mylonitic as the region rose from amphibolite facies into greenschist metamorphic facies. Most of the mylonitic shears less than about one centimetre thick and up to a few metres long, are almost random in orientation.

On a regional scale a later diffuse foliation due to alignment of biotites is concentric and confined to within a few kilometres of the contacts of younger (1350-1400 Ma) Göttemar and Uthammar granites and is apparently due to early ductile stages of their

emplacement. Zones of epidote veins tend to follow the mylonites. They mostly trend N and NNW and are believed to have been created in a semiductile cooling phase of the Göttemar-Uthammar granites. These veins also often contain quartz and are most probably older than other fracture sets investigated. There are obvious indications that some of these are hydraulic conductors today.

At about 1100 Ma red-stained dilational fractures, mostly striking about N-NW, probably acted as transport channels for hot, oxidizing solutions which coloured plagioclase red in the adjoining granitic wall rock in zones from a few millimetres up to decimetres wide /Munier, 1989/. This alteration postdates epidote and predates rare surviving filling of prehnite, indicating a transition from epidote - to zeolite facies.

A NNW trending basic dike swarm that fed sills now dipping approximately 20° SW was probably intruded soon after about 1000 Ma. It is interesting to note that basic sills of this kind - dipping about 20° SW - are reported by Talbot /1990/ to be exposed in two caves, described by Nordenskjöld /1944/ as examples of gently dipping mylonitic thrusts. Some younger dolerites are encountered in Äspö as dikes only a few decimetres wide and with a strike approximately N-S.

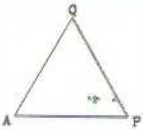
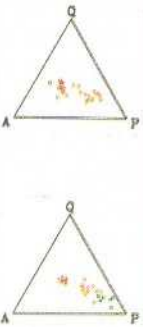

A period of erosion (about 960-600 Ma) of the Sub-Cambrian peneplain included the Varangian glaciation with associated glacial depression and uplift of the lithosphere. This period ended with injection of "Cambrian" sands into open fractures in the Sub-Cambrian peneplain, forming mostly NE and ENE trending subvertical clastic dikes.

By about 500 Ma, Cambrian limestone covered parts of the Baltic Shield. From observations of the limestone along the west coast of Öland - about 20 km to the east of Äspö - Talbot /1990/ reports NE trending faults which display similarities to some chlorite-filled fracture zones and faults on Äspö. Milnes and Gee /1990/ present joints, with the preferred orientations NNW, NE, WNW and N-S, from the west coast of Öland.

A definite effect caused by Quaternary glaciations in the Äspö area seems to be disruption of surface bedrock to a depth of at least 2-3 m /Mörner, 1989/. There is today no evidence in bedrock of deeper glacial disturbance. /Talbot, 1990/. Quaternary glaciations may in some way have affected various mineral fillings (e.g. younger calcite) in fractures which are known to be hydraulic conductors /Tullborg, 1989/.

The main rock units and events in the Simpevarp area are summarized in a chronological schedule /Figure 3.5/.

CHRONOLOGIC SCHEME OF THE MAIN ROCK UNITS AND EVENTS IN THE SIMPEVARP AREA.

TIME SCALE, Ma (1)	ROCK UNIT (1)	MODAL CLASSIFICATION	ROCK TYPE (1) STRUCTURES (4, 5)	SEQUENCE OF EVENTS (2,3,4)	FRACTURE FILLINGS (2)
2000-1850	Oldest supracrustals		Metaandesites		
1925-1800	Primorogenic rocks		Gneissic granites Granodiorites		
1840-1760	Postorogenic Småland-Värmland granitoids		Porphyritic granite-granodiorite-diorite. Fine-grained granite. Mafic dykes and enclaves. Greenstone.	Continuous magmamingling and magma-mixing process. Regional deformation. Folding E-W to ENE-WSW foliation. Mylonitic shear zones.	Mylonites or "shear-bands" containing fine-grained epidote, muscovite and recrystallized quartz
1400-1350	Anorogenic rocks		Coarse-grained granite (Göttemar-granite) Fine-grained granite Dolerite Chlorite veins.	Tension Post-magmatic hydrothermal circulation of the anorogenic granite	Fe-rich, idiomorphic epidote. One generation of fluorite. Growth of idiomorphic quartz, muscovite, hematite, fluorite, calcite and spherulic chlorite.
~1100				Burial metamorphism.	Prehnite, hematite-stained laumontite, calcite and fluorite.
600-300			Clastic dykes. Cambrian (?) sandstone. Post-chlorite veins. Fault scarps?	Burial metamorphism. Reactivation of older structures?	Gypsum, chlorite, illite, probably calcite and possibly Fe-oxyhydroxides.
Synglacial-present time			Fault scarps? Fractures?	Fracturing? Reactivation of older structures?	Calcite, Fe-oxyhydroxides and clay-minerals like kaolinite. Present groundwater circulation?

1 Kornfält-Wikman (1987) 2. Tullborg (1989) 3. Wikström (1989) 4. Talbot-Munier (1989) 5. Mörner (1990)

Figure 3.5 Summarized chronological schedule of the main rock units and events in the Simpevarp area/1. Kornfält and Wikman, 1987, 2. Tullborg, 1989, 3. Wikström, 1989, 4. Talbot and Munier, 1989, 5. Mörner, 1990/

3.1.4

REGIONAL SCALE: Geological - tectonic model of the Simpevarp area

Interpretation of geological field investigations and geophysics show that the Simpevarp area is mainly of granitic composition. Different types of Småland granite dominate in the study area. Some E-W elongated massifs of basic rocks, greenstone, have been indicated by positive magnetic and gravity anomalies.

Besides the more coarse-grained types, such as gabbro and diorite, fine-grained irregular bodies and xenoliths of greenstone are found as remnants within the granite mass. Greenstone occupies only a minor part of the Simpevarp area.

Some circular-semicircular structures in the investigated area are interpreted as granite diapirs. They are all represented by a more or less round, non-magnetic pattern and negative Bouguer anomalies. The Götemar and Uthammar granites are two of these structures which have been indicated as true diapirs.

Magnetic-gravity modelling with different density contrasts has given outward-pointing moderately-low dips. The joints in and around the granite diapirs are of several types but especially important are the flat ones, which can be seen in some quarries. Very low-dipping pegmatites and, to lesser degree, aplite granite are characteristic of the area around the Götemar granite. This granite may be very extensive below the Småland granites and may perhaps have caused not only joints but also gently dipping shear zones.

Information from all geological and geophysical investigations corroborates a tectonic picture of the Simpevarp area dominated by one almost orthogonal system of 1st order lineaments (N-S and E-W) /Figure 3.1/. These lineaments, extending in the order of 20-50 km, often coincide with some hundred-metres-wide, low-magnetic zones with a central fracture zone up to some tens of metres wide.

The N-S zones most probably have vertical-subvertical dips and seem to be of a tensional, more open, character according to coincident magnetic and VLF indications. The zones trending E-W are mostly vertical or moderately low dipping to the north or south. They seem to be more complicated, with an early dip-slip ductile phase indicated by intense mylonites, followed by a semi-ductile strike-slip phase and a late stage of reverse faulting, with local development of thrust sets with a mainly low to moderate dip to the SSE.

Besides the system of 1st order lineaments, there are also 2nd order zones trending NW and NE and forming another almost orthogonal system. The 2nd order zones are mostly in the order of 100 to 200 m wide and extend 1 to 20 km.

The most prominent of the N-E trending zones, running immediately west of Simpevarp and crossing the island of Äspö, is indicated by mylonites in some outcrops in the granite. For many of the zones trending N-W there seems to be a better coincidence between VLF and magnetic indications than for the N-E trending zones. According to a general interpretation most of the zones trending N-E and N-W are older than the N-S and E-W fracture zones. /Nisca, 1989 a,b, Tiren et al 1987/

Lineaments trending NNW and NNE (3rd order zones) are geophysically interpreted as being a conjugate shear set to the tensional fracture zones trending N-S.

Most of the regional fracture zones in the Simpevarp area have been preliminarily interpreted as being vertical or sub-vertical. Both geological and geophysical indications, however, point to the possibility of more flat or low-dipping structures, especially connected to the anorogenic granites (e.g. flat pegmatite dikes in the Göttemar granite area). Dikes of fine-grained granites and aplitic dikes are probably more sub-vertical or moderately dipping.

There are probably also low-dipping shear zones, especially connected to the E-W lineaments. Earlier geomorphological investigations report thrust zones, especially trending NW, and with low dips to the WSW /Nordenskjöld, 1944/.

On the island of Ävrö a fracture zone at least 120 m wide was encountered in three boreholes at depths varying between 100 and 500 m. This fracture zone is interpreted as having a N-S strike and dipping about 40° towards the west /Gentzschein et al, 1987/.

3.1.5

REGIONAL SCALE: Correlation between geological data and the water-bearing ability of different rocks and fracture zones

Metavolcanic rocks show no prominent foliation. Compared with the intrusive rocks, the metavolcanics show more intense and closely spaced fracturing. The fracture length is often shorter than that of the granitic rocks. Common fracture fillings are epidote and quartz. Highly fractured dikes or remnants of metavolcanic rocks in a surrounding granitic rock mass, are probably conductive.

Greenstone in large massifs normally has fracture lengths significantly shorter than those of all other rock types in the Simpevarp area. The fracture fillings are often calcite and chlorite. Greenstone can normally be regarded as having low permeability. In areas with greenstone xenoliths and dikes, however, the contacts with the surrounding bedrock can be hydraulically conductive.

Anorogenic rocks, such as the Göttemar granite, often have a very characteristic cubic fracture pattern, with a few long persistent fractures. The fracture density, however, is often low. Especially notable are the flat fractures which can be seen in the quarries. Highly permeable open, single fractures and flat dikes of fractured pegmatite and aplite seem to be very important conductive elements in the anorogenic granite. The vertical fractures, especially those with N20°W and N55°E orientations, seem to be more tight than the flat fractures.

The Småland granites (including the "tonalite" variant) are always more or less foliated and rather heterogeneous. The fracture length is normally rather long and the fractures are often filled with quartz, epidote and calcite. Fine-grained granite in dikes, often 0.5- 5 metres wide, frequently occur following the foliation in the direction about E-W to NE-SW and dipping sub-vertical. Typical of these dikes is that many of them are highly fractured and highly permeable. Flat pegmatite dikes, probably also permeable, cannot be excluded in the Småland granite mass, especially at greater depth and connected to the anorogenic granites. Xenoliths of greenstone are very common in the Småland granite in some parts of the Simpevarp area. Their contact zones with the granite are sometimes chemically and mineralogically altered and, in the case of fracturing, more or less conductive.

The N-S and the NE trending fracture zones, are interpreted as being the most permeable subvertical zones. The NW trending zones are probably less permeable than the NE striking ones. The zones running E-W seem normally to be less important as conductive elements but local variations may occur due to reactivation of these zones. Sub-horizontal fracture zones like the Ävrö zone are likely to be very important hydraulic conductors.

3.1.6

REGIONAL SCALE: Evaluation of the methods of investigation

During the regional phase of the pre-investigation for the Hard Rock Laboratory numerous geological and geophysical techniques were applied to characterize the geological and geohydrological conditions in the Simpevarp area. A first evaluation of the usefulness of the different methods applied, based on our present experience, is presented here.

The gravity and aeromagnetic methods were found very useful, especially for studies of a regional nature, i.e. for investigating the boundaries of the Götömar-Uthammar diapirs in three dimensions and the basic rocks of large extent. The densities and magnetic contents of these granitic rocks usually vary from those of the surrounding rocks and they were therefore good targets for both these methods. Based on these investigations it was possible to carry out a first three-dimensional lithological-tectonic modelling on a regional scale.

The aeromagnetic method was also used for mapping possible fracture zones in which oxidation of magnetite to non-magnetic minerals may cause magnetic minima. Aeromagnetic and VLF measurements seem to be far superior to the EM measurements in respect of interpretation of possible fracture zones. Coincident magnetic and VLF fracture zones may be of special interest in the search for the most permeable fracture zones. It is important, however, to point out the necessity of checking the aerogeophysical data with ground investigation methods before the final interpretation. The VLF measurements, however, are strongly disturbed by the salt water in the coastal area outside Simpevarp. The high outcrop density in the actual area made the radiometric measurements valuable in the bedrock interpretation work.

The petrophysics, based on physical measurements in the laboratory of a large number of representative samples, is necessary for making a good interpretation of the geophysical data.

Ground geophysical methods were used for more detailed investigations in some areas (Ävrö, Äspö, Laxemar, Bussvik). The VLF method may, under favourable circumstances (though they are strongly disturbed by the salt water), indicate water-bearing fracture zones and the ground magnetic measurements can provide bedrock information, like the locations of mafic xenoliths or dikes, if the contrasting magnetic susceptibility is big enough in relation to the surrounding granitic rocks.

Lineament interpretation of relief maps and structural analysis based on different digital models on a regional scale seem to be a very good base for further site investigation work, especially when this interpretation has been compared with the topographic expression of aeromagnetic lineaments.

Structural analysis of terrain features on a more detailed scale, based on topographical contour maps, is also valuable but the subdivision of an area into more than third order blocks seem to be questionable.

The detailed maps with modern petrographic descriptions, complemented with fracture mapping and a characterization study of the main fracture zones, performed in the Simpevarp area, have been very valuable in the geological and geohydrological modelling work.

3.1.7

SITE SCALE: Summarized presentation of main geological investigation data, interpretation and analyses

In order to get more detailed information about the geological conditions on Äspö a number of geological and geophysical studies were performed.

The aim of the geological field study was to obtain information to make a description of the lithological distribution and petrological and structural characteristics of the different rocks on Äspö. Very detailed mapping was performed along cleaned trenches across the island, and a geological map to a scale of 1:2 000 was prepared. A classification of the rocks based on chemical and mineralogical analyses is presented.

A complementary study of structural elements including a fracture mapping programme was also performed along the cleaned trenches to obtain results for use in geohydrological and rock mechanics model studies. Data concerning 4500 mapped fractures - such as orientation, length, aperture and fracture filling - is presented.

The main aim of the detailed geophysical investigation was to indicate fracture zones on Äspö, using mainly geomagnetic, geoelectric and seismic methods. Especially important was the interpretation of the dip of the fracture zones.

Lithology


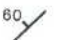





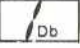
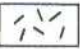






The dominant rocks on Äspö belong to the 1700-1800 M-year-old Småland granite suite, with mafic enclaves and dikes probably formed in a continuous magma-mingling and magma-mixing process /Kornfält and Wikman, 1988/, Figure 3.6.

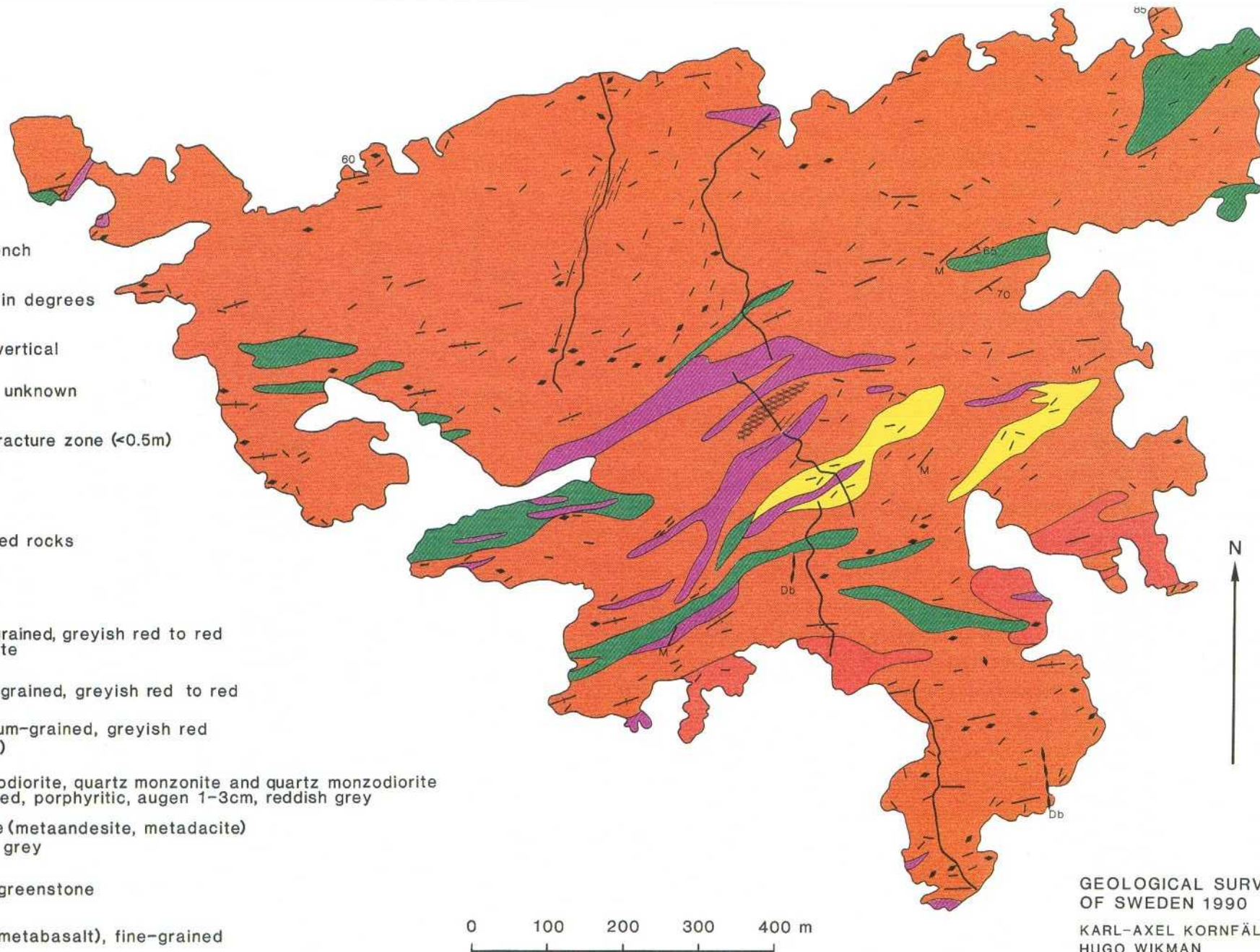
The result of this mingling (mixing) process is a very inhomogeneous rock mass, ranging in mineralogical composition from true granites to dioritic or gabbroid rocks. Rather large irregular bodies of diorite/gabbro have been located in boreholes at great depth in the site area /Wikström, 1989/.

Older folded basic sheets and xenoliths, often hybridized by the granitoids, are more or less dispersed in the rock mass, especially in a NE-ENE trending belt crossing central Äspö. Basic sheets tens of metres thick seem to have more gentle dips than sheets only about one metre thick /Talbot and Munier, 1989/.

All the rock mass in Äspö is intruded by fine-grained granites of at least two or three generations, related to the Småland granites and the 1300-1400 M-year-old anorogenic Götemar granite. The fine-grained granites form dikes of different widths - often trending NE and almost vertical - but also very irregular masses and veins which have been found by coring at different depths.

LEGEND

-  Uncovered trench
-  Foliation, dip in degrees
-  Foliation, dip vertical
-  Foliation, dip unknown or vertical
-  Mylonitized fracture zone (<0.5m)
-  Mylonite
-  Strongly foliated rocks
-  Diabase
-  Dikes of fine-grained, greyish red to red younger granite
-  Granite, fine-grained, greyish red to red
-  Granite, medium-grained, greyish red (Ävrö granite)
-  Granite, granodiorite, quartz monzonite and quartz monzodiorite medium-grained, porphyritic, augen 1-3cm, reddish grey
-  Metavolcanite (metaandesite, metadacite) fine-grained, grey
-  Xenoliths of greenstone
-  Greenstone (metabasalt), fine-grained



GEOLOGICAL SURVEY
OF SWEDEN 1990
KARL-AXEL KORNFÄLT
HUGO WIKMAN

Figure 3.6 Map of the solid rocks of the island of Äspö

Using the IUGS classification system, different rocks can be distinguished in the Småland granite group ranging in mineralogical composition from true granite - to granodiorite -monzonite and diorite /Kornfält and Wikman, 1987a/ Figure 3.7.

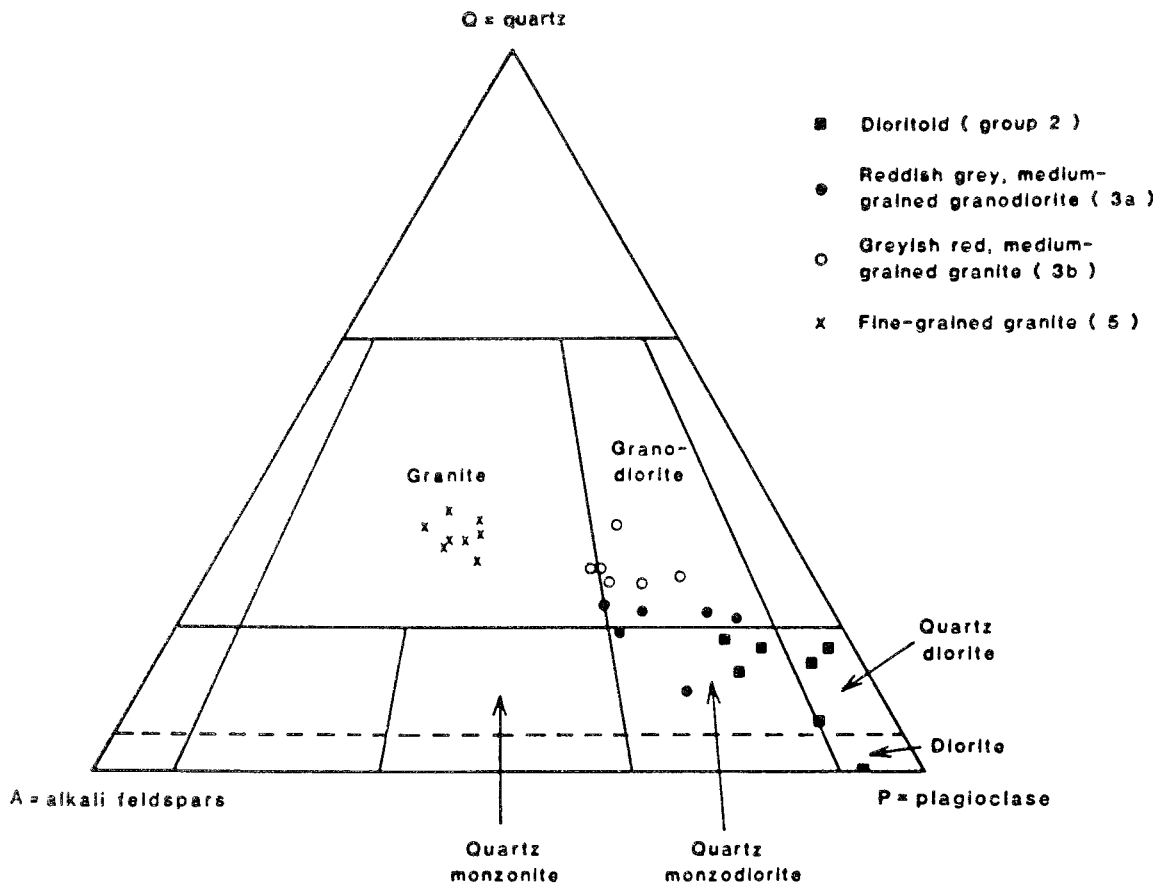


Figure 3.7 Modal classification of rocks from Äspö (KAS 02) according to IUGS (1973, 1980)

Based on surface observations and drill core logging a practical classification limit was later fixed at the silicate density 2.65-2.70 g/cm³ between what is now called Småland granite and Äspö diorite /Sehlstedt et al, 1990/. The most basic variant observed in some boreholes in Äspö, with a silicate density above 2.75 g/cm³, is assigned to the Greenstone Group.

In small areas on southern Äspö a redder variety of the Småland granite was observed. This rock, which is called Ävrö granite, is a true granite with rather small microcline megacrysts which are sparsely scattered compared with the porphyritic granitoids.

Across the island of Äspö, from SW to NE, there are a number of outcrops with greyish black, fine-grained basic rocks with a basaltic composition. They are very often strongly altered and called greenstone. Grey to dark-grey fine-grained rocks with a dacitic composition only constitute minor parts of the Äspö island. Most of these metavolcanic rocks seem to be older than the Småland Granite, based on the fact that they form thin sheets and xenoliths in the granitoid. Along the border between the medium-grained granitoid and greenstone, there are sometimes accumulations of fine-grained greyish-red granite.

Fine-grained granite also occurs frequently on Äspö as more or less well-defined dikes or veins intersecting the older rocks. The width of the often NE trending dikes is normally from one decimetre to some metres, but there are also wider dikes of this rock - up to 25 metres across. The fine-grained granites can be classified as true granites as can be seen from the triangular diagram, Figure 3.7.

Most of the fine-grained granites on Äspö seem to be anorogenic and related to the 1300-1400 M-year-old Göttemar-Uthammar granites, but there is certainly also at least one generation of fine-grained granite related to the older Småland granitoids.

Aplite and pegmatite as well as diabase have only been observed as very narrow dikes seldom more than a few decimetres wide.

Fracture mapping

The mapping has mainly been done on outcrops following the two cleaned N-S profiles on Äspö island. The principal aim of the fracture mapping measurements was to produce results for geohydrological and rock mechanics model studies. The project report includes (in different manners) geographically integrated results regarding strikes, dips, fracture densities, fracture lengths and spacing /Ericsson, 1988/.

The fractures, exceeding 0.5 m, have been measured on outcrops which have surface areas from about 30 m² to 200 m². A description may thus be made for the geometric fracture structure of an outcrop, where the outcrop is considered as a geological unit. This observation scale could be considered mesoscopic. The outcrops concerned have not been stochastically chosen on the island. The choice of outcrops mainly follows the two N- S profiles where the bedrock has been cleared of overburden. The requirement of fractures during a surface cell mapping is about 100-150 fractures per outcrop. The assembly of data on the two rather narrow exploratory profiles implied that there is a relationship between the fracture density and the surface area.

Summarized rosette diagrams show dominating sectors around N 60° W, N 5° W and N60°E. E-W fractures are more scarce but still occur in a narrower, prominent peak, /Figure 3.8/. About 85% of the 4500 mapped fractures are steep, with dips in the range 70°-90°. The relatively few observed inclined fractures with dips in the range 0-65° show predominant strikes around N60°E and dip mainly to the north. The foliation is commonly N60°E - N80°E and implied a fracture frequency increase within this sector.

The apertures were not measured but fractures with widths of millimetres have been noted. The "open fractures" verify the brittle pattern, with a predominant peak at N 55° W. An obvious similarity has been found between the rosette diagrams of the open fractures and the red-stained fractures. Quartz-filled fractures strike N-S and E-W.

In respect of the bedrock type, the longest fractures are found in the porphyritic granite and the shortest ones in the mylonite. The fracture density of the fine-grained granite is significantly higher than that of the porphyritic granite.

The outcrops have been grouped into three classes according to their situation on Äspö island, i.e. the Northern Block, the Äspö shear zone and the Southern Block. The Äspö shear zone has a dominant sector around N60°E. Within the Southern Block the N55°W fractures dominate strongly. The Northern Block is relatively more homogeneous but four conspicuous sectors appear around E-W, N60°W, N5°W and N60°E. The Äspö shear zone has a higher fracture density than the surroundings and the Southern Block is more fractured than the Northern Block.

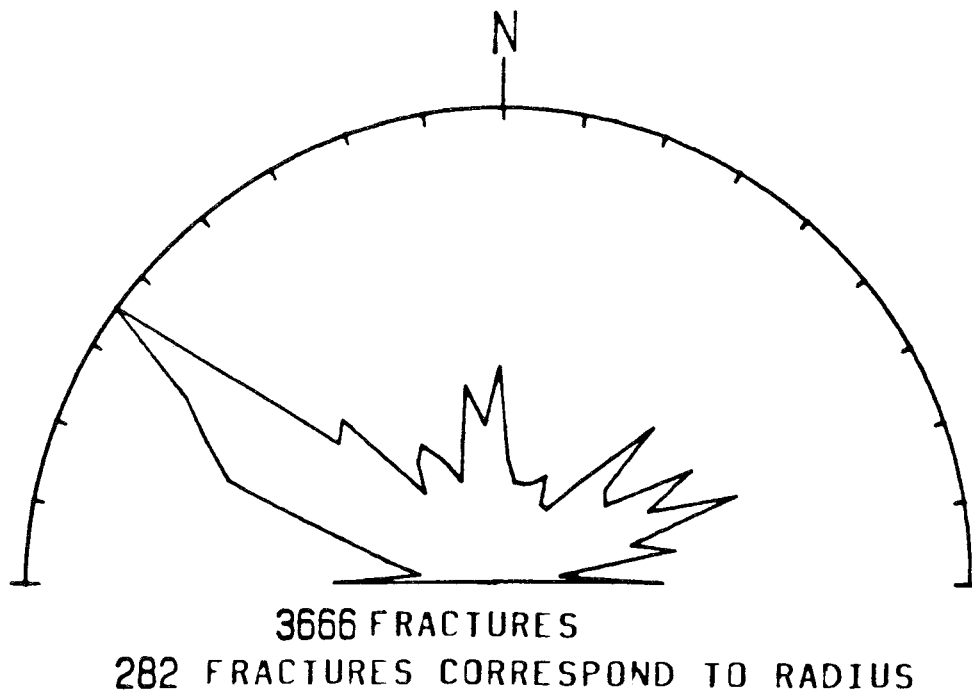


Figure 3.8 Rosette diagram for all mapped outcrop fractures with dips 70°-90° on Äspö island /Ericsson, 1988/.

The rosette diagram for the Äspö shear zone has a main peak which coincides with the direction of the Äspö shear zone. The Southern Block has one dominant peak at N55°W. The Northern Block has a somewhat greater fracture intensity within the sector N40°E - N65°E.

By way of conclusion some mean spacing estimates were made within the four sectors E-W, N45°W, N-S and N45°E, for the tectonic blocks. The spacing results reflect what was earlier mentioned about the fracture lengths and sector frequencies, i.e. the Northern Block is rather homogeneous, with mean spacings around 2.0 m. The fractures in the Äspö shear zone are denser and shorter, with mean spacing from 0.50 m to 1.80 m. The Southern Block seems to be the most heterogeneous, with mean spacings of 0.90 m in the NW direction and up to 2.0 m in the NE direction.

Compared with the previous results of the regional study this analysis shows confident determinations and estimations regarding strikes, dips, lengths and fracture densities. The former conductive fracture mean spacing evaluations of Äspö /Ericsson, 1987/, seem, however, to have been somewhat overestimated because fractures which are crossed by more than two other fractures were neglected.

Development of ductile structures and fracture zones

A NE-ENE trending almost steep, penetrating foliation is the most dominant structural element in the 1700-1880 M-year-old Äspö granitoids and seems to be the oldest sign of the ductile deformation related to the sub-horizontal NNW-SSE compression. This deformation is also marked by the orientation of mafic sheets often backveined by two or three generations of fine-grained granites /Talbot, 1990/.

Intensified strain formed in the amphibolite-facies is marked by gneissic zones trending NE-ENE, dipping to the NNW. Elevated to a higher structural level between 1700-1400 Ma, these old gneissic zones were reactivated as mylonitic NE trending shear-zones especially in central Äspö in a ductile-semiductile deformation phase.

Strong foliation and mylonites are common in the Äspö shear zone - where more than 10-metre-long bodies of mylonite occur trending E-W and dipping steeply to the north. Regional evidence suggests that the E-W trending mylonites are older than those trending NE /Talbot and Munier, 1989/. Small scale mylonitic shear planes less than about one cm wide and up to a few metres long, almost ubiquitous in orientation, are to be found in many parts of the island.

The first brittle faults probably developed in the region in response to the emplacement of younger granites. These faults and older ductile zones were reactivated several times. The rock mass becoming increasingly brittle as it was uplifted and unroofed about 1000 M years ago. Epidotic vein systems became chlorite, zeolite and carbonate filled fractures with time.

Fracture zones on Äspö (Figure 3.9) have a wide range of orientations and styles and most of them reactivate older structures. The style of each fracture zone tends to depend on the nature of any older structure being reactivated, such as EW gneissic zones, NE or E-W trending mylonites and gently dipping alteration zones. Fracture zones trending N, NE or E-W on Äspö normally had ductile precursors whereas those trending NW apparently did not.

Except for the fracture zone which reactivated the NE trending Äspö shear zone, there is no fracture zone of a regional order crossing the island. Geophysically indicated fracture zones trending ENE and NE border Äspö to the north and south. Fracture zones of a more local order - outside the Äspö shear zone - are most prominent in an E-W direction. Narrow fracture zones trending approximately N-S and NNW are common.

A number of gently dipping fracture zones, trending ENE, intersect the surface of Äspö /Talbot, 1989/. Their dips are presumed to be gentle between 10-40° to the NNW. It has been found, however, to be difficult to identify these zones unambiguously in the sub-vertical boreholes.

Gently SW dipping thrusts like those described by Nordenskjöld /1944/ and Palmquist /1988/ from the inland area west of Simpevarp have not been clearly indicated on the surface of the Äspö area, but probably some kind of narrow, gently SW dipping (clay altered) fracture zones occur underground in the Äspö-Hälö area.

The fracture sets described earlier /Ericsson, 1988/ are, with some exceptions, also present in the fracture sets of the zones. The difference between the sets in the surrounding region and those in the zones is that individual fractures in the region have different functions in the different zones /Munier, 1989/.

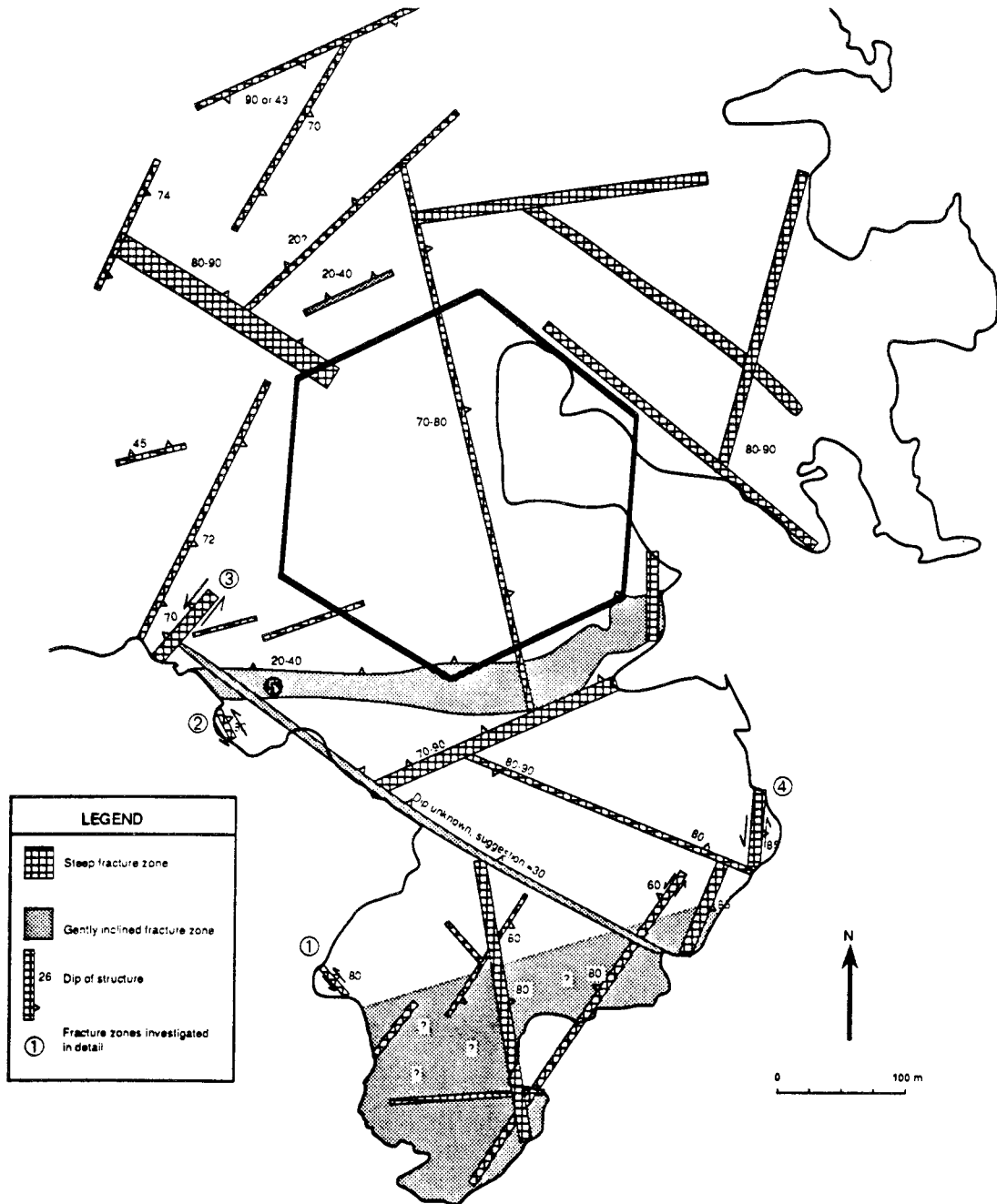


Figure 3.9 Interpretation of fracture zones on southern Äspö /Talbot and Munier, 1989/.

Lineament study

Structural analysis of terrain features on Äspö has been performed as a complement to an earlier regional study of lineaments in the Simpevarp area. The study is based on topographical maps (scale 1:4 000), with 0.5 m contour interval. The pattern of lineaments on the island is analogous to the regional pattern on the adjacent mainland, (scale 1:50 000), presented by Tirén et al /1987/.

According to Tirén and Beckholmen /1987/, Äspö is situated within a triangular block, which is transected by three regional discontinuities. In the middle of Äspö an E-W and a NE trending discontinuity intersect, splitting Äspö into four rock blocks. The third discontinuity trends N80°E and runs along the northern part of the island. This discontinuity is a shear zone. The orientations of the most frequent directions of lineaments on Äspö are N5°W, N45°W and N80°E. The southern part of Äspö appears to be the least deformed part.

In the regional interpretation of lineaments, based on digital terrain models, only structures on land were considered. The regional study pointed out that most expressed lineaments on Äspö island trend E-W and ENE. These lineaments are in agreement with the local interpretation. According to the regional study a sharp and narrow N-S trending lineament crosses Äspö. This lineament is not identified as a lineament in the local study but can be traced as a zone of low blocks.

Talbot et al /1988/ report a very high correlation between the topographic lineaments and structures on the ground but also point out their inability to identify the nature of the structures (mylonites, fracture zones, veins, etc.) and the general inability to recognize gently dipping structures in an area of such low relief, as on Äspö.

Detailed geomagnetic and geoelectric mapping of Äspö

As a part of the investigation of the structural pattern of Äspö detailed ground magnetic and electric mapping were carried out /Nisca and Triumf, 1989/.

Magnetic measurements were made every fifth metre along profiles in an east-west direction, with profiles at 10 metre centres in the geomagnetic survey and at 40 metre centres in the geoelectric survey.

Different geometrical arrangements of currents and potential electrodes can be used in geoelectrical mapping. In order to effectively map relatively narrow zones (2 m thick), and low-resistivity zones near the surface, a 5-10-5 metre dipole-dipole configuration was used /Barmen and Stanfors, 1988/.

A combined analysis of geomagnetic and geoelectric data has been performed, especially with respect to fracture zone delineation.

Fracture zones are probably encountered in areas where the bedrock is covered with till, sediments and organic material. An interaction between apparent resistivity anomalies caused by the relatively low-resistivity overburden and water or clay-filled fracture zones could then be expected. By using complementary information provided by magnetic data, it is possible to make a meaningful connection between low-resistivity zones in different profiles, in spite of the large distance between profiles. Magnetic data also provided information important for the extraction of

overburden induced anomalies from anomalies induced by fracture zones.

Figure 3.10 is a general map of the fracture/fracture zones filled with water and/or clay which were delineated by combining geoelectric and geomagnetic data.

It is evident from Figure 3.10 that low-resistivity zones differ somewhat in length and orientation within the central Äspö shear zone in comparison with the Northern and Southern blocks. Low-resistivity zones are more common in the shear zone and the mean length of low-resistivity zones is slightly larger than elsewhere in the area.

In addition to the low-resistivity zones connecting profiles, several low-resistivity cross-overs are marked along the profiles, Figure 3.10. Some of them are probably caused by overburden effects, but it is also probable that some of them are due to the presence of fractures not indicated by the geomagnetic survey.

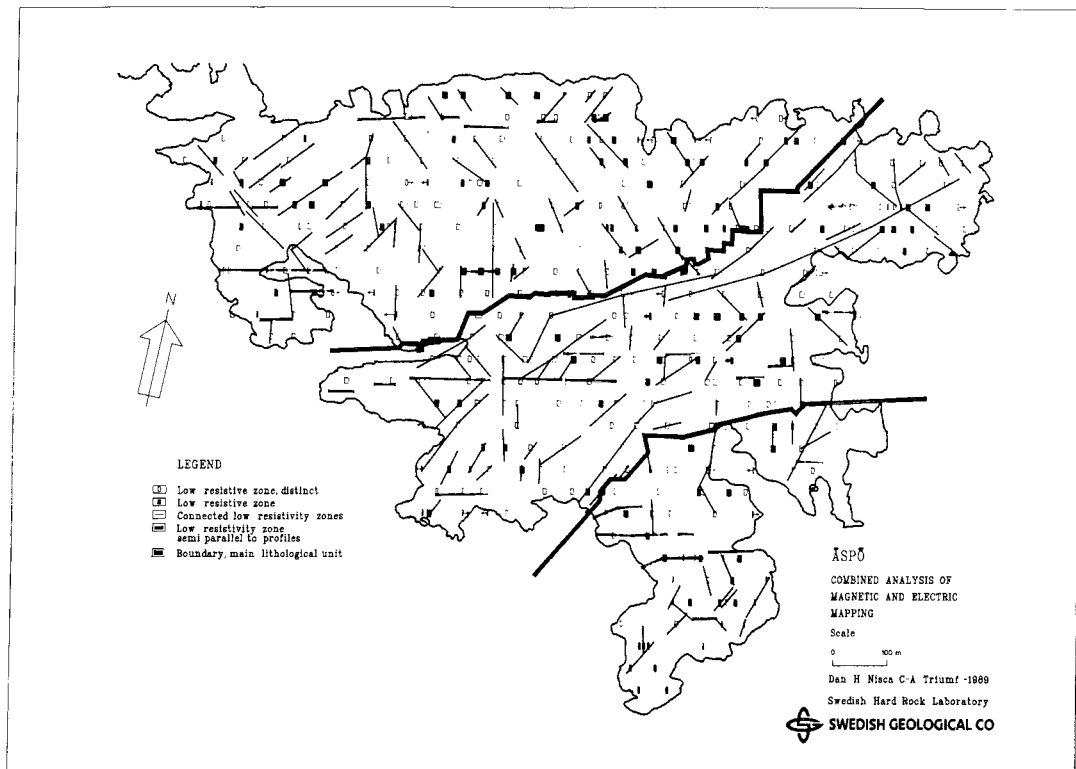


Figure 3.10 Combined analysis of geomagnetic and geoelectric mapping. /Nisca and Triumf, 1989/.

It is obvious that a similar principal trend, with two orthogonal sets of fractures, as presented for the magnetic data, can be found. This is not surprising as magnetic data largely controlled the connection of low-resistivity zones between the profiles.

The orthogonal fracture set N-S/E-W is almost consistent in all the three sub-areas, the Northern Block, the Äspö shear zone and the Southern Block. The directions of the

second orthogonal fracture set, however, vary from area to area. The fractures in the Northern Block and the Äspö shear zone run in similar directions, though the directions of fractures within the shear zone are more scattered around N35°E. In the Southern Block, however, a shift is obvious in the dominating angle to about N15°E for the same fracture set. Furthermore, the concentration of fracture directions around N55°W, recognizable in the Northern Block and the shear zone, is lacking.

As a complement to the magnetic and resistivity investigations, VLF measurements were also performed along N-S profiles on Äspö and Hälö. A number of presumed fracture zones seem to have been successfully detected by a combination of magnetic, VLF and electric resistivity measurements. However, disturbances, especially from electric cables and saline sea-water, constituted an important obstacle to VLF and other electrical methods.

To check the correlation between the ground geophysical indications (magnetic and resistivity) and structures seen on the ground, a systematic investigation was performed along the trenches /Talbot et al, 1989/. A very good correlation (more than 80%) was found especially between magnetic indications and different geological structures. However, it is interesting to note that only about 25% of the correlated structures were fracture zones and that as many as 15% apparently corresponded to "single fractures". Most of the EW magnetic lineaments turned out to be fracture zones, the NE lineaments to be mylonites, and the N-S structures, to be single fractures.

The correlation between magnetic indications and "single fractures" is in very good agreement with the results presented by Barmen and Dahlin /1989/ from a very detailed ground susceptibility study along the cleaned trench on southern Äspö. They found increased susceptibility values up to some metres wide in red stained zones close to these fractures, probably due to oxidation of the magnetite in the bedrock.

Seismic refraction

As a complement to the electric and magnetic measurements, which were partly severely disturbed by man-made installations and saline water, seismic refraction has been used to locate and characterize fracture zones on Äspö /Sundin, 1988/.

A 22-channel seismic instrument of SEMAB type was used in these investigations and the signals were generated by explosives.

When surveying in the sea the distance between geophones was 5 m and between shot points 25 m. The geophones and charges were pressed down through the uppermost layer of organic soil to firmer layers using a special tool.

The investigations on Äspö were performed with geophones at 2.5-m centres and shot points at about 12.5-m centres. For the other profiles on land, the corresponding distances were 5 and about 30 m, respectively.

In some profiles, in the sea area, records were also taken far from shot points (300-400 m) in order to find out if the bedrock velocity increased with depth and, if possible, to obtain some indications of the dip of the structures. These results, when compared with the velocities from the standard investigation, indicate that the low-velocity zones are more or less vertical and that the velocity in the surrounding rock

increases with depth.

Especially important were the results from seismic profiling in the sea areas along the Äspö-Hälö access tunnel, where we have no results from electric measurements. Along these profiles a number of low-velocity zones were recorded, indicating fracture zones /Rydström et al, 1989/. These indications are in good agreement with low-magnetic data recorded from proton magnetometer measurements made on water from a plastic rowing boat in this area /Triumpf et al, 1989/.

The seismic refraction profiles on Äspö were performed mainly to check topographic and geophysical lineaments indicating possible fracture zones. The thickness of the overburden along these profiles is nowhere calculated to exceed 10 m and a number of pronounced - mostly only some metres wide - low velocity zones (2000-3500 m/s) were recorded. These indications correspond in most cases very well to other indications of narrow fracture zones. The seismic velocity in the bedrock surrounding the presumed fracture zones is between 5000-6000 m/s, indicating sound crystalline rock with a fracture frequency which is low-normal.

Seismic reflection

The main aim of using seismic reflection was to test the ability of this method in mapping especially low-dipping fracture zones in crystalline bedrock. The target area was from as near the surface as possible down to approximately 1500 metres. Two seismic profiles were recorded across Äspö island. One NW-SE line (01) passes the cored boreholes KAS 02, KAS 03 and KAS 04 - another one (02), approximately perpendicular to the first, passes close to KAS 03 /Plough and Klitten, 1989/, Figure 3.11.

The investigation identified two sub-horizontal "zones" situated at depths of from 300 to 500 metres and 950 to 1150 metres along both profiles and characterized by several rather short and irregular reflectors. However, two rather planar and strong reflectors were identified in the deeper zone of 02 and are approximately 300 metres long. The same reflectors, but shorter and more irregular, were in a similar way identified in 01. Both these "zones" are probably reflecting a system of more or less interconnected and irregular heterogeneities in a fractured and weathered rock mass /Figure 3.15/.

Based on the much higher intensity of events in the deeper zone than in the upper one, the deeper zone must be expected to contain many more heterogeneities and to be a more strongly tectonically affected and coherent zone than the upper one. In general such large, sub-horizontal tectonically affected zones cannot be expected to constitute well defined planar, regular and widespread reflector horizons as are typical of layer boundaries in sedimentary rock sequences. Instead, they will occur as more or less planar zones with varying contrast in the physical conditions along very irregular boundaries and constitute a very inhomogeneous, fractured and weathered rock mass.

The seismic reflectors can only to some extent be correlated to zones with increased frequency of low-dipping fractures in drill cores. The correlation seems to be most relevant for the reflectors at greater depths /Juhlin, 1990/.

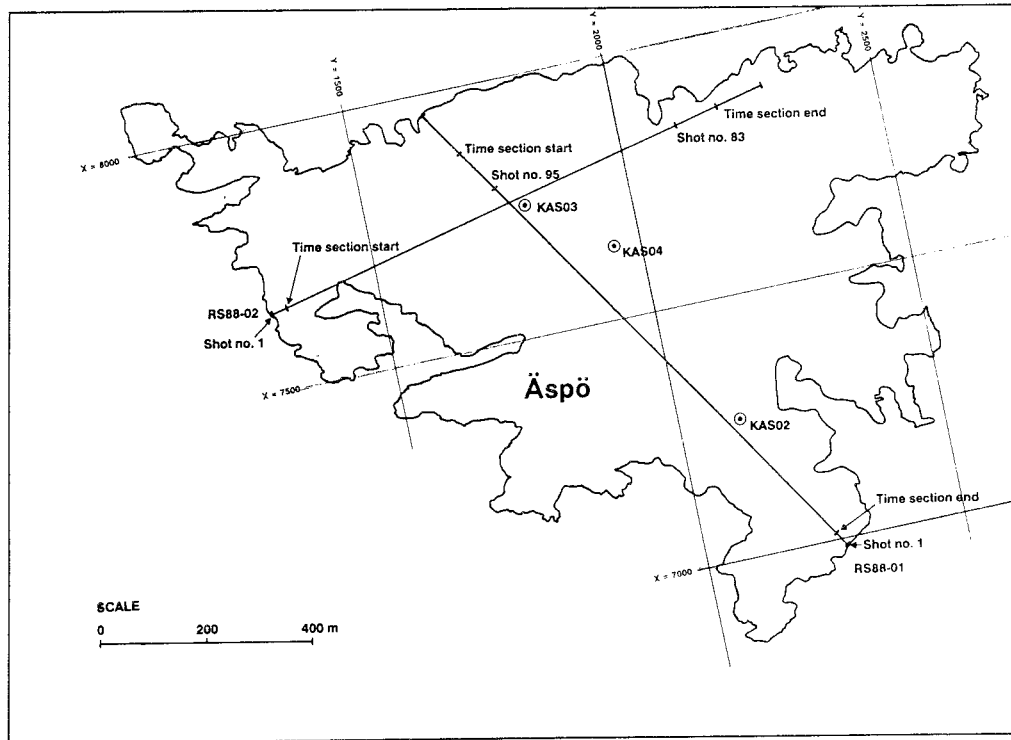


Figure 3.11 Reflection seismics location map / Plough and Klitten, 1989/.

Ground radar investigation

The objectives of the surface radar project were to make a study of the RAMAC borehole radar system operating as a ground probing radar system and to test its ability to locate reflections, especially from low-dipping fracture zones at the southern part of Äspö /Sandberg et al, 1989/.

The ground surface radar measurements at the southern part of the Äspö site comprised reflection measurements with a centre frequency of 60 MHz. These profiles, P27-P34, P35-P47 and P51-P59, were measured using measurement points at 0.5 m centres. The radar range obtained was approximately 20 m and the estimated speed 133 m/ μ s in the rock.

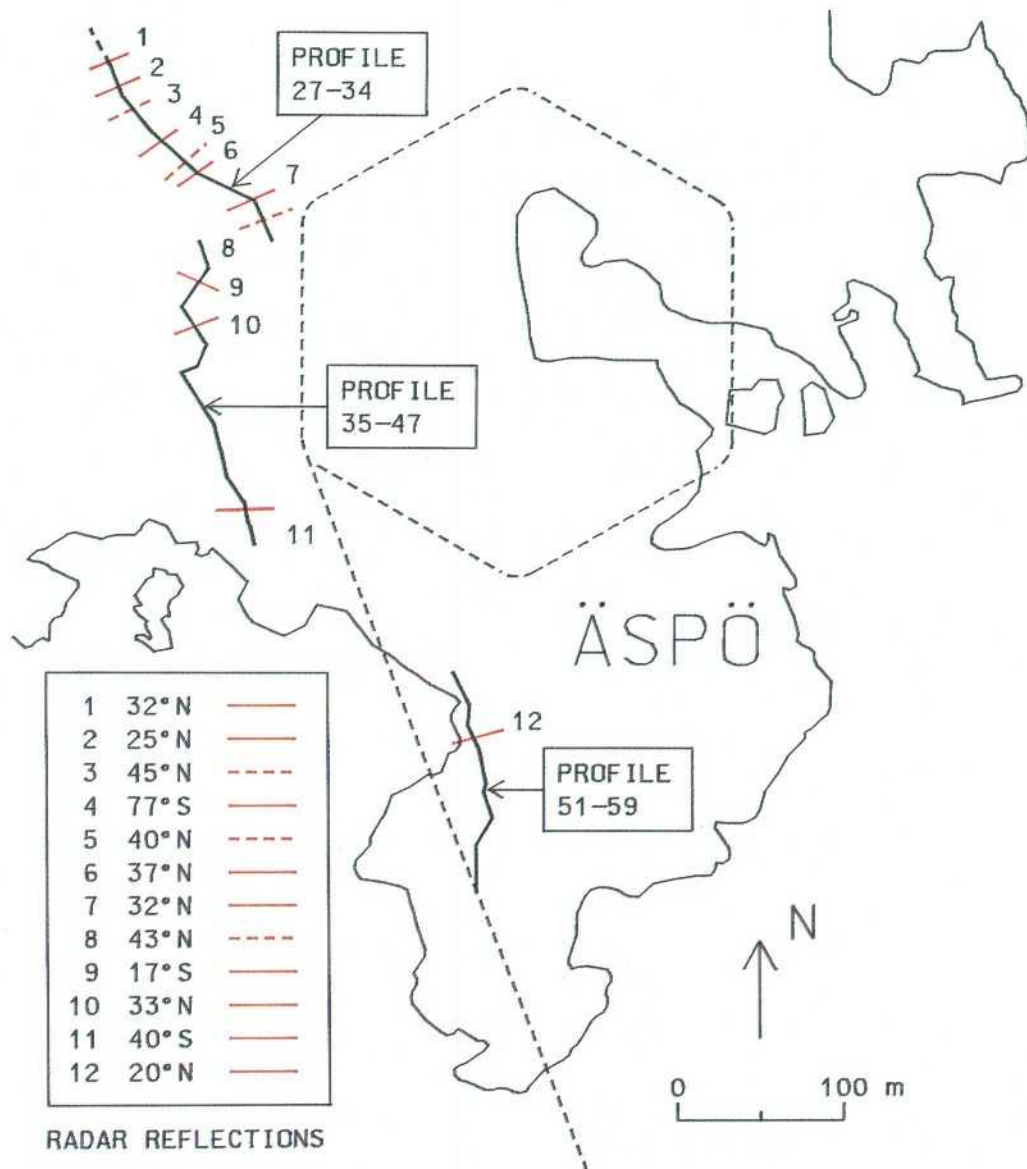


Figure 3.12 Location of profiles P27-P34, P35-P47 and P51-P59 on the southern part of Äspö /Sandberg et al, 1989/.

The three measured profiles, P27-P34, P35-P47 and P51-P59, Figure 3.12, were all striking N-S. There was no overburden along the profiles which resulted in excellent conditions for ground probing radar measurements.

The measurements revealed several interesting reflections, probably from fractures and contact surfaces between different rock types. 12 more or less prominent reflections are reported from the three profiles - 8 of them from the northern profile. For 9 of these reflectors an apparent dip of less than 45° to the north were recorded. Two of the reflectors have low dips to the south.

It should also be noted that in order to get the true dip of reflections from fracture zones which are not perpendicular to the profiles, the strike of the fracture zones must be known before the true dip of the fracture zone can be determined. As pointed out previously, the polarization of the transmitted radar waves is perpendicular to the measured profile. The strike of the fracture zones at the Äspö site was, however, not used in the interpretation of the results in this report.

Some of the reflections have been analyzed to see how well they correlate with reflections identified in the borehole radar measurements from KAS 02, KAS 04, KAS 05, KAS 06, KAS 07 and KAS 08. These results are discussed later in this report.

Drilling campaigns

The detailed lithological and structural mapping performed along the well-exposed trenches and ground geophysical measurements contributed to a better understanding of the two-dimensional geological model of Äspö. To improve this model, to a three-dimensional lithological and structural model, a comprehensive drilling programme was performed.

In the first core drilling campaign two cored boreholes were drilled sub-vertically to a depth of approximately 1000 m in the southern part (KAS 02) and the northern part (KAS 03) of Äspö. The main aim of a third borehole (KAS 04) - inclined 60°SE - was to cross the geophysically and geologically indicated shear zone trending NE in central Äspö.

Småland granite is the most common rock type in all the cores except KAS 02, where Äspö diorite is by far the most common from about 315 m to the bottom of the hole. Fine-grained granite is represented in dikes and veins in the three cores but is much more common (approximately 30% of the core length) in KAS 03 and KAS 04 than in KAS 02 (only 15%). Dark fine-grained greenstone occurs as some metre-wide remnants - often strongly altered - in the younger granitic and dioritic rocks. The greenstone constitutes 4% of the total core length in all the boreholes /Figure 3.17/.

The foliation of the rocks in the cores varies in intensity from scarcely detectable to very strong mylonitic. It is generally more intense close to mylonites. Mylonite was observed, especially in KAS 04 at 170-182 m and 214-217 m. In KAS 02 mylonitic zones occur at the depths 455-485 m and 550-570 m, both associated with 1-2 m wide crushed zones. In KAS 03 approximately 1 m wide mylonites are intersected at the depths 397, 403, 865 and 920 m. These zones correspond to increased fracturing. The dips of the mylonites in relation to the core axis are mostly about 60-70° /Riad and Munier, 1988/. It seems to be possible to correlate some of the mylonite zones in KAS 04 and KAS 02 to mylonite outcrops in the Äspö shear zone.

The fracture frequency is generally higher in KAS 03 than in KAS 02 down to a depth of approximately 750 m. Below this level the core in KAS 02 is highly fractured. In KAS 04 the whole core shows signs of strong mechanical deformation.

Calcite and chlorite are the most frequent fracture minerals throughout all cores. Hematite and epidote are concentrated to distinct zones. There seems to be some agreement between the open fractures detected in the geophysical logging and the frequency of Fe-oxyhydroxide and hematite /Tullborg in Munier et al, 1988/.

Sections with increased fracturing and crushed zones (normally only 1-2 m wide) are more or less evenly distributed throughout the three boreholes - but are most frequent in KAS 04 and KAS 02 and least in KAS 03. Core losses were very rare and more complete alteration is normally noticed only in the greenstones. Fine-grained granite appears to be more brittle and more highly fractured than the Småland granite and Äspö diorite. Main fracture zones occur in KAS 02 at approximately 300-700 m and below approximately 800 m, in KAS 03 at approximately 300-350 m and approximately 725-750 m, and in KAS 04 at approximately 325-450 m.

To sum up, it can be said that the first borehole campaign corroborates the first simple two-dimensional model of Äspö island divided into two main blocks by a NE-trending tectonic zone of a regional order, Figure 3.13. In both these blocks Småland granite with veins and xenoliths of greenstone and dikes and irregular masses of fine-grained granite dominate but from about the 300 m level and downwards especially in the Southern Block, the Småland granite is of more basic varieties (Äspö diorite).

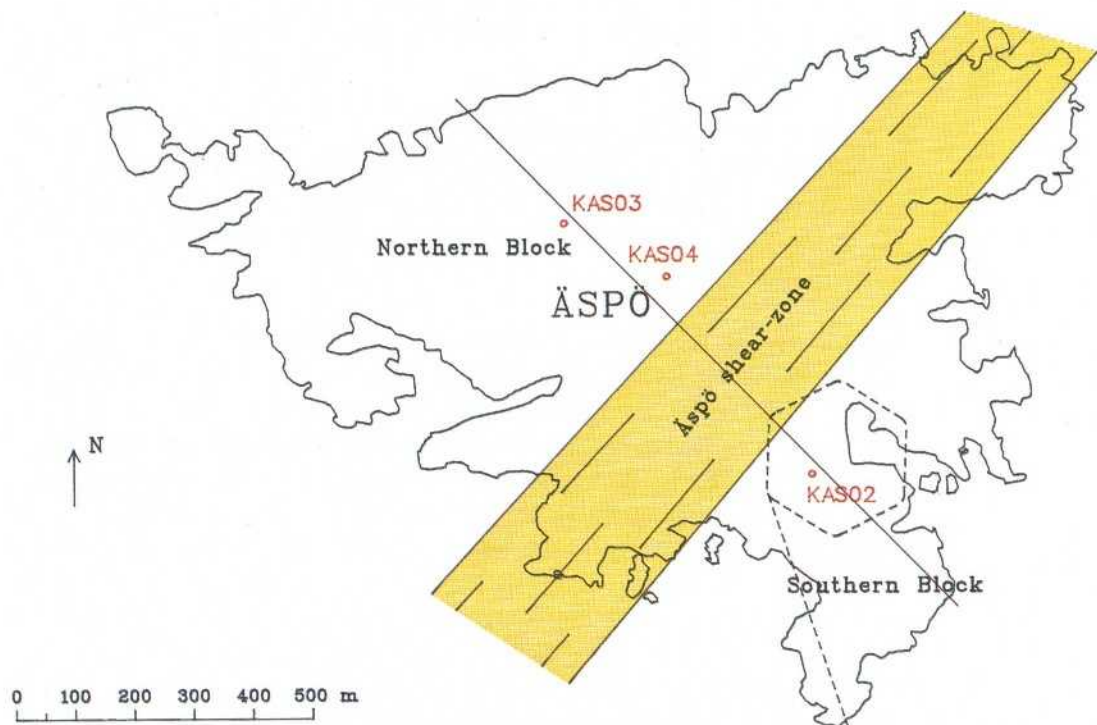


Figure 3.13 Generalized geological - tectonic model of the island of Äspö based on the first deep drilling campaign.

The central NE-trending Äspö shear zone comprises strongly foliated inhomogeneous Småland granite, with a large number of mylonite lenses and xenoliths of greenstone, seems to be almost vertical or steeply dipping to the north. The zone is very complex, comprising 5-10-metre wide highly fractured parts alternating with more normally fractured rock. Characteristic of the entire Äspö shear zone is the oxidation of magnetite in the granitic rocks.

The two sub-horizontal "zones" identified at the depths 300-500 m and 950-1150 m by seismic reflection measurements can only to some extent be correlated to highly fractured sections or rock contacts in the two boreholes, KAS 02 and KAS 03, (Figure 3.14).

b. Generalized interpretation

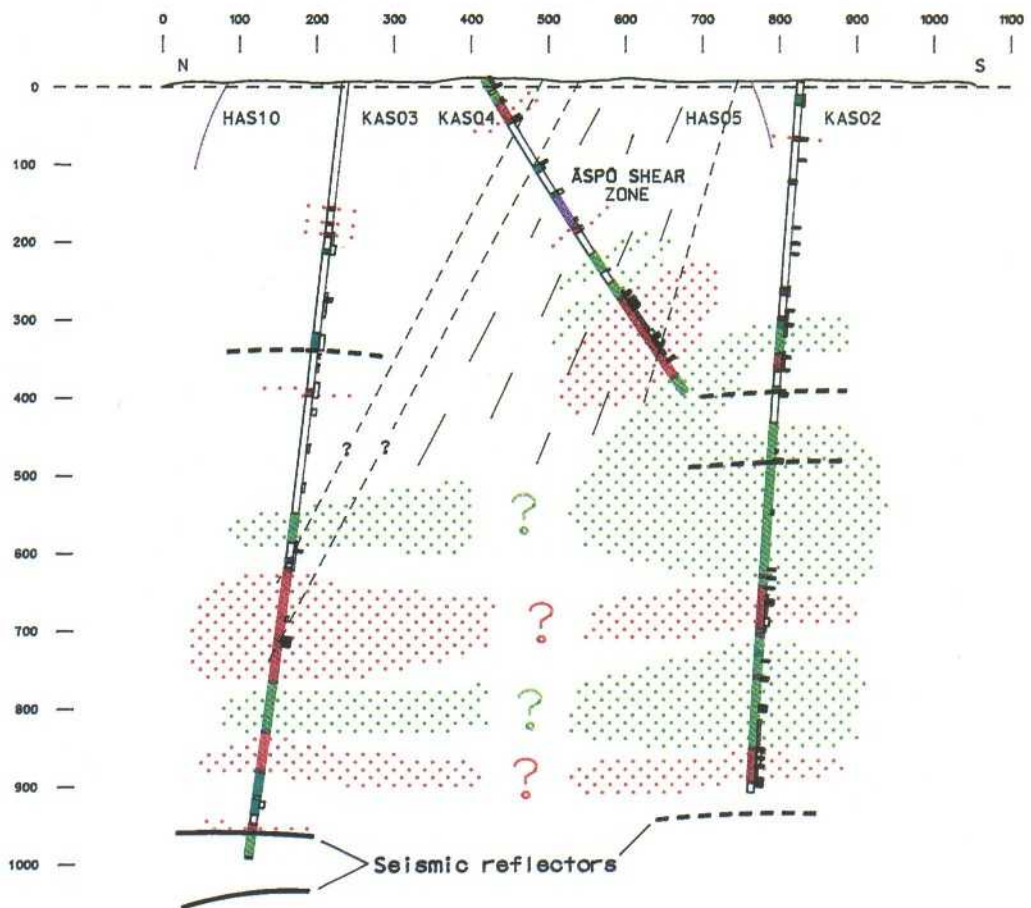


Figure 3.14 Section across Äspö island, see Figure 3.13. Generalized geological-tectonical model, based on the first drilling campaign.

According to surface investigation results and borehole data the rock mass in the southern part of Äspö was estimated to be less fractured than the northern part. The hydraulic conductivity, especially in the more basic rock types at depth in the southern block, was also found to be low.

Based on the investigation results mentioned above the second drilling campaign was concentrated to the southern part of Äspö. The object of this campaign was to make a characterization of the vertical and lateral distribution of lithological and structural units within the possible site area. The second drilling programme comprised 4 cored boreholes (KAS 05-08) and 4 percussion holes (HAS 13-17), later complemented with 7 cored boreholes (KAS 09-14 and KBH 02) and three percussion boreholes (HAS 18-20), Figure 3.15.

Continuous analyses based on surface investigations, combined with borehole data, provided the information for preparation of the structural model presented in Figure 3.16.

Cored borehole KAS 05, see Figure 3.18, confirmed the existence of the Äspö diorite at a depth below about 300 m. Increased fracturing in the section at about 100-115 m may possibly indicate the low-dipping fracture zone EW-5.

A highly fractured and partly clay altered section at 60-72 m in KAS 06 confirmed the orientation and character of fracture zone EW-3. Borehole radar and VSP indications confirmed the almost vertical dip of this zone which is also clearly indicated in KAS 07 (425-430 m). A highly fractured and mylonitic section between 40-60 m in KAS 08 seems to be a good indication of fracture zone NE-2. Increased fracturing between 20-80 m in HAS 16 as well as the mylonitized section at about 260-300 m in KAS 12 also corroborates the presumed extent of this zone which was also indicated by borehole radar.

Cored boreholes KAS 09, KAS 11 and KAS 14 were mainly sited to investigate the surface indication of fracture zones EW-5 and NE-1 bordering on Äspö to the south. In all these boreholes NE-1 is very well indicated (increased fracturing, clay alteration). Borehole radar and VSP results also confirm the extent and moderate NW dip of NE-1, which have been found to be very hydraulically conductive. Concerning EW-5 there are possible but no unambiguous indications in these boreholes, (Figure 3.19).

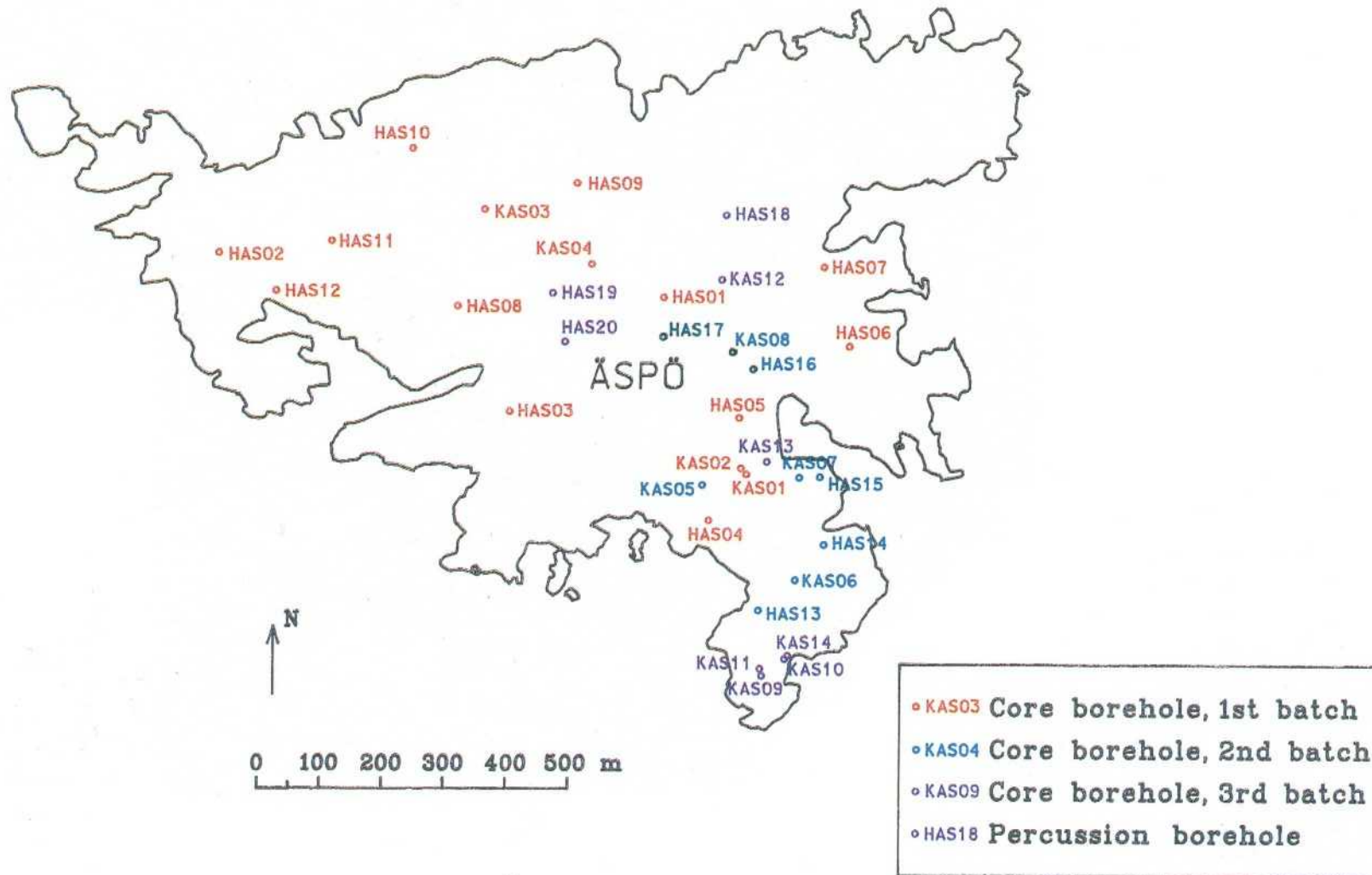


Figure 3.15 Location map of boreholes on Äspö

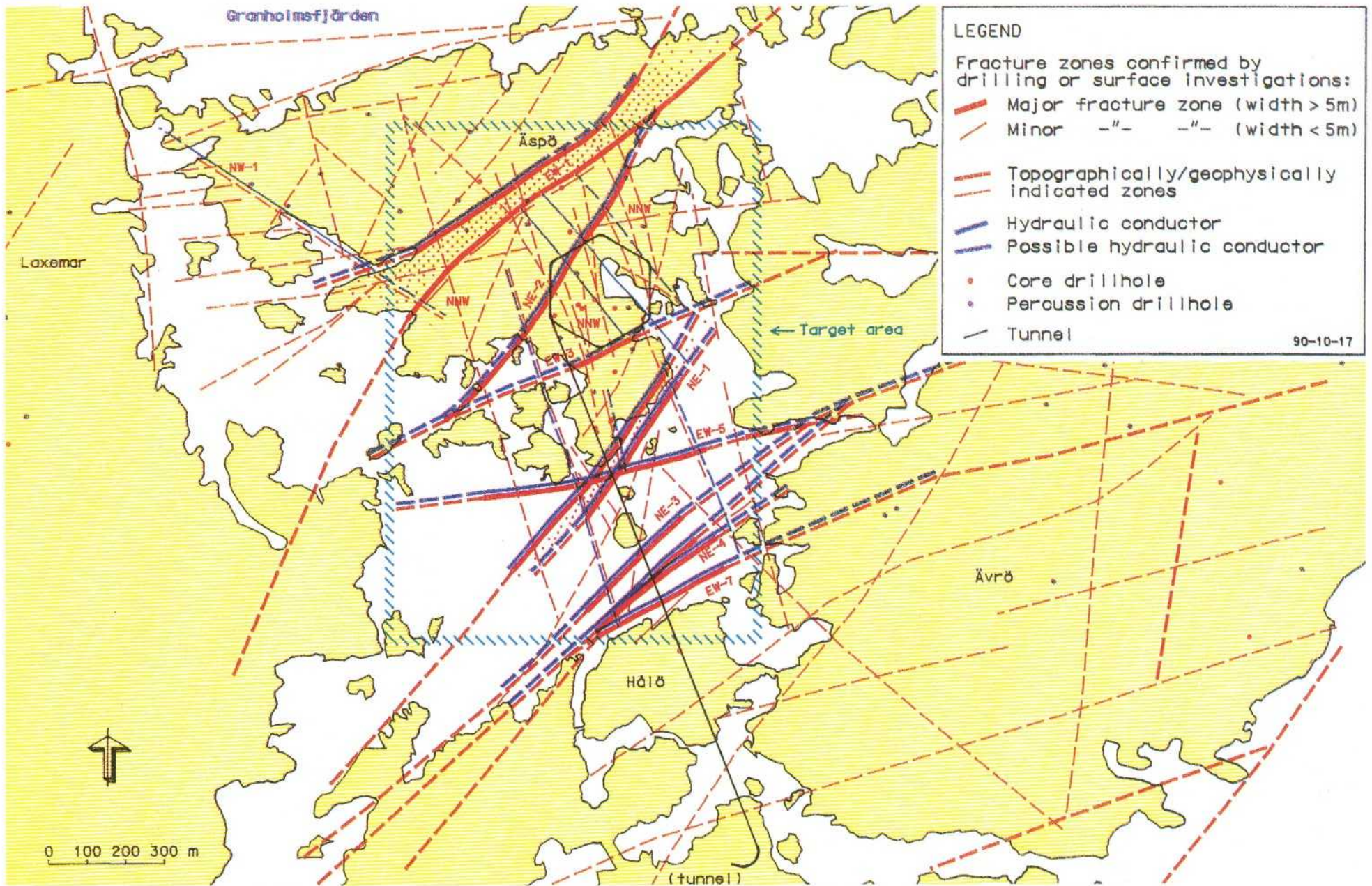


Figure 3.16 Fracture zone interpretation

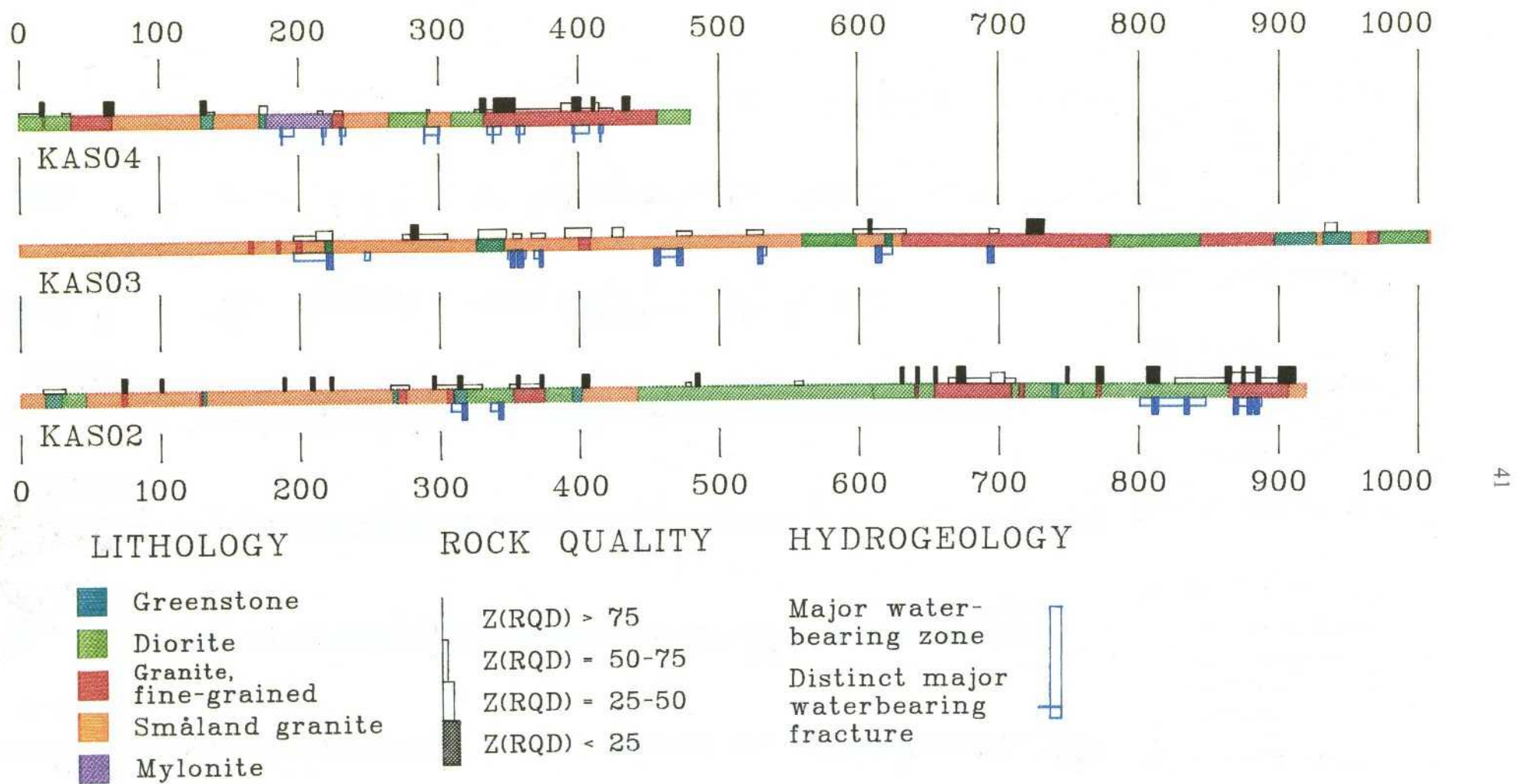


Figure 3.17 Äspö Hard Rock Laboratory core borehole description

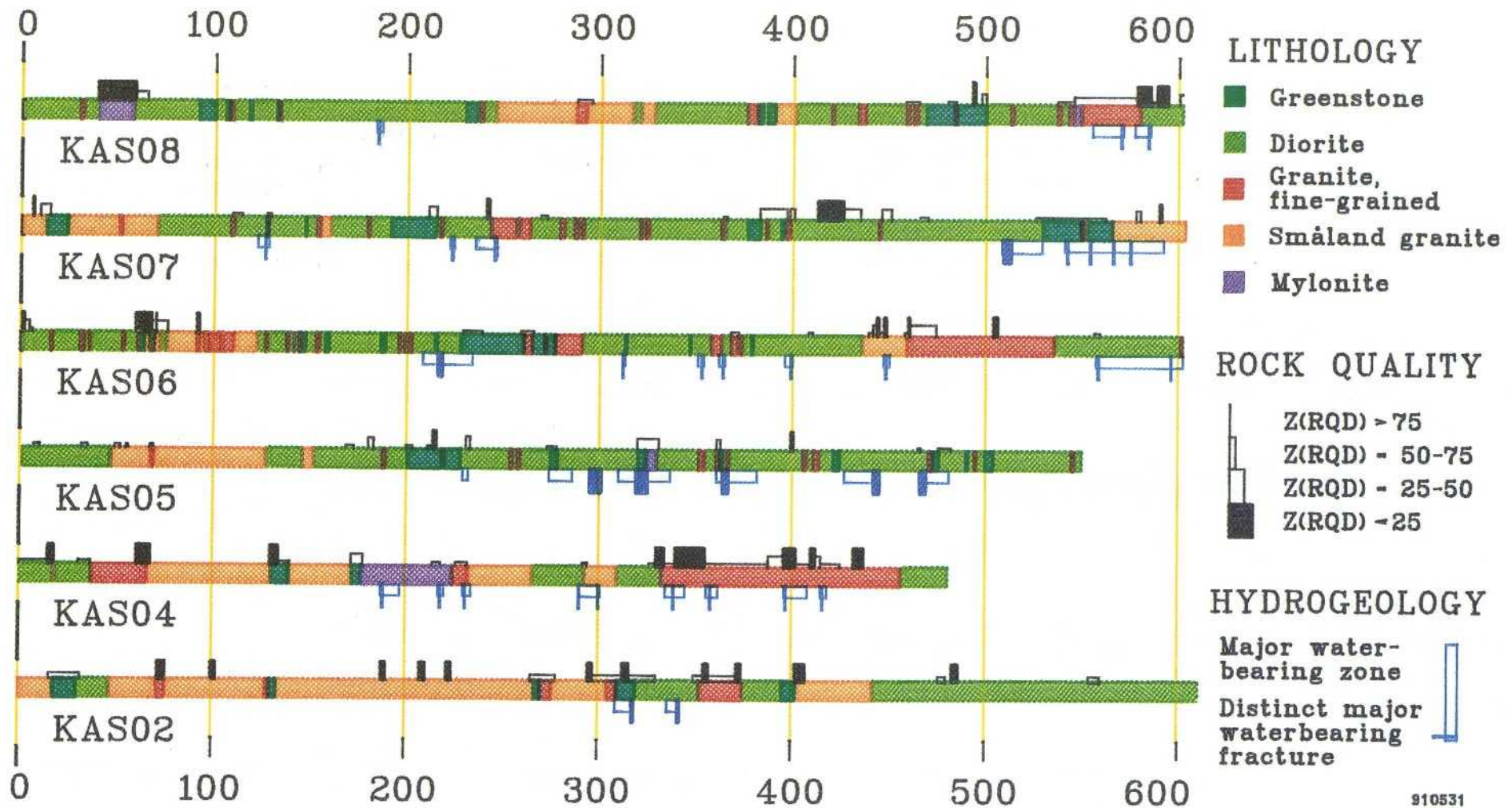


Figure 3.18 Äspö Hard Rock Laboratory. Core borehole description.

910531

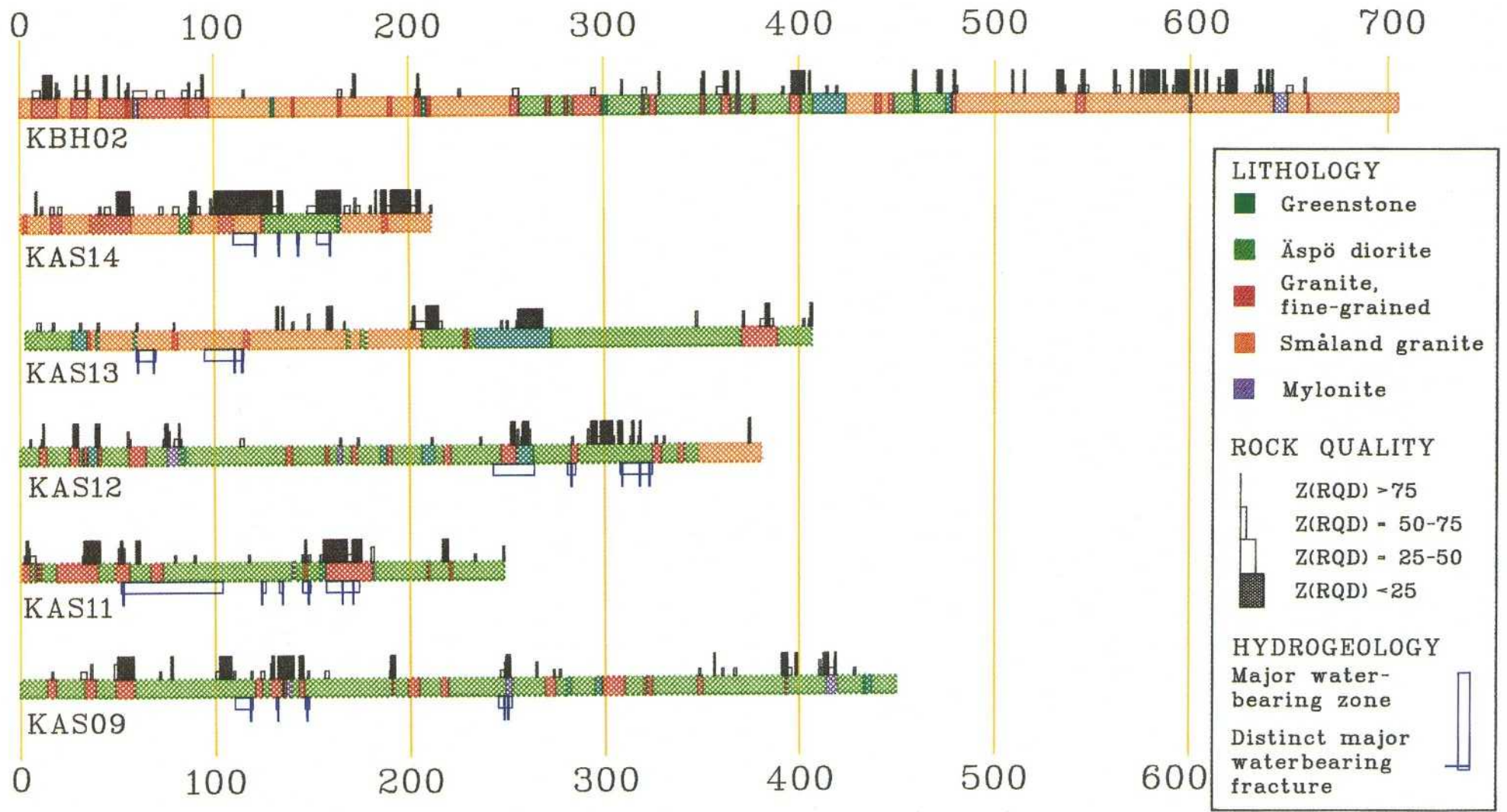


Figure 3.19 Äspö Hard Rock Laboratory. Core borehole description

Cored borehole KAS 13 provided very important complementary information in the E-W direction of the site area. Metre-wide highly fractured sections in the core confirmed the proposed set of narrow fracture zones trending almost N-S in the southern part of Äspö called NNW. VSP and borehole radar reflectors indicate the steep dip of these zones.

Cored borehole KBH 02 was inclined about 80° from the vertical and is almost parallel to the planned tunnel from Hälö to Äspö. Fractured sections especially at about 200-300 m, confirmed the existence of the proposed regional fracture zones NE-3 and NE-4 trending approximately ENE in the strait to the north of Hälö. Highly fractured sections at about 600-700m in the borehole can be correlated to fracture zone NE-1. Core mapping results from KBH 02 contribute very well to the possibility of good characterization of the rock mass in the Hälö - Äspö tunnel area.

The three percussion boreholes, HAS 18, HAS 19 and HAS 20, confirmed the interpretation of EW-1 as a wide complex zone built up by elements trending E-W and NE, with very different characters concerning rock quality, alteration and hydraulic conductivity. In cored borehole KAS 12 increased fracturing in the upper 50 metres confirms the idea of a somewhat wider extension of EW-1 to the south.

The integrated results from interpretation of geological core mapping and geophysical borehole logging greatly improved our knowledge of the lithological contribution in southern Äspö.

One of the main difficulties was to find a simple way to make a rock type classification, especially in order to distinguish between the Småland granite and the Äspö diorite. It was found that the density log ($\gamma\text{-}\gamma$) gave the best results. The granite/diorite density limit was set at about 2650 kg/m³. However, one should note that "diorite" here probably ranges from granodiorite to diorite (density range 2650-2650 kg/m³). As can be seen from Figure 3.20 the dominating rock type in the site area is Småland granite and granodiorite-diorite.

Normally, there is no distinct contact between the different varieties of the granitic-dioritic rocks which gradually melt into each other. Fine-grained granite is very common in the whole rock mass, mostly in the form of narrow dikes and veins, but also as bigger irregular masses, especially at the level between about 300 and 450 m (KAS 03 and KAS 06) and at the level below about 750 m in KAS 02. Dark, fine-grained greenstone occurs as some metre-wide lenses and xenoliths - often highly fractured and altered. Wider sections of a more coarse-grained gabbroid rock were recorded especially in boreholes KAS 05 and KAS 13. Mylonite was mainly observed in KAS 04, KAS 08 and KAS 05.

Summarizing, it can be said that lithologically the rock mass in the southern Äspö-Hälö area is very inhomogenous and it seems to be difficult to distinguish the extent of the different rock types more accurately.

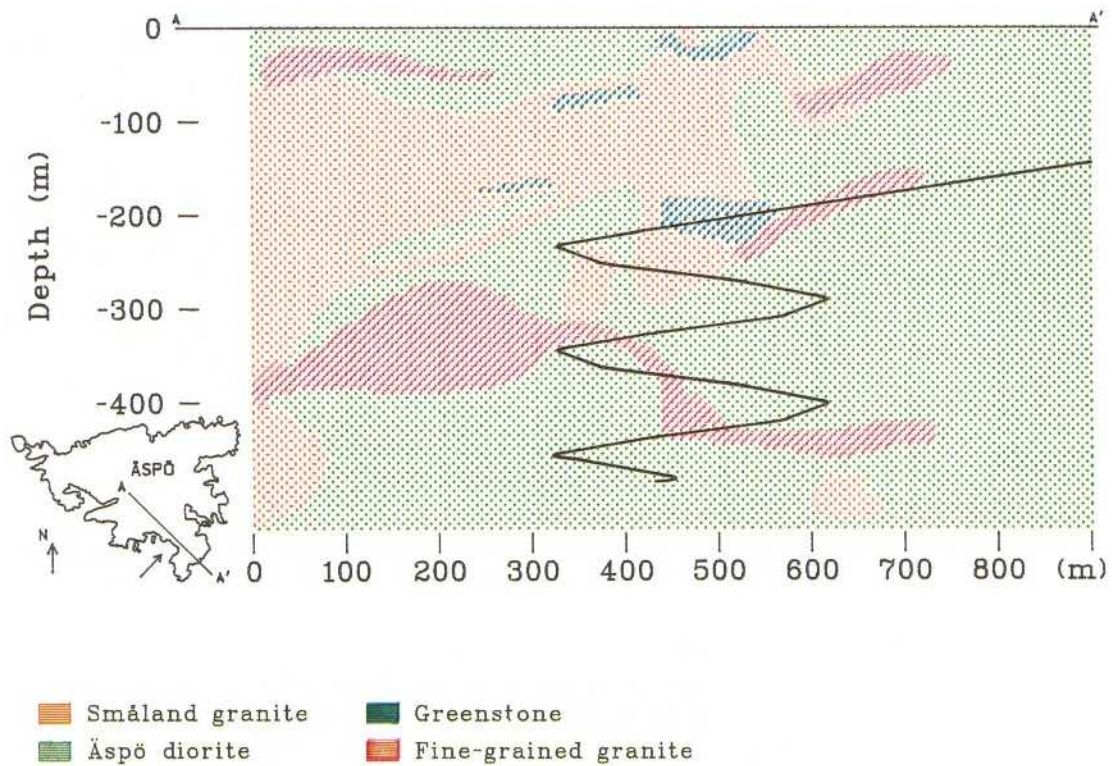


Figure 3.20 Lithological model of southern Äspö

Borehole investigations

During the pre-investigations a drilling programme was executed at different stages comprising 20 percussion boreholes and 14 cored boreholes in the Äspö area. In addition a large number of boreholes - mostly percussion boreholes - were also sited in the surrounding area (Laxemar-Ävrö).

The aim of the boreholes was to obtain basic information on the bedrock composition, orientation and characteristics of the major fracture zones and the hydraulic properties of the rock mass at increasing depth.

When drilling was finished a great number of different investigation methods were used in the boreholes and the drill cores were mapped and investigated in great detail.

The geophysical logging programme carried out in the boreholes generally comprised most of the following logging methods:

- gamma-gamma
- neutron (cored boreholes only)
- borehole deviation
- caliper (cored boreholes only)
- sonic
- natural gamma
- single-point resistance
- self-potential (SP)
- magnetic susceptibility
- normal resistivity (1.6 m)
- lateral resistivity (1.6-0.1 m)
- temperature
- borehole fluid resistivity
- radar measurements

The gradient of the temperature and the equivalent content of sodium chloride were calculated using the temperature and borehole fluid resistivity methods.

The aim of the interpretation was to describe the geophysical logging data in terms of lithology, fracturing and hydrogeology. The logging methods applied make their specific contributions to the different subjects above, the amount varying with the physical property measured /Sehlstedt and Triumph, 1988/.

A combination of the density (gamma-gamma) and magnetic susceptibility logs were preferred for the rock type classification.

The sonic logging, single point resistance, normal resistivity, caliper and self-potential methods were mainly used for delineation and classification of fracturing in core borehole walls.

Observations of water movements and temperature signatures in boreholes were obtained mainly from temperature measurements and borehole fluid-resistivity logs. Water transport in a borehole is common and occurs when the borehole serves as a connection between water-bearing fractures/fracture zones with different hydraulic heads.

Borehole radar measurements were made in all the cored boreholes and some of the percussion boreholes using the RAMAC system. The radar measurements were performed as single-hole measurements in all boreholes except KAS 12, KAS 13 and KAS 14, using omni-directional dipole antennas with a 22 MHz frequency. Measurements with directional radar antenna were made as single-hole measurements in boreholes KAS 12, KAS 13 and KAS 14 using antennas with a 60 MHz frequency. Borehole KAS 11 was measured with directional antenna using a 60 MHz frequency, but only the dipole component was used for the interpretation, due to technical reasons. The radar range obtained in the single-hole reflection mode reaches 60 metres in a borehole /Niva and Gabriel, 1988; Carlsten, 1989, 1990/. A number of prominent structures were indicated in the boreholes using the directional antenna and dipole antenna radar measurements, which corroborated the presumed orientation of most of the major fracture zones and some of the minor zones interpreted. There is good agreement between results from the present radar investigation using directional antennas and results from earlier radar investigations using dipole antennas.

As a complement to the borehole radar investigation, a VSP-survey was carried out in borehole KAS 07 on southern Äspö /Cosma et al, 1990/. Measurements were made in this hole, down to a depth of 410 m. The diameter of the hole is 56 mm. A multi-detector geophone chain and digital recording equipment were used. Small dynamite charges (50 g) were exploded at five locations around the deep hole with offsets vaying from 35 to 80 m. The charges were placed in shallow water-filled boreholes. The data were then organized in profiles containing seismograms recorded at increasing depths from the same shot point. Five offset VSP profiles were thus formed for this deep hole. The trace spacing in the profiles is 5 m. An estimate of the position and orientation after three-dimensional processing of the reflectors found using VSP is shown in Figure 3.21.

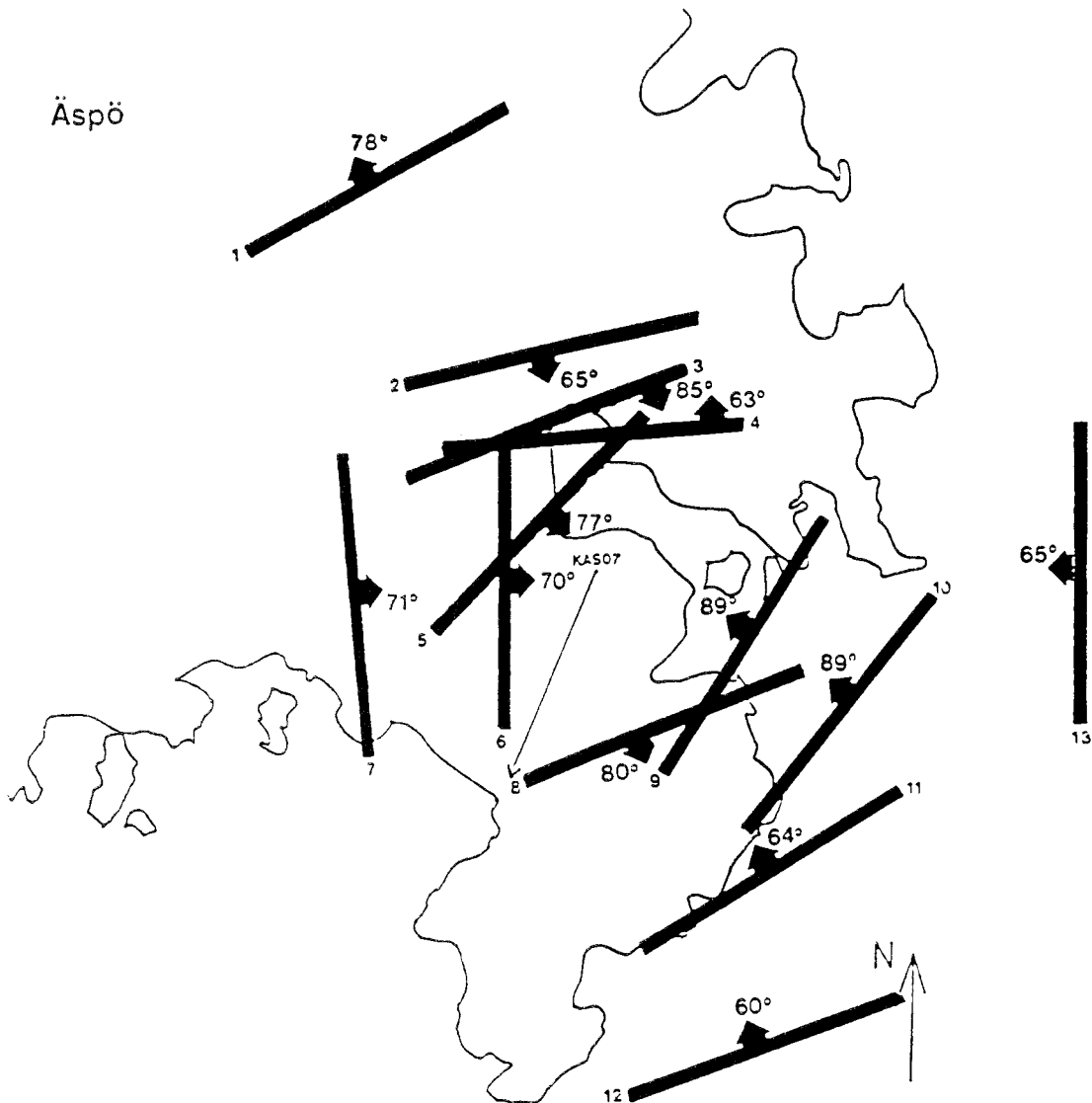


Figure 3.21 Map of VSP reflectors in KAS 07, Äspö /Cosma et al, 1990/.

The drill cores were investigated using many different methods in order to improve our information at depth about the petrological, structural and petrophysical quality of the rock mass in the target area. The drill cores were mapped with the highest precision using the Petro Core System. Considerable attention was devoted to the characterization and mapping of the fractures. Basic data on fracture orientations, fracture spacing and the surface characteristics of the fracture planes, including mineral filling and coatings, were obtained by logging drill cores. Rock types and alteration variation along the cores were also mapped /Strähle, 1988/.

Different orientation methods were used to obtain information on the location of the fractures intersecting the boreholes. During the core mapping procedure the drill core was reconstructed and the relative orientation of long or short orientation sections obtained. The absolute orientation of the relatively oriented sections was obtained using a TV-logging device in KAS 02, KAS 03 and KAS 04. In KAS 04, which is inclined, absolute orientations were also defined by the drillers, using an iron rod indenter with a wire. A test investigation using a WBK televiewer system was also performed in boreholes KAS 05 and KAS 06 in order to evaluate this system with respect to its ability to detect and orient fractures in small diameter boreholes (76 and 56 mm) /Fridh and Strähle, 1989/. During the interpretation work there were many problems, especially concerning the correlation between fractures in the cores and oriented fractures recorded by the TV- and Televiewer-devices. Not until the ramp in the HRL penetrates the actual borehole area we will be able to evaluate the ability of these absolute orientation methods.

The examination of the colour, grain-size and structure of the cores, together with the results of the chemical and thin-section analyses, combined with geophysical logging data, has led to a practical classification of the rock types /Wikman, 1988; Sehlstedt and Strähle, 1989; Sehlstedt et al, 1990/.

A special study of fracture minerals was made in many of the cores from Äspö. The fracture mineralogy is dominated by chlorite, calcite, hematite and epidote but also minerals, like quartz, muscovite, laumontite, prehnite, fluorite and pyrite, are frequent, as well as low-temperature minerals Fe-oxyhydroxide and clay minerals /Tullborg in Munier et al, 1988/. Results from the core mapping correspond well to the results from the XRD-analyses and most of the unidentified mineral phases from the core mapping appeared to be colour- and textural varieties of chlorite, hematite, fluorite, clay minerals or quartz.

A fracture-filling history based on textural studies of thin sections resulted in the following sequence (all of which postdates the foliation (1) in the granite/granodiorite):

- 2) Mylonitization with growth of fine-grained quartz, epidote and muscovite.
- 3) Growth of iron-rich, idiomorphic epidote and fluorite.
- 4) Formation of idiomorphic quartz, muscovite, hematite, fluorite, calcite, spherulitic chlorite and possibly some Fe-oxyhydroxide.
- 5) Mineralization of prehnite, hematite-stained laumontite, calcite and fluorite.

- 6) Formation of gypsum, chlorite, illite and probably clay-minerals like kaolinite.

Ages for listed mineralizations above are suggested to range from Middle Proterozoic (1660 Ma) to the present.

To provide general information for the interpretation of ground geophysical and logging data, measurements of physical properties were made on core samples from two holes. The following physical properties were determined in the laboratory: density, magnetic susceptibility, remnant magnetization, resistivity, and induced polarization. Laboratory spectrometry measurements of uranium (U), thorium (Th) and potassium (K) were made on samples from one of the boreholes, KAS 02 (Äspö). The total number of measured samples was 212 /Nisca, 1988/.

Rock stress measurements were made in boreholes KAS 02, KAS 03 and KAS 05 /Bjarnason et al, 1989/.

KAS 02 and KAS 05 are located in the Southern Block and KAS 03 in the Northern Block of Äspö. The first measurements were made by hydraulic fracturing in borehole KAS 03. Laboratory tests on rock samples from borehole KAS 02 were also performed. The results of the rock stress measurements and laboratory tests are presented and discussed in 3.5 "Mechanical stability" in this report.

3.1.8

SITE SCALE: Correlation to geohydrology and groundwater chemistry

The fine-grained granite which is normally more fractured than the other rock types in southern Äspö is estimated to be the most hydrologically conductive rock and especially more than the contact zones between narrow dikes of this rock type and the wall rock.

The fine-grained greenstone in the form of big lenses or xenoliths with normally a few and irregular fractures (clay or chlorite-filled) are probably mostly tight but the contact zones or narrow dikes (sheets) of the same rock type may be conductive due to increased fracturing

The more acid varieties of the Småland granitoids are normally more fractured than the basic ones (Äspö diorite) and for that reason considered to be more conductive.

Mylonites are very often found to be almost tight.

The dominating hydraulic paths in the site area are, of course, the major fracture zones. It is important, however, to note that single open fractures - which are very often especially persistent in the Småland granite - can also act as highly conductive elements in the rock mass.

Among the major fracture zones, NE-1 has been established to be the most conductive but the other NE trending zones (NE-3 and NE-4) are also considered to be partly highly-conductive, except NE-2, which seems to be more mineralogically altered and less permeable.

The more E-W trending zones, EW-1 and EW-3, are also regarded as being more or less tight except for occasional open paths.

The NNW fracture zone system is considered to comprise a series of more or less vertically dipping narrow fracture zones trending NNW-NNE in the central part of the target area. These zones are regarded as being hydraulically very important, especially in co-operation with the low-dipping fracture zones EW-5 and EW-x, which probably comprise a series of more or less parallel, partly open fractures with stepped offsets in the NNW dip direction.

3.1.9

SITE SCALE: Evaluation of the methods of investigation

Based on the results of the initial phase of pre-investigations the main aim of the second phase of investigations was to characterize the geological conditions for the HRL on a more detailed scale. For this reason a great number of investigation methods were used. Most of these methods are reliable and were used conventionally, but for some of them no earlier experience of importance was available.

A three-dimensional model of a rock mass must be based on the characterization of the distribution of lithological units, fracture systems and fracture zones on different scales.

Recognition of small-scale structures, petrographic variations and fracture orientation within and near the site area on Äspö was achieved by means of detailed surface mapping along cleaned trenches across the island. The results of these investigations, complemented with subsurface information, have been very useful in the geological characterization of rock volumes in the site area.

Aero-geophysical measurements made earlier in the Simpevarp area constituted a good base for the analysis of the tectonic setting on a regional scale. In order to investigate the pattern of the fracture zones and the boundaries of the different bedrock units on a more detailed scale ground geophysical measurements were made over the entire island of Äspö. The combination of detailed geoelectric and geomagnetic data provided very good basic information concerning the possible extent and orientation of fractures and fracture zones, but it is very important to carry out correlation between the geophysical indications and the geological features in the field. VLF measurements were mostly strongly disturbed by the saline water and man-made installations in the Äspö area and have for this reason not been very useful.

Seismic refraction profiling across the island of Äspö and surrounding water confirmed some of the regional fracture zones and gave a good picture of the fracture density and the rock quality in different parts of the island. Seismic refraction is a very useful method, especially in areas where salt water makes it almost impossible to use electrical methods. A disadvantage, however, is the need for explosives during the field work.

Seismic reflection may be useful to detect fracture zones with low dips at depths of about 300 m or more but there is still need for much more development both concerning field techniques and data processing before this method can be regarded as practicable for fracture zone identification in crystalline rocks /Juhlin, 1990/.

An interesting study of the borehole RAMAC radar system operating as a ground probing radar system was made to test the ability of this system to locate shallow, low-dipping zones on Äspö. A number of reflections were recorded along the cleaned trenches. For some of these reflections it was possible to carry out correlation with indications from borehole radar measurements in the boreholes. After further development it is felt that this method will be very useful, especially as a complement to seismic reflection and borehole radar for identification of low-dipping fracture zones.

Single-hole radar reflections give very valuable information about the orientation of fracture zones - especially those intersecting the borehole at rather low angles. A number of prominent structures were indicated in the boreholes using the directional antenna and dipole antenna radar measurements which corroborated the presumed orientation of most of the major fracture zones and some of the minor zones interpreted. There is generally good agreement between results from present radar investigation using directional antennas and results from earlier radar measurements made using dipole antennas.

VSP results from KAS 07 were found to be very important as a complement to the borehole radar data especially after three-dimensional processing using a new technique with Image Space filtering, which has been developed for seismic reflection studies in crystalline rock.

The objectives of the geophysical borehole surveys were to aid definition of the location and character of the lithological units and their contacts and to determine the distribution and character of fractures and fracture zones in the rock mass.

The sonic log and magnetic susceptibility and gamma-gamma logs seem to be very relevant for lithological characterization of an inhomogeneous rock mass like that in the Äspö area. There is specially significant correlation between high gamma radiation and the fine-grained granites in the boreholes. The results from the caliper log and the electric logs were of greatest interest in detecting fractures and fracture zones. It seems, however, to be rather unnecessary to use three different electric logs which give largely identical results, so in most of the geophysical logging surveys, only the single-point resistance log was used.

To obtain the absolute orientation of structures like rock contacts and fractures TV-logging and Televierer measurements were made. In the inclined borehole, KAS 04, the absolute orientation was also obtained using an iron-rod indenter during the drilling operation, but this method does not seem to be generally useful due to practical problems.

The use of the TV-logging and Televierer methods for absolute orientation of fractures in core boreholes was accompanied by many problems, especially concerning depth measurement. It is very difficult to identify the same feature in the core as in the TV-log and Televierer records. On the other hand it is equally important that the logging depth measurement is correct. The reconstruction and relative orientation of the core, which is necessary to permit absolute orientation, is also very time consuming.

From our experience of the different orientation methods available today it is obvious that it is very difficult to obtain a reliable picture of the orientation of fractures at depth using borehole information only.

3.2 GEOHYDROLOGY

3.2.1 Purpose of the investigation

The purpose of the investigations up to 1990 was to describe the natural groundwater distribution and flow in a selected rock volume. Of particular interest is to describe the geometric distribution of the groundwater flow in the rock volume and quantify transmissivity and pressure head in these volumes, zones or fractures. A further goal of the investigations was to supply the data necessary for setting up mathematical groundwater models for a selected rock volume. The models should be devised in such a manner that they are able to describe with good accuracy the natural groundwater situation and the changes that take place in the ambient groundwater head and flow when a tunnel or shaft is excavated in the selected rock volume. The main parameters, variables and structures are

- hydraulic conductivity of the rock mass
- main conductive structures
- precipitation and infiltration
- boundary conditions for mathematical models

The results from the investigations are discussed in Chapter 3.2 and the geohydrological conceptual model is presented in Chapter 4.

The purpose of the investigations at this stage was not to find parameters governing the transport process in the groundwater flow. This will be studied more in detail later in the Äspö HRL project.

3.2.2 An overview of the geohydrological investigation

The preinvestigations were started in 1986 and have been carried out successively from a regional scale down to a detailed scale. An overview of the investigations is shown in Tables 3.2.1 and 3.2.2

Table 3.3 Overview of geohydrological investigations in the Simpevarp area - regional scale

Compilations of available data in databases and reports
- regional hydrology
- hydraulic conductivity
Hydraulic tests
- air-lift tests
- interference tests
Generic modelling

Table 3.4 Overview of geohydrological investigations in the Äspö-area. Site scale

Hydrology on Äspö scale
Hydraulic tests in 14 coreholes and 20 percussion holes
- air-lift tests
- injection tests
- flowmeter (spinner) survey
- interference tests
- dilution tests
Numerical modelling

The investigation was started by making an inventory of available geohydrological and hydrological data in reports and databases concerning the Simpevarp area in order to provide the initial estimates of important parameters and variables, such as

- hydraulic conductivity
- precipitation, evapotranspiration and run off
- possible directions for conductive structures

Percussion drillings were then made in several areas and hydraulic tests performed (Äspö, Ävrö and Laxemar). The purpose was to obtain a more detailed picture of the geology and geohydrology. The first conceptual model was based on the results from the investigations mentioned above /Gustafson et al, 1988/.

After evaluation of these results, three core boreholes (KAS 02-04) and five more percussion holes (HAS 08-12) were drilled on Äspö to get more detailed information about the island, which had been found most suitable for the HRL. The second conceptual model was based on these and some other results /Gustafson et al, 1989/.

Numerical modelling was performed simultaneously to the investigations. The first models were generic models (not site specific in detail). The purpose was to study some specific aspects of groundwater flow that could be useful in later modelling stages.

3.2.3

REGIONAL SCALE: Summarized presentation of main geohydrological data - Interpretation and analysis**Regional hydrology - compilation of available data**

The hydrological conditions in the Simpevarp area have been reported by Svensson /1987/.

The area is situated on the eastern coast of southern Sweden. Despite the coastal position the climate is governed by the prevailing westerly winds, which are comparatively dry. The total mean precipitation is 675 mm/year. The average temperature in Oskarshamn is 6.4°C, with February as the coldest month, -2.9°C, and July as the warmest, 16.2°C. Of the annual precipitation, about 125 mm/year falls as snow, and the durability of the snow cover is on average 91 days. The total evapotranspiration is calculated to be 490 mm/year, leaving a run off of 150-200 mm/year.

In the region around Simpevarp there are two major catchment areas, Virboån ($Q_m = 3.6 \text{ m}^3/\text{s}$) and Marströmmen ($Q_m = 2.9 \text{ m}^3/\text{s}$) and some small streams like Gerseboån and Laxemarån. The lake area comprises 7-12 % of the catchment area for all streams except Laxemarån which has only 1.2 % of lakes.

The groundwater levels in the area are at maximum in the spring, during the snow melt-period. At a distance from the coast winter minimum levels may occur, but the annual absolute minimum is the summer one. The annual recharge has been estimated to be 128 to 218 mm/year in pervious ground.

Hydraulic conductivity - compilation of available data

Data from a great number of water wells in the region around Simpevarp are stored in the Well and Borehole records of the Swedish Geological Survey. Several geological studies mentioned earlier, such as geological mapping, geophysics and structural geology, permit correlation with the geohydrological data from the different boreholes. Statistical evaluation of these data was performed by Liedholm /1987a/.

The area studied in this report corresponds to the area covered by the regional map of the bedrock geology. Within this area, 162 wells in bedrock are registered in the Well Records. In this study the specific capacity, Q/s_w , was used as a significant measure of the transmissivity of the upper part of the bedrock. In different statistical analyses the specific capacity is then correlated to rock type, fracture frequency, geophysical structures and other relevant factors.

The median of the logarithm of the specific capacity (m^2/s) of the 162 wells was -5.4 and the median depth was 57 m.

The coarse-grained granites of Götemar-Uthammar type have the greatest specific capacity in the area. The tonalite and medium-grained grey gneissic granite have a somewhat lower specific capacity than the average. Least pervious are the greenstones.

The specific capacity follows log-normal distribution. The variation in specific capacity is greater for bedrock with a lower median specific capacity. The data for the greenstones are, however, an exception in which a small specific capacity coincides with a moderate spread.

An analysis of the specific capacities from different sub-areas showed that the most pervious rock is found in an area directly west of Simpevarp. This can also be correlated to an area of the bedrock with low magnetization levels and the occurrence of radial fracture systems, possibly indicating a granite diapir not reaching to the surface.

A correlation to the fracture mapping indicated that structures striking NE-SW and to some extent NW-SE are associated with a high specific capacity. No other significant correlations to terrain features was found.

Geohydrological data from the Simpevarp peninsula and the island of Ävrö were analysed by Rhén /1987/.

During pre-investigations and construction of the power plants and the CLAB installation on the Simpevarp peninsula, geohydrological information was produced. On the island of Ävrö immediately east of the Simpevarp peninsula, preliminary investigations were performed within SKB's fracture zone project /Gentzschein et al, 1987/.

All data from the area show that the fracture system is dominated by two main sets striking N60-70°E and N30-40°W. The foliation and dykes of aplite strike in the sector NE-E.

The hydraulic conductivity of the rock was analysed from a large number of tests performed in investigation boreholes for the power plants, the tunnel for cooling water for OIII, the CLAB installation and in the investigation boreholes at Ävrö. Conductivity distributions for the Simpevarp peninsula are shown in Figure 3.22 On Ävrö there is an evident tendency of decreasing conductivity with depth, interrupted, however, by a fracture zone in the eastern part of the island. In the upper 300 m the conductivity is in the range of $K = 10^{-8} - 10^{-7}$ m/s. On the Simpevarp peninsula the conductivity is in the range of $K = 10^{-9} - 3 \cdot 10^{-8}$ m/s. This lower value may be caused by the occurrence of volcanites.

The groundwater level was found to be 8-10 m below ground level. Measurements made near the existing facilities show that these have only a small influence on the level fluctuations.

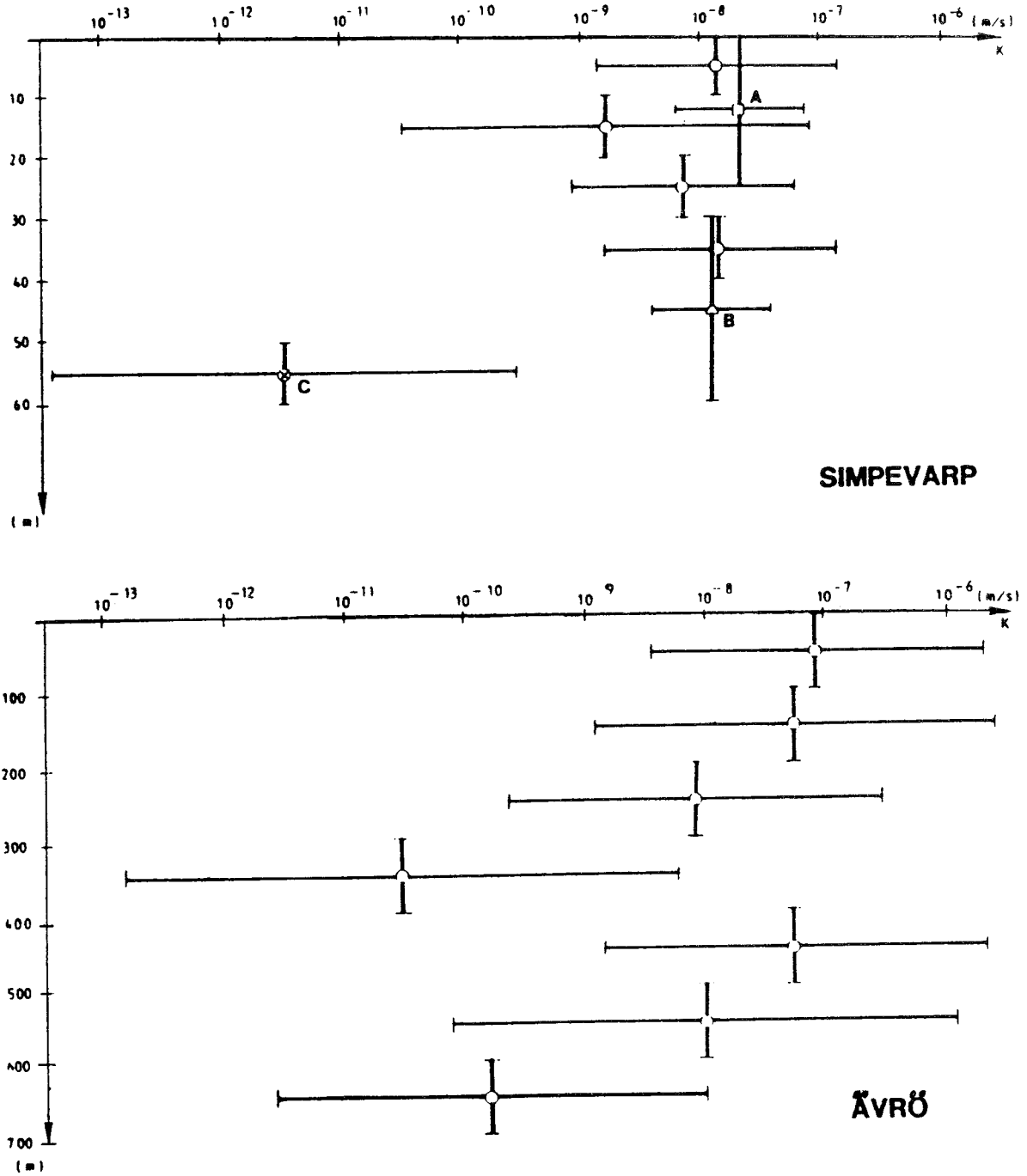


Figure 3.22 Hydraulic conductivity (K) for the Simpevarp peninsula and Ävrö. The median value and \pm one standard deviation are shown for different depths.

K is calculated from:

A: Specific capacity

B, C: Single-packer injection tests

The rest: Mainly double-packer injection tests /Rhén, 1987/

Hydraulic tests - introduction

During the regional investigations a few hydraulic tests were performed in percussion holes at Äspö, Ävrö and Laxemar. Later in the investigations four coreholes were drilled, three on Äspö and one in Laxemar. Results from tests performed at Ävrö and Laxemar are discussed in this chapter and the main part of the results from tests performed at Äspö are discussed in Chapter 3.2.6. The test methods are also presented in 3.2.6. and by Almén and Zellman /1991/.

Hydraulic tests - regional scale

Eight percussion holes were drilled at Ävrö, eight at Äspö and seven at Laxemar to a depth of approximately 100 m.

In the percussion boreholes at Ävrö, Äspö and Laxemar recovery and interference tests were performed. Data from these tests were evaluated by Nilsson /1987, 1988/. From the preliminary data obtained a direct comparison with the data from the Well Records of the Geological Survey can be made (see Figure 3.23).

Thus, data show that the medians of the specific capacities for the areas studied are lower than what is normal for the different rock types. The figure also shows that the variation in the data for the three areas increases with decreasing specific capacity, which corresponds to what was reported above under "Hydraulic conductivity - compilation of available data".

Interference pumping tests were performed in the boreholes with higher yields. Analyses of these data showed transmissivities as high as $T = 2.2 \cdot 10^{-4} \text{ m}^2/\text{s}$ on Ävrö, $T = 3.3 \cdot 10^{-4} \text{ m}^2/\text{s}$ at Äspö and $T = 9.0 \cdot 10^{-5} \text{ m}^2/\text{s}$ at Laxemar. These are values that exceed the corresponding median specific capacities shown in Figure 3.23 by one or two orders of magnitude. The transmissivity (T) was on average estimated to be $6 Q/s_w$ for all areas.

Hydraulic interference with other boreholes occurred in all four tests at Ävrö, in one test at Äspö and in one test at Laxemar. However, strict interference within the same conductor was only shown in the fracture zone in the eastern part of Ävrö (HAv3) and in one test in the Laxemar area (HLx1). Although no complete set of observation boreholes existed some conclusions on the direction of the conductive structures could be drawn, since interference occurred mainly in the NW-SE and NE-SW directions. This is probably caused by the major fracture sets found to run roughly in these directions in the whole area, but also on Äspö by the foliation and the direction of greenstone bodies in the rock.

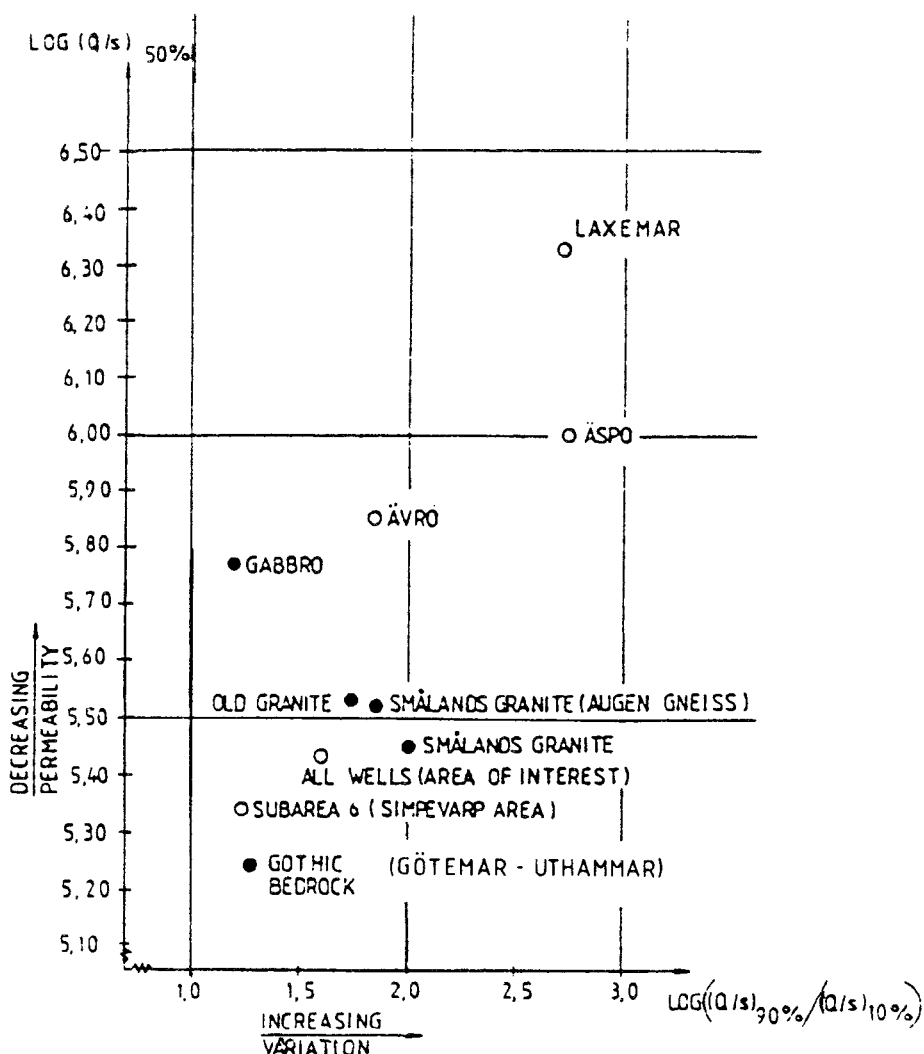


Figure 3.23 Bedrock-related median and variation of specific capacity, Q/s . (Note that only eight percussion holes on Äspö are included in the calculations) /Nilsson, 1988/

Hydraulic tests in KLX 01

In 1987 the cored hole KLX 01 was drilled down to 688 m and several hydraulic tests were performed during 1988 /Nilsson, 1989/. In 1990 KLX 01 was drilled down to 1078 m and a few hydraulic tests were performed in the new part of the borehole /Rhén et al, 1991c/. Some results from the tests are shown in Table 3.5 . From a pumping test between section 0 and 688 m the transmissivity was estimated at $8 \cdot 10^{-5} \text{ m}^2/\text{s}$ or as an average hydraulic conductivity to $1.2 \cdot 10^{-7} \text{ m/s}$. A cumulative plot of the integrated hydraulic conductivity is shown in Figure 3.24 for the different tests between section 0 and 688 m.

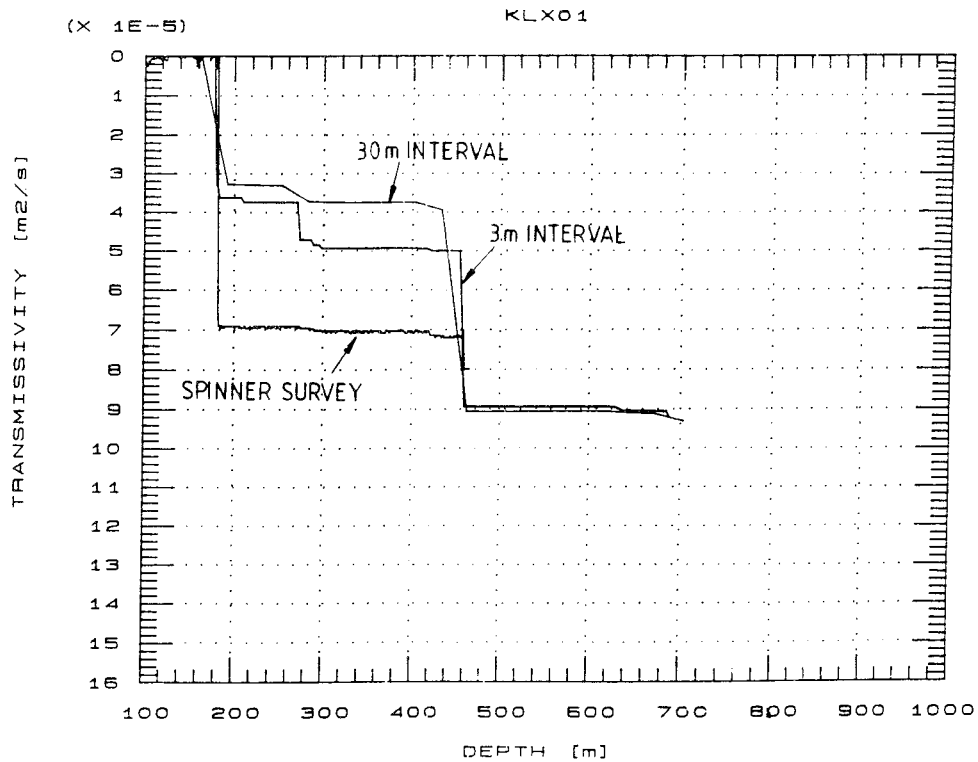


Figure 3.24 Cumulative plot of integrated hydraulic conductivity versus depth for KLX 01 (0-688 m). /Nilsson, 1989/.

3.2.4

Generic modelling

Test of two layouts

Generic modelling of two possible layouts for the Äspö HRL was performed using the analytical element method /Axelsson, 1987/.

The two layouts chosen were a double shaft down to a depth of 500 m and a spiral ramp down to 331 m. The study was performed under the simplified assumptions of a homogeneous bedrock and a constant head at ground level.

All calculations were made using the hydraulic conductivity as the basic unit, making it easy to convert calculated flows to real values when the parameters become known. The calculated potentials are, however, directly applicable.

The draw-down during the construction period was simulated by a series of steady state models for different stages.

The calculations show that the radius of influence around the shafts will be approximately 1 900 m in the final stage and will probably be of the same order of magnitude for the ramp design (see Figure 3.25).

For a homogeneous bedrock the inflow will increase rather drastically with depth. However, an assumption of a conductivity that decreases with depth as shown by Rhén /1987/ reduces the total inflow to about 1/4 of the amount calculated using homogeneous conductivity.

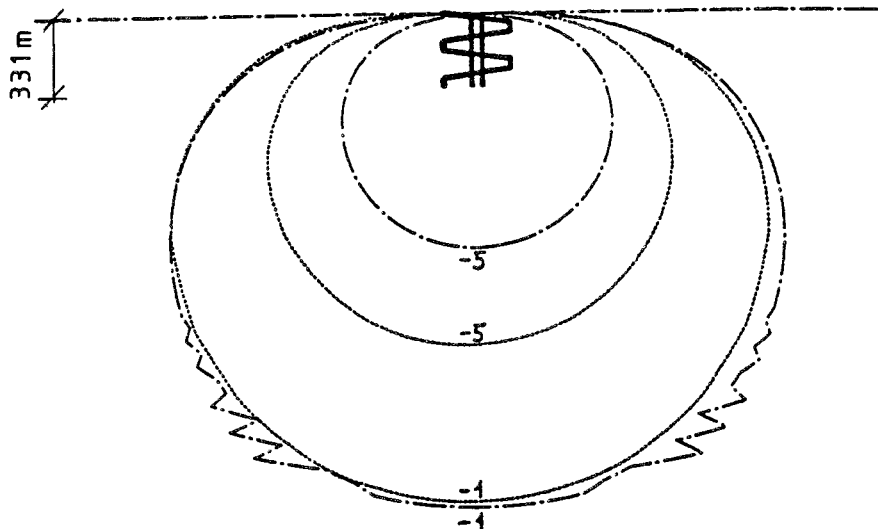


Figure 3.25 Comparison of the radius of influence for the shaft (---) and the spiral (.....) layout. Figures indicate draw-down in metres /Axelsson, 1987/.

Two and three-dimensional regional models

Groundwater flow calculations on a regional scale around the Äspö laboratory were performed /Gustafson et al, 1989b/, on the basis of the conceptual model given in the previous report /Gustafson et al, 1988/.

Two-dimensional modelling

In order to achieve satisfactory understanding of the groundwater flow conditions around the site, several numerical models of the geohydrological situation were used. The study presented here, which comprises regional models, was aimed at describing the groundwater situation in a wide area round the planned laboratory and to assess the influence of it in order to define the boundary conditions for models

covering smaller areas. However, it is difficult to find natural limits to an area to be modelled at this scale, i.e. the positions of the confinements of the model are extremely uncertain. Since the application of boundary conditions is essential for the model results, these would suffer from inherent uncertainties, if incorrect positions for the boundaries were assumed.

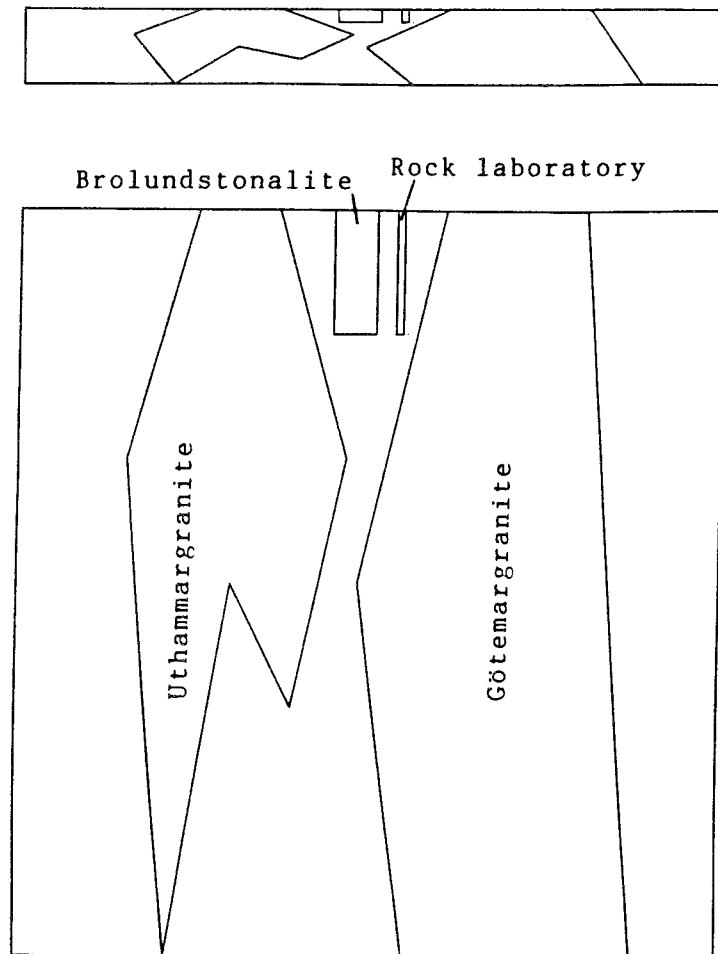


Figure 3.26 The geometry of the geological formations as modelled. The upper figure has the same vertical and horizontal scale. The Småland granite is between other rock areas /Gustafson et al, 1989b/.

It was deemed feasible to perform this study in two steps. First, a two-dimensional-calculation was performed to investigate the impact of the different lithological units. The position of this 2-D model was based on gravimetric investigations and the boundaries of it were considered to be rather well established (see Figure 3.26).

Four two-dimensional cases were modelled using different material properties; the laboratory was generically modelled in two of these cases. The purpose of the exercise in two dimensions was to elucidate whether or not there are hydrological means for a conceptual transfer of boundary conditions from the two-dimensional calculation to a

three-dimensional model covering the potential location of the laboratory and to estimate the radius of influence from the shaft.

The properties of the two-dimensional domain are shown in Table 3.7, corresponding to the representative conductivities at the surface.

Table 3.7 Properties of the two-dimensional domain

Gravity modelling Geological dominance	Property areas	K (m/s)
Uthammar granite	Götemar- Uthammar	$1.12 \cdot 10^{-6}$
Brolund tonalite	Tonalite	$1.82 \cdot 10^{-7}$
Götemar granite	Götemar- Uthammar	$1.12 \cdot 10^{-6}$
Ambient rocks (Småland granite)	Granite to granodiorite	$3.01 \cdot 10^{-7}$

The relevant factor in determining the size of the three-dimensional model is the radius of influence. If the laboratory is introduced as an atmospheric pressure boundary, the head difference between this model and the previous one will define the draw-down caused by the laboratory.

The calculations show that the radius of influence is in the order of 3-4 km.

Three-dimensional modelling

Two three-dimensional models were considered, both consisting of ten lithological units. The first one was referred to as the basic case, which was used to analyse the regional flow system, and to investigate whether the vertical limits around Äspö are significant enough to be regarded as boundary conditions for future modelling exercises on a local scale around Äspö. The second model was a generic model of the laboratory. This was done by assigning atmospheric pressure to the nodal points located near an imaginary line of symmetry (to a depth, Z, of -500) of the excavation. The purpose of this exercise was to study the regional effects of the presence of the laboratory.

With the extent of the model defined by the radius of influence of the laboratory calculated in two dimensions, the same type of boundary conditions can be used in a three-dimensional model, i.e. an upper constant head boundary defined by the topography and no lateral flow and bottom boundaries. The model chosen was a horizontal trapezoid measuring some 10 x 7 km in area with a depth of 3 km, divided into 8 layers.

The gravimetric model formed the basis for defining the property areas for the two-dimensional model. In this case the profile was used to give the geometry of the pervious Göttemar granite in the model area. This granite probably exists at depth in the whole model domain. The other property volumes were defined by the different investigation areas within the model domain. For areas outside the investigation areas data from Liedholm /1987/ were used. As in the two-dimensional models, the lithological units defined the property volumes.

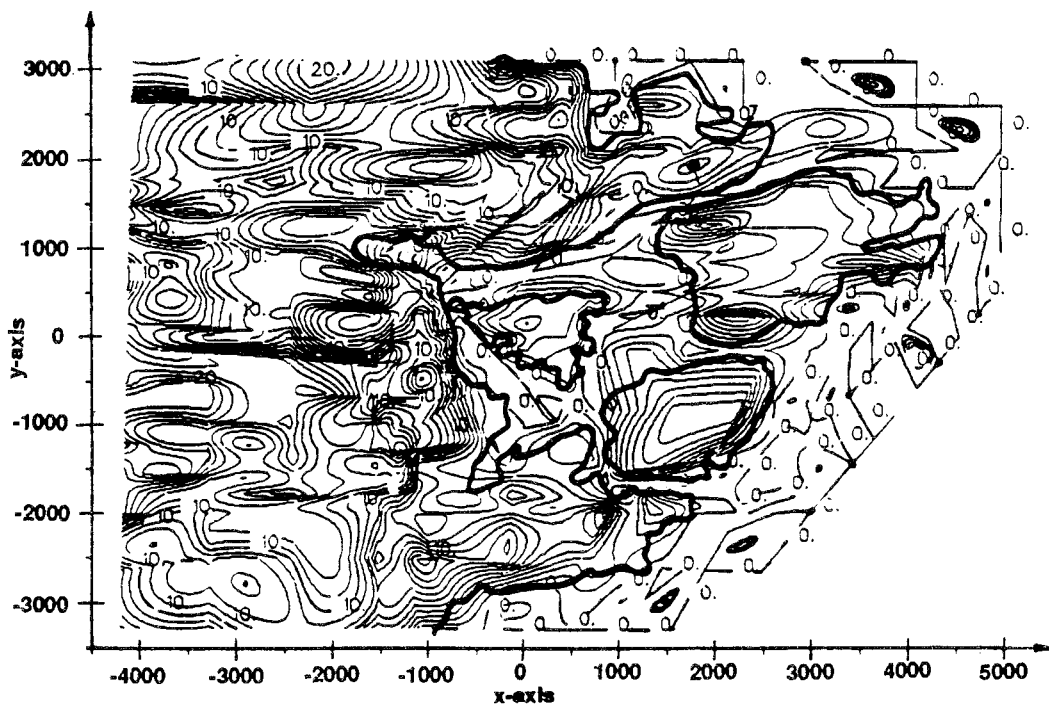


Figure 3.27 Top surface (i.e. the groundwater table) of the three-dimensional model. Values of pressure are expressed in metres (piezometric level) above sea level. The coastline is indicated by a thick solid line /Gustafson et al, 1989b/.

Figure 3.27 shows the groundwater table in the area. This is assumed to be governed by the topography and acts as a constant head boundary.

Figure 3.28 shows the calculated piezometric head 500 m below the surface, corresponding to the depth for the experiment area under natural conditions. As expected the lines of equal pressure potential are smoothed out.

In the two-dimensional modelling a crucial matter is the radius of influence from the laboratory. Figure 3.29 shows the draw-down around the Äspö laboratory at a depth equal to the level of the proposed laboratory.

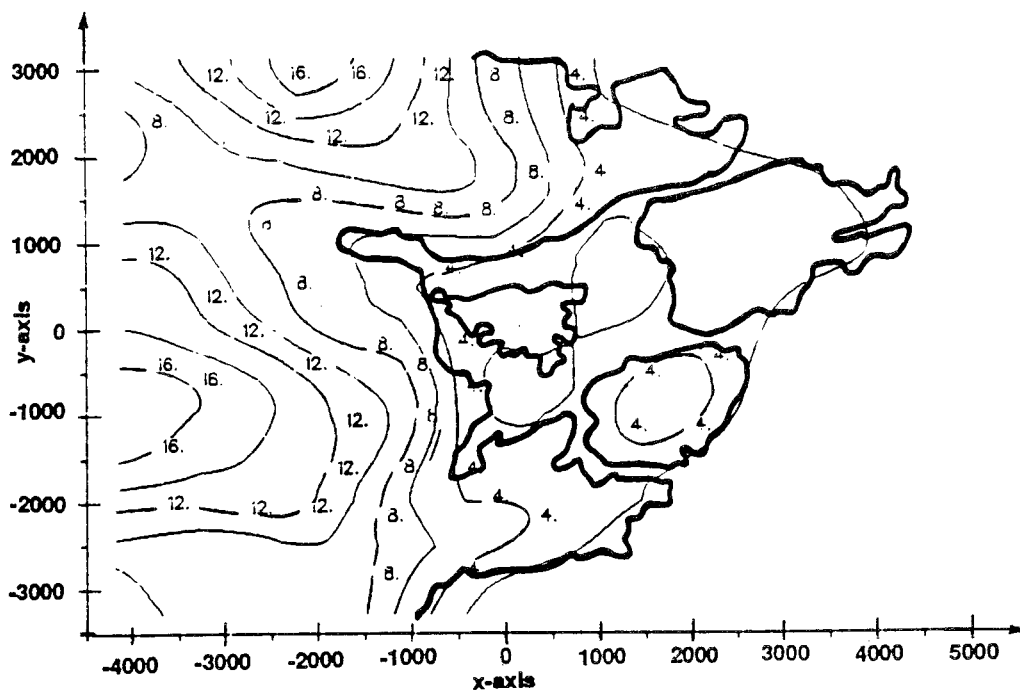


Figure 3.28 The distribution of pressure potentials at a level of 500 m below sea level. Values of potentials are expressed in metres (piezometric level) above sea level. The coastline is indicated by a thick solid line /Gustafson et al, 1989b/.

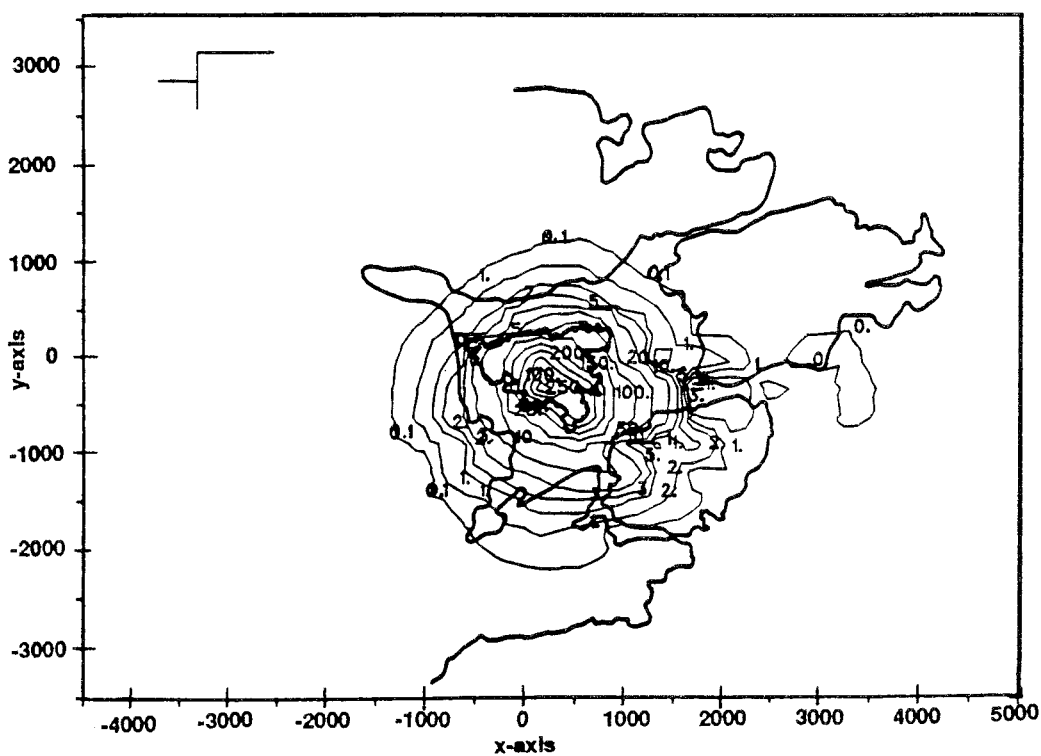


Figure 3.29 Distribution of differences in pressure potentials at a level of 500 m. Values of pressure potentials are expressed in metres (piezometric level). The coastline is indicated by a thick solid line /Gustafson et al, 1989b/.

Although saline groundwater exists at depth, the influence of this on the pressure potential and flow conditions has not been considered in this model.

Numerical models of the saline water front

In order to understand the behavior of a saline water front with small salinity contrast in a hydraulically inhomogeneous medium a few numerical simulations were performed. The work is reported by Svensson /1988/ and Hemström and Svensson, /1988/.

Specification of the problem

In the Simpevarp area fresh groundwater meets the brackish seawater. Measurements also revealed the existence of more saline water (1 %) in the bedrock, which at sea resides more than 20 m below the sea bed. We therefore need to consider water of three different salinities and hence different densities. Due to the density differences, it is expected that the 1 % saline water will be found at a lower level under the land (see Figure 3.30).

The purpose of the report by Svensson /1988/ was to:

- Demonstrate that the numerical model used is compatible with other existing codes for density-stratified groundwater flows.
- Establish a realistic, although idealized, scenario that can be used as a reference case when carrying out sensitivity tests.
- Carry out sensitivity tests of parameters that specify the properties of the fractured porous medium, i.e. hydraulic conductivity, relations for the dispersion coefficient, etc. and, in particular, to investigate the effect of stochastically generated conductivities.

Verification simulations

In order to verify this application of the computer code used, PHOENICS /Spalding, 1981/, two reference problems were studied: Henry's problem /Voss and Souza, 1987/ and the Saline Dome problem /Herbert and Jackson, 1987/. In both cases the solution calculated using PHOENICS agreed well with the ones presented in literature.

The reference case

The porosity, dispersion coefficient and hydraulic conductivity for the reference case are given in Figure 3.30 and the predicted salinity and flow field can be found in Figure 3.31. The salt water is found at a depth of 300 - 400 m at the left boundary, which represents the centre of the island.

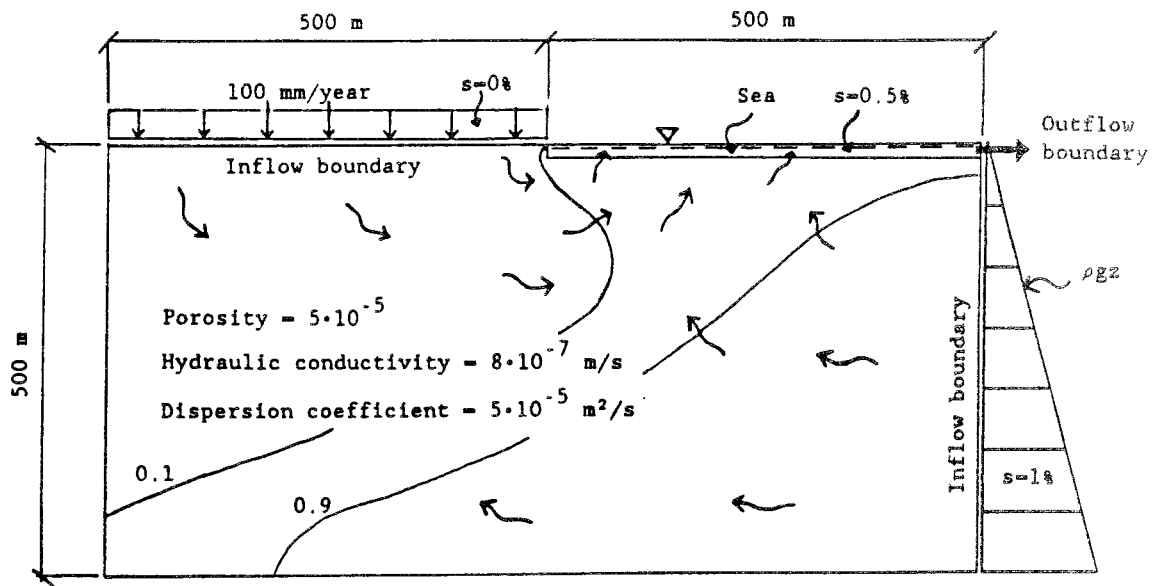


Figure 3.30 The reference case with assumed parameters /Svensson, 1988/.

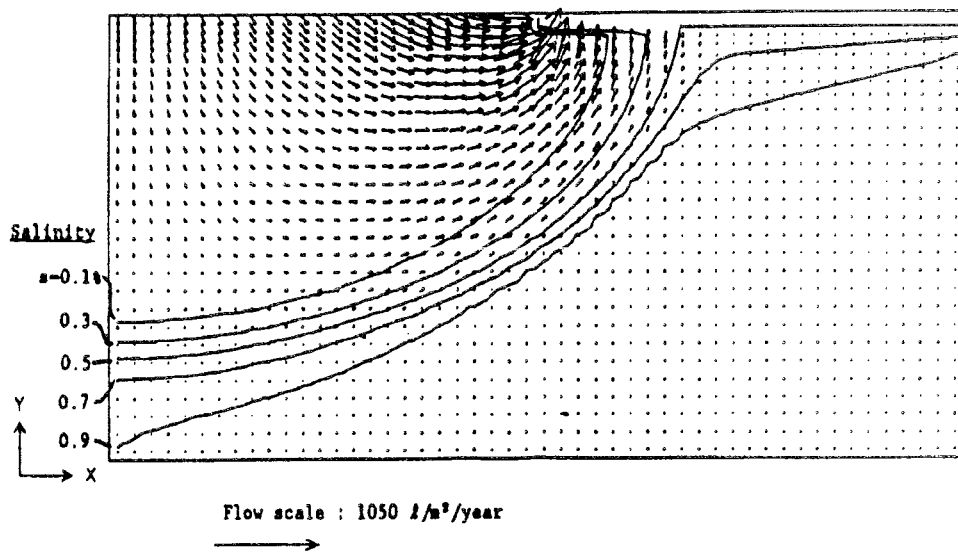


Figure 3.31 The homogeneous reference case /Svensson, 1988/.

Two additional, homogeneous cases were also tested, one with a dispersion coefficient proportional to the Darcy velocity, giving results very similar to the reference case, and one with a hydraulic conductivity decreasing with depth, showing that this forces the flow close to the surface, but also that the boundary between fresh and saline water is forced downwards.

Stochastically generated conductivities

All results for the homogenous model look very "smooth", which is a consequence of assuming constant or smoothly varying properties of the rock. The fractured rock can, however, only be given mean properties in a statistical sense. An attempt was therefore made to generate random hydraulic conductivities having a log-normal distribution. The mean conductivity used is the same as in the reference case. Results for three different standard deviations of $\ln K$ (1, 2 and 4), but with the same set of random numbers, are shown in Figure 3.32. It is interesting to note that although the conductivities do not have any spatial correlations, streaks, as formed in the velocity field, develop. This can to some degree be understood by first noting that due to the boundary conditions prescribed the average pattern must be the same as in the reference case, i.e. the precipitation must find its way out to the sea. If a new series of random numbers were used, another flow and salinity field would, of course, be obtained.

The results are exciting and show many features, such as higher salinities overlying lower ones, that have been recorded in the field investigations.

In conclusion, it can be stated that numerical models of the kind used in this study are useful tools for improving our understanding of the flow in a fractured medium.

Hydraulic conductivity and infiltration rate

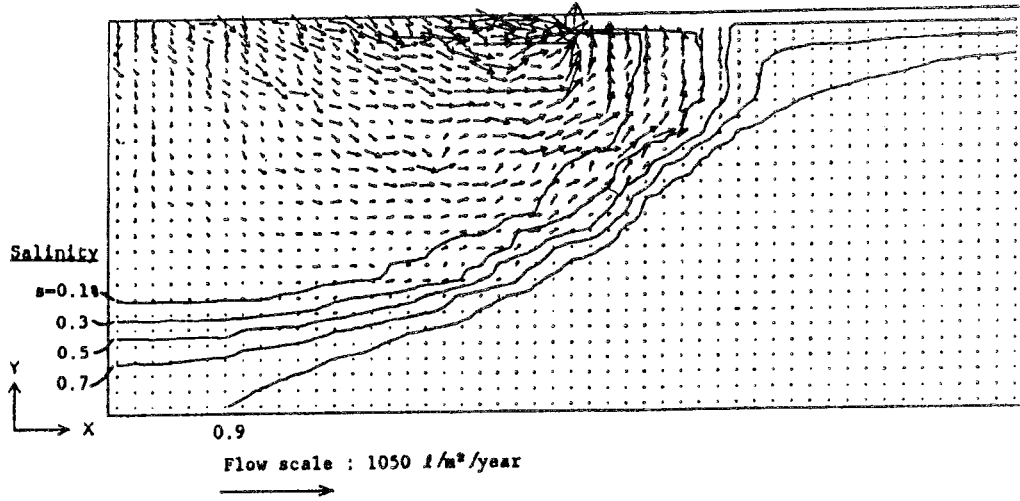
A sensitivity analysis was performed by Thunvik et al./1989/ in order to check the response of the piezometric head to perturbations of the hydraulic conductivity in various layers, and of the infiltration rate.

An axi-symmetric FE-model, with the HRL tunnel system 400 - 500 m below ground level was used. Infiltration rates of 59 mm/year and 185 mm/year resulted in a maximum draw down in the laboratory domain of 70 m and 0 m respectively. The time required to reach steady state was approximately 4 years. The sensitivity study showed that changes in the hydraulic conductivity at, levels deeper than 750 m do not influence the pressure or flux distribution around the HRL. The flux to the tunnel was most sensitive for the hydraulic conductivity changes between 120 and 500 m depth.

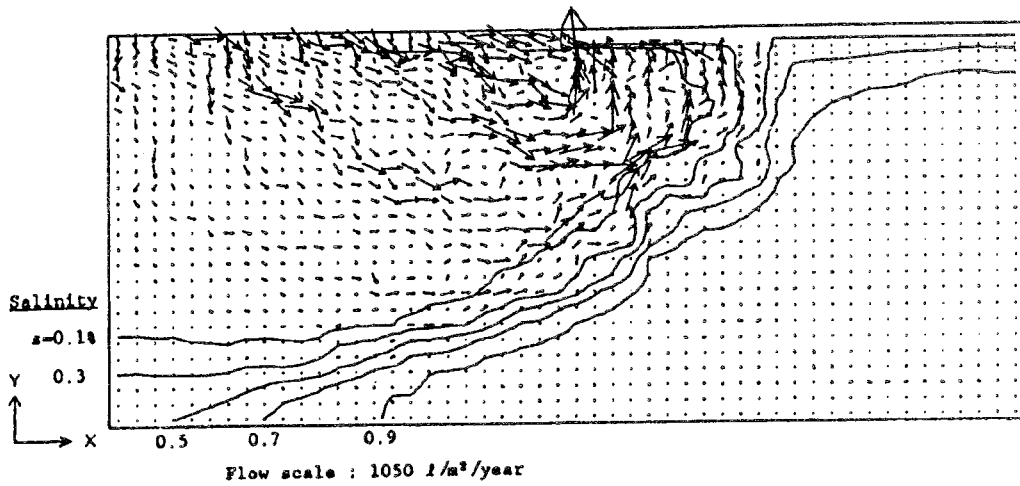
3.2.5

REGIONAL SCALE: Evaluation of the methods of investigation

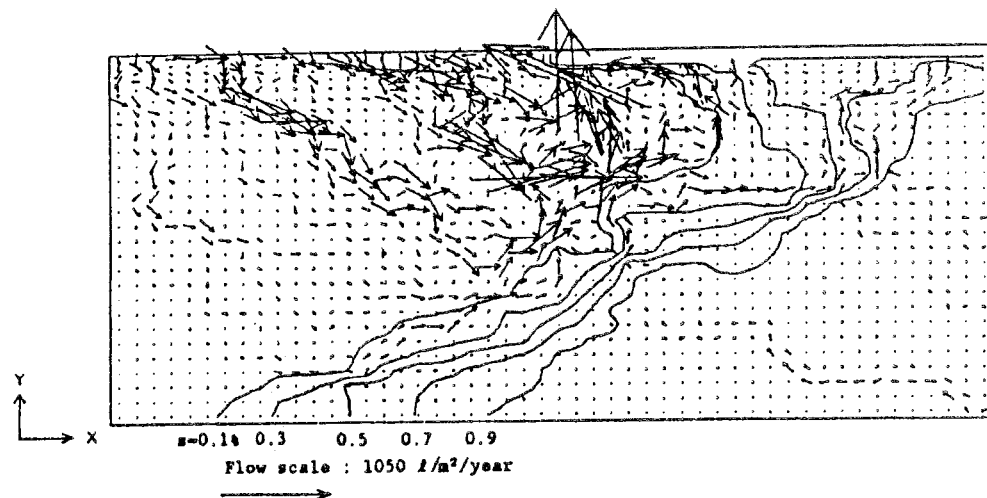
When evaluating the geohydrological work, the importance of a thorough analysis of existing data must be emphasized. At an early stage of an investigation, the main features of the surface hydrology, the bedrock properties and the groundwater regime can be rapidly obtained from sets of existing data in reports and data bases.



a) Standard deviation, $\ln K = 1$



b) Standard deviation, $\ln K = 2$



c) Standard deviation, $\ln K = 4$

Figure 3.32 Simulations with stochastically generated hydraulic conductivities. Velocity and salinity fields /Svensson, 1988/.

The use of shallow percussion boreholes for pumping tests is a valuable technique for determining the basic properties of the upper part of the bedrock, such as hydraulic conductivity, anisotropy and hydraulic connections in fracture zones.

The generic modelling has been useful in assessing the area of influence of the HRL and understanding the influence of the saline water on the groundwater flow.

3.2.6

SITE SCALE: Summarized presentation of main geohydrological data - interpretation and analysis

Surface hydrology and groundwater recharge

The land surface of Äspö is slightly undulating, with a maximum height of a little more than 10 m above the sea. The valleys are filled with wet land and the hills consist mainly of bare rock and some till. This means that there are no perennial streams in the area: the surface water is drained to the sea by the wet lands. There are some open surfaces of fresh water, at least in the spring and autumn.

The small run-off basins, however, imply that the terrain may be subdivided into a mosaic of in and outflow areas, thereby giving a small average annual recharge as long as the groundwater is not utilized or drained to an underground utility.

On a regional scale (see Chapter 3.2.3) the mean precipitation (P) is estimated to be 675 mm/year, and the evapotranspiration (E) is calculated to be 490 mm/year /Svensson, 1987/. This leaves a surplus of $P-E = 185$ mm/year to be distributed as groundwater recharge and run-off. The main recharge takes place in conjunction with the melting of snow, thereby giving a maximum water level in the spring and a minimum in the late summer.

The mean annual snow cover corresponds to approx 125 mm/year. Table 3.8 shows the precipitation, air temperature and potential evapotranspiration for the period 1987 to 1989.

Table 3.8 Precipitation, air temperature and evapotranspiration for 1987-89. Precipitation and temperature measured at Oskarshamn and the evapotranspiration is calculated as the mean of the evapotranspiration for Västervik and Ölands Norra Udde /Nyberg et al, 1991/.

Year	Precipitation (mm/year)	Air temp (°C)	Evapotranspiration (mm/year)
1987	639	4.9	535
1988	733	6.8	545
1989	430	8.3	635

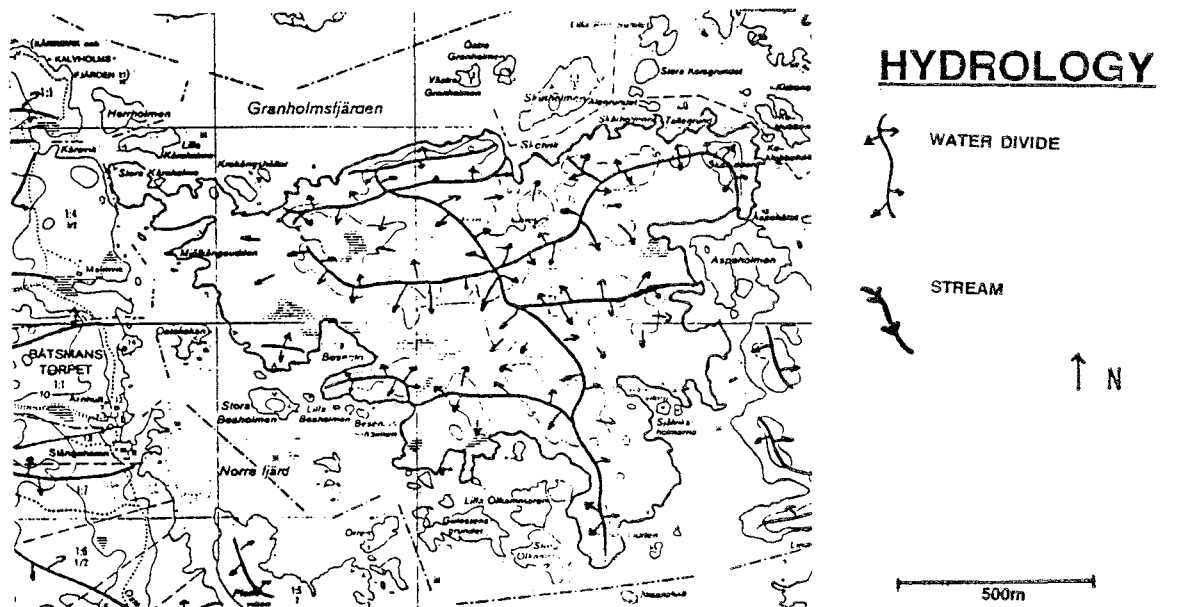
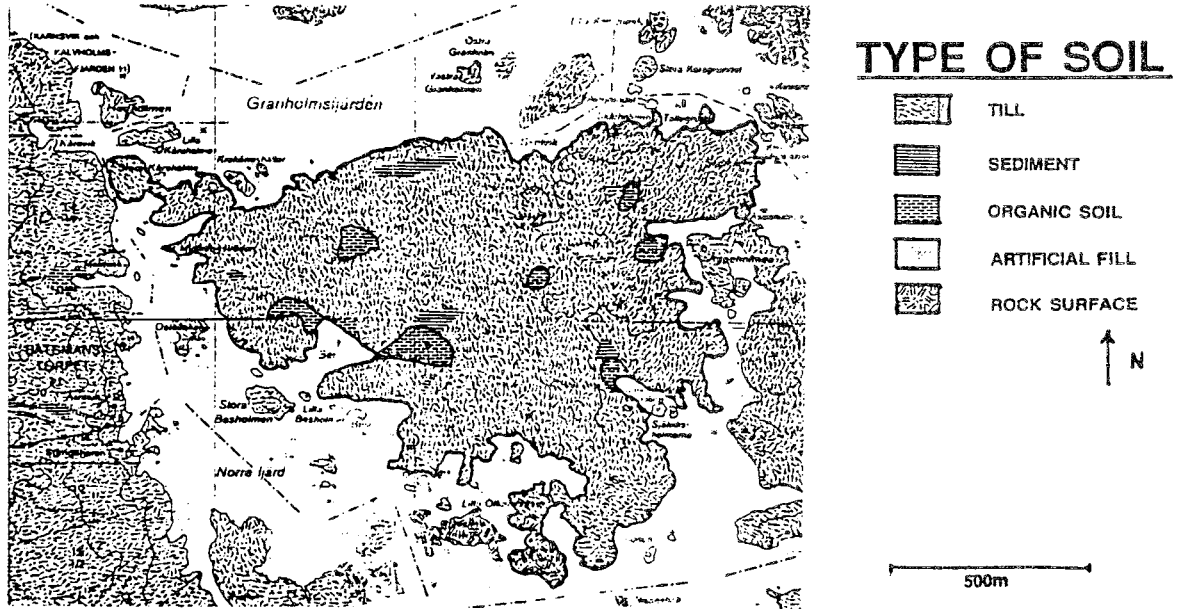


Figure 3.33 Surface conditions and water divides on Äspö /Lindahl, 1989/.

Groundwater levels

The natural fluctuation of the water level during a year is expected to be less than about 1 m. In some of the boreholes the water level may rise up to 1 m during a few days or weeks if the precipitation is large. The maximum water level on Äspö is about +4 m. A contour map of the water table is presented in Figure 3.34.

The map is based on measurements in boreholes except for six values of the water table. These values were estimated for the areas where there were no boreholes from a regression curve showing the relationship between the water table and the topography.

An overview of piezometric levels 1987-1989 is shown in /Nyberg et al, 1991/.

Sea level

During 1987-1989 the levels of the Baltic sea ranged from -0.5 to +0.8 m above sea level, with normal fluctuations within ± 0.3 m /Nyberg et al, 1991/.

GV1ARKA

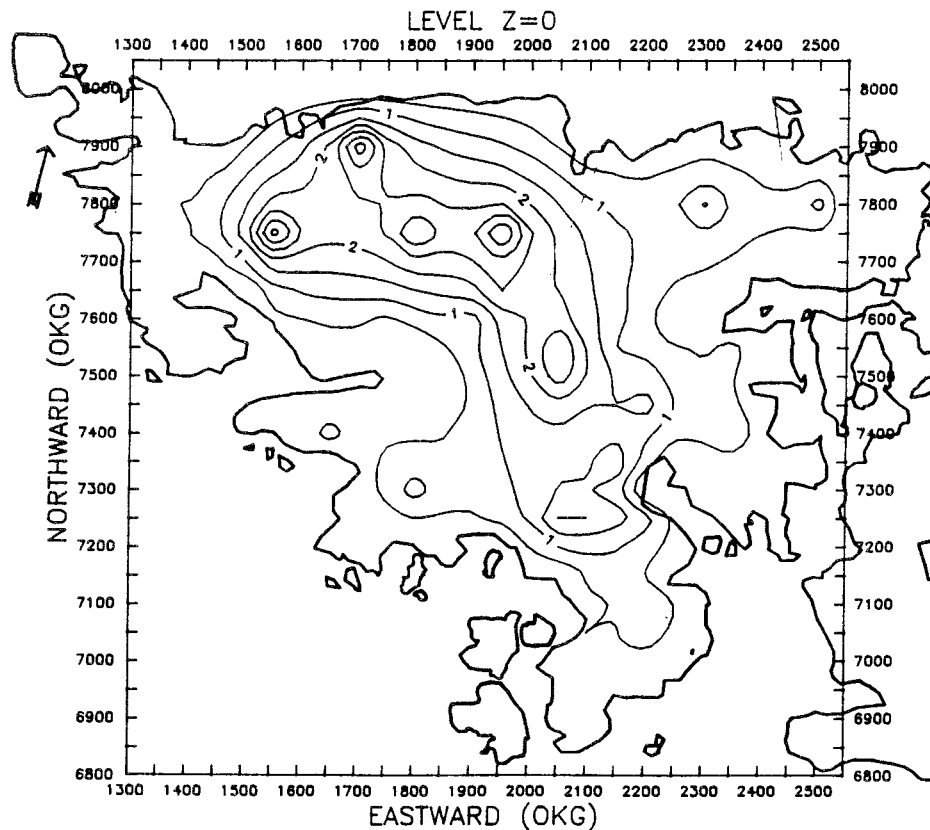


Figure 3.34 The water table on Äspö under undisturbed conditions /Liedholm, 1991; 31/.

Hydraulic tests in the boreholes - introduction

Hydraulic tests were performed in the boreholes in connection with the drilling operations. The tests were made at different stages in the operation and on different

scales. These single-hole tests are evaluated and reported by Nilsson /1987/, Nilsson /1988/, Nilsson /1989/, Nilsson /1990/ and Rhén et al, /1991c/.

The single-hole tests are:

- air-lift tests, in part or all of the borehole
- injection tests over 3 and 30-m sections
- pumping test of the entire borehole
- flow meter (spinner) survey

Based on the test results some conductive sections of the boreholes were selected for transient interference tests. These tests are summarized below under Transient interference tests and reported in Rhén /1989/, Rhén /1990/ and /Rhén et al, /1991c/.

Dilution tests were also performed in some of the sections in most of the coreholes. /Almén and Zellman, 1991/.

Air-lift tests

Air-lift tests were performed in percussion borehole HAS 01-20. The tests in the percussion boreholes were performed as one-hour of air-lift pumping followed by a recovery period. In the core boreholes drilling was interrupted at approximately every 100 m. A packer is set about 100 m above the bottom of the hole, and the air-lift test was done through the packer string. Most tests were performed in an approximately 100-m length of borehole.

The transmissivity in several of the percussion boreholes was very low, so low that the well bore storage in the boreholes made conventional transient analysis impossible. The specific capacity of the boreholes can, however, be related to the previous boreholes (see Figure 3.35), and the transmissivities can be estimated from the relationship between known transmissivities and corresponding specific capacities.

The air-lift tests in the coreholes and percussion holes are presented in Table 3.9 and Table 3.2.8.

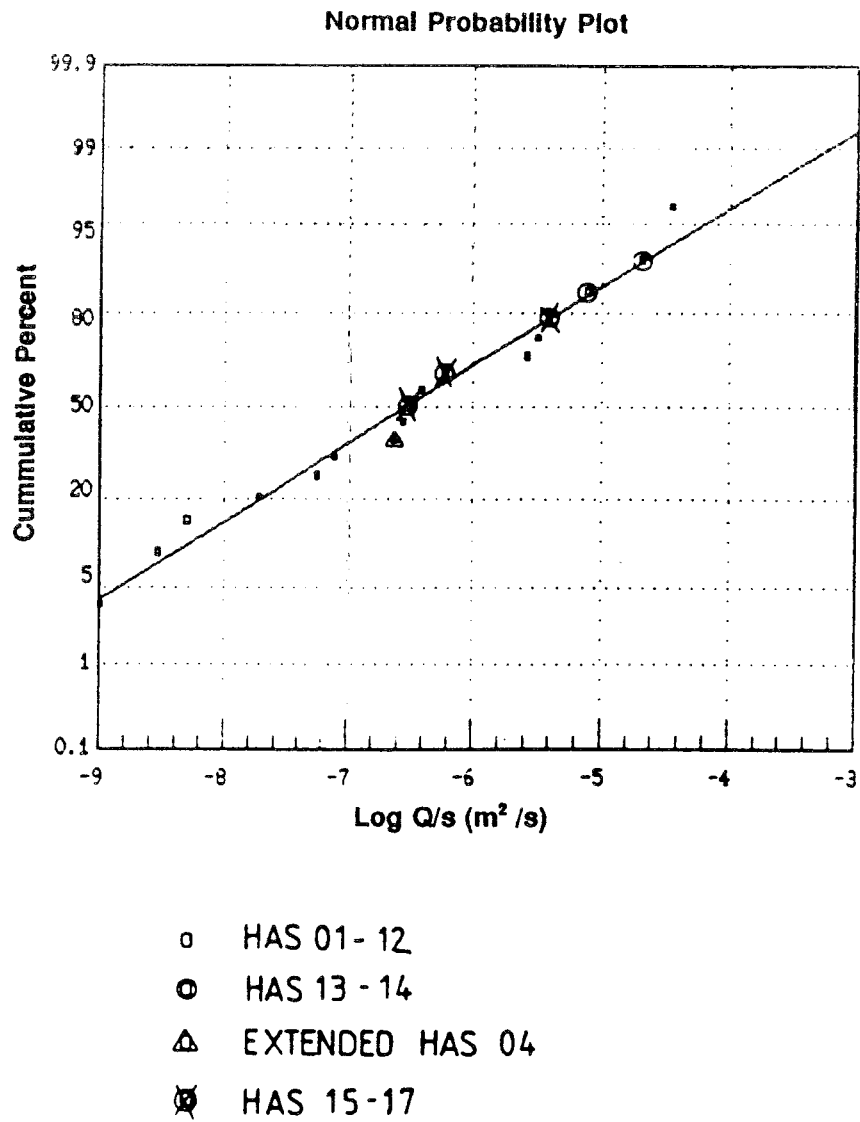


Figure 3.35 Cumulative plot of specific capacities for percussion boreholes on Äspö (HAS 01-17), /Nilsson, 1990/.

Table 3.9 Air-lift test on Äspö coreholes

Borehole	Test level top-bottom (m)	Transmissivity (T) (m ² /s)	Specific capacity (Q/s) (m ² /s)
KAS01	0-101	-	9.0 · 10 ⁻⁸
KAS03	540-638	1.4 · 10 ⁻⁵	1.2 · 10 ⁻⁵
KAS03	640-780	1.3 · 10 ⁻⁵	1.2 · 10 ⁻⁵
KAS04	102-202	7.5 · 10 ⁻⁶	0.5 · 10 ⁻⁵
KAS04	202-325	2.1 · 10 ⁻⁵	1.2 · 10 ⁻⁵
KAS05	0-154	-	1.0 · 10 ⁻⁶
KAS05	156-388	5.5 · 10 ⁻⁶	1.2 · 10 ⁻⁶
KAS05	388-550	1.8 · 10 ⁻⁶	2.3 · 10 ⁻⁶
KAS06	0-100	-	1.4 · 10 ⁻⁶
KAS06	106-217	3.2 · 10 ⁻⁶	8.5 · 10 ⁻⁶
KAS06	217-317	5.9 · 10 ⁻⁶	8.6 · 10 ⁻⁶
KAS06	317-396	8.1 · 10 ⁻⁶	2.4 · 10 ⁻⁶
KAS06	396-505	6.8 · 10 ⁻⁵	2.5 · 10 ⁻⁵
KAS06	505-602	6.5 · 10 ⁻⁶	8.3 · 10 ⁻⁶
KAS07	0-105	-	1.5 · 10 ⁻⁶
KAS07	106-212	1.4 · 10 ⁻⁶	1.8 · 10 ⁻⁶
KAS07	212-304	5.7 · 10 ⁻⁶	2.6 · 10 ⁻⁶
KAS07	372-604	2.9 · 10 ⁻⁵	1.3 · 10 ⁻⁵
KAS07	462-604	1.6 · 10 ⁻⁵	1.1 · 10 ⁻⁵
KAS08	0-104	-	7.1 · 10 ⁻⁶
KAS08	106-208	1.4 · 10 ⁻⁵	1.7 · 10 ⁻⁵
KAS08	208-306	5.7 · 10 ⁻⁶	8.6 · 10 ⁻⁷
KAS08	306-447	-	5.0 · 10 ⁻⁷
KAS08	447-601	1.3 · 10 ⁻⁴	1.5 · 10 ⁻⁵
KAS09	0-100	-	4.8 · 10 ⁻⁶
KAS09	102-189	5.6 · 10 ⁻⁴	5.6 · 10 ⁻⁵
KAS09	189-305	4.2 · 10 ⁻⁴	4.0 · 10 ⁻⁵
KAS09	303-450	2.9 · 10 ⁻⁴	3.3 · 10 ⁻⁵
KAS11	99-244	4.1 · 10 ⁻⁴	5.3 · 10 ⁻⁵
KAS12	0-99	-	5.0 · 10 ⁻⁸
KAS12	102-202	-	1.2 · 10 ⁻⁶
KAS12	204-303	2.9 · 10 ⁻⁵	2.3 · 10 ⁻⁶
KAS12	303-380	4.1 · 10 ⁻⁵	5.1 · 10 ⁻⁶
KAS13	0-100	-	8.0 · 10 ⁻⁸
KAS13	104-211	3.2 · 10 ⁻⁵	2.4 · 10 ⁻⁵
KAS13	210-314	2.9 · 10 ⁻⁵	2.3 · 10 ⁻⁵
KAS13	312-407	2.7 · 10 ⁻⁶	2.7 · 10 ⁻⁶
KAS14	0-100	-	4.2 · 10 ⁻⁶
KAS14	105-212	5.7 · 10 ⁻⁴	2.8 · 10 ⁻⁵
KAS14	154-212	1.4 · 10 ⁻³	5.5 · 10 ⁻⁵
KBH01	0-75	1.6 · 10 ⁻⁴	4.4 · 10 ⁻⁵
KBH02	100-183	3.2 · 10 ⁻⁴	6.2 · 10 ⁻⁵
KBH02	192-304	3.5 · 10 ⁻⁵	3.8 · 10 ⁻⁶
KBH02	408-706	6.5 · 10 ⁻⁴	4.0 · 10 ⁻⁵

Table 3.10 Air-lift tests on Äspö. Percussion holes

Borehole	Test level top-bottom (m)	Transmissivity (T) (m ² /s)	Specific capacity (Q/s) (m ² /s)
HAS01	0-100	-	$1 \cdot 10^{-9}$
HAS02	0- 93	$1.4 \cdot 10^{-4}$	$3.4 \cdot 10^{-5}$
HAS03	0-100	$3.4 \cdot 10^{-4}$	$3.8 \cdot 10^{-6}$
HAS04	0-100	-	< $2.7 \cdot 10^{-7}$
HAS04	0-201	-	$2.4 \cdot 10^{-7}$
HAS05	0-100	$7.5 \cdot 10^{-6}$	$3.2 \cdot 10^{-6}$
HAS06	0-100	-	$2.8 \cdot 10^{-7}$
HAS07	0-100	$1.5 \cdot 10^{-6}$	$3.8 \cdot 10^{-7}$
HAS08	0-125	-	$5.7 \cdot 10^{-9}$
HAS09	0-125	-	$2.9 \cdot 10^{-9}$
HAS10	0-125	-	$5.0 \cdot 10^{-9}$
HAS11	0-125	-	$1.9 \cdot 10^{-8}$
HAS12	0-125	-	$7.9 \cdot 10^{-8}$
HAS13	0- 50	-	$1.8 \cdot 10^{-6}$
HAS13	0-100	$2.5 \cdot 10^{-4}$	$3.6 \cdot 10^{-5}$
HAS14	0- 50	-	$1.3 \cdot 10^{-5}$
HAS14	0-100	-	$7.7 \cdot 10^{-6}$
HAS15	0- 50	-	$5.3 \cdot 10^{-7}$
HAS15	0-120	-	$3.0 \cdot 10^{-7}$
HAS16	0- 50	-	$1.1 \cdot 10^{-7}$
HAS16	0-120	-	$2.6 \cdot 10^{-6}$
HAS17	0- 50	-	$2.5 \cdot 10^{-7}$
HAS17	0-120	-	$6.0 \cdot 10^{-7}$
HAS18	0-150	-	$4.2 \cdot 10^{-6}$
HAS19	0-102	-	$7.0 \cdot 10^{-7}$
HAS19	0-150	$2.6 \cdot 10^{-5}$	$1.1 \cdot 10^{-6}$
HAS20	0-102	$4.9 \cdot 10^{-5}$	$1.8 \cdot 10^{-5}$

Injection tests over 3-m sections

Injection tests over 3-m sections were performed in coreholes KAS 02-08. Due to technical problems with the equipment it was not possible to test the full depth of all holes. The sections tested are summarized in Table 3.11.

Each test was performed as a 10-minute injection period at 200 kPa followed by a 10-minute fall-off period before the packer set was moved.

Data were evaluated in two steps. First a conventional steady-state evaluation was performed for the sections where a reliable flow could be measured using the flow gauge. Based on these data and a regression on the after-flow determined from the pressure decline periods, a new set of flows was calculated. In the second run both steady-state and transient evaluations were performed. Data was found to exhibit approximately log-normal distribution and an example from borehole KAS 03 is shown in Figure 3.36. The results are summarized in Table 3.11.

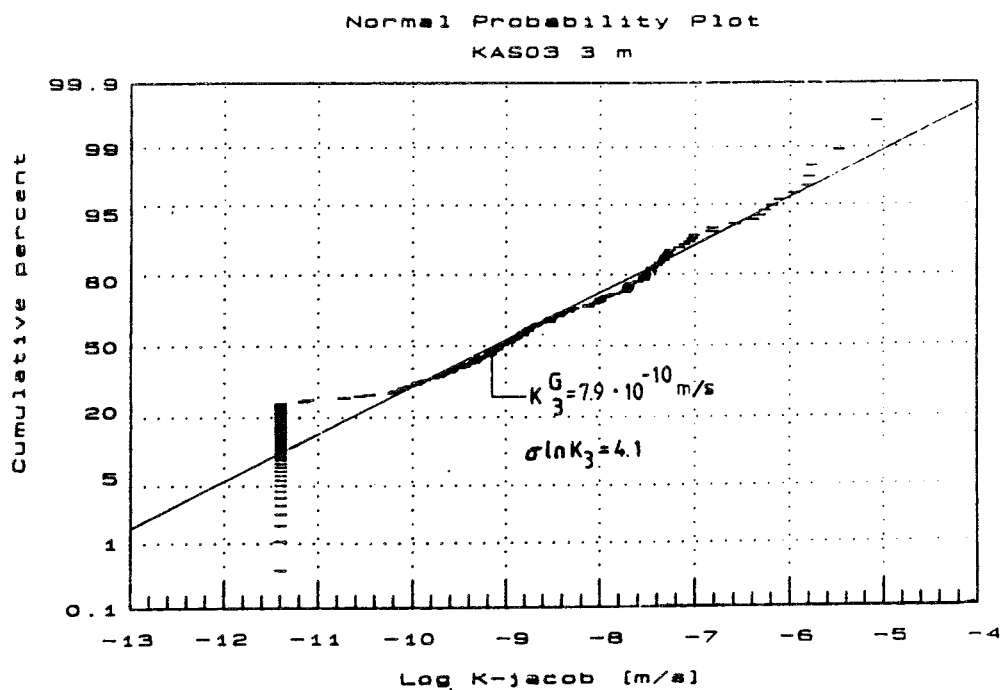


Figure 3.36 Cumulative plot of hydraulic conductivities for 3-m sections in KAS 03. /Nilsson, 1989/.

Table 3.11 Conductivity distribution for 3-m section

Borehole	Section level top-bottom (m)	Arithmetic mean K_a (m/s)	Geometric mean K_g (m/s)	Standard deviation $S_{\ln K}$
KAS02	102-801	$1.7 \cdot 10^{-8}$	$1.3 \cdot 10^{-11}$	4.5
KAS03	103-547	$2.2 \cdot 10^{-8}$	$8.0 \cdot 10^{-10}$	4.2
KAS04	133-454	$7.8 \cdot 10^{-8}$	$8.9 \cdot 10^{-10}$	3.9
KAS05	157-541	$2.6 \cdot 10^{-7}$	$4.6 \cdot 10^{-10}$	4.9
KAS06	105-591	$8.9 \cdot 10^{-7}$	$2.5 \cdot 10^{-10}$	6.2
KAS07	106-592	$5.9 \cdot 10^{-7}$	$4.8 \cdot 10^{-10}$	4.8
KAS08	106-577	$1.3 \cdot 10^{-6}$	$1.0 \cdot 10^{-10}$	6.4

Injections tests over 30-m sections

The injection tests over 30-m sections were performed in three core boreholes. Some sections of the boreholes were also excluded from these tests due to equipment problems. The sections tested are shown in Table 3.12.

Each test was performed as a 120-minute injection period at 200 kPa followed by a 120-minute fall-off period before the packer set was moved.

Data were evaluated under transient conditions for the fall-off period. The hydraulic conductivities were found to exhibit approximately log-normal distribution. An example is shown in Figure 3.37 and the results are summarized in Table 3.12.

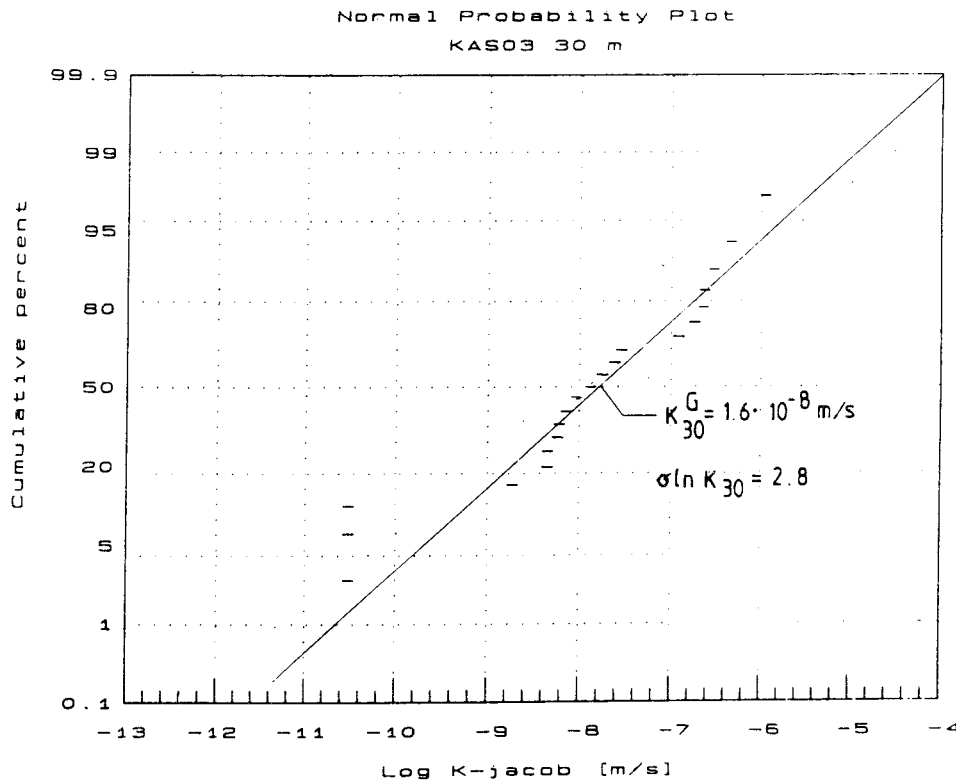


Figure 3.37 Cumulative plot of hydraulic conductivities for 30-m sections in KAS03 /Nilsson, 1989/.

Table 3.12 Conductivity distribution for 30-m sections

Borehole	Section level top-bottom (m)	Arithmetic mean K_a (m/s)	Geometric mean K_g (m/s)	Standard deviation S_{LNK}
KAS02	102-810	$2.9 \cdot 10^{-8}$	$6.3 \cdot 10^{-9}$	2.7
KAS03	103-703	$7.1 \cdot 10^{-8}$	$7.9 \cdot 10^{-9}$	2.5

Pumping tests and spinner surveys

After the end of drilling and testing operations the core boreholes were pumped in order to clean them up and to perform a hydraulic test on the entire borehole. This was made possible because of the telescope design of the boreholes, /Almén and Zellman, 1991/.

This design also made it possible to log the vertical water velocity in the boreholes by means of flow meter logging.

Data from the draw-down period of the pumping test were evaluated by a normal transient analysis and interference with other boreholes was checked. The hydraulic conductivity could then be determined approximately as the derivative of the spinner curve multiplied by the transmissivity of the entire borehole.

Figure 3.38 is shown as an example of the evaluation of data from KAS 03. The figure shows a conventional Jacob plot with an expressed straight line portion and a curve that eventually approaches steady state.

The spinner curve for the same test is shown in Figure 3.39. As can be seen the inflow of water is restricted to very narrow zones, shown as steps in the graph.

The pumping tests in KAS09, KAS11-14 and KBH02 were also performed as interference tests and interference data is discussed later.

The results of the core borehole pumping tests are summarized in Table 3.13.

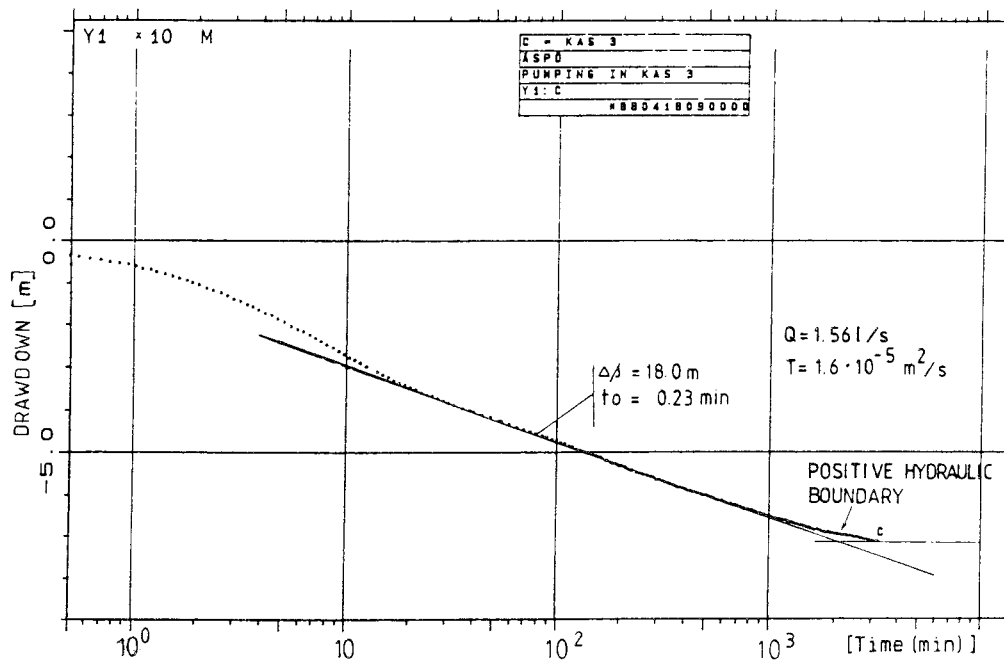


Figure 3.38 Draw-down graph of KAS03 in semilog plot /Nilsson, 1989/.

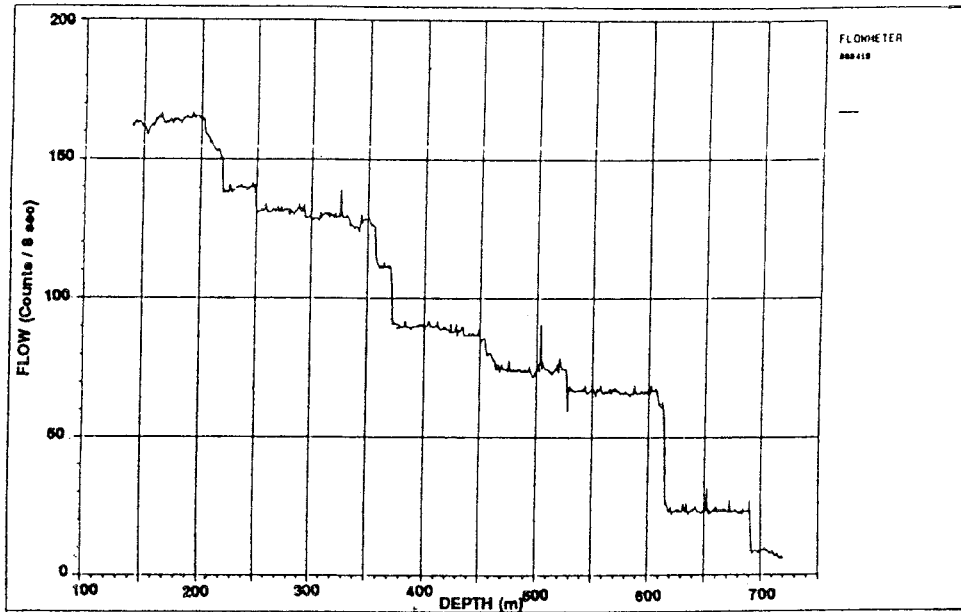


Figure 3.39 Spinner or flow meter curve for KAS03 /Nilsson, 1989/.

Table 3.13 Results from pumping tests in core holes

Borehole	Section level top-bottom (m)	Transmissivity (m ²)	Average hydraulic conductivity (m/s)	Skin factor (-)
KAS02	0- 924	$1.5 \cdot 10^{-4}$	$1.6 \cdot 10^{-7}$	26.0
KAS03	0-1002	$1.6 \cdot 10^{-5}$	$1.6 \cdot 10^{-8}$	-5.0
KAS04	100- 481*	$2.4 \cdot 10^{-5}$	$6.3 \cdot 10^{-8}$	-4.5
KAS05	0- 549	$2.6 \cdot 10^{-5}$	$4.7 \cdot 10^{-8}$	12.2
KAS06	0- 602	$1.0 \cdot 10^{-4}$	$1.7 \cdot 10^{-7}$	5.7
KAS07	0- 604	$4.7 \cdot 10^{-5}$	$7.8 \cdot 10^{-8}$	4.4
KAS08	100- 601*	$2.2 \cdot 10^{-4}$	$4.4 \cdot 10^{-7}$	18.0
KAS09	0- 100	$5.2 \cdot 10^{-5}$	$5.2 \cdot 10^{-7}$	13.0
KAS09	0- 450	$9.7 \cdot 10^{-4}$	$2.1 \cdot 10^{-6}$	2.9
KAS11	0- 249	$4.1 \cdot 10^{-4}$	$1.6 \cdot 10^{-6}$	-4.3
KAS12	0- 380	$4.2 \cdot 10^{-5}$	$1.1 \cdot 10^{-7}$	13.0
KAS13	0- 407	$4.8 \cdot 10^{-5}$	$1.2 \cdot 10^{-6}$	-2.0
KAS14	0- 212	$9.6 \cdot 10^{-4}$	$4.5 \cdot 10^{-6}$	0.6
KBH02	0- 706	$1.0 \cdot 10^{-3}$	$1.4 \cdot 10^{-6}$	2.1

* Casing was set down to 100 m. The casing depth was 1-2 m for the rest of the boreholes.

Summary of results from single-hole tests

The hydraulic testing programme was designed to provide tests on different scales in the different boreholes. It is also evident that the tests gave different results. The reason for this will be discussed later in the text.

A simple way to present the results is to plot data from all tests performed in a borehole as the cumulative transmissivity versus depth, i.e. in the same manner as a spinner survey graph. Figures 3.40 - 3.51 show cumulative plots of all the test methods employed as a function of depth for the core boreholes.

Figure 3.40 shows that the main hydraulic conductor is situated at the bottom of the borehole. The fractures in that section made it impossible to perform packer tests.

It is, however, clear that conductive sections show up in the same places for all the methods employed, which is common for all plots. It is also common that the spinner survey shows the smallest transmissivity, followed by the 30-m packer tests and the 3-m tests.

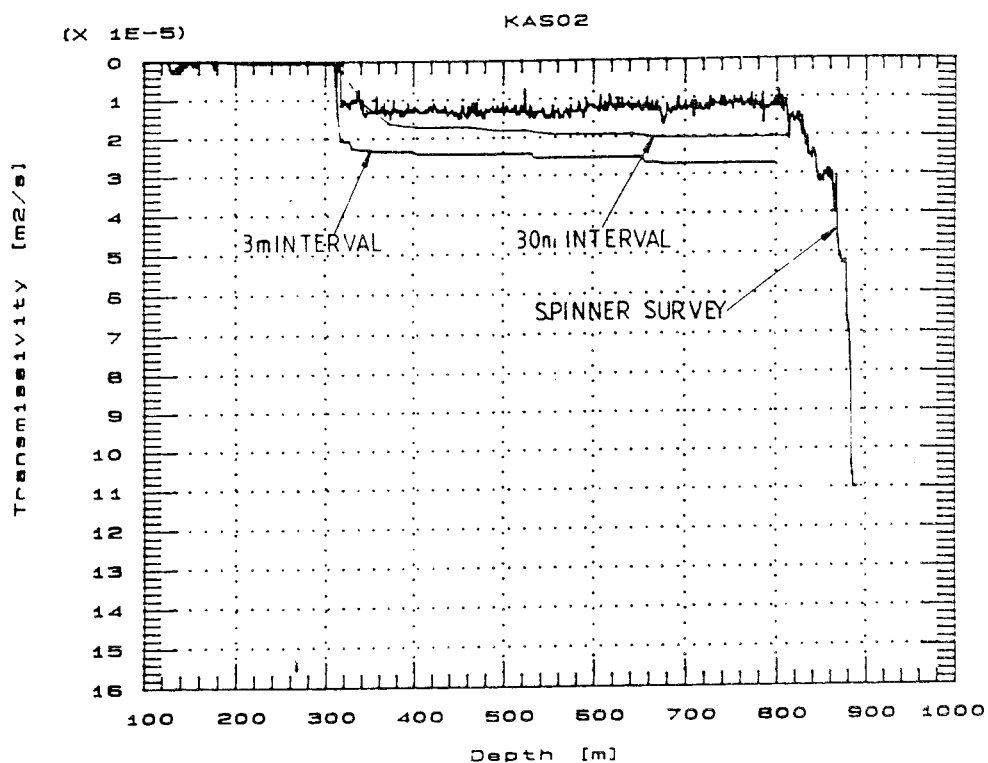


Figure 3.40 Cumulative plot of the integrated hydraulic conductivity versus depth for KAS02 /Nilsson, 1989/.

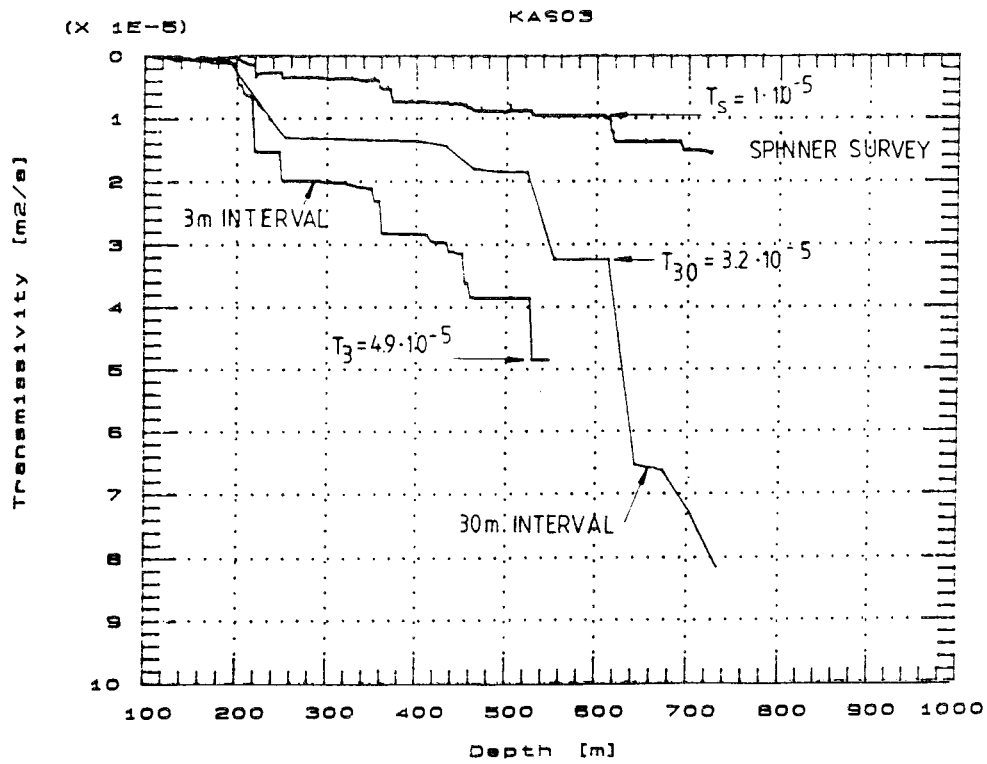


Figure 3.41 Cumulative plot of the integrated hydraulic conductivity versus depth for KAS03 /Nilsson, 1989/.

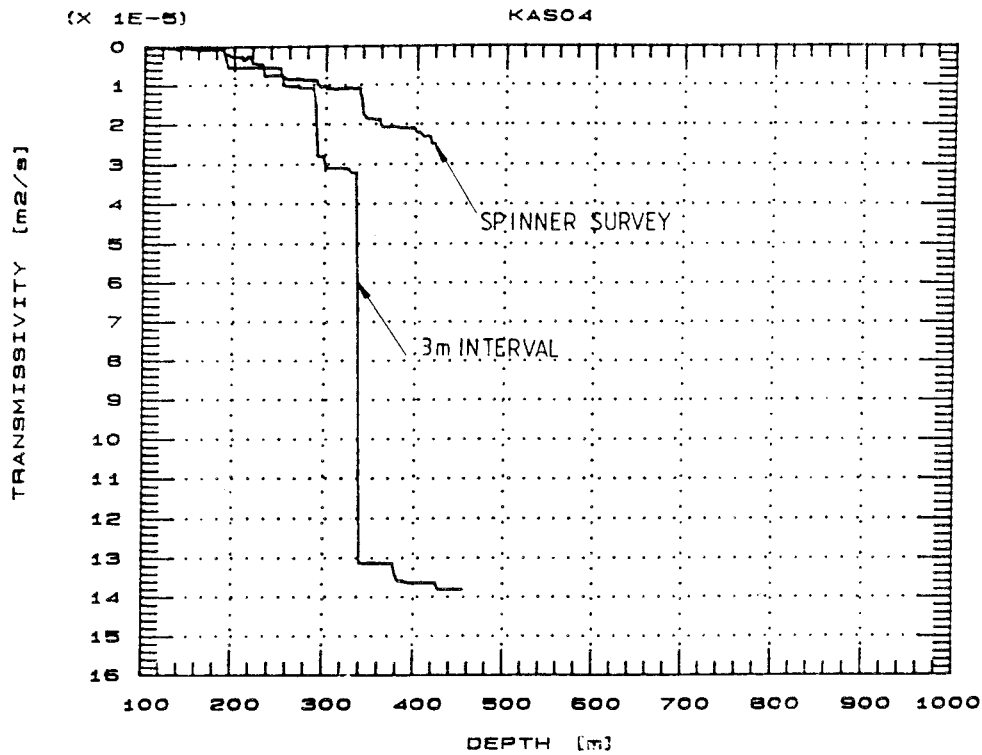


Figure 3.42 Cumulative plot of the integrated hydraulic conductivity versus depth for KAS04 /Nilsson, 1989/.

iii

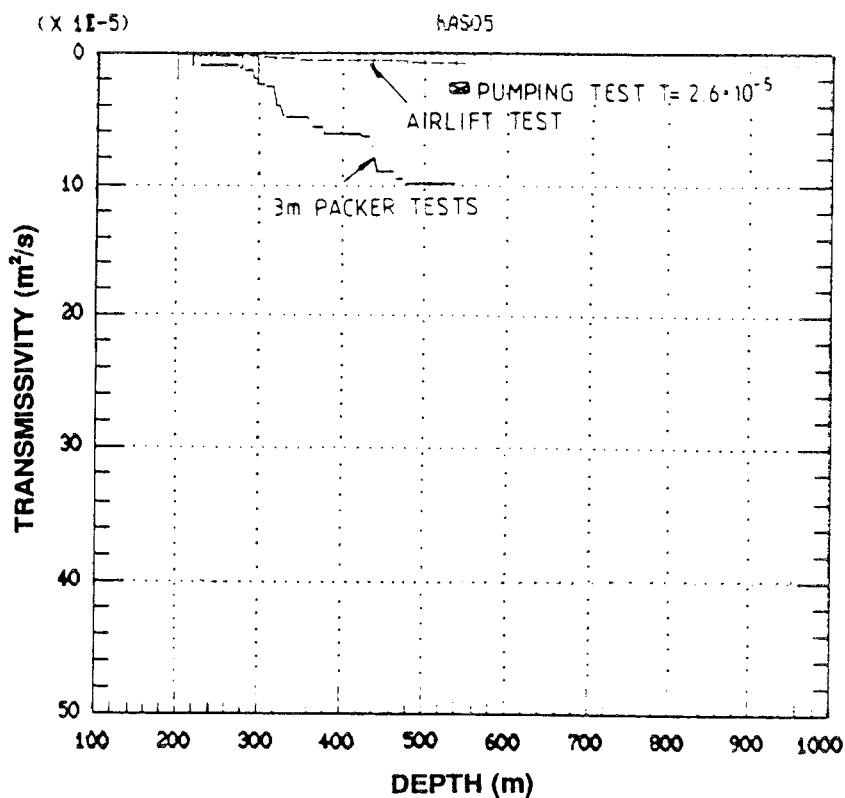


Figure 3.43 Cumulative plot of the integrated hydraulic conductivity versus depth for KAS05 /Nilsson, 1990/.

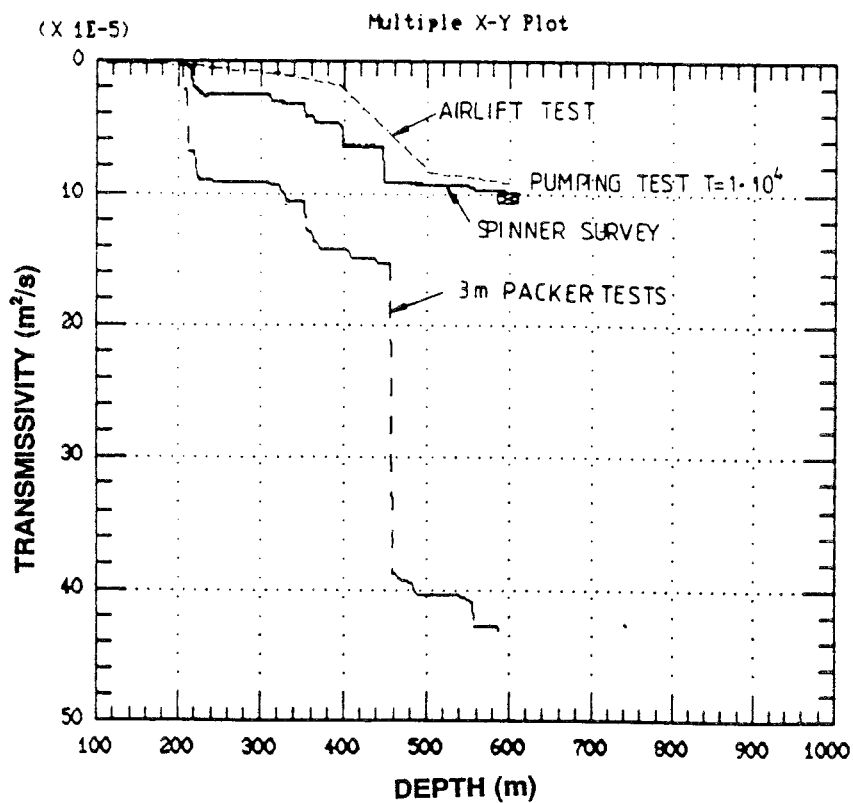


Figure 3.44 Cumulative plot of the integrated hydraulic conductivity versus depth for KAS06 /Nilsson, 1990/.

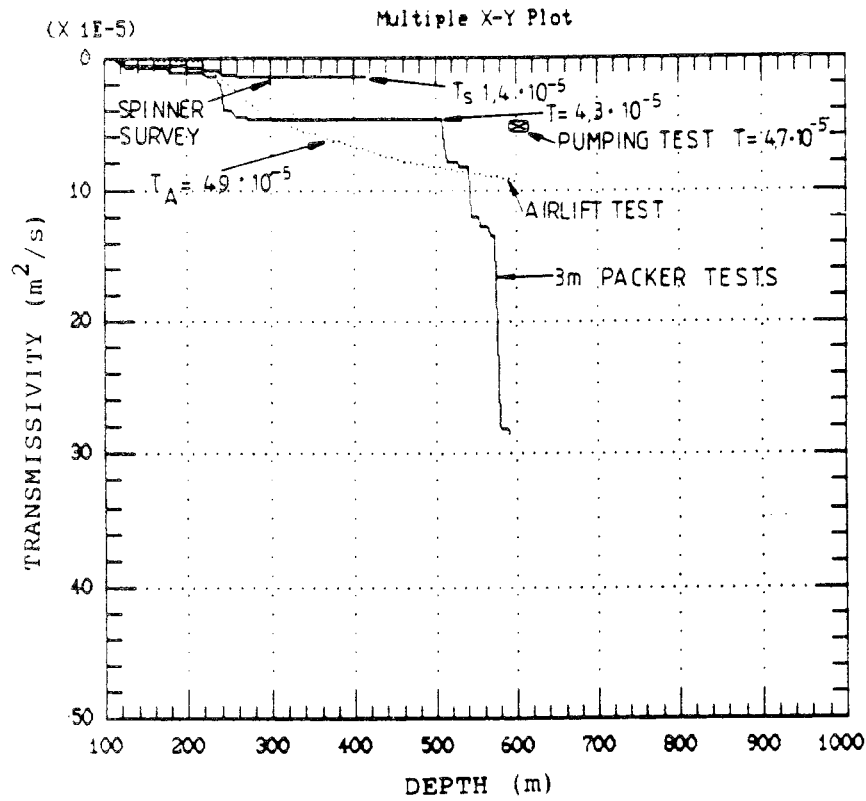


Figure 3.45 Cumulative plot of the integrated hydraulic conductivity versus depth for KAS07 /Nilsson, 1990/.

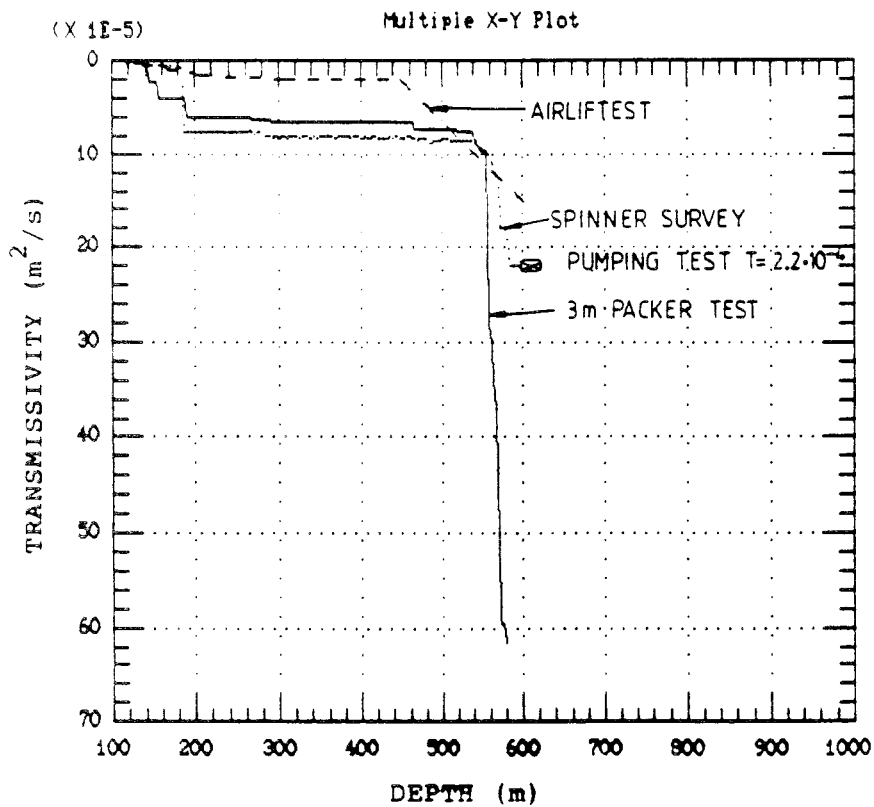


Figure 3.46 Cumulative plot of the integrated hydraulic conductivity versus depth for KAS08 /Nilsson, 1990/.

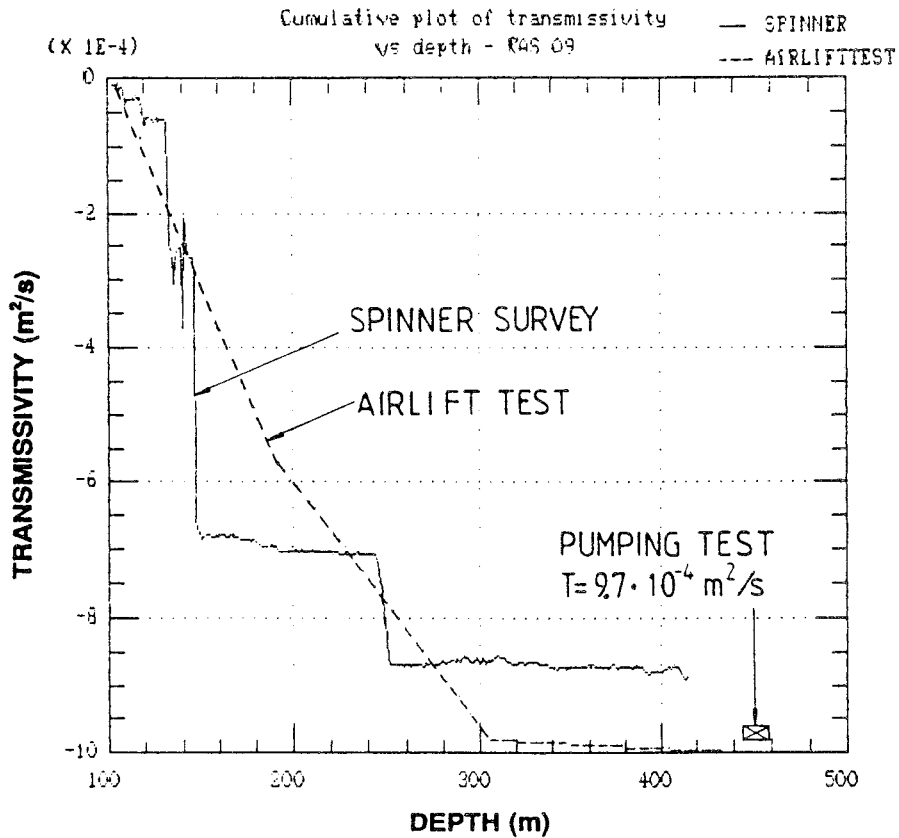


Figure 3.47 Cumulative plot of the integrated hydraulic conductivity versus depth for KAS09 /Rhén et al, 1991c/.

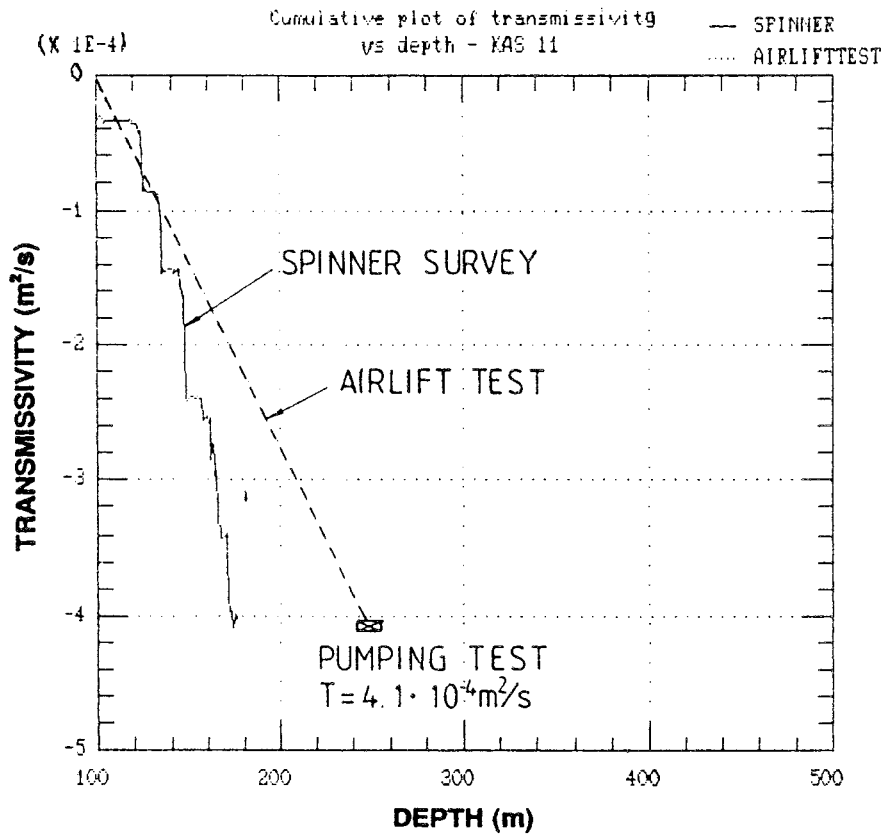


Figure 3.48 Cumulative plot of the integrated hydraulic conductivity versus depth for KAS11 /Rhén et al, 1991c/.

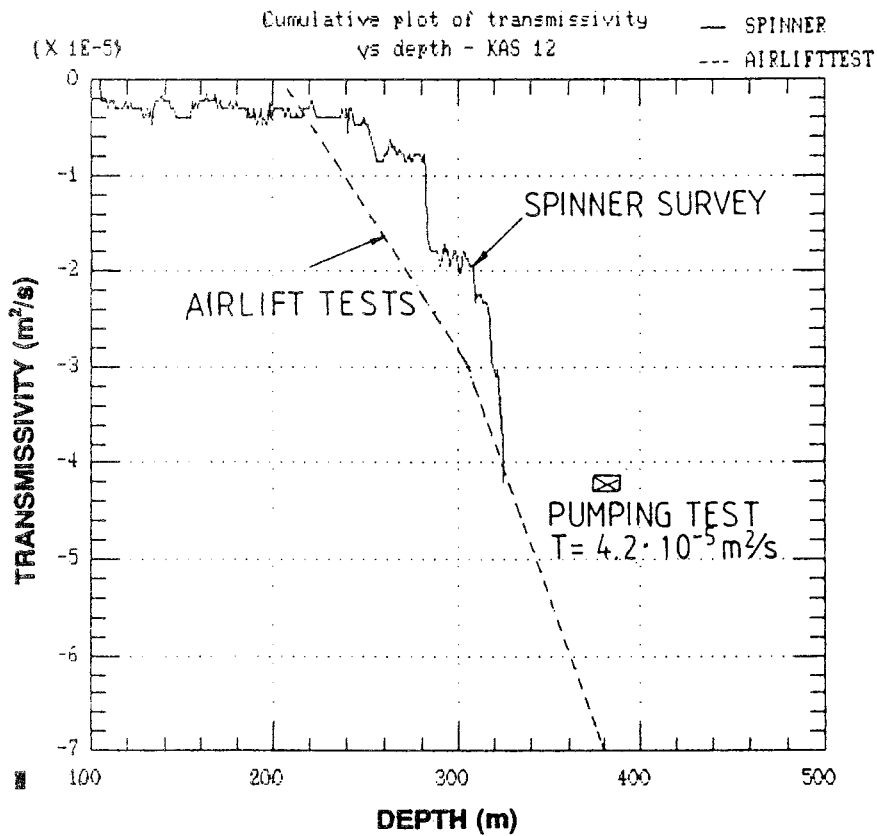


Figure 3.49 Cumulative plot of the integrated hydraulic conductivity versus depth for KAS12 /Rhén et al, 1991c/.

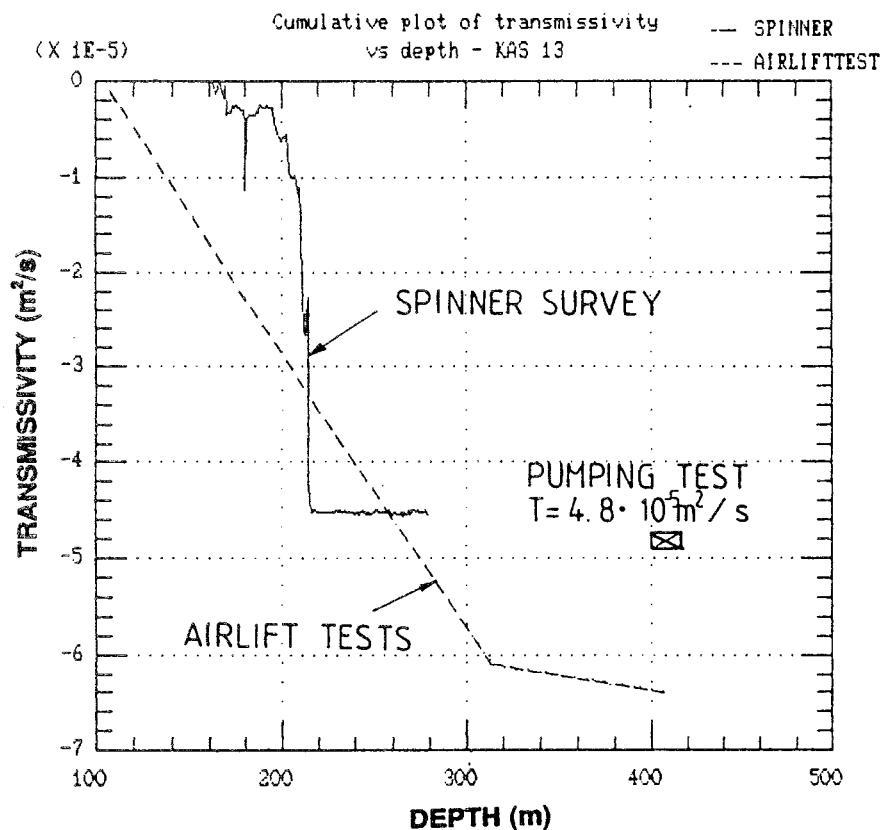


Figure 3.50 Cumulative plot of the integrated hydraulic conductivity versus depth for KAS13 /Rhén et al, 1991c/.

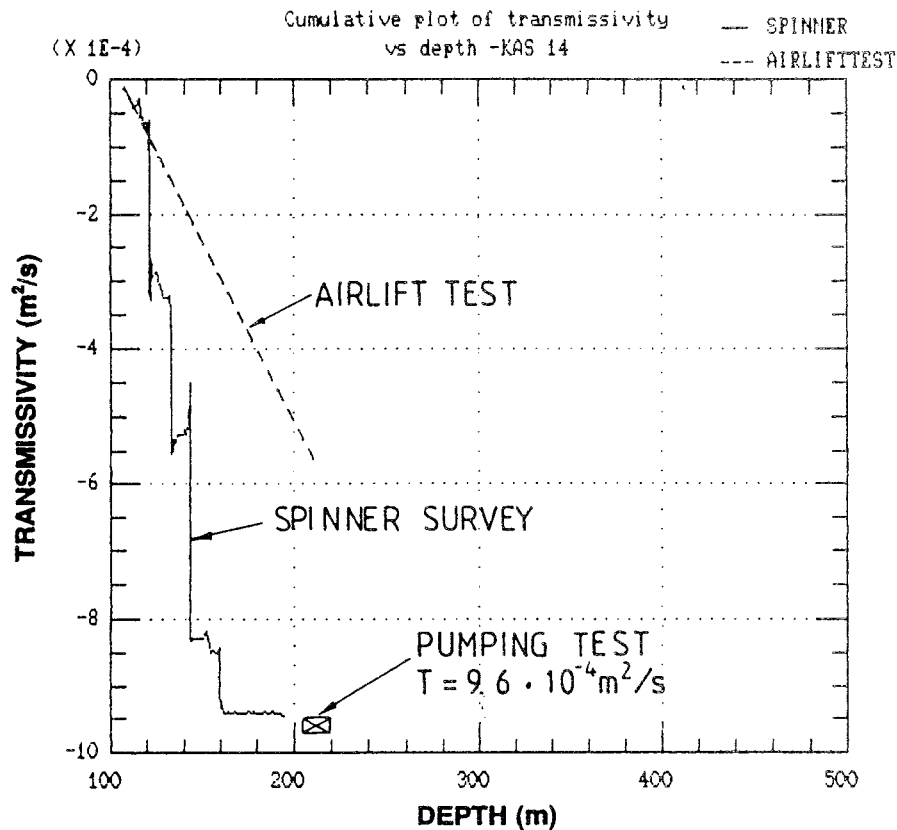


Figure 3.51 Cumulative plot of the integrated hydraulic conductivity versus depth for KAS14 /Rhén et al, 1991c/.

Transient interference tests

In the deep core boreholes, KAS 02-04 and KAS 06, interference pumping tests were performed in selected sections. The test sections were selected on the basis of spinner surveys and packer tests in the boreholes. Pumping tests were also performed in the core boreholes KAS 07, KAS 09, KAS 11-14, KBH 02 and percussion holes HAS 13 and HAS 20. In these cases the entire borehole was pumped.

Three pumping tests were performed in KAS 02, six in KAS 03 and four in KAS 06. One pumping test was performed in each of the remaining holes tested (see Figure 3.53).

The field data are presented in borehole reports and the evaluation of test data is reported by Rhén /1989/, Rhén /1990/ and Rhén et al, /1991c/.

The object of the tests was to determine the hydraulic properties of identified hydraulic conductors on Äspö, their extent and geometry.

Test procedure

Tests in KAS 02, KAS 03 and KAS 06 were made on sections within straddle packers (see Figure 3.52). The packers were connected by steel tubing to the pump, which was placed in the wide, upper part of the borehole. During tests the pressure in the borehole was measured between, below and above the packers. The rate of pumping was measured using double flow gauges.

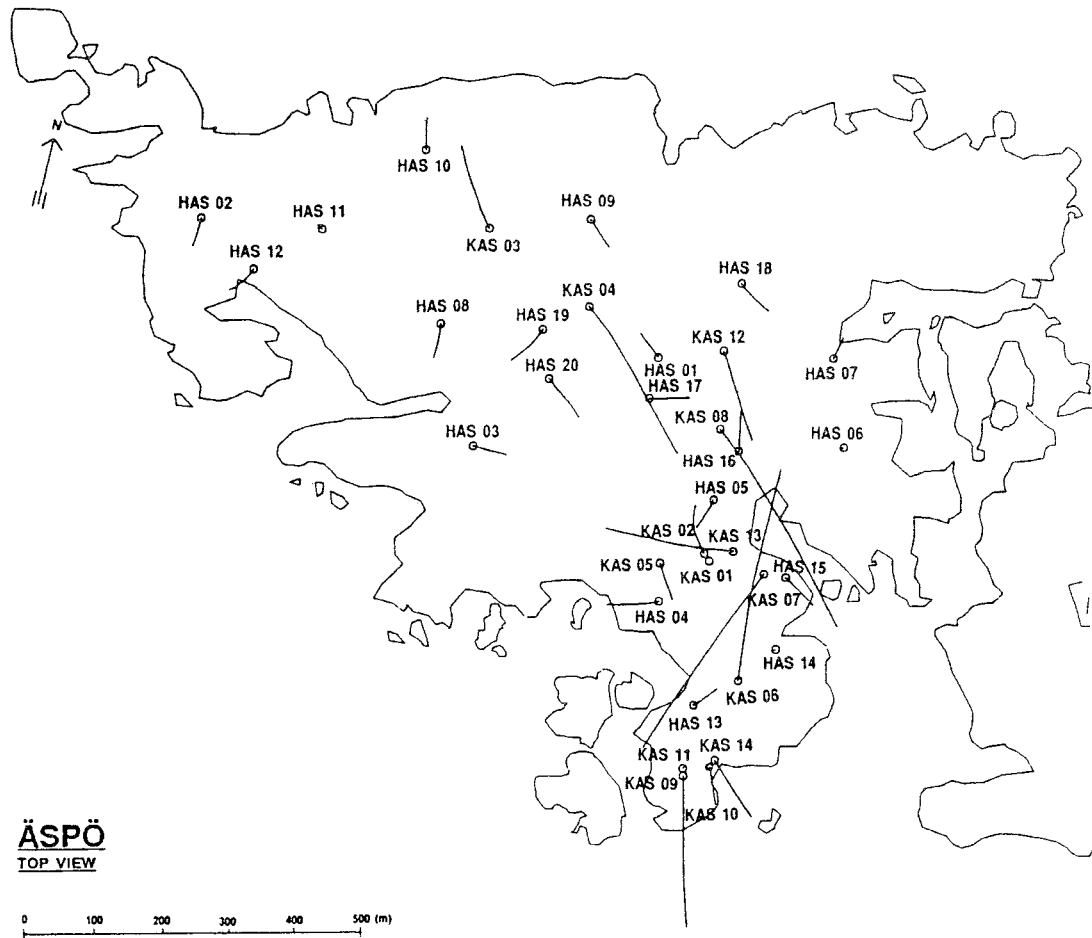


Figure 3.53 Boreholes on Äspö, 1990.

Evaluation

The evaluation of test data was made to clarify three matters:

- The hydraulic properties of the conductor tested as seen from the well. The transmissivity and storage coefficient. The connection of the well to the conductor.
- The geometry and character of the conductor as seen from the well. The boundary conditions.
- The hydraulic properties of the conductors and their geometry as seen from the interference data measured in the surrounding boreholes.

All pumping tests were evaluated under transient conditions using type-curve and lin-log methods. As an example, the evaluation of test No 1 in borehole KAS 03, level 196-223 m, is summarized below. For a complete description see Rhén /1989/.

In Test No 1, section 196-223 m was pumped at a rate of $Q = 1.75 \cdot 10^{-4} \text{ m}^3/\text{s}$ (10.5 l/min). The total draw-down during the 72-h test was measured to be 48.5 m. The conductive section was identified by a spinner survey of the corehole and confirmed by packer tests (see Nilsson /1989/). A lin-log plot of the draw-down between the packers is shown in Figure 3.54.

The curve is interpreted as being an initial linear fracture flow period, deduced from a log-log plot, followed by a dual porosity or layered system, with two straight line portions, 1 and 3, showing the transmissivity of the structure, separated by a transition period. The hydraulic properties evaluated from the straight line portions are shown in Table 3.14.

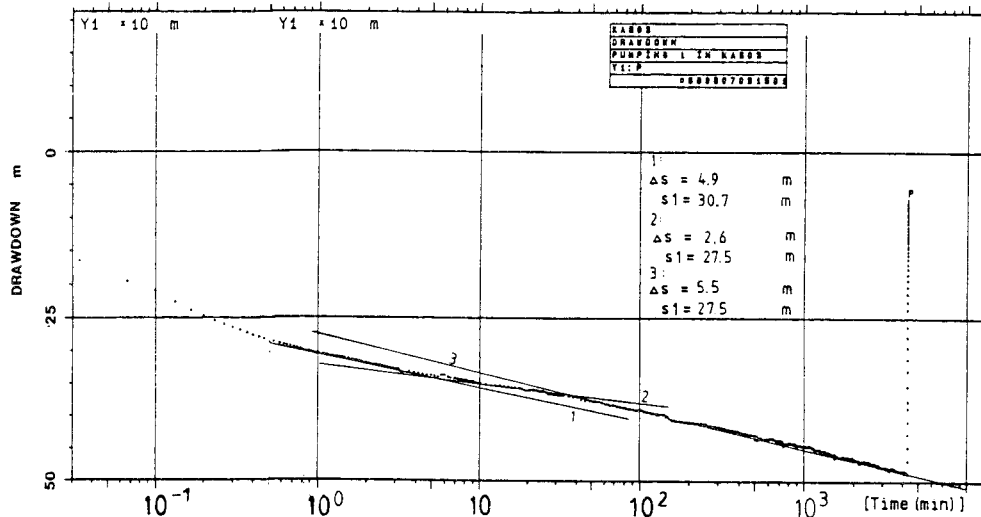


Figure 3.54 Draw-down between packers, KAS 03, 196-223 m /Rhén, 1989/.

Table 3.14 Hydraulic properties in KAS 03, 196-223 m determined for a draw-down period

Straight line No.	Transmissivity T $\times 10^{-5}$ (m^2/s)	Storativity S $\times 10^{-5}$ (-)	Skin factor SK (-)	Well bore storage C_D
1	0.65	0.5	1	24
3	0.58	0.8	0	15

In the test no influence from boundaries can be inferred within approximately 300 m of the section tested. The conductive structure acts as a plane on which radial flow to the well takes place.

The measurements in the surrounding boreholes were analysed both as time-draw-down plots and distance - draw-down plots, one of which is shown in Figure 3.55.

From the distance-draw-down plot it can be seen that several measured draw-downs lie close to the theoretical Theis curve. The hydraulic properties evaluated for different observation points are shown in Table 3.15.

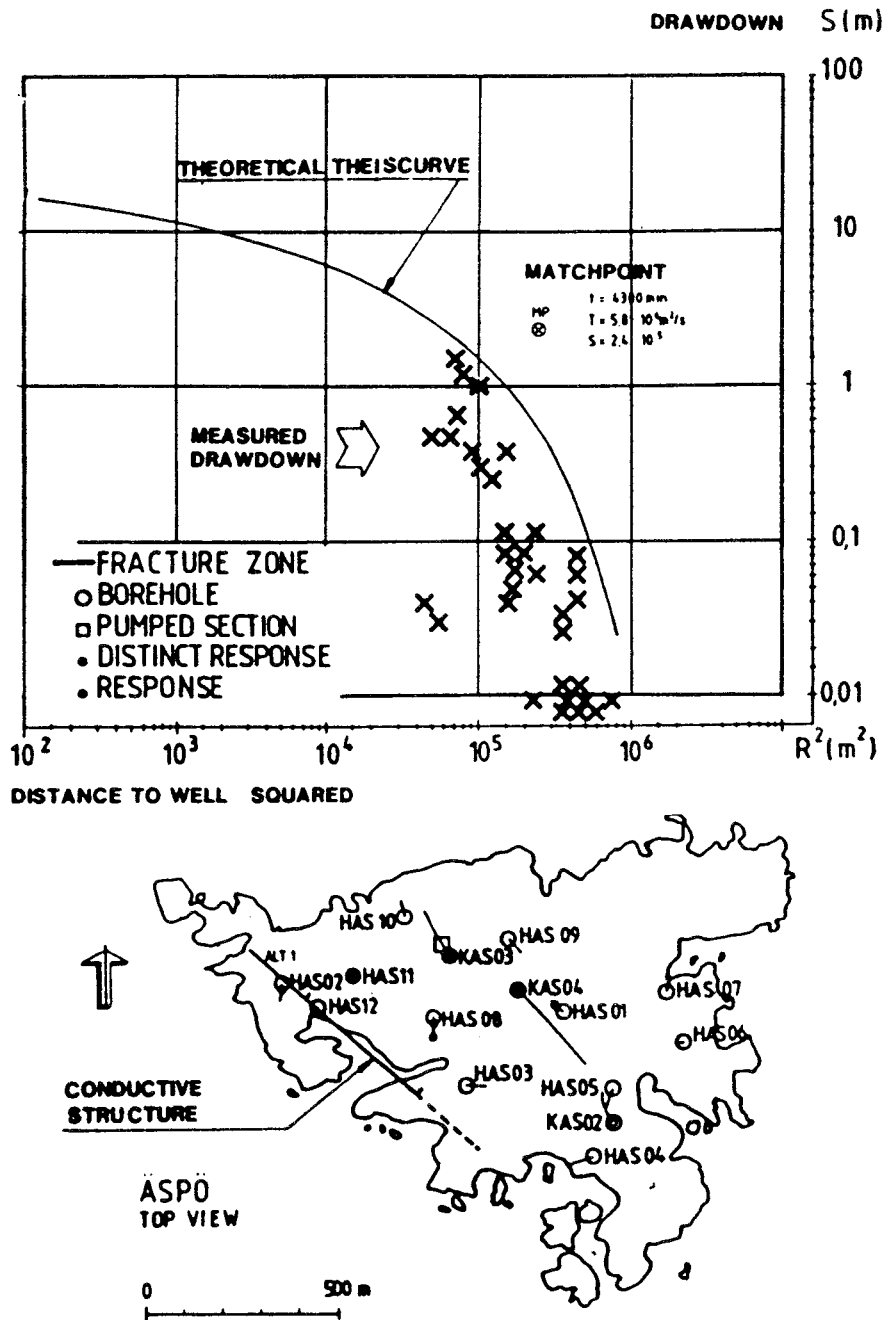


Figure 3.55 Distance-draw-down plot for the test in KAS 03 at 196-223 m /Rhén, 1989/.

Table 3.15 Hydraulic properties evaluated for different observation points, KAS 03, 196-223 m, draw-down period

Borehole	Level	Transmissivity $\times 10^{-5}$ (m ² /s)	Storativity $\times 10^{-5}$ (-)
HAS 08	lower	2.6	1.6
HAS 08	upper	3.5	6.7
HAS 11	lower	2.3	4.3
Distance	Draw-down	0.6	2.4

Apart from the borehole shown above a hydraulic conductor was found in boreholes HAS 01, HAS 02, HAS 04 and KAS 01.

If the boreholes with good contact with the well are assumed to penetrate the same conductive structure, the position of the structure can be deduced geometrically. Figure 3.56 shows its possible intersection with the ground surface. It has a strike of 130° and a dip of approximately 30° towards the N-E.

An evaluation of this type has been made for all tests and a summary of the results is given below.

Test results

A summary of the results is given in Table 3.16 below, together with some comments.

The test performed in borehole KAS 03 showed two groups of conductive structures (see Figure 3.56). The first group has a shallow strike, 130°, with a dip of 30° (Tests 1 and 4). The structures may, however, be the same zone, which in Test 4 is connected to the borehole by a distinct open fracture. The zone strikes parallel to the SW coast of Äspö and dips under the island. The extension towards the SE is not clear.

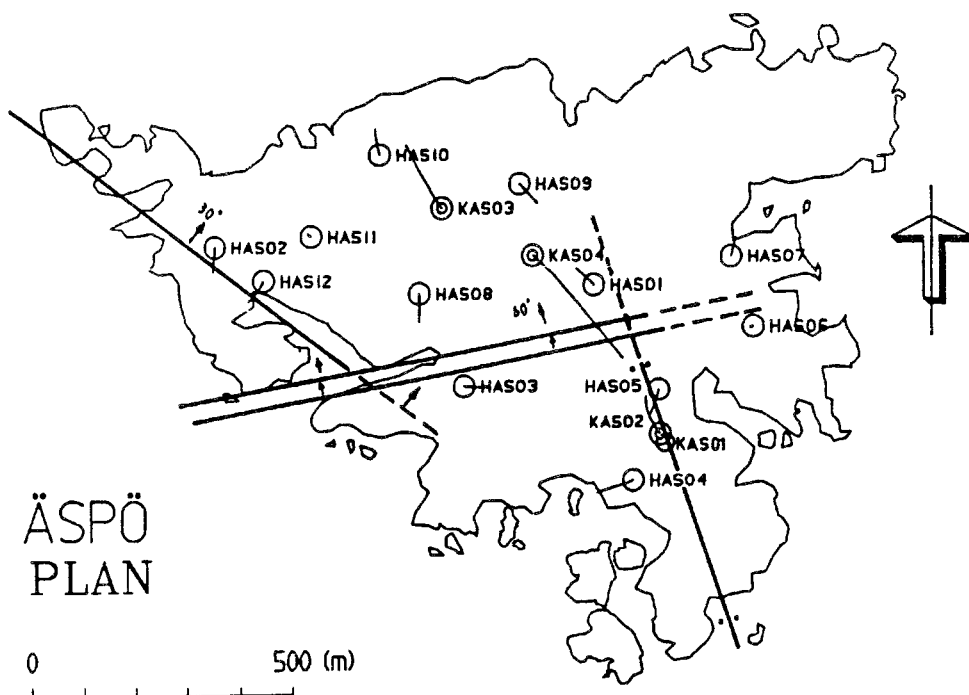


Figure 3.56 Conductive structures determined by interference tests from the first interference tests in KAS 02 and KAS 03 /Rhén, 1989/.

The second group consists of a series of interpreted zones striking 70-80°, dipping towards the north. These zones comply well with the E-W portion of the Äspö shear zone that forms the southern border of NW Äspö.

Tests in KAS 02 also show two distinct features. At depth the conductive structure complies well with the lower boundary of the diorite found in the core borehole, which also was possibly indicated by the reflection seismic investigation. The conductive structure at 308-344 m complies well with the upper boundary of the diorite, but interference data show a vertical conductive structure striking approximately 160°.

Table 3.16 Summary of results from the transient interference tests

Test No	Section	Transmissivity $\times 10^{-5}$ (m ² /s)	Storativity $\times 10^{-5}$ (-)	Distance to boundary R _e (m)
KAS03-1	196- 223	0.7	0.8	> 300
KAS03-2	347- 374	0.6	1.0	> 600
KAS03-3	453- 480	1.0	2.0	> 400
KAS03-4	248- 251	0.7	1.0	
KAS03-5	609- 623	1.0	1.0	large
KAS03-6	690-1002	0.5	0.1	large
KAS02-1	802- 924	25	1.0	150
KAS02-2	308- 344	1.8	1.0	
KAS02-3	117- 126	0.004	1.0	
KAS06-1	204- 277	1.1	0.5	-
KAS06-2	304- 377	3.1	1.	-
KAS06-3	389- 406	4.2	1.	-
KAS06-4	439- 602	10.5	1.	-
KAS07				
LPT	0- 604	27.	1.	probably large
KAS09	0- 450	97.		
KAS11	0- 249	41.		
KAS12	0- 380	4.2		
KAS13	0- 407	4.8		
KAS14	0- 212	96		
KBH02	0- 706	100		
HAS13	0- 100	25.		
HAS20	0- 150	4.9		

The first test in KAS 06 also indicates a NNW striking almost vertical structure at about the same position as Test 2 in KAS 02. The structure is called NNW-1.

The second pumping test in KAS 06 indicates a subhorizontal structure striking E-W and with a dip of 37°N. This structure corresponds fairly well with the gently dipping fracture zones called GDFs in Talbot and Munier, /1989/. In Chapter 3.1 this structure is called EW-5 and is thought to be a complex structure. In the conceptual model the conductive structure EW-5_w is put forward as a single planar structure. This is probably an over simplification but so far the structure cannot be described better geohydrologically for numerical modelling purposes. The pumping test also indicates that the structure may not continue to the east, as no major responses were found in KAS 08.

The responses in interference test KAS 06-3 are complex and probably several fracture systems, such as NNW-1, EW-5 and some E-W and NNW striking structures, affect the draw-down.

Pumping Test No. 4 in KAS 06 indicates another NNW striking vertical structure, here called NNW-2. It is probably not a single fracture zone. The conductor may

consist of several fracture systems with a NNW strike and with approximately vertical dip.

The test in HAS 13 shows that the borehole is in contact with a structure of high transmissivity but does not penetrate the structure as indicated by the large skinfactor. The structure with high transmissivity was probably NE-1 with a ENE strike and a dip of 60-70°N. There were also responses in the upper part of KAS 06 which is an indication that EW-3 may be conductive although the geological interpretation suggests it to be a low or non-conductive structure. EW-5 was also probably active in the test.

The rest of the interference tests were performed by pumping the entire borehole because there was not time for both pumping tests, as described earlier in the text, and interference tests by pumping selected sections of the boreholes. In one sense these interference tests are of lesser quality compared to those already described because there are fewer possibilities to test and identify properties of separate structures. Furthermore, many activities, like drilling, were performed at the same time as testing and in some cases these have made the interference data difficult or impossible to evaluate. In spite of this, the testing was useful for identifying some new structures, giving indications of some possible ones and confirming some structures that had already been indicated in previous tests.

A long-term pumping test was performed in KAS 07 (53 days) and a positive boundary was probably reached during the pumping. The interpretation was difficult because of heavy rainfall during the test. The test clearly indicated the structure NE-1. KAS 07 does not seem to penetrate NE-1 or at least the transmissivity close to KAS 07 is less than the main part of NE-1. NNW-1 and EW-3 were also probably responsible for some reaction in the boreholes.

The aim of drilling KAS 09, KAS 11 and KAS 14 was to penetrate NE-1 to identify its location and hydraulic properties. The pumping tests in these boreholes indicated a conductive structure with high transmissivity. According to a spinner survey the structure comprises two parts, NE-1a and NE-1b, both of which probably have a dip of approximately 70°N. The depth of the structure is probably large, as indicated by responses at the bottom of KAS 02. The pumping tests also showed responses in all sections in KAS 08 and in some of the sections in KAS 12 and HAS 18. This is a good indication that NNW-2 exists and another structure, NNW-4, is also put forward as a possible structure. The responses in sections close to NNW-1 are relatively small which indicates that NNW-1 terminates before it reaches NE-1 or at least its transmissivity is low in the southern part. The responses in HAV 08 and some response in HAV 02 indicate that there must be some N-S striking conductive structures south of Äspö, because EW-5 and NE-1 cannot explain the responses. It has not been possible to identify this or these structures by geohydrological measurements but geophysical measurements indicate several possible structures and two of the major structures have been selected as possible conductive structures, NNW-5 and NNW-6. Responses in HAS 04 in some of the tests also indicate that NNW-5 may be conductive.

NNW-3 was also identified from geophysical measurements as a possible hydraulic conductor which could possibly explain the rather good contact between HAS 13 and NE-1. It was impossible to evaluate the test in KAS 11 as an interference test because of pressure disturbances from other activities.

KAS 12 was drilled to corroborate identification of NE-2. Geologically NE-2 is anticipated to have a rather small transmissivity and the pumping test also shows that it is the NNW striking structures which dominate. Unfortunately the pumping technique with an open borehole gives a high wellbore storage value, which makes it impossible to evaluate early time data and therefore the properties of NE-2, but the responses and the skin factor show that the transmissivity of NE-2 should probably be less than a magnitude of the transmissivity of NNW-2.

KAS 13 was drilled to see if it was possible to better identify the structures with a strike NNW, whose extent and location are difficult to define, and possibly also to reach NE-2. In the test NNW-1 shows up but there may exist a NNW conductive structure west of NNW-1, which it has not been possible to identify. This structure should, however, be of limited extent to the south because it has not been seen in tests performed in the southernmost part of Äspö. NE-2 is thought to be conductive in this part of Äspö because of responses seen in HAS 04.

The properties and direction of the conductive zones intersecting the southern part of KBH 02 have been evaluated from air-lift tests and geophysical measurements (NE-3, NE-4 and EW-7). The tests also show responses which are similar to tests in KAS 09, KAS 11 and KAS 14, which is natural because KBH 02 intersects NE-1. Clear responses in HAV 08 and HAV 02 indicate that the systems EW-7, NE-3 and NE-4 extend a great distance to the east.

The interference test in HAS 20 gave obvious responses at the northern part of Äspö. This test and all the others show that the conductivity of the Äspö shear zone, or at least the northern part of it, is very low, which hydraulically separates northern Äspö from the southern part. The listed boreholes are considered to belong to the northern part of Äspö:

HAS 01
 HAS 02
 HAS 03
 HAS 08
 HAS 09
 HAS 10
 HAS 11
 HAS 12
 HAS 19
 HAS 20
 KAS 04, D6

The storativity indicated in Table 3.2.14 is uncertain. In most of the tests it was difficult to estimate the storativity or specific storativity but the specific storativity (S_s) is estimated to be in the range from 10^{-8} to 10^{-6} (1/m).

The results from all interference tests, together with the geological structural model, formed the basis for the model of the main conductive structures shown in Figure 3.57. This model, with the transmissivities of the structures, is presented in detail in the conceptual model.

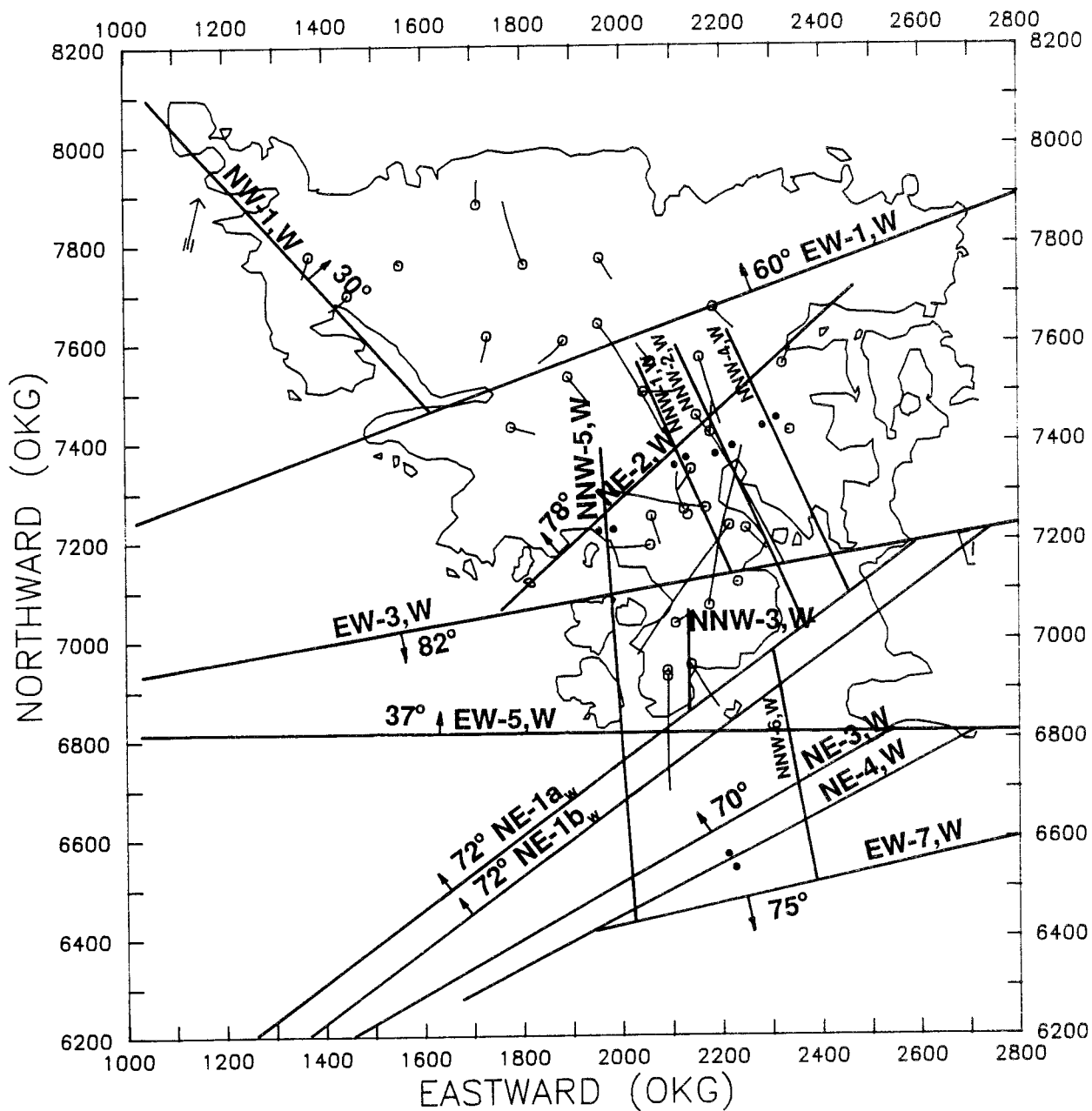


Figure 3.57 Conductive structures determined mainly by interference tests. Some of the structures, in the figure were not seen in the interference test but are considered to be possible conductors. They have been identified from geophysical measurements.

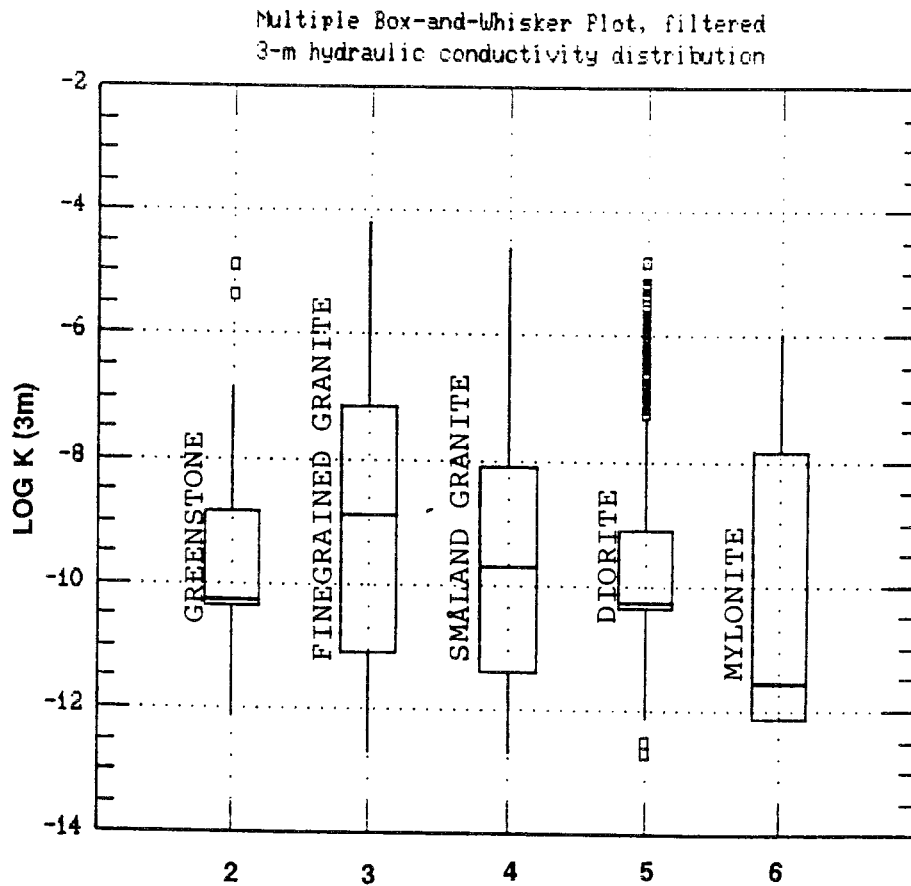


Figure 3.58 Hydraulic conductivity distribution of different rock types. The basis for the calculations were the 3-m injection tests in KAS 02-08.

Rock type 2 = Greenstone
 3 = Fine-grained granite
 4 = Småland granite
 5 = Diorite
 6 = Mylonite

/Liedholm, 1991; 29/

The average hydraulic conductivity of the whole borehole is not simply reflected in the frequencies and hydraulic properties of the most abundant rock types. Thus, it is hardly possible to obtain a simple site-scale model of the average hydraulic conductivity as a function of lithological unit frequency and a representative value of the hydraulic conductivity of the lithological units /Liedholm, 1991; 16/. The relationship is probably complex, as the same lithological units may have different properties in different boreholes.

There is, however, a weak correlation between the lithology and the median hydraulic conductivity on the 3-m scale /Liedholm, 1991; 16/. The correlation for southern Äspö is: $\log K^3_{50\%} = -0.099 \cdot Sg - 0.147 \cdot D - 0.078 \cdot Fg + 0.172 \cdot G$

Sg:	Småland granite (%)	$10\% < Sg \leq 62\%$
D:	Diorite (%)	$12\% \leq D \leq 70\%$
Fg:	Fine-grained granite (%)	$4\% \leq Fg \leq 32\%$
G:	Greenstone (%)	$0.5\% \leq G \leq 13\%$

The 95% confidence interval for $\log K^3_{50\%}$ is approximately $\log K^3_{50\%} \pm 1.2$. The uncertainty increases if the fracture frequency is included in the model.

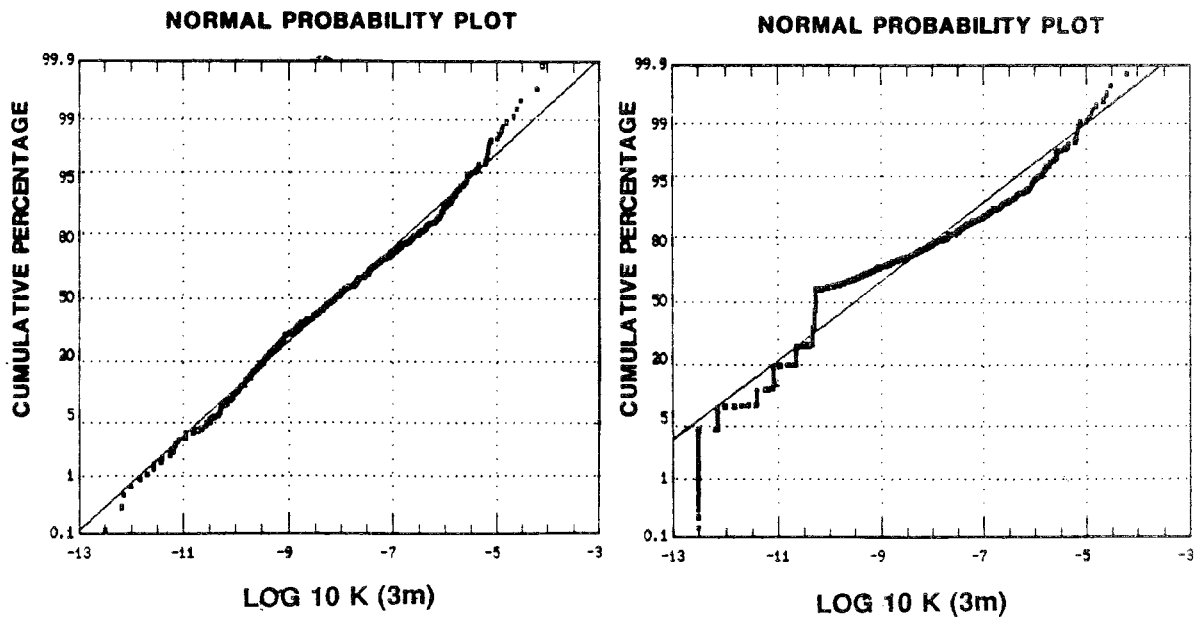


Figure 3.59 Distribution of hydraulic conductivity. Injection test on 3-m scale in KAS 02-08. The figure to the right includes values at the limit of detection or analysis - thus the steps in the graph. Values at the limit of detection or analysis were omitted from the graph to the left /Liedholm, 1991; 8/.

Spatial distribution of hydraulic conductivity

There is no apparent areal pattern in the hydraulic conductivity distribution on the site scale at Äspö, besides, the geometric borehole means of 3-m hydraulic conductivities in the most northern boreholes KAS 03 and KAS 04 are higher. Thus, the SE part of Äspö seems less pervious than the NW part.

The median hydraulic conductivity in the upper part of Äspö (0-100 m below sea level) was estimated to be $K^{100} = 1 \cdot 10^{-8}$ m/s. The distribution of the hydraulic conductivity is shown in Figure 3.59. This is lower than the value for the neighbouring mainland /Liedholm, 1991; 23/. The hydraulic conductivities in the upper part of Äspö tend to increase towards the W. The conductivities in the upper part of Äspö correspond well to the geometric mean hydraulic conductivity from all packer tests if this value is scaled up to 100 m. This means that the hydraulic conductivity in the upper part of Äspö does not differ greatly from the conductivity found at deeper levels.

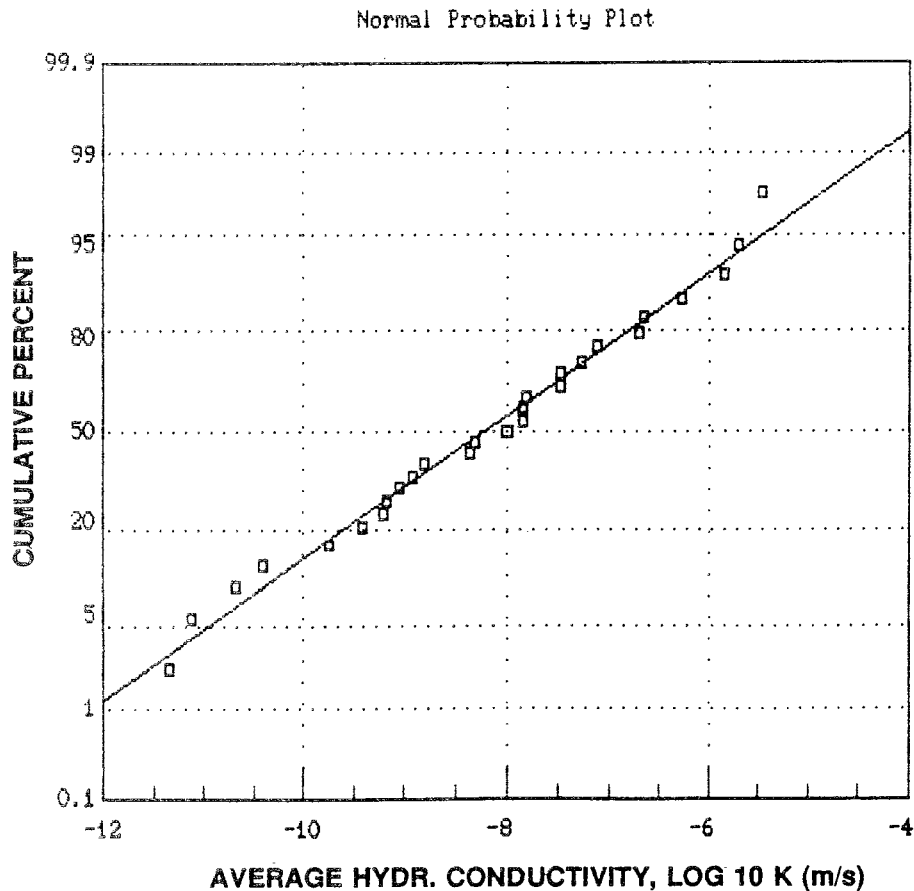


Figure 3.60 Estimated hydraulic conductivity for the upper part of Äspö, 0-100 m below sea level. Conductivity estimated on the 100 m scale /Liedholm, 1991; 23/.

There is, however, a general but weak correlation between depth (100-800 m below sea level) and hydraulic conductivity (K) if all packer tests in KAS 02-08 are merged into one sample /Liedholm, 1991; 14/ (see Figure 3.61). The hydraulic conductivity decreases with depth, according to the figure. However, if boreholes are analyzed individually the hydraulic conductivity may also increase with depth in some of the boreholes /Liedholm, 1991; 8/. The reason for the decreasing conductivity according to Figure 3.61 is the low conductivity in KAS 02, where diorite dominates. The decrease is therefore uncertain because it is based on data from only one borehole. Furthermore, no packer tests were performed at the bottom of KAS 02, which has been proved very conductive.

The standard deviation of log K for all packer tests decreases with depth (see Figure 3.62). The variation in the hydraulic conductivity is, thus, higher in the upper part of Äspö than at deeper levels.

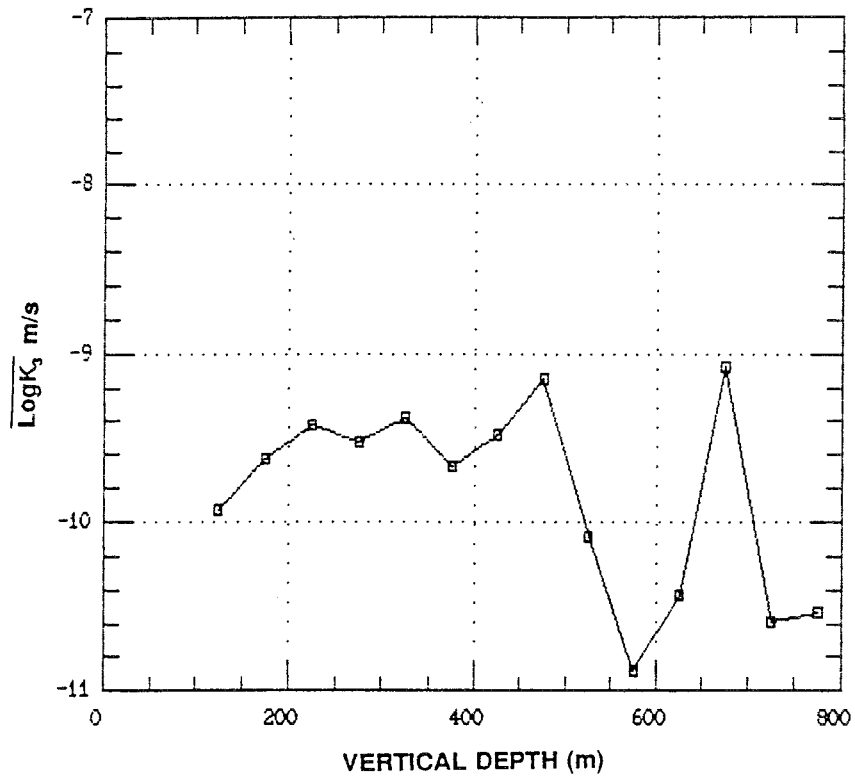


Figure 3.61 Geometric mean over 50-m sections of the logarithmic hydraulic conductivity, KAS 02-08, 3-m scale /Liedholm, 1991; 14/.

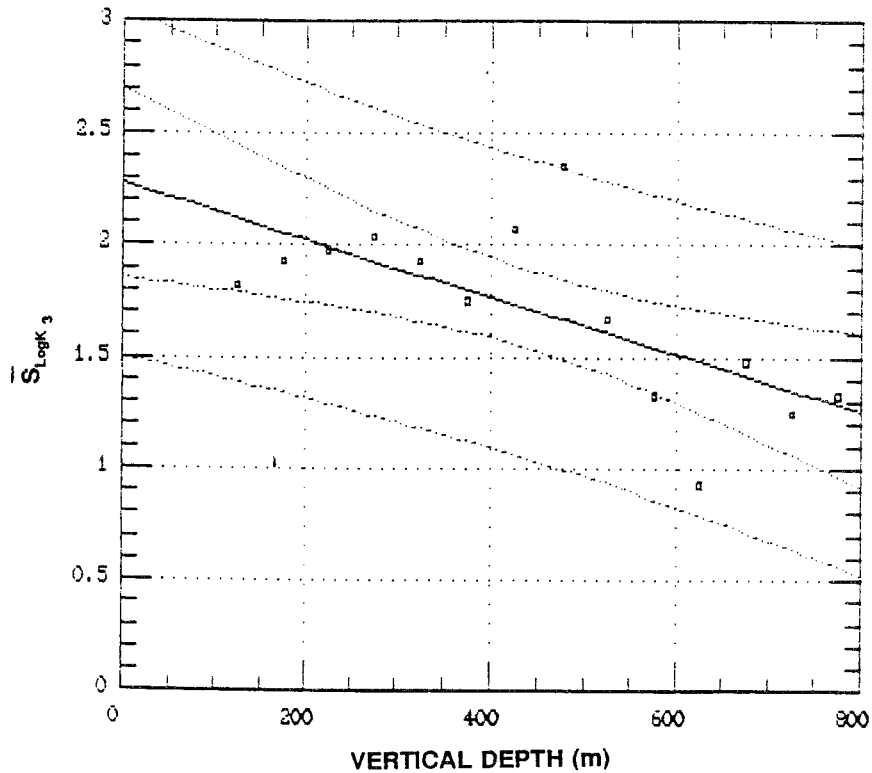


Figure 3.62 Standard deviation of logK for 50-m sections. KAS 02-08, 3-m scale /Liedholm, 1991; 14/.

Over the whole of Äspö, there exists a significant increase in hydraulic conductivity between 100-200 m and 400-500 m depth, as can be seen in Figure 3.61.

Considering the individual measurements on the 3-m scale between 0-500 m below sea level a higher frequency of high conductivity sections ($K > 10^{-6}$ m/s) can be expected between 300-350 and 450-500 m below sea level on southern Äspö /Liedholm, 1991; 15/.

There seems to exist a cyclicity of the logarithmic hydraulic conductivity versus depth. The cyclicity of 120-140 m wave-length /Liedholm, 1991; 2 and 5/ with depth is in accordance with the anticipated distance between gently dipping fracture zones (GDF) /Talbot and Munier, 1989/.

Hydraulic conductivity and scale

Hydraulic tests on different scales produce different conductivity distributions. The characteristic means converge towards the borehole average.

Based on information from KLX 01 and KAS 02-08 a significant correlation exists between the geometric mean and relative scale as well as arithmetic mean and relative scale /Liedholm, 1991; 19/. This means that the averages of the hydraulic conductivity in a borehole cannot be used to predict properties on another scale. The result may, however, be transformed to another scale. The transformation factors that have been calculated are shown in Figure 3.63.

The standard deviation of the hydraulic conductivity also decreases as the sample scale increases /Liedholm, 1991; 19/ (see Figure 3.64).

For small scales the impact of extreme hydraulic conductivities become prominent (few individual fractures) whereas the larger scale samples comprise a large number of "extremes" which smoothen out the impact of individual fractures.

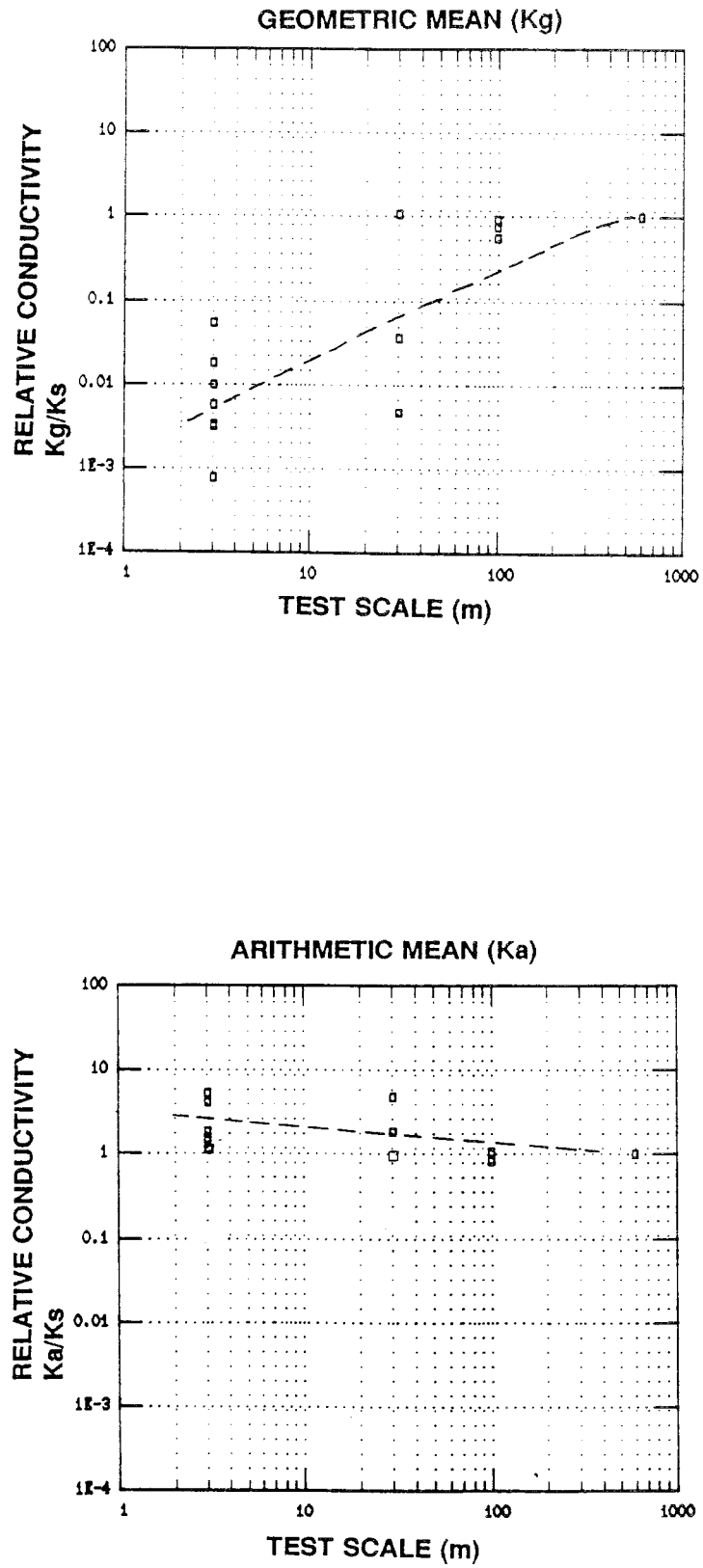


Figure 3.63 Relative hydraulic conductivity for different test scales. Full scale conductivity = the average hydraulic conductivity calculated from the transmissivity value evaluated from the test on the whole borehole /Liedholm, 1991:19/

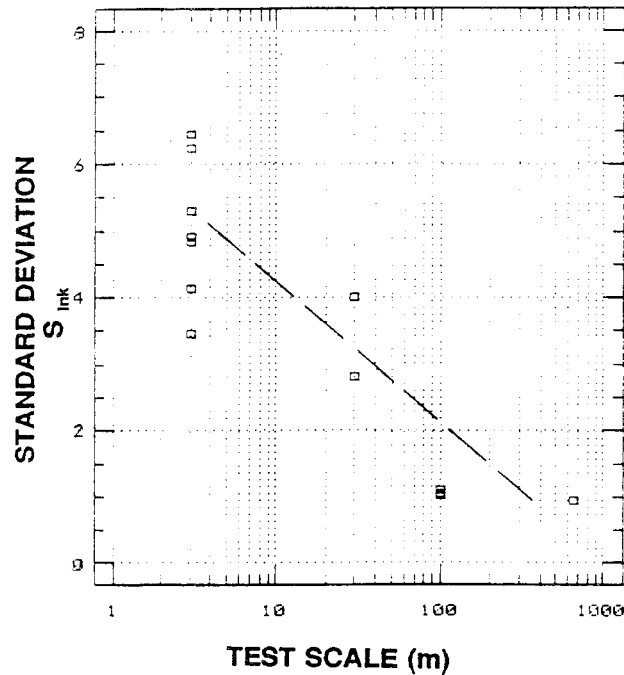


Figure 3.64 Standard deviations for the distributions of logK /Liedholm, 1991; 19/.

Hydraulic conductivity and fracture characteristics

A wide range of transmissivities may be found for individual conductive fractures /Liedholm, 1991; 6 and 13/. Transmissivities of conductive fractures may commonly be up to the order of 10^{-4} m²/s /Liedholm, 1991; 6 and 13/.

In Axelsson et al, /1990/ and Liedholm /1991; 6/ the transmissivity distribution of individual fractures has been estimated using a computer model. The transmissivities estimated from the 3-m injection test fracture trace length was used as input data and it was assumed that the conductive fractures were in accordance with the Poisson distribution and that the fracture transmissivities were in accordance with a log-normal distribution. The results are presented in Table 3.18.

Table 3.18 Estimated transmissivity distribution of individual fractures. Fractures with transmissivity $< 1 \cdot 10^{-11}$ m²/s were considered non-conductive /Axelsson et al, 1990/, /Liedholm, 1991; 6/

Rock type	Mean transmissivity Log $T_i^{50\%}$ (m ² /s)	Standard deviation $S_{\log T_i}$	Non-conductive fractures (%)	Number of conductive fractures per 3-m interval
Småland granite	-5.9	0.9	61	0.51
Fine-grained granite	-7.3	1.4	44	0.84

In Liedholm /1991; 12 and 13/ sections 380-430 m and 510-560 m in KAS 06 were examined. The number of conductive fractures in each section that was subjected to injection testing (3-m scale) was identified by means of geological core mapping, geophysical borehole logging, geohydrological tests and spinner measurements /Sehlstedt and Strähle, 1991/.

Three types of fracture were identified in core mapping: Coated fractures, sealed fractures and breaks. Only coated fractures were analysed, except for what are called "conductive fractures", in the paper below. The "conductive fractures" identified by Sehlstedt are a part of the coated fractures.

The transmissivities of the conductive fractures seemed to follow a log-normal distribution with $\text{Log } T_i^{50\%} = -7.3$ and $S_{\text{Log } T_i} = 1.1$. The arithmetic means of the number of conductive fractures were 1.3 and 1.6 per 3-m section respectively /Liedholm, 1991; 12/. Only a weak correlation was found between the number of conductive fractures and the transmissivity /Liedholm, 1991; 13, Liedholm, 1989/.

The conductive fractures seem to be clustered /Liedholm, 1991; 12/. The distance between the clusters was subjectively estimated at 3-13 m.

The distance between individual conductive fractures and between individual coated fractures followed an approximately log-normal distribution Liedholm /1991; 12/ (see Figure 3.65), and the statistics shown in Table 3.19.

Table 3.19 Distance characteristics for KAS 06, sections 380-430 m and 510-560 m /Liedholm, 1991; 12/.

		Arithmetic mean distance (m)	Median distance (m)	Standard deviation
380-430	conductive fr	2.28	0.80	3.67
"-	coated fr	0.44	0.28	0.64
510-560	conductive fr	1.84	0.71	2.39
"-	coated fr	0.51	0.31	0.66

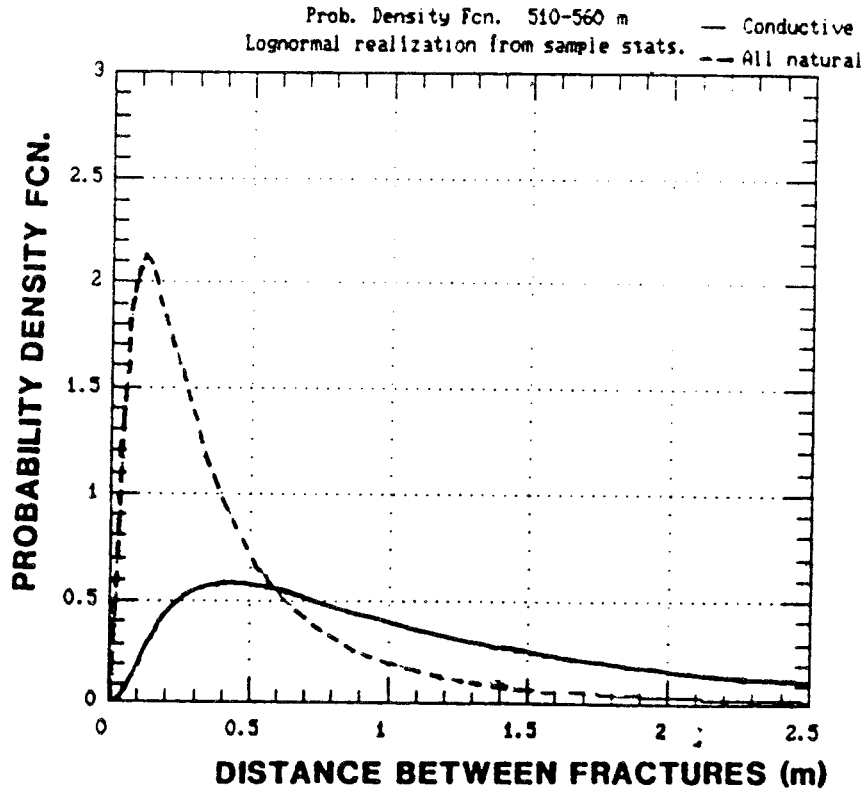
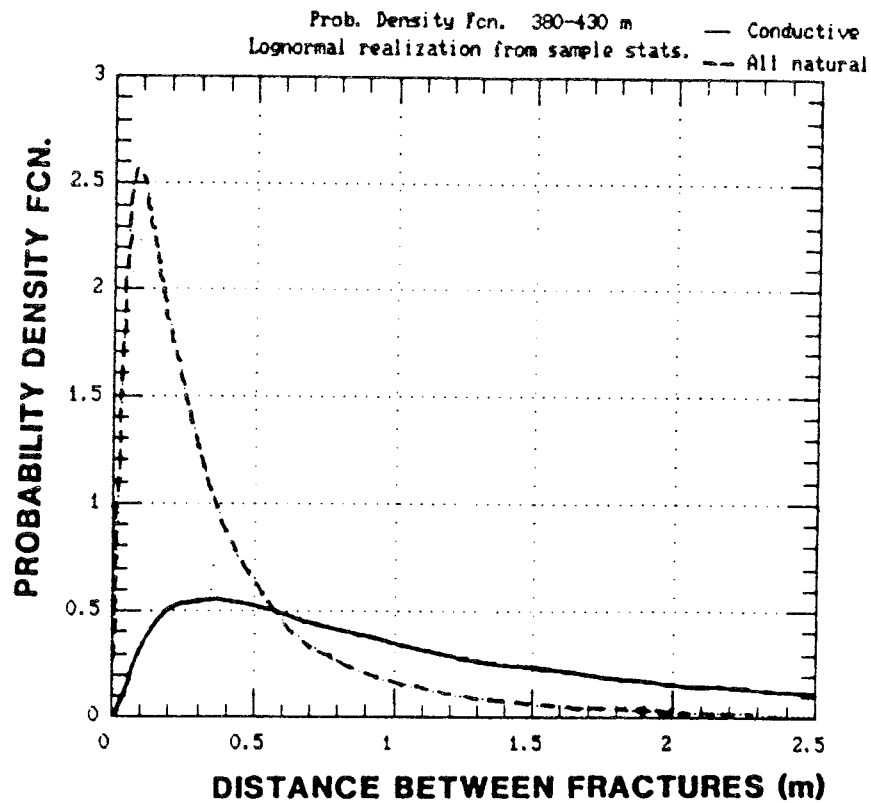
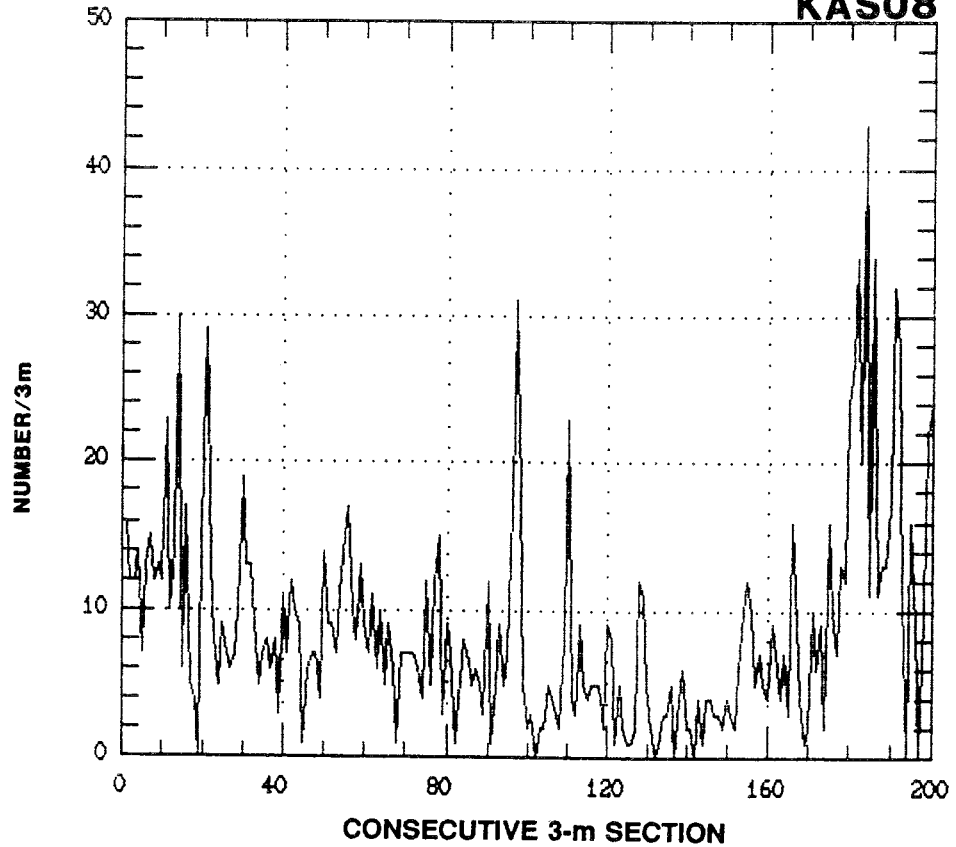


Figure 3.65 Frequency distribution of conductive fractures and coated fractures (= all natural) for KAS 06 sections 380-430 and 510-560 /Liedholm, 1991; 12/.



Estimated Autocorrelations

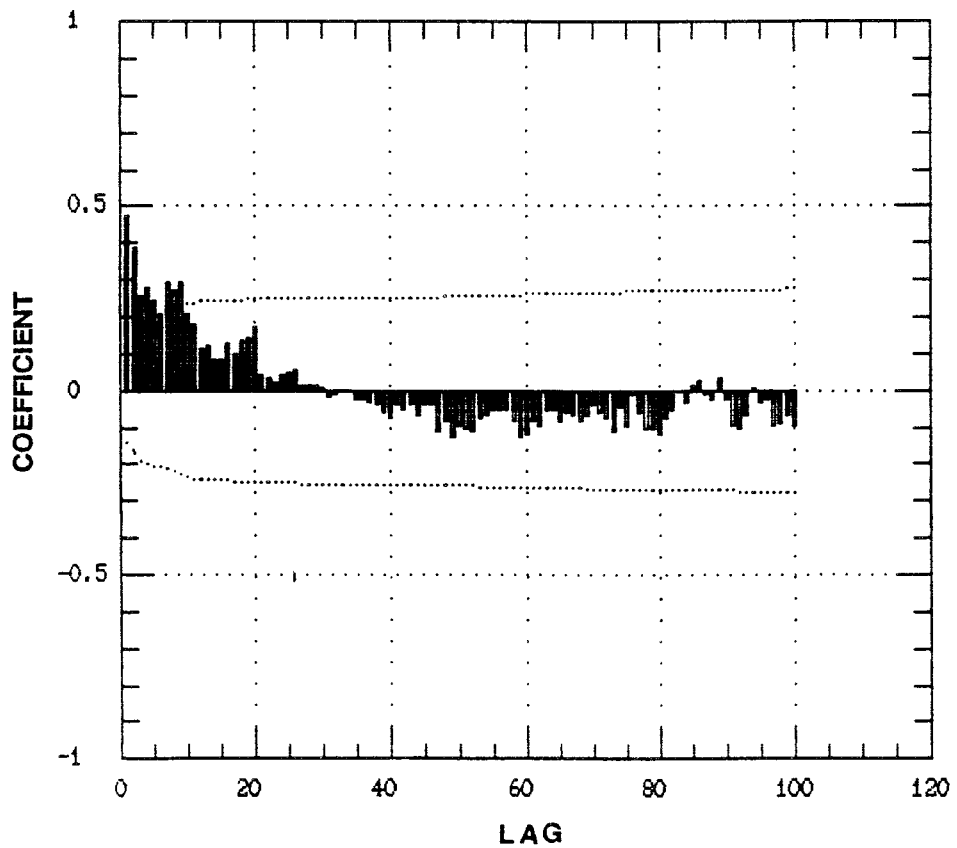


Figure 3.66 The correlation ranges of fracture frequency series. The correlation range is in the figure estimated to be $30 \text{ m} = 3 \text{ m} \cdot 10 \text{ lags}$. Borehole KAS 08. The data is in this case has not been adjusted for the trend. The dashed lines are plotted at zero plus and minus twice the large standard error for each coefficient /Liedholm, 1991; 27/.

The series of hydraulic conductivities and fracture frequencies are correlated for the same boreholes /Liedholm, 1991; 27/ with regard to correlation ranges, that is, the distance of sections with related magnitudes. The correlation ranges for an average value of a 3-m section is commonly less than 6 m for the logarithmic hydraulic conductivity series /Liedholm, 1991; 9/ and about 10 m for the fracture frequency series /Liedholm, 1991; 27/.

The linear correlation between the average logarithmic hydraulic conductivity and the number of open, coated fractures is weak but significant. The number of coated fractures probably only explains a minor part of the variation in hydraulic conductivity. About 20 additional coated fractures per 3-m increases the average hydraulic conductivity about ten times /Liedholm, 1991; 21/. The coated fracture frequency was in the order of 3 fractures per m /Liedholm, 1991; 11/ and the frequency is higher between 0-100 and 350-400 m below sea level. Borehole KAS 02, KAS 04-08 was examined in the two articles.

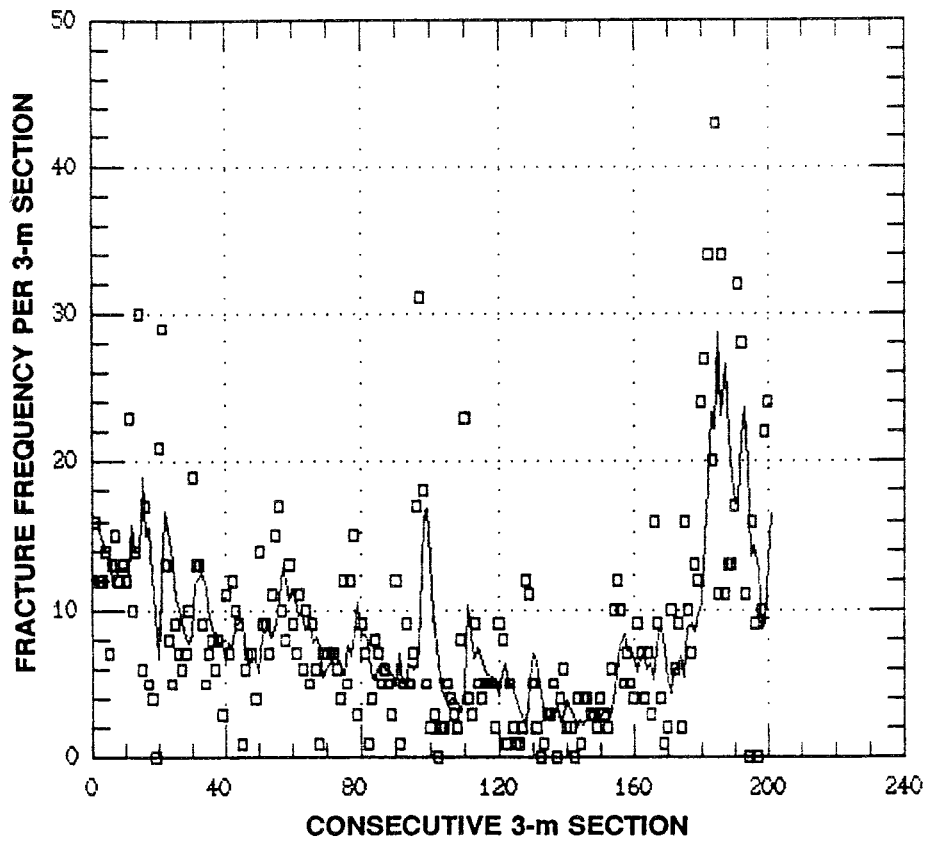
Hematite and iron oxide were often found in fractures where the hydraulic conductivity is relatively high. Fractures with a chlorite coating seem to be less conductive than fractures with hematite and iron oxide and fractures with calcite seem to be even less conductive than fractures with chlorite. (KAS 08 was examined in the study using the hydraulic conductivity from the injection tests with 3-m packer settings.) The fractures within the hydraulically conductive zones are also often coated with chlorite, calcite and epidote /Tullborg, 1989/. However, chlorite and calcite are generally by far the most dominating primary coatings in all open fractures /Liedholm, 1991; 22/.

Forecasting the hydraulic conductivity and fracture frequency

Simple exponential smoothing forecasting models to predict the hydraulic conductivity and fracture frequency one period ahead /Liedholm, 1991; 25 and 28/ were tested and found to perform better than a simple extrapolation of the last period, the so-called naive forecast. The hydraulic conductivity and fracture frequency are partly governed by the weighted average of neighbouring magnitudes and the neighbouring random disturbances (ibid). In conclusion, the deterministic part of the fracture frequency and of the hydraulic conductivity is less than the random component, but these variables may to some extent be predicted one period ahead.

It is not possible on the detailed and block scale to satisfactorily forecast the hydraulic conductivity nor the fracture frequency between the sampled points. The reason is that the correlation ranges and exponential model characteristics both indicate the range of a prediction to be at least one order of magnitude less than the distance between the sampled points. The basic reason is the large variance of the variables.

Original Series with Forecasts
KAS08 alpha=0.31



Original Series with Forecasts
KAS08 alpha=0.31

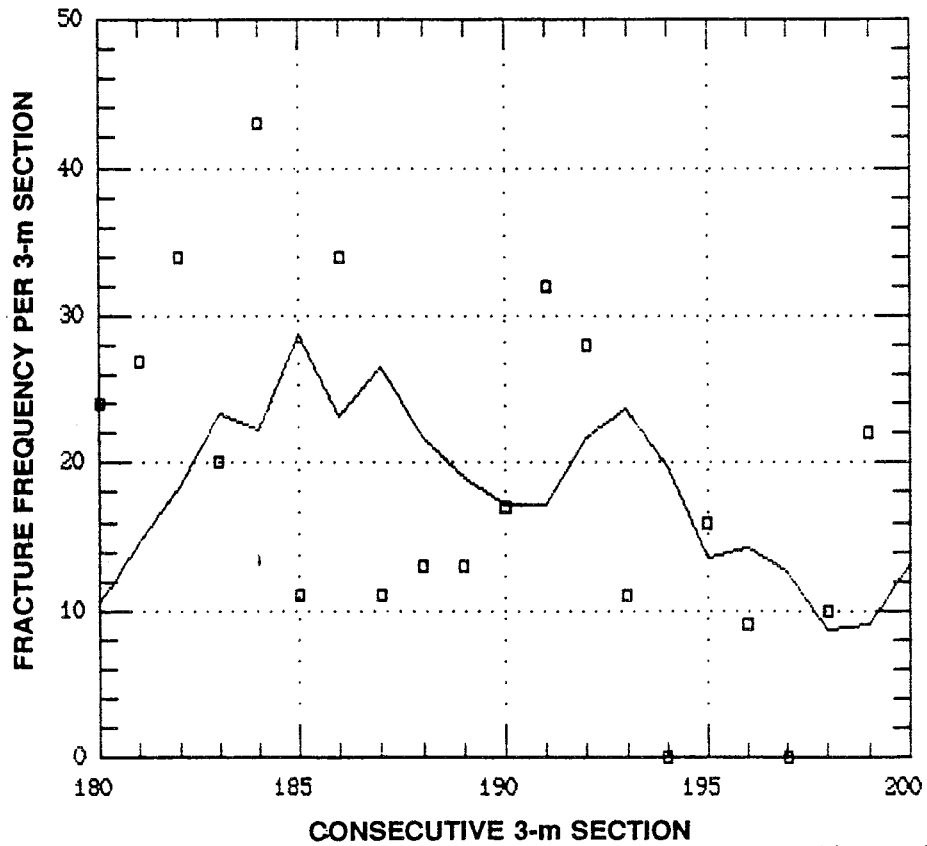


Figure 3.67 Forecasting the fracture frequency by an exponential smoothing model with $\alpha = 0.38$. Borehole = KAS 08. Squares represent measured data /Liedholm, 1991; 25/.

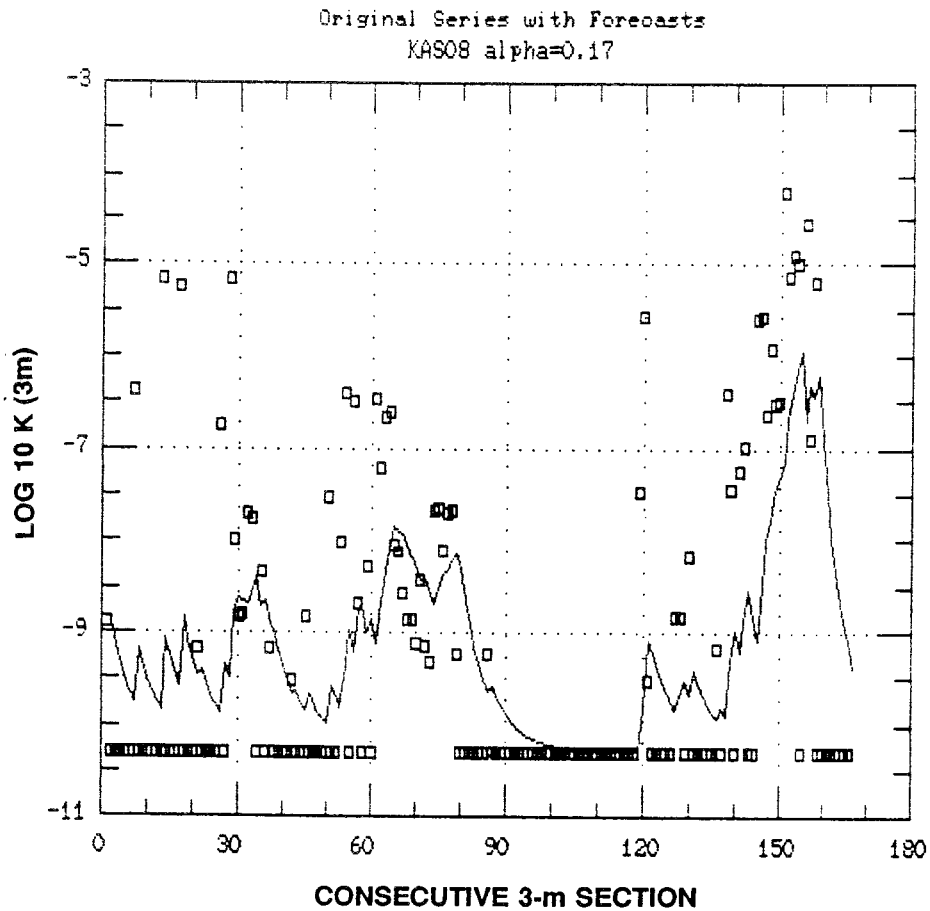


Figure 3.68 Forecasting the hydraulic conductivity by an exponential smoothing model with $\alpha = 0.17$. Borehole KAS 08. Distance down the borehole = $3 \cdot (\text{consecutive 3-m section})$ /Liedholm, 1991; 28/.

Distribution of hydraulic conductivities

The expected distances between 3-m sections with magnitudes of the hydraulic conductivity higher than $10^{-9}/10^{-7}/10^{-5}$ m/s are in the order of 3-9 m /6-16 m/45-130 m /Liedholm, 1991; 18/ (KAS 02, KAS 04-08 were studied).

3.2.7

SITE SCALE: Numerical modelling**LPT1 - Long-term pumping test in KAS 07**

A long-term pumping test was in the summer of 1989 performed in KAS 07 as an interference test. Before the pumping test, predictions of the draw-down were made using two numerical models, which are reported in Grundfelt et al, /1990/ and Svensson /1990a/. They were both based on the conceptual model presented in Gustafson et al, /1989a/. The main conductive structures implemented in the models can be seen in Figure 3.56. The object of the modelling was to test the ability to make predictions based on the data collected up to 1988, which formed the basis of the conceptual model.

Both models were first calibrated using three pumping tests (Interference tests KAS 03-3, KAS 02-2 and the pumping test in KAS 07) and the undisturbed water level.

In Svensson /1990a/ a finite difference code called PHOENICS was used. The cells in the model were orthogonal and the transmissivity of the conductive structure was superimposed on the hydraulic conductivity field for the rock mass. The conductivity field was generated as a stochastic field with a log-normal distribution. The salinity

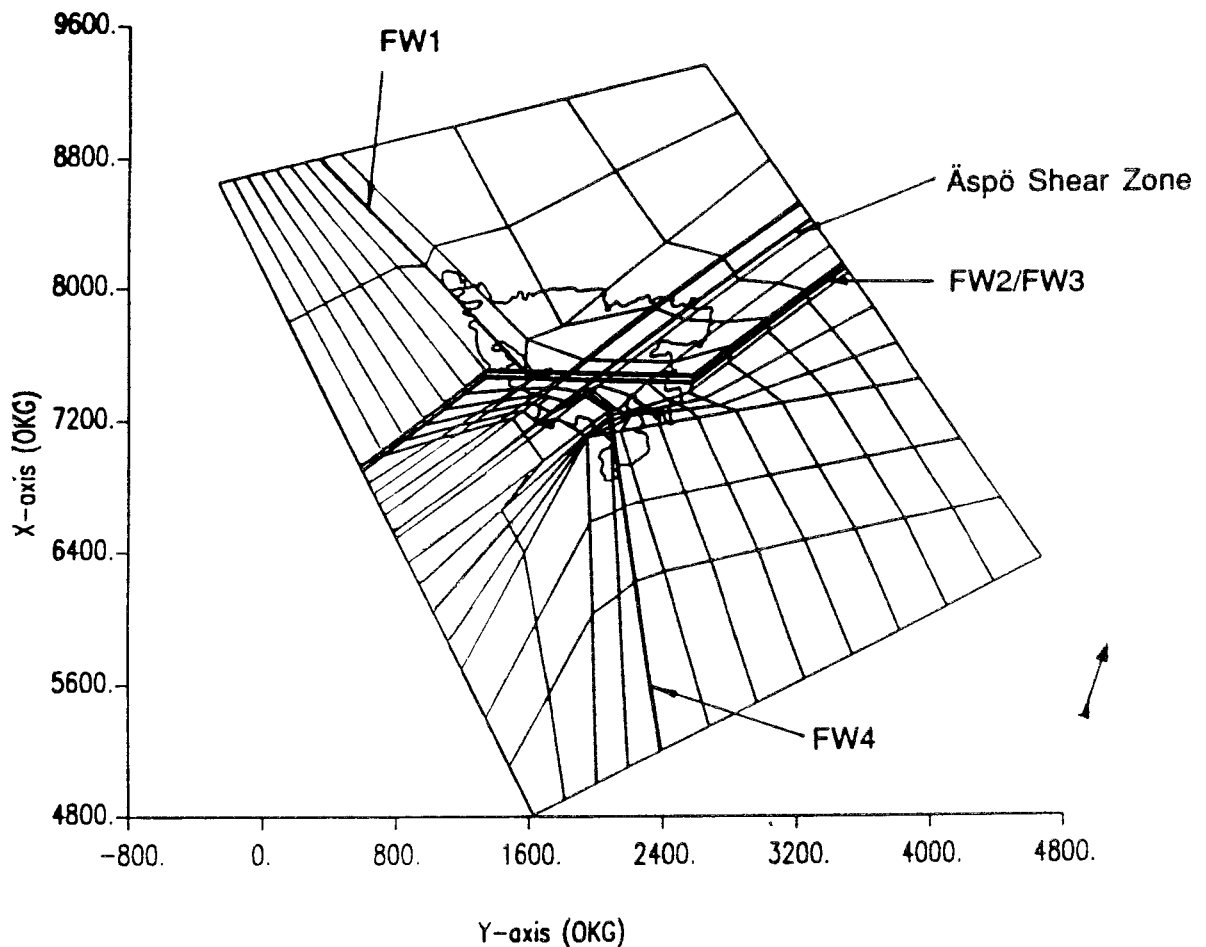


Figure 3.69 Plan of the finite-element mesh. The shore line of Äspö is indicated by a solid line. The depth of the model was 2 000 m. y-axis and x-axis in m /Grundfelt et al, 1990/.

was also included in the model. In Grundfelt et al, /1990/ a Finite Element Method (FEM) code called NAMMU was used and each conductive structure was defined by elements in a plane. The models are shown in Figure 3.69-70.

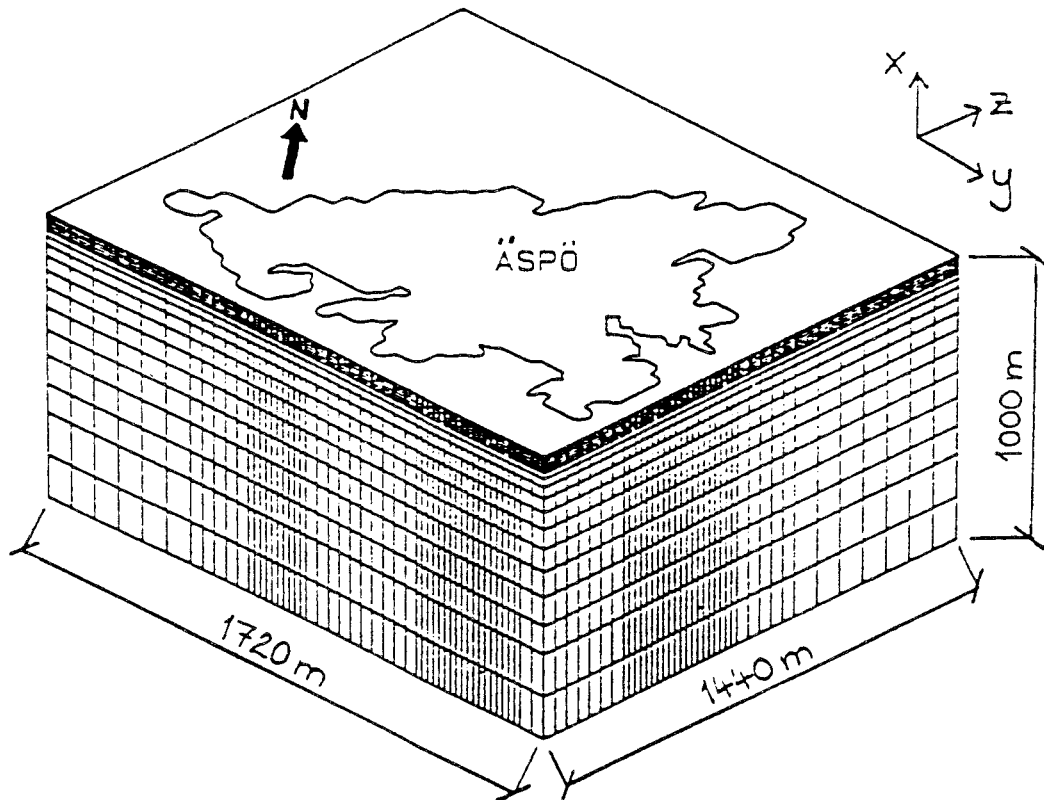


Figure 3.70 Computational grid /Svensson, 1990a/.

Even during the calibration phase it was obvious that the conceptual model covering southern Åspö was insufficient as regards geohydrology. The calibration indicated that there should be more conductive structures in the model. At this phase of the modelling, however, it was not possible from the available investigations to introduce new structures.

The measured draw-downs after 53 days (maximum pumping time) were compared with the predicted draw-downs in two ways:

$$ds = \frac{\sum_{i=1}^n (s_i^m - s_i^c)}{n}$$

$$Ds = \left(\frac{\sum_{i=1}^n (s_i^m - s_i^c - ds)^2}{n-1} \right)^{0.5}$$

n =	number of points with measured data used in the calculation
s =	draw-down (m)
ds =	mean error of the model (m)
Ds =	accuracy of the model (m)
m =	index for measured data
c =	index for calculated data

The equation tests two different properties of the model. The value of Ds tests the shape of the piezometric "surface". In a pumping test, Ds is the most sensitive of the results in the central part of the model. The value of ds is more a test of the boundary conditions in the model. Naturally, these two parameters do not show all aspects of how successful the prediction has been, but still, they are an objective measure of the result. The results are shown in Table 3.20.

Table 3.20 Comparison of measured and predicted draw-downs for the long-term pumping test in KAS 07 (LPT 1) /Svensson, 1990a/ and Grundfelt et al, 1990a/. Max (s^m) is the maximum draw-down in an observation section.

	Svensson /1990/	Grundfelt /1990/
n	33	44
ds	0.16 m	1.64 m
Ds	3.3 m	2.9 m
Max(s ^m)	18.4 m	18.4 m
ds/Max(s ^m)	0.0087	0.009
Ds/Max(s ^m)	0.18	0.15

Both models indicated that important conductive structures were missing from the model because unrealistic pressure drops were calculated near the well and the differences between measured and calculated values were large in a few borehole sections. If a few of these observations are not included in the calculations the values of ds and Ds for Grundfelt et al, /1990/ in Table 3.2.18 become much less.

Discrete fracture modelling

In /Axelsson et al, 1990/ three-dimensional discrete-fracture flow modelling is performed for cubes with sides 50 m long. In character the modelling was semi-generic and the object of the simulations was to apply heterogeneity, anisotropy and uncertainty due to discrete fractures in the flow model and to study how the flow through the cube changed under different conditions. The object was also to test the technique of discrete fracture flow modelling.

Blocks were modelled for two types of granite, Småland and fine-grained. Within the blocks, individual fractures were treated as probabilistic features, with locations and other properties described by probability distributions. Fracture statistics were derived from site characterization data that included scanline surveys, core logs and single-hole hydrological test results. Forward modelling was used to match the field data for fracture transmissivity, intensity and size, while explicitly accounting for many of the biases arising from site characterization methods. Orientation data were analysed to determine distribution forms, but because the data did not fit Fisher distributions, a non-parametric, bootstrap method was used in the simulations. Uncertainties exist for the statistics thus derived, because of uncertainties in the data and methodology. The effect of these uncertainties could be quantified through sensitivity studies, but only limited sensitivity studies were performed for this report.

Both fracture data analysis and fracture geometric simulations were performed using the FracMan Discrete Simulation Model. For each Monte Carlo realization, a finite element mesh was produced and the flow equation was solved using the finite element program MAFIC.

Using this approach, the hydrological heterogeneity and anisotropy of the rock mass were quantified for the HRL site. Heterogeneity on the scale of 50-m blocks was expressed in terms of probability density functions for hydraulic conductivities. Anisotropy was expressed in terms of the ratio of effective hydraulic conductivities in the North-South and East-West directions. Heterogeneity on the scale of canisters was expressed in terms of probability density functions and autocorrelation functions of hydraulic conductivities. Distributional forms were characterized using Pearson charts. The modelling approach is outlined in Figure 3.71.

Monte Carlo simulation results were obtained for two different types of boundary condition. One type of boundary condition ("no-flow") has no-flow conditions on the faces of the generic blocks (except for the faces perpendicular to the direction of flow), and the other type ("declining-head") has fixed-head conditions on all faces of the blocks, with heads decreasing linearly in the direction of flow. The no-flow condition gives a stricter test of conductivity, but tends to underestimate values of conductivity. The declining-head condition tends to overestimate hydraulic conductivity substantially.

The results for the no-flow boundary condition indicated that, for the simplest conceptual model in which fractures are uniformly, randomly distributed in space, the simulated 50-m blocks of Småland granite are generally non-conductive. This results in a strongly bimodal distribution of block conductivity. Other conceptual models, which are based on the assumption that fractures are non-uniformly distributed in space, resulted in from 5 to 30 per cent of the simulated 50-m cubes of this granite

being conductive, with mean effective hydraulic conductivities of the order of 10^{-10} m/s. The quantity and quality of results for no-flow boundary conditions were limited due to a precision problem that was identified in MAFIC, but could not be rectified until after the simulations had been performed.

The results of simulations using declining-head boundary conditions were more complete. Hydraulic conductivities were determined for all simulated blocks, for both types of granite. The mean effective hydraulic conductivities calculated using declining-head boundary conditions were of the order of 10^{-7} m/s for both Småland and fine-grained granites. Mean values of anisotropy ratios for both granites were approximately unity, but anisotropy was predicted to vary by as much as a factor of ten for principal directions running either North-South or East-West.

The simulations indicate that discrete fracture modelling can be a useful tool for understanding the flow in crystalline rock, but there still remain several questions to be answered, for example, how does one obtain proper statistical distributions of the fracture properties? The problem of boundary conditions noted in the report is probably a good illustration of the fact that the representative element volume is much larger than 50 m. If the fluctuations had been studied on a 50-m cube inside a model cube with sides much larger than 50 m, the difference between the boundary conditions would have been less but the computer time much longer.

Äspö Hard Rock Laboratory model

Predictions of inflow into the tunnel, pressure changes in the rock mass, etc. during several excavation stages of the Äspö HRL were made and reported in Svensson /1991/. The program code used is called PHOENIX. The calculations, in which salinity was included, are based on the conceptual model presented in Chapter 4 of this report, and a detailed presentation of the background is given in Chapter 5. The main part of the results is shown in Gustafson et al /1991/ and Rhén et al /1991d/.

3.2.8

SITE SCALE: Evaluation of methods of investigation

The water movement in the bedrock is governed by the distribution in space of the hydraulic conductivity and the specific storage and also by boundaries and sources. If water transport of solutes is also considered several other parameters have to be estimated. The object of the hydraulic tests so far performed, was to find main hydraulic structures in the bedrock and to estimate the hydraulic conductivity and specific storage of these hydraulic structures and the less conductive rock mass. Several tests have been performed and some brief comments are made below.

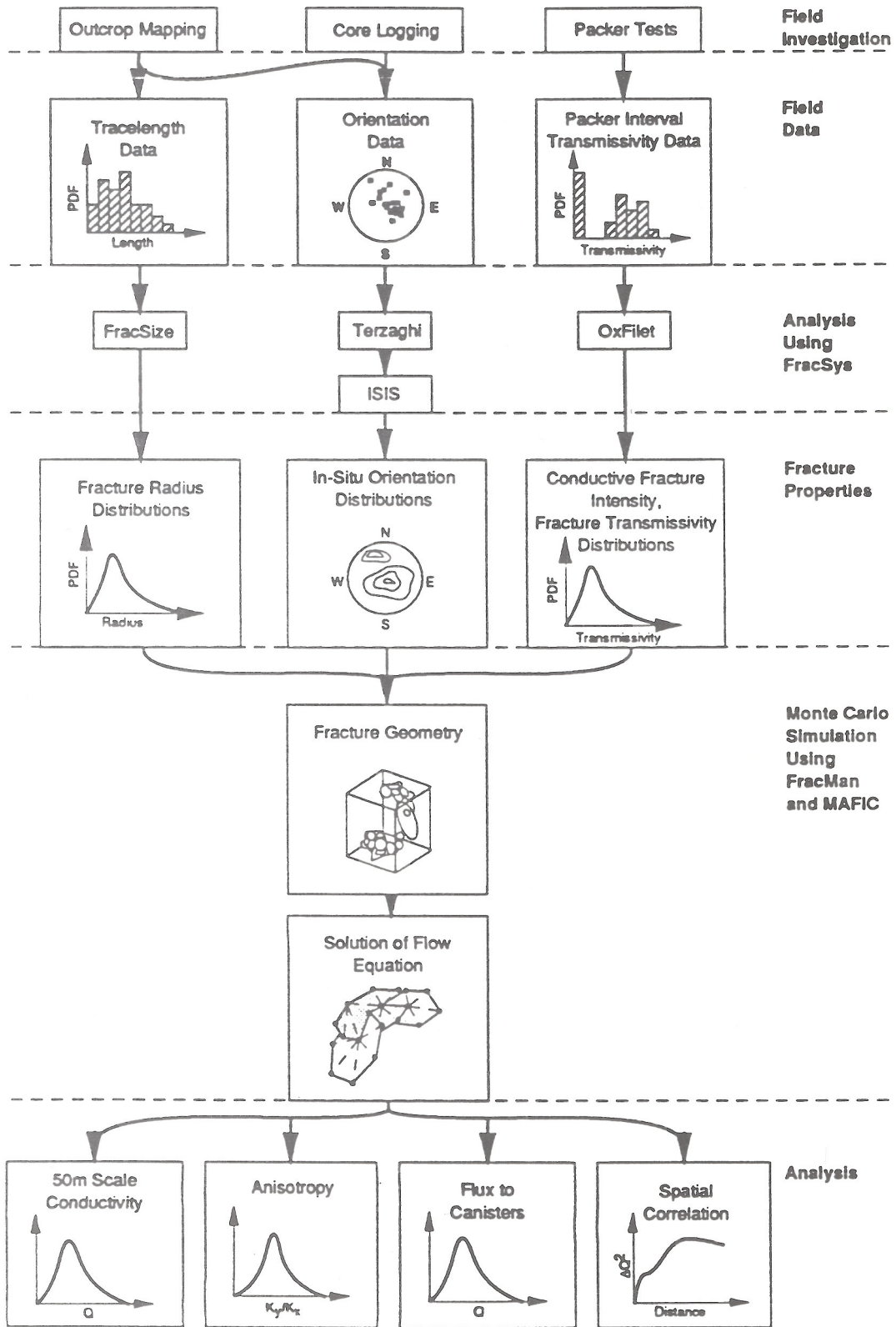


Figure 3.71 Outline of modelling approach /Axelsson et al, 1990/.

Borehole configuration

The core boreholes were all drilled to a telescope design. This has been an important advance compared with the traditional layout /Almén and Zellman 1991/. During drilling the telescope configuration made it possible to have an air-lift pump unit running in order to minimize contamination of the bedrock by drilling water. The telescope configuration also permitted flow meter logging to be done during the final test and clean-up pumping. The telescope configuration permitted the carrying out of transient interference pumping tests on selected sections of boreholes. Finally the telescope configuration also simplified the installation of packer systems and sensors, and also calibration and exchange of pressure transducers.

The disadvantage with the telescope design was that neither spinner surveys nor injection tests were performed in the uppermost 100 m of the boreholes.

The disadvantage of having the pressure transducers in tubes above the uppermost packer is that it can be difficult to estimate the absolute pressure at deeper levels in the borehole because of uncertainty in borehole deviation and fluid density in the pipes. On the other hand pressure transducers with small range can be used, which increases the accuracy of the measurements.

Hydraulic tests

The tests performed were:

- Air-lift test
- Pumping test of the whole borehole
- Spinner test
- Injection test
- Interference test

Useful and inexpensive information can be obtained during percussion drilling if the drillers register carefully the drilling performance, levels and the amount of water leaking into or out of the borehole.

Air-lift tests were often done during the drilling operation. This is also a cheap test to obtain a quick estimate of the hydraulic properties of the bedrock. The tests must, however, be performed carefully to give accurate flow and recovery results.

Pumping tests on the whole borehole give a more accurate estimate of the effective hydraulic properties of the rock mass on a relatively large scale. If observation wells are used it may be possible to obtain indications of hydraulic anisotropy if the duration of pumping is long enough. Brief pumping of the cored holes is also necessary to clean the borehole before packer installation.

Spinner tests can be performed during the pumping tests and give very important information on the location and character of main hydraulic conductors. Together with pumping tests spinner tests make it possible to obtain a transmissivity distribution along the borehole.

The injection tests were performed with a double-packer system on 3 and 30-m sections. Transient analyses were performed when possible. With the injection tests on

these scales it is possible to identify levels of main hydraulic conductors but not with the same precision as with spinner tests. The main purpose of the injection tests was, however, to find the statistical distribution of the hydraulic conductivity on different test scales. Together with the pumping tests and air-lift tests these tests are very useful for understanding the hydraulic behaviour of the rock mass.

Interference tests provided information on the hydraulic properties of some main hydraulic conductors and, in some cases, it has also been possible to determine the likely geometry of the conductors. In some cases it was difficult to evaluate the interference tests because activities, as for example drilling, disturbed the pressure response. This should be avoided when planning investigation activities.

The tests provided, above all, significant information on water transport and, in some cases, a weak or strong indication of an important hydraulic structure. None of the tests gave individually comprehensive information but together they provided fairly comprehensive information on the hydraulic features of the target area.

Geophysical logs

The geophysical logs are extremely dense in terms of the information they provide, with one measurement every 0.1 m, and they provide information of which only a small portion can yet be used.

With respect to the magnitude of the hydraulic conductivity, no comprehensive correlation with high accuracy has been found to any of the 12 logs. For each log five different statistics measures were correlated to the hydraulic conductivity from 3m-injection tests. Only when it is impossible to perform hydraulic tests, should some information be retrieved by using the above electric logs. The magnitude of the hydraulic conductivity can to some extent be determined from the (median) Normal Resistivity, the (minimum) Single-Point Resistance and the (minimum) Lateral Resistivity readings.

These geophysical logs provide information about the magnitude of the hydraulic conductivity just beyond or within the range of the judgmental approach. They hardly provide selective information nor do they probably provide complete information about the hydraulic conductivity.

The hydraulic conductivity is to some extent dependent on the number of fractures. The numbers of fractures provide important information, but neither complete nor selective information about the magnitude of the hydraulic conductivity.

Numeric modelling

It is necessary to use numerical models if the groundwater flow has to be calculated in a heterogeneous medium like the rock mass below Äspö. The flow field in a fractured crystalline bedrock is, however, much more complicated than a porous medium and there are several aspects that must be investigated to get a better understanding of the flow. In the previous phase of the Äspö HRL several numerical models were used to study different aspects of the groundwater flow and the results have been useful for the understanding of these aspects in a qualitative and sometimes in a quantitative way. They have also been the basis for making successively more complex and

realistic models of the Äspö HRL and were also indicative of areas where geohydrological information was lacking. The models have so far handled pressure and flow. Transport predictions have been tested but it is still too early to make any realistic predictions with the models because we do not have enough information about the transport properties in the rock mass and it has also not been the purpose of the investigations up to 1990 to estimate these parameters. The transport problem will be studied later in the Äspö HRL.

It should also be emphasized that it is important to have interference tests because all the models that can be used for predictive purposes of a real case should be calibrated before prediction if there is to be any confidence in the numerical prediction.

In the models of the Äspö island the bedrock properties have been divided into main conductive structures and the rock mass between them. The rock mass has been handled as a continuum or a stochastic medium. A developed system of superimposing the conductive structures on the rock mass has been a very useful tool because building of the model becomes much more flexible.

3.3 CHEMISTRY

3.3.1 Purpose of the investigation

The goal of the chemical investigations is to describe the ambient chemical composition of the groundwater and the fracture mineral and their distribution in different portions of the rock. A subgoal is to describe and model the changes that take place in the groundwater's main components, trace-quantity components (especially of redox-sensitive constituents), content of natural isotopes, possible drilling water markers and tracers. Hydraulic conditions will have a strong influence on the composition of groundwater. Therefore, the geohydrological evaluation should agree with the observed variation in chemical composition on the site scale.

An overview of the investigations are given in 3.3.2 and 3.3.4.. The interpretation of the results is given in 3.3.3 and 3.3.5. The results and evaluation of the fracture mineral chemistry are given in a separate section, 3.3.6.

The full evaluation of all the groundwater and geochemical investigations is given in 3.3.7. These results are presented in the different conceptual units in Chapter 4 and also in the form of direct predictions /Gustafson et al, 1991/.

3.3.2 REGIONAL SCALE: Overview of the groundwater and geochemical investigations

Well water analysis

Existing data from chemical analyses of well water in Kalmar County have been compiled and evaluated statistically by Liedholm /1987/. The material consists of

results from 86 well water analyses. Both saline and non-saline waters were included in the study. The maximum and minimum values of the main element concentrations are given in Table 3.21.

The results of the statistical evaluation point to the fact that it is difficult to find statistically defined correlations between the bedrock type, groundwater composition or any other non-chemical parameter. The most firm correlations found by Liedholm are:

- The chloride concentration is high in wells with a high capacity.
- The chloride concentration in the water is higher in wells close to the coast.
- The pH-carbonate system is determined by the thickness of the soil cover through which the water percolates.

Shallow groundwater chemistry at Laxemar, Äspö and Ävrö

An analysis of the chemistry of the shallow groundwaters at Laxemar, Äspö and Ävrö was performed by Laaksoharju /1988/. In order to find the major water conducting zones in the upper part of the bedrock, shallow percussion holes were drilled at the three sites. Water samples were collected and analysed from 13 of these boreholes. The maximum and minimum values of the main constituents are given in Table 3.21.

The results of the analyses were evaluated and modelled /Laaksoharju, 1988/. The equilibrium modelling indicates that the groundwater, even in the shallow part of the bedrock, has a long residence time. This is supported by the results of tritium analyses, showing that only a few samples contain large amounts of water precipitated later than the 1950s.

Both saline and non-saline water were encountered. The saline water source can be either present or relict Baltic Sea water. Chloride concentrations above the present one of the Baltic Sea strongly suggest the relict sea water source, and groundwater rock interaction.

With respect to the composition, the waters were classified as sea water, mixed water and fresh water (see Figure 3.72), and illustrated schematically for Äspö, Laxemar and Ävrö (Figure 3.73).

Surface waters from Laxemar, Äspö and Ävrö

Surface waters from lakes, streams, ditches, etc. were analysed for their composition of main constituents. The material consists of twenty samples on which the natural radioactivity and radium contents have also been analysed /Lindén, 1988/. The results, in the form of maximum and minimum values of the main constituents, are given in Table 3.21.

These data were used by Laaksoharju, /1988/, who compared the "evolution line" of the surface waters with that of the shallow groundwaters. The result of the exercise shows that the surface water has a composition similar to diluted sea water. All sampled waters lie on the mixing line between the sea water and the fresh water. The

reason for this is thought to be sea spray evaporating on the leaves of the trees. The rain water dissolves the evaporites from the leaves as it precipitates. The salinity varies depending on the time between rainfalls and the amount of precipitation. The shallow groundwaters have passed through an ion exchange process, giving them a composition different from the surface water and sea water.

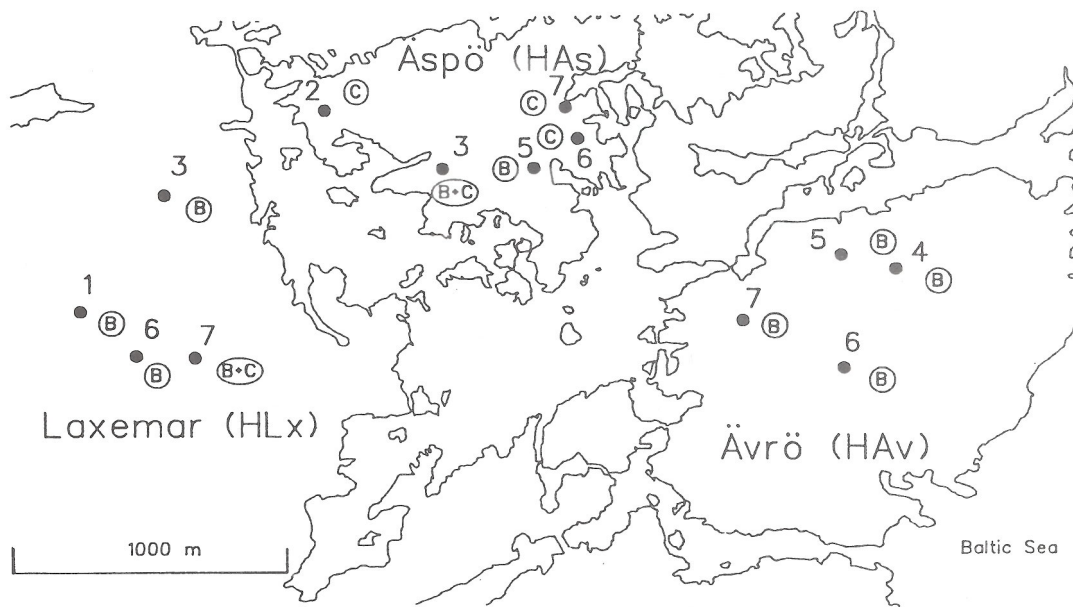


Figure 3.72 The water types in boreholes at Laxemar, Äspö and Ävrö.

Table 3.21 Maximum and minimum values of the concentrations of major elements in the water samples from wells, shallow boreholes and the surface.

Element	Wells (25-75) % quartiles	Boreholes all data	Surface all data
pH	6.8 - 8.6	6.5 - 8.4	4.9 - 6.7
Cond. mS/m	11 - 190	40 - 1550	5 - 120
Bicarbonate (mg/l)	1 -	334 102 -	373 0 -83
Sulphate (mg/l)	1 -	430 9 -	283 4 -66
Chloride (mg/l)	2 -	840 6 -	5500 1 -236
Potassium (mg/l)	1 -	21 2 -	28 0.4 -16
Calcium (mg/l)	17 -	135 10 -	818 4 -74
Magnesium (mg/l)	3 -	17 1 -	244 0.5 -10
Sodium (mg/l)	5 -	335 33 -	2300 3 -220

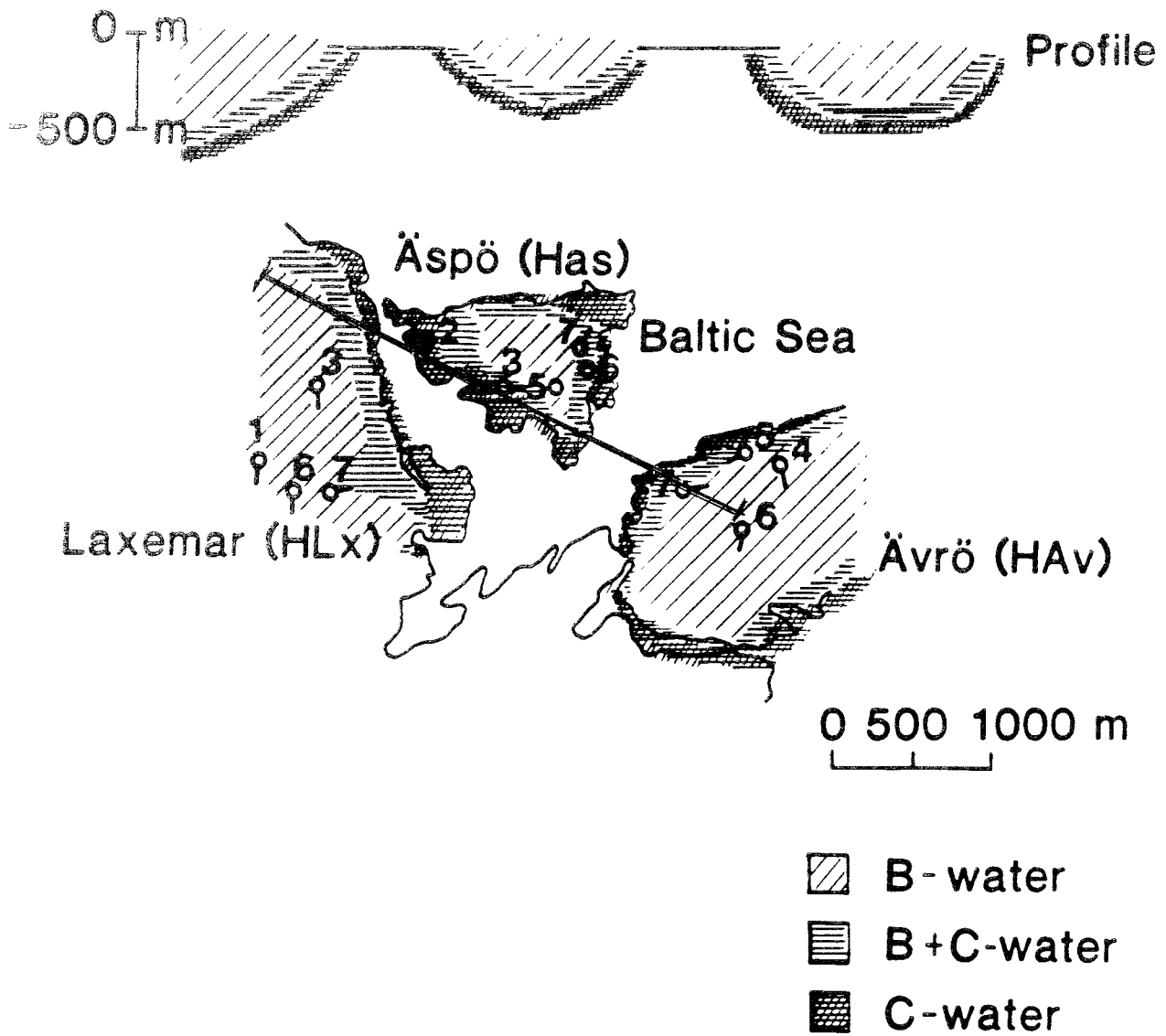


Figure 3.73 A schematic profile through Laxemar, Äspö and Ävrö showing the water types /Laaksoharju, 1988/.

3.3.3

REGIONAL SCALE: Interpretation and evaluation of the results

The data in Table 3.3.1 indicate that all three categories of water are fairly similar in composition. The well water material therefore, despite its being gathered from a very large area, can also be considered representative of the local area in the vicinity of Äspö. Because of this one can conclude that the Laxemar, Äspö, Ävrö area is characteristic of the Kalmar County as far as a groundwater chemistry is concerned. This also suggests a certain similarity in both the geological and the geohydrological conditions of the three areas.

The rather limited amount of data does not give a very detailed picture of the groundwater chemistry situation in the region. However, the work by both Laaksoharju and Liedholm suggests that both saline and fresh water can be encountered. From the pumping tests at Äspö it is obvious that the borehole giving the highest salinity has hydraulic connections with the sea. The saline water reaches ground surface at the shore line. At any other location the saline/fresh water interface is solely determined by the local hydrogeological conditions. There is perhaps neither a well established interface nor a distinct depth for the interface. The major conducting fracture zones mostly appear as depressions in the ground surface. Because of this they constitute local discharge areas. Saline water is therefore encountered in these, whereas the fracture systems visible on the outcrops are local recharge areas for the precipitating fresh water.

A washing-out process, in which saline water is gradually replaced by freshwater, is also evident from the results of sampling from the percussion boreholes in the Laxemar, Äspö and Ävrö areas. In Figure 3.74 the salinity of the sampled water is graphically presented in relation to where it was collected. The chemical composition of the water is given in Table 3.3.3.

From Figure 3.74 it is obvious that the salinity of the water at Äspö is considerably higher than that at Laxemar and Ävrö. The reason for this is that the washing-out of saline water at Äspö has not reached as deep as it has at Laxemar and Ävrö. This is because the island of Äspö rose above the sea only a few thousand years ago, while the Ävrö and Laxemar areas have been exposed to infiltrating freshwater for a much longer time.

3.3.4

SITE SCALE: Overview of groundwater and geochemical investigations

The sampling and chemical analyses of groundwater were made in connection with the drilling campaigns. The first one being the drilling of three deep boreholes on Äspö and one reference borehole on Laxemar. In a second drilling campaign water samples were collected from four additional deep boreholes and one, 100-m deep percussion borehole. In a third drilling campaign five more deep boreholes were sampled.

The sampling of groundwater has been done in three very different ways:

- Complete chemical characterization/field laboratory

- Sampling and analysis during hydraulic pumping tests/field laboratory
- Sampling during core drilling/conventional laboratories

The complete chemical characterization was made by the SKB mobile laboratory connected to the multihose system for convenient operation of down hole equipment for Eh and pH monitoring and in-situ gas sampling. The methods and equipment used are described in Wikberg et al./1987/. This programme of complete chemical characterization was carried out in KAS 02 (five sections), in KAS 03 (two sections), and in KAS 04 (three sections) (see Table 3.22).

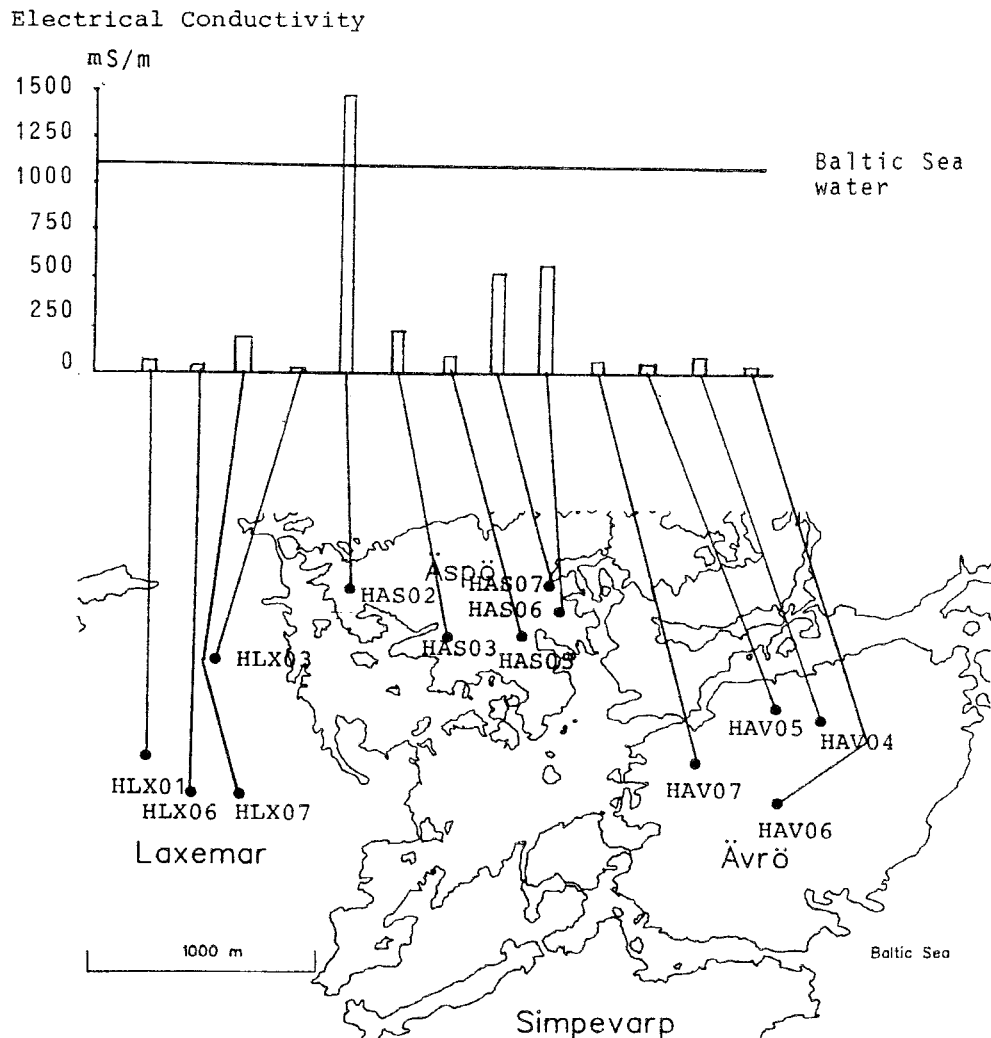


Figure 3.74 The electrical conductivity (proportional to salinity) of the water sampled in percussion boreholes at Laxemar, Äspö and Ävrö. The horizontal line shows the conductivity of the Baltic Sea water /Laaksoharju, 1988/.

Table 3.22 Groundwater sampled borehole sections at Äspö

CCC = Complete chemical characterization
 SPT = Sampling during pumping tests
 SDD = Sampling during drilling

Borehole	Sampled section/m		
	CCC	SPT	SDD
KAS02	202-215 314-319 463-468 530-535 860-924	308-344 802-924	
KAS03	129-134	196-223 248-251 347-374 453-480 609-623 690-1002	540-640 640-800
KAS04	860-1002 226-235 334-343 440-481		102-202 202-325
KAS05			155-388 387-550
KAS06		204-277 304-377 389-406 439-602	106-217 217-317 319-396 396-505 505-602
KAS07			106-212 212-304 372-604 462-604
KAS08			106-208 208-306 306-447
KAS09			303-450
KAS11			99-249
KAS12			204-303 303-380
KAS13			104-211 210-314 312-407
KAS14			105-212 153-211
KBH02			100-183 192-304
HAS02			44-93
HAS03			46-100
HAS05			45-100
HAS06			40-100
HAS07			71-100
HAS13		0-100	

The groundwater was pumped out of a section sealed off by packers and the chemical analyses were made once a day. In this way the composition as a function of time is known. When the composition is constant the samples are thought to be representative. Due to the highly varying hydraulic conductivity of the sampling sections, 10^{-9} - 10^{-5} m/s, the time required to obtain stable composition cannot be defined in advance. The specific conditions in the borehole are also important for the time it takes to obtain representative water samples. Therefore, the on-site analyses are necessary in order to optimize the time sampling will be carried on.

The mobile field laboratory was also used for the sampling during the hydraulic pumping tests, see section 3.2 and Almén and Zellman, /1991/. The same chemical analyses were done as in the complete characterization programme. However, the down-hole equipment for Eh and pH monitoring and for gas sampling was not used. Sampling and analysis during the hydraulic pumping tests were done in KAS 02 (two sections), in KAS 03 (six sections), in KAS 06 (four sections) and in HAS 13 (one section) (see Table 3.3.2).

During the core drilling of the deep boreholes the operation was interrupted every 100 m and water was pumped out from the deepest 100-m section. Water samples were collected and sent to ordinary laboratories for main constituent analyses. Such sampling was done in KAS 05, 06, 07, 08, 09, 11, 12, 13, 14 and KBH 02 (see Table 3.3.2).

First sampling campaign

From the three deep core boreholes, KAS 02, KAS 03 and KLX 01, groundwater was sampled during the hydraulic pumping tests and independently as part of the complete chemical characterization programme. The same field laboratory was also used as for the complete characterization of the deep groundwaters. With the exception of redox-sensitive elements and Eh, the sampling during the pumping tests gave results which were as accurate and representative as those from the separate sampling campaign, specifically aimed at obtaining good groundwater samples /Laaksoharju and Nilsson, 1989/.

Figure 3.75 presents graphically the dominating constituents: Na, Ca and Cl. The ion concentrations are presented in (mol/l). It should be noted that sulphate is present in such a low concentration that it is not visible in the figure.

From Figure 3.75 it is evident that the content of main constituents is rather similar in the water of all three boreholes. The most saline water is more of a (Ca, Na-Cl) type, whereas the less saline waters are dominated by sodium (Na > Ca-Cl).

The accuracy of the chemical analyses were checked by means of ion balance calculations. The results are statistically presented in Figure 3.76. For groundwater analyses a variance of +/- 10% is acceptable whereas +/- 5% is considered excellent. Out of the 45 samples only one falls within the error range -(5-6)%. Half of the samples lie in the interval -(1-2)% (see Figure 3.76). It is, therefore, concluded that the sum of anions agrees very well with the sum of cations.

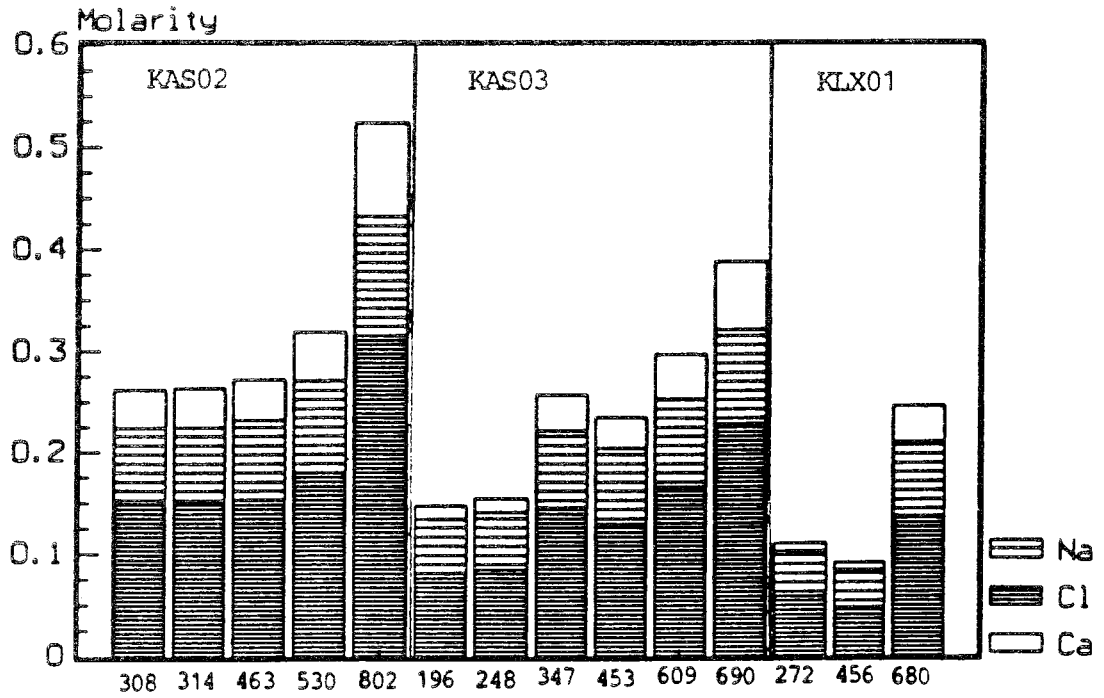


Figure 3.75 The composition of groundwaters sampled at different depths in the deep boreholes KAS 02, KAS 03 and KLX 01 /Laaksoharju and Nilsson, 1989/.

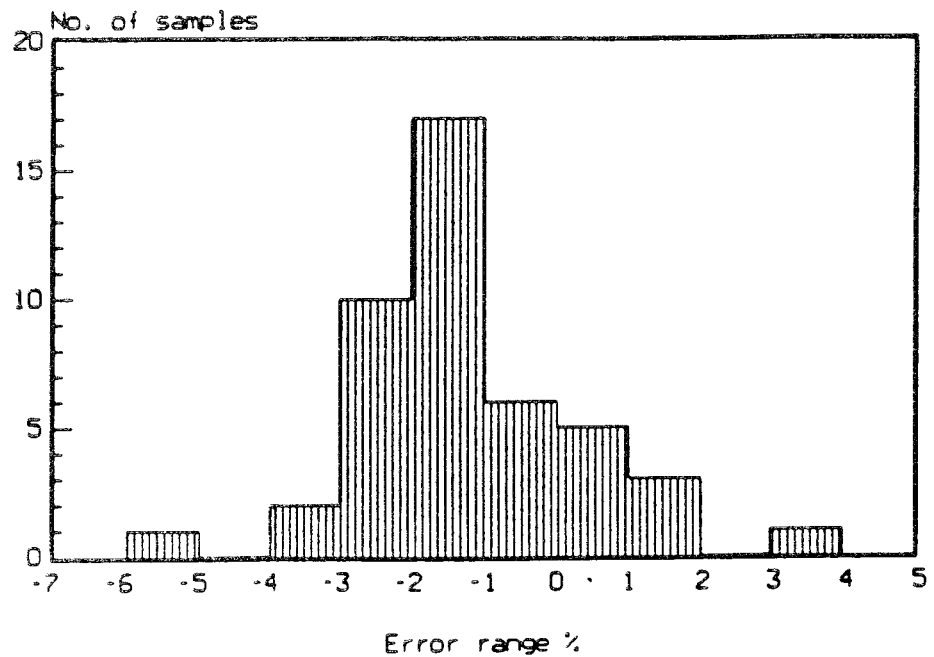


Figure 3.76 Statistical presentation of the ion balance calculations made on the analyses of water samples. The error is defined as the difference between the sum of cations and anions divided by the sum of all of them /Laaksoharju and Nilsson, 1989/.

A statistical evaluation of the fracture filling minerals has been made by Tullborg /Munier et al, 1988/. The percentage of, among others, calcite-filled fractures in the drill cores has been analysed as a function of depth. The results show that the calcite fillings are common in all the boreholes regardless the depth. This supports the conclusions from the results of the water analyses that near stagnant conditions prevail. Deep infiltration of surface water would have caused a depletion of calcite in the upper part of the bedrock. Such a decrease can only be traced down to depths of some ten to twenty metres by studying the drill cores. This suggests that there has been relatively little intrusion of carbon-dioxide-rich surface water into the rock mass.

Second sampling campaign

Groundwater from three sections in KAS 04 has been subject to complete chemical characterization. Water was also analysed in conjunction with hydraulic pumping tests in four sections in KAS 06 and one in HAS 13.

The quality of the analyses was checked in the same way, by means of ion balance calculations as described above. Based on the total set of complete analyses, 108 data sets, the error range decreased, c.f. Figure 3.77 /Nilsson, A-C, 1989/.

Third sampling campaign

The groundwater sampled in connection with the drilling operation was only analysed for the major constituents. The results were used to define the specific characteristics of the groundwater in the conductive zones penetrated by the boreholes. The quality of the samples is considered to be too low for any kind of quantitative evaluation. The main reasons for this are mixing in the 100-m long sampling section and occasional occurrences of large quantities of drilling water.

A statistical evaluation of the fracture filling minerals in the drill cores from KAS05-08 give a result similar to the evaluation of KAS02-04 /Tullborg, 1989/. In these drill cores no calcite dissolution can be observed, only a small decrease in the upper 10 to 20 m in KAS06 and KAS07. The frequency of hematized zones is also lower than in KAS02-04.

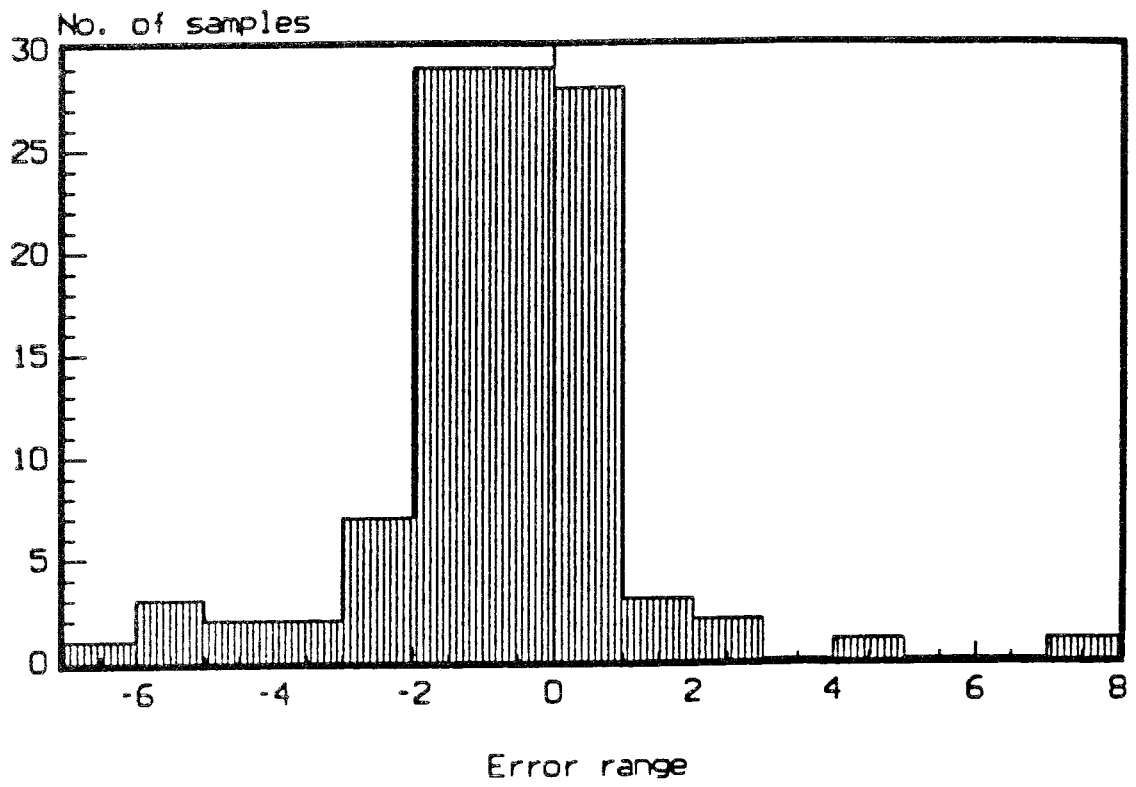


Figure 3.77 The distribution of the charge balance error /Nilsson, A-C, 1989/.

3.3.5

SITE SCALE: Interpretation and evaluation of the results**Shallow groundwater chemistry**

The chemical composition of the groundwaters sampled from the percussion boreholes are presented in Table 3.23. From the data on the Äspö waters it can be concluded that the freshwater pillow does not reach a depth of 40 m. It should be noted that the definition of fresh water in this context means water with a chloride concentration of less than 300 mg/l. Below the fresh water pillow there is a very large portion of infiltrated freshwater mixed with the saline water (c.f. Table 3.24).

Deep groundwater chemistry

The depth correlation of the groundwater chemistry was evaluated from the data collected in the two deepest, almost vertical, boreholes, KAS 02 and KAS 03, both of which reach a depth of 1000 m. A multivariate analysis called Chemometri was used in order to divide the groundwater samples into different classes /Laaksoharju and Nilsson, 1989/. Based on the results of this classification the different waters are explained as being the result of mixing between saline and non-saline water. The mixing proportions turned out to be affected by the hydraulic head of the flow system.

The deepest (most saline) and the most shallow (fresh) water samples were used as end members describing the mixing proportions in the rock mass. All sampled waters were found to lie roughly on a straight line on a graph at the chloride concentration is plotted versus depth, see Figure 3.80. Deviations from the straight line were examined and found to correlate to abnormal hydraulic heads, both higher and lower than the average. A higher salinity corresponded to a negative piezometric head and a lower salinity corresponded to a higher head (= positive piezometric head). The explanation to such a situation is found in the salinity-density relationship. In order to have a hydrodynamic balance the water columns at the same vertical depth need to have the same weight even when they differ in height. This is achieved when the density of the water column compensates for the variations in groundwater level.

Two different types of prediction were presented, both based on the assumption that the salinity of the water is a linear function of depth and that the only factor causing a deviation from the linearity is the relative pressure difference in the bedrock. The hydraulic head of the sampled section is calculated on this basis. With the additional assumption that the topography determines the groundwater level the same concept was used to calculate the salinity of the water in the rock mass where no boreholes are situated (see Figure 3.78).

The predicted hydraulic heads were compared to the measured heads in the boreholes of the next drilling campaign /Laaksoharju, 1990/. The predictive model was now also extended to include all major constituents. Thus, a renewed calculation of the hydraulic heads gave an improved fit with the observed data. The comparison between the predicted groundwater heads and the measured ones showed that out of 89 observations and calculations the standard deviation is 0.49 m and 0.67 m for the refined and the original model respectively. The maximum deviation is 0.9 m and 1.1 m for the refined and original model respectively. These variations are thus in the same order of magnitude as the uncertainty of the measured pressure heads. The predicted and the measured heads are presented graphically in Figure 3.79.

Table 3.23 Groundwater composition from percussion drilled holes at Laxemar, Äspö and Ävrö.

Borehole	depth m	Na mg/l	K mg/l	Ca mg/l	Mg mg/l	Cl mg/l	SO ₄ mg/l	HCO ₃ mg/l
HLX01	50	140	3	12	2	41	63	233
HLX03	21	67	4	17	4	6	23	204
HLX06	45	92	2	12	2	12	23	249
HLX07	20	430	6	42	9	440	260	200
HAS02	44	2250	28	741	244	5200	155	219
HAS03	46	336	12	87	39	608	104	235
HAS05	45	237	4	25	6	119	118	370
HAS06	40	900	12	297	56	1760	283	155
HAS07	71	656	5	361	55	1740	116	106
HAV04	35	202	4	13	3	106	71	290
HAV05	49	144	3	12	2	15	97	271
HAV06	73	127	2	111	1	36	71	223
HAV07	69	133	2	21	2	72	69	257

Table 3.24

The concentration of selected major and minor constituents and parameters in the groundwater sampled at Äspö. All concentrations are given in mg/l, µg/l for uranium, unless specified.

Borehole/ section (m)	W.flow ml/min	Drilling water %	Na	K	Ca	Mg	Sr	Fe ^{tot}	Fe(+II)	HCO ₃	F	Cl	Br	SO ₄	S ²⁻	pH	Eh	TOC	¹⁴ C- age	U ^{tot}	²³⁸ U/ ²³⁴ U	¹⁸ O SMOW	² H SMOW	³ H Tu
KAS02/202-215	61	0.80	1300	6.6	980	68		0.502	0.483	71.0	1.3	3840	14	108	0.50	7.4		6.0	10435	0.15	3.16	-13.9	-108.9	0.30
KAS02/308-344	5000	0.70	1720	8.8	1480	75	27	0.715	0.622	32.7	1.3	5300	29	290	0.16	7.6		2.0		0.15	4.11	-12.7	-99.8	< 8
KAS02/314-319	180	0.60	1700	9.0	1540	75	26	0.794	0.788	26.6	1.3	5340	23	270	0.01	8.2	-300	2.4	12670	0.34	3.06	-12.3	-100.6	< 8
KAS02/463-468	160	0.40	1800	8.2	1570	66	30	0.507	0.505	25.6	1.4	5450	28	290	0.13	8.3	-300	3.0	13910	0.32	2.99	-12.8	-99.9	< 8
KAS02/530-535	117	0.30	2100	8.1	1890	42	35	0.228	0.226	10.4	1.6	6370	42	550	0.18	8.3	-300	1.0		0.13	3.25	-12.3	-97.2	< 8
KAS02/802-924	15200	0.20	2800	11.7	3690	39	61	0.027	0.023	7.1	1.6	11000	78	522	0.01	8.2		0.5		0.64	3.16	-13.0	-96.8	< 8
KAS02/860-924	130	0.22	3000	10.9	3830	30		0.051	0.049	11.0	1.7	11100	74	520	0.72	8.5				0.54	4.56	-13.1	-96.8	0.20
KAS03/129-134	120	0.07	600	2.4	162	20	3.3	0.120	0.120	61.3	2.1	1230	5	32	0.70	8.0	-260	2.0	31.365	0.15	4.56	-15.8	-124.8	0.10
KAS03/196-223	10000	2.70	1200	6.3	480	60	10			60.0	1.8	2900	27	31	0.05	7.7		1.0	21695	0.19	3.54	-14.6	-115.3	< 8
KAS03/248-251	4000	1.00	1300	6.6	500	54	10	0.290	0.288	53.0	1.8	3000	18	40	0.17	7.8		0.5	20090	0.49	4.23	-14.5	-118.1	< 8
KAS03/347-374	18000	0.80	1730	6.3	1400	45	26	0.200		12.0	1.6	5180	30	340	0.05	7.8		0.5		0.08	3.00	-13.3	-104.9	< 8
KAS03/433-480	16000	2.10	1710	6.2	1200	40	21	0.196	0.194	27.0	1.5	4600	28	300	0.11	7.8		0.5		0.36	2.90	-13.6	-109.6	< 8
KAS03/609-623	18800	2.20	2000	6.3	1740	39	28	0.072	0.068	11.2	1.5	5880	46	470	0.10	8.0		1.1		0.15	3.34	-13.3	-103.4	< 8
KAS03/690-1002	13000	2.60	2130	6.6	2660	63	44	0.065	0.059	11.0	1.6	8100	51	680	0.10	8.0		0.5		0.58	4.83	-13.0	-99.7	< 8
KAS03/860-1002	120	0.15	3050	7.3	4400	50	75	0.075	0.075	10.6	1.6	12300	85	720	1.10	8.0	-240	0.5		0.13	6.30	-12.7	-96.4	0.40
KAS04/226-235	100	0.16	400	2.4	95	6.8		0.040	0.040	215.0	4.0	530	3	180	1.10	8.2	-300	6.9		0.46	5.10	-11.0	-84.8	4.3
KAS04/334-343	100	0.55	1180	6.1	750	30	13	0.315	0.315	70.0	2.6	3030	15	210	0.40	7.9	-260	5.3		0.29	4.60	-13.0	-99.6	0.50
KAS04/440-481	95	0.06	2000	7.8	1700	60	29	0.260	0.260	20.6	1.5	5900	26	410	0.60	8.0		1.3		2.20	7.20	-11.9	-92.3	< 0.10
KAS06/204-277	15000	0.72	1130	6.9	809	72	15	0.442	0.440	90.0	1.7	3630	17	150	0.17	7.6		4.7	7435	0.39	2.60	-10.7	-94.3	3.8
KAS06/304-377	16300	0.03	1850	9.0	1490	119	25	0.430	0.425	49.0	1.6	5680	24	283	0.02	7.5		0.1	13280	0.22	6.00	-9.2	-77.8	0.30
KAS06/389-406	1500	0.03	2060	11.8	1410	153	22	0.850		64.0	1.8	5970	23	362	0.01	7.3		0.1		0.27	4.40	-7.4	-69.2	0.60
KAS06/439-602	2500	0.05	2200	11.1	1560	130	26	0.627	0.627	50.0	1.8	6150	30	439	0.02	7.3		0.5		0.23	4.90	-8.2	-70.8	3.5
HAS13/0-100	11500		1880	32.8	1040	219	12	2.730	2.690	132.0	2.0	5070	37	136	< 0.005	7.3		1.7		6.11	3.50	-7.2	-69.3	1.2

* Eh measured in the down-hole probe

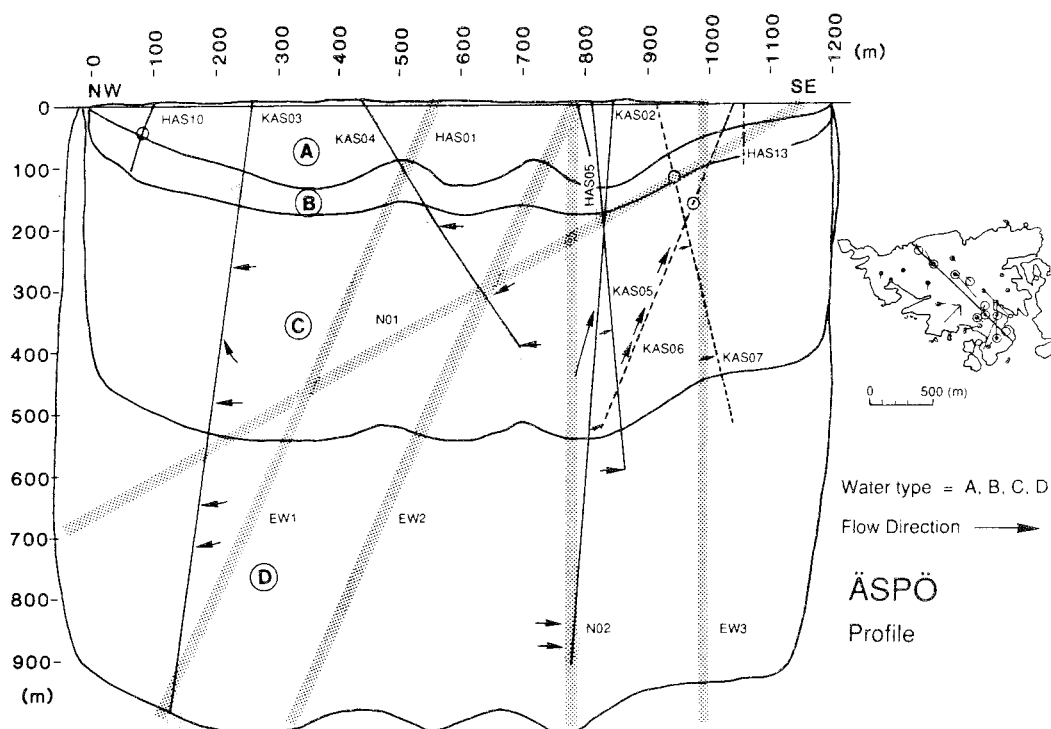


Figure 3.78 The distribution of different water classes in the Äspö rock mass. Groundwater sampling points where the chemical composition and the hydraulic head do not match are indicated by an arrow in the direction of the groundwater flow /Laaksoharju, 1990/.

The complete data set of the deep groundwaters is presented in Table 3.24. These data have been sorted into different classes according to their chloride concentration and ion ratio /Laaksoharju, 1990/.

Four classes were easily separated. The composition of the different classes are presented in Table 3.25

Table 3.25 Characteristics of the four different groundwater classes representing the groundwater in Äspö.

Class	Chloride mg/l	Bicarbonate mg/l	Sodium mg/l	Calcium mg/l
A	174±92	338±58	240±13	32±10
B	580±70	213±15	393±32	98±14
C	4171±1694	58±49	1392±553	1080±565
D	11001±1434	11±2	2776±587	3826±598

The distribution of the different water types on Äspö is presented in Figure 3.78.

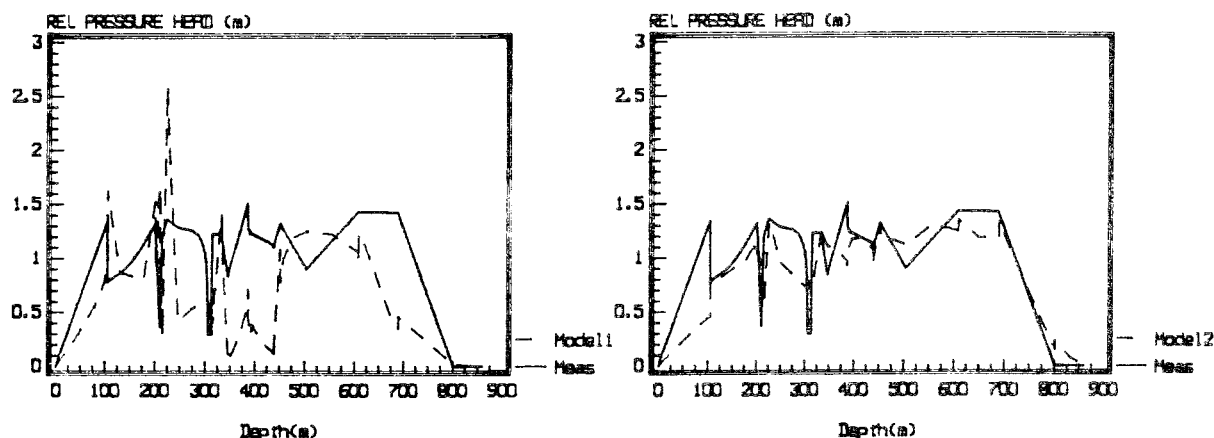


Figure 3.79 Measured hydraulic heads of borehole sections compared with values calculated from two different models correlating the hydraulic head with the chemical composition of the groundwater /Laaksoharju, 1990/

For an operational classification only the chloride concentration was used:

Class A	0 - 300	mg/l chloride
Class B	300 - 1000	mg/l chloride
Class C	1000 - 6500	mg/l chloride
Class D	6500 - 13000	mg/l chloride

The Laxemar reference borehole KLX 01

From borehole KLX 01 water was sampled at six different levels. The results are presented in Table 3.26. A comparison with those from Äspö show that the waters are of the same type. There are a few differences that should be mentioned.

The chloride concentration in the Laxemar borehole is much lower as a function of depth than in the Äspö boreholes. Such a situation is in good agreement with the results obtained in the percussion boreholes, which at Laxemar showed much less salinity than in the boreholes on Äspö. This simply states that the amount of infiltration of surface water into the bedrock of Laxemar is larger than it is at Äspö. The reasons for this are obvious. Äspö is an island (surrounded by the sea on all sides), whereas Laxemar belongs to the mainland, and the fact that Äspö rose above the sea level only three thousand years ago and that the washing-out process of the saline water has been going on only since then. It should be noted, however, that the salinity at a depth of 1000 m is as high at Laxemar as it is on Äspö.

Table 3.26

The concentration of selected major and minor constituents and parameters in the groundwater sampled from KLX 01. All concentrations are given in mg/l, µg/l for uranium, unless specified.

Borehole/ section (m)	W.flow ml/min	Drilling water %	Na	K	Ca	Mg	Sr	Fe ^{tot}	Fe(+II)	HCO ₃	F	Cl	Br	SO ₄	S ²⁻	pH	Eh	TOC	¹⁴ C- age	U ^{tot}	²³⁸ U/ ²³⁴ U	¹⁸ O SMOW	² H SMOW	³ H Tu
KLX01/272-277	140	4.7	1000	6.0	240	26	4	0.21	0.20	85	2.3	2000	8	50	0.60	8.4	-250	-		4.8	-11.5	- 89.9	< 8	
KLX01/456-461	130	14	850	6.1	220	17	4	0.09	0.08	77	2.4	1700	7	110	0.60	8.6	(-300)	2.2		4.1	-12.2	- 94.5	< 8	
KLX01/680-702	90	1.9	1600	7.2	1300	24	20	0.34	0.34	22	1.8	4700	5	380	0.60	7.8	-250	1.2		2.9	-11.8	- 98.8	< 8	
KLX01/830-841	50	0.2	2800	6.8	3000	15	42	0.35	0.35	6.2	1.6	9200	73	700	0.08	8.2	(-270)							
KLX01/910-921	100	0.9	3100	7.6	3700	9	60	0.05	0.05	5.9	1.7	11100	88	780		8.4	-							
KLX01/999-1078	80	2.3	3400	8.5	4500	7	71	0.56	0.55	12	1.6	12600	93	600	0.20	8.2	-							

Evaluation of Carbon-13 and Oxygen-18 in calcites from borehole KLX 01 indicated three classes with different signatures /Wallin, 1990/. The first one is the result of the turnover of present day freshwater, the second results from a complex mixing of glacial and marine sources and the third class indicates a possible hydrothermal signature. The Sulphur-34 content of the dissolved sulphate agrees with that of the seawater. This points towards a marine origin of the saline water. However, there are also other possible explanations for the Sulphur-34 content /Wallin, 1990/.

3.3.6

Fracture mineral chemistry on Äspö

The fracture minerals of the drillcores at Äspö have been carefully mapped in the core-mapping programme. The data has been evaluated in the form of frequency diagrams for the different type of fracture mineral /Tullborg, 1989, Munier et al, 1988/. In these studies the fracture minerals which could be the result of low temperature water-rock interaction have been focussed on; iron minerals and calcite. The major part of all fracture minerals are formed under hydrothermal conditions and are therefore of no interest for tracing the history of the groundwater chemistry. Of special interest are the calcite minerals which react rapidly with the groundwater.

Fracture mineral samples were collected from the drillcores of KAS 02 and 06. By comparing the results of spinner, point resistance and sonic surveys and the hydraulic injection tests with the drill core it was possible to find the actual water-conducting single fractures /Sehlstedt and Strähle, 1991/. These fractures were analysed for trace elements and carbon and oxygen isotopes of calcites /Tullborg, Wallin and Landström, 1991/.

Oxygen-18 and Carbon-13 values are typical for calcites in equilibrium with meteoric water at ambient underground temperature. At shallow depths there is a change towards more positive Oxygen-18 values corresponding to equilibrium with today's precipitation. Calcites with a hydrothermal signature are few, even in combination with epidote, fluorite and phrenite. Consequently there has been a re-equilibration of practically all the calcites in the fractures, since they were initially formed.

Trace element concentrations, rare earth elements, Uranium and Thorium, both in fracture minerals and in the groundwater, were analysed. These data can be used to calculate an in-situ value of K_d for the different elements. In Table 3.27 the calculated distribution coefficients for the different elements are presented and compared with those found for Klipperås, one of the earlier sites investigated.

Table 3.27 Distribution factors for the trace elements in fracture fillings and in the groundwater /Tullborg et al, 1991/

Element	Distribution factor m ³ /kg	
	Äspö	Klipperås
Sr	0.003-0.11	1-4
Rb	0.7-13.4	22-160
Ba	0.7-13	5-30
Cs	0.06-24.0	19-6030
Eu	14-142	900-1400
U	3-440	10-97
Ce	60-1231	2900-6800
Sc	75-3750	2000-7600

According to the Table 3.27, there is a variation in the calculated distribution factor of one to two orders of magnitude for each element. This is due to the variation in sorption capacity of the different minerals. It is obvious that the trend in the distribution coefficients is the same for the Äspö and Klipperås data. The difference in magnitude is likely to be due to the difference in groundwater composition. The content of the rare earth elements is up to one to two orders of magnitude higher in the Äspö groundwater than in the Klipperås groundwater.

3.3.7

Chemical conditions of the Äspö groundwaters

Salinity

The process determining the distribution of the salinity at Äspö is a transient washing-out of the saline water by the infiltrating fresh water. This process has, since Äspö rose above the sea level 3000 years ago, replaced the saline water completely to a depth of only a few tens of metres. The fact that only one of the percussion boreholes gave fresh water at a depth of 40 m is strong evidence of that. However, the infiltrating fresh water has reached much deeper, as can be seen from the Figure 3.80, in which the chloride concentration is presented graphically as a function of depth. Figure 3.80 indicates that the salinity increases linearly with depth. In the uppermost part of the rock a major part of the saline water has been replaced by the fresh water. Gradually the proportion of fresh water decreases and the proportion of the saline water increases. It must also be kept in mind that the mixing does not only occur at the interface between the saline and fresh water but also at any other place where the water moves. An already mixed volume of water mixes with the next previously mixed volume and so on.

Figure 3.80 includes the data collected during complete chemical characterization and pumping test campaigns. Data from the sampling during drilling is presented in Table 3.28. These data are not included in Figure 3.80. Instead they are used to characterize or identify the major fracture zones according to the specific composition (salinity) of the groundwater.

Table 3.28

The chemical composition of groundwater sampled during the drilling operation

Borehole	Sampling method	Section (m)	Drilling water %	Na mg/l	K mg/l	Ca mg/l	Mg mg/l	HCO ₃ mg/l	Cl mg/l	SO ₄ mg/l	SiO ₂ -Si	pH
KAS05	SDD	155-388	39.80	1525	12.5	1380	55	29	5400	270	3.3	6.9
		387-550	28.40	2080	13.5	1980	44	15	6680	535	2.9	6.4
KAS06	SDD	106-217	31.60	1778	34.0	1022	213	87	5410	152	2.5	7.4
		217-317	25.00	1570	1.0	1220	115	61	5000	130	3.6	7.6
		319-396	0.93	1740	9.3	1430	70	44	5410	240	5.4	7.1
		396-505	0.77	2190	11.0	1523	158	55	6300	440	5.6	7.4
		505-602	8.40	2100	17.0	1720	100	48	6300	450	3.7	7.2
KAS07	SDD	106-212	22.60	460	8.2	244	20	231	1100	136	3.6	8.0
		212-304	8.76	1055	10.3	868	57	78	3220	125	4.2	7.6
		372-604	41.40	2500	11.2	2820	100	11	8700	505	2.3	7.0
		462-604	43.80	2550	13.4	2860	75	14	8950	500	1.9	7.0
KAS08	SDD	106-208	0.64	1440	7.3	1430	85	37	5060	210	5.8	7.2
		208-306	9.28	1300	11.2	1145	89	68	4350	165	3.0	7.3
		306-447	29.20	615	6.8	329	39	195	1470	138	3.7	7.6
KAS09	SDD	303-450		2080	41.0	836	194	247	5300	93	4.7	7.4
KAS11	SDD	99-249	0.5	2050	20.0	1140	163	267	5580	61	5.9	-
KAS12	SDD	204-303	0.5	1710	19.0	1090	115	47	4810	279	3.2	7.2
		303-380	0.5	1930	12.0	1350	122	69	5610	300	3.9	7.2
KAS13	SDD	104-211	0.5	965	7.8	420	53	196	2110	210	6.0	7.7
		210-314	0.5	1140	15.0	480	72	166	2520	234	4.5	7.6
		312-407	0.5	1070	10.0	1430	77	50	5370	318	3.8	7.0
KAS14	SDD	105-212	0.5	2215	54.0	860	224	288	5660	90	5.7	7.4
		153-211	0.5	2180	52.0	866	217	280	5640	84	5.3	7.3
KBH02	SDD	100-183	0.5	1770	48.0	410	188	250	2840	245	3.7	-
		192-304	0.6	1860	41.0	684	173	278	4450	285	3.4	-

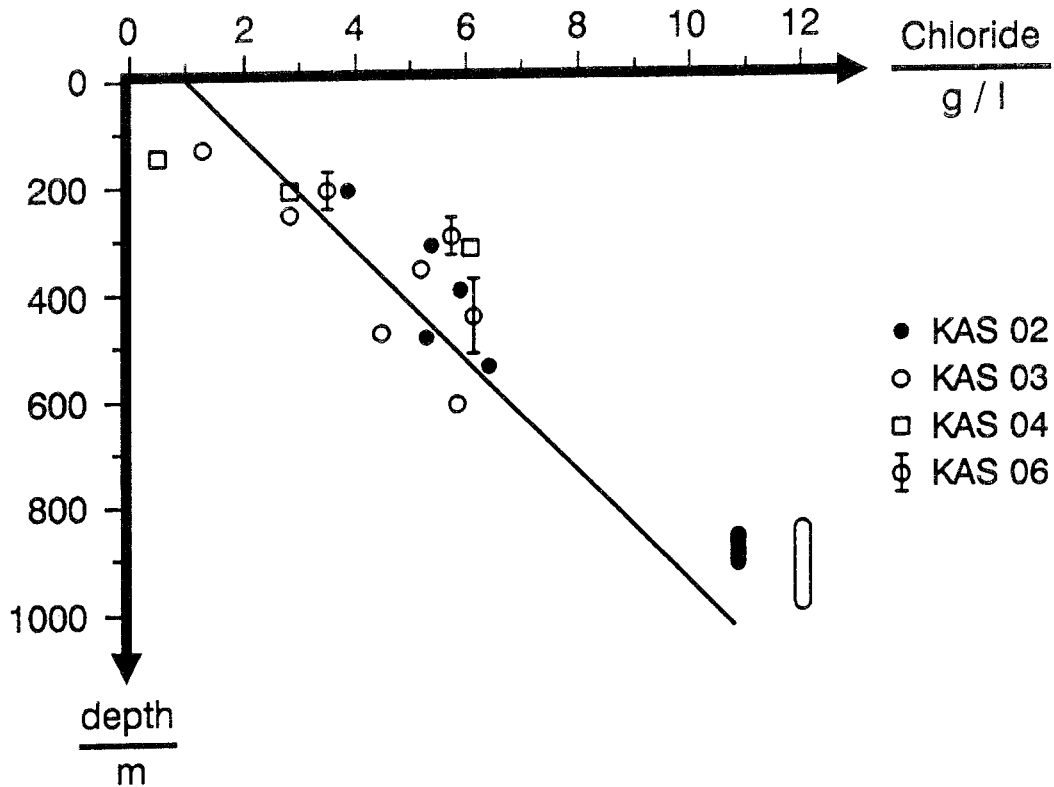


Figure 3.80 The chloride concentration of the waters sampled in sections sealed off by packers in boreholes KAS 02, 03, 04 and 06 and as a function of depth.

There is quite a large variation in the salinity and obviously not only the depth influences the chloride concentration. The correlation between hydraulic head and salinity mentioned in 3.3.5 is capable of explaining the observed variation as a result of differences in hydraulic head. The variation in the hydraulic head is reflected in the topography which, in turn, reflects the groundwater surface. Assuming that the controlling process for the groundwater flow is the very slow washing-out of the saline water, the groundwater level will adjust to remove the gradients which are caused by the washing-out process. Thus, the groundwater level reflects the degree to which this process has occurred and the process can be traced simply by analysing the chloride concentration and measuring the hydraulic head.

The reason for the very heterogenous mixing of fresh and saline water is likely found in the range of variation of the hydraulic conductivity. The variation of four orders of magnitude, see Figure 3.58 in section 3.2, for the hydraulic conductivity in adjacent spots will have a dramatic consequence for the penetration of e.g. freshwater into the saline aquifer even at a very moderate pressure gradient.

Salinity - density relationships

The correlation between the density and the electrical conductivity has been established from a large number of samples on which both have been measured /Nilsson,A-C, 1989/. The relationship between the electrical conductivity and the density is

$$D = 0.9972 + 4.6 \cdot 10^{-6} \cdot C \text{ (ms/m) valid at } 25^{\circ}\text{C}$$

This equation is valid at 25°C, the temperature at which the density was measured. The electrical conductivity is also sensitive to temperature variations. The measured data are automatically compensated for the variation. This compensation is made by a thermistor in the conductivity meter. The temperature reference is therefore 25°C.

The temperature dependence of the density of pure water is extremely well known. This temperature dependence is used for calculating the weight of the water columns in the rock and in the pressure monitoring tubing /Liedholm 1990,26/.

The salinity is related to the measured electrical conductivity in accordance with the formula

$$S = \frac{4.67 \cdot 10^{-3}}{0.741} \cdot C$$

C = electrical conductivity (m S/m)

S = salinity (g/l)

D = density (kg/l)

Residence time of the groundwater

The radioactive isotopes tritium and carbon-14 can be used as indicators of the residence time of the groundwater in the rock. Tritium which has a half-life of 11 years, if present, indicates a proportion of young water, whereas carbon-14 can in principle be used to determine ages of up to 30000 years. As can be seen from Table 3.23 the carbon-14 ages range from 7000 to 30000 years. Even though the carbon-14 data cannot be considered as the age of the water the results indicate a very long residence time, on the scale of thousands to tens of thousands of years. However, the water has no uniform turnover time and it is therefore dangerous to interpret the residence time as the turnover time of the infiltrating water. The tritium data are well below the detection limit of 8 TU. Out of the complete set of samples a few were selected for analyses with a much lower detection limit. Most of these are in the range of 0,1-0,6 TU. The ones with an enhanced tritium content were sampled from borehole sections considered to penetrate the NNW fracture zone system.

The high salinity of the Äspö groundwaters can be the result of a sea water intrusion or simply a long groundwater residence time. Oxygen and carbon isotope data of the calcites indicate a meteoric water interacting with the calcite, as mentioned in 3.3.5. However, it seems unlikely that the high salinity of the water has resulted solely from a long contact time between the water and the rock.

On the other hand, the composition of main constituents in the water is very different from sea water. By increasing chloride concentration the Ca/Na ratio increases. At the highest chloride concentrations the ratio is greater than unity. The corresponding ratio for Baltic Sea water is 1/27. The gradual change in the Ca/Na ratio probably results from an exchange of sodium in water to calcium in the minerals or is caused by a very slow dissolution of minor impurities of calcium chloride in the rock matrix.

Since the last glaciation the island of Äspö has been covered by sea and freshwater lakes during the past 12000 years. During this period the most saline water existed during the Litorina stage which started about 7000 years ago and lasted until Äspö rose above the sea level some 3000 years ago. Assuming that before the Litorina stage, the fractures contained fresh water or water with a lower salinity than the overlying sea, an overturning of the fresh water and saline water would be expected, due to the higher density of the saline water. Such an inversion would have affected the groundwater down to a depth where the density is the same as in the infiltrating sea water.

In Figure 3.81 the Oxygen-18 data are presented as a function of the chloride concentration. Through some of the points a straight line is drawn. This line represents the mixing of a marine water with a meteoric water of low Oxygen-18 character. The intercept at zero chloride concentration is around -18 per thousand. This implies that the fresh water end member is precipitated at cold climatic conditions. Present day Oxygen-18 data from this area are around -10 per thousand; -18 per thousand is possibly resulting from glacial melt water. Thus the data points following the straight line will represent the mixing of marine sea water with a glacial melt water. This is in good agreement with the hypothesis of inversion where Litorina sea water or other precursor to the Baltic Sea has gradually replaced glacial melt water.

At a chloride concentration above 6 g/l the Oxygen-18 versus chloride data in Figure 3.81 do not follow the glacial water - sea water mixing line. Thus the inversion process described above has not affected water with a chloride concentration above 6 g/l. The constant Oxygen-18 data of -14 per thousand could be a result of very long time water-rock interaction. The water could therefore be classified as a pre-glacial water.

There are also other possible explanations to the chloride and Oxygen-18 data which cannot be ruled out even though the overturning process seems more likely. One such process which would give the observed Oxygen-18 and chloride relationship is a slow freezing of the groundwater giving the most shallow ice a very negative Oxygen-18 value and a low salinity. Gradually the Oxygen-18 and chloride content increase until the maximum depth of the permafrost is reached. Even with this explanation the Äspö water is very old.

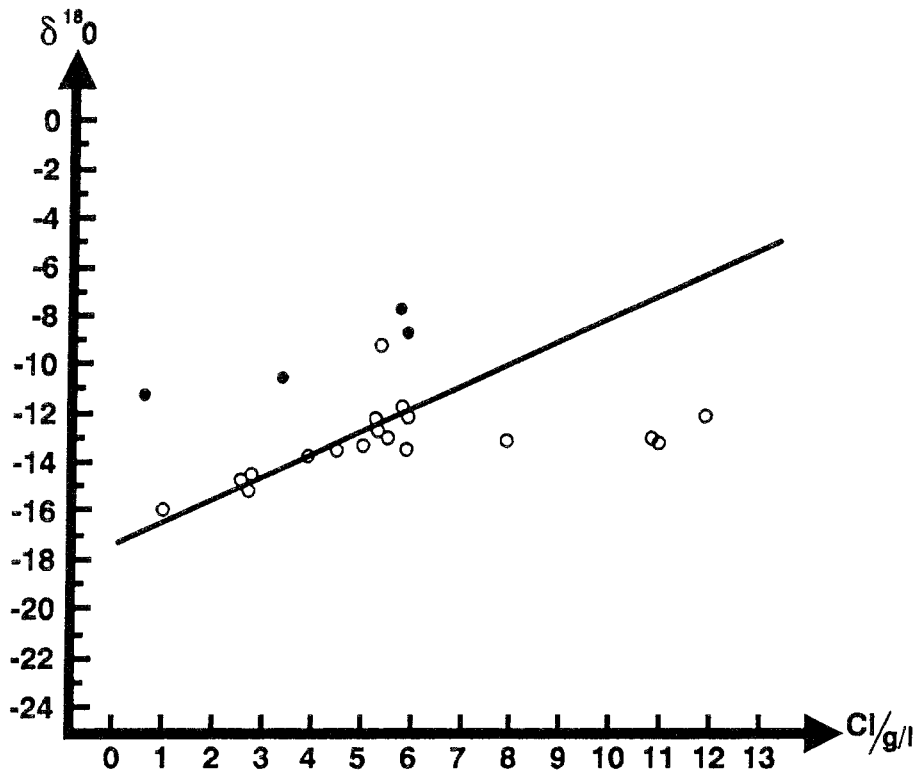


Figure 3.81 The Oxygen-18 data of the Äspö groundwater as a function of the chloride concentration. The straight line represents the mixing between sea water and fresh water with the Oxygen-18 character given by the intercept on the Oxygen-18 axis. Filled circles represent waters with measurable tritium contents.

A third set of data in Figure 3.81 is the one above the mixing line. The filled circles represent water samples where tritium concentrations in the range 1-4 TU have been measured. This means that a portion of the water has penetrated from surface to the sampling level during the last 40 years. The portion of such young water is in the order of parts per thousand. The higher Oxygen-18 values of these water samples agree with the tritium concentration. The present Oxygen-18 content in precipitation is in the order of -10 per thousand. Therefore the infiltration of present day fresh water shifts the overall Oxygen-18 content towards more positive values.

Calcite saturation

The calcite saturation has been calculated using the PHREEQE computer code for all the groundwater analysed. The saturation index is presented in Figure 3.82 as a function of depth.

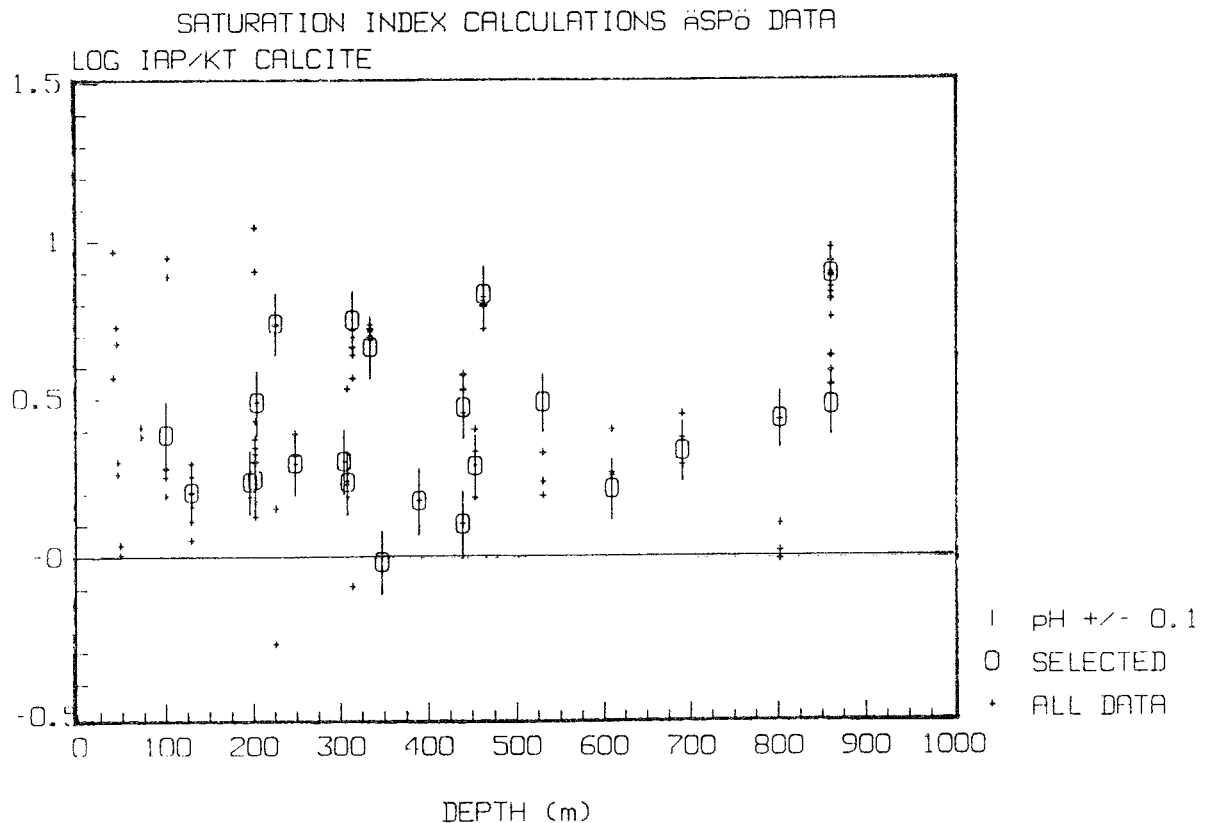


Figure 3.82 Saturation index for calcite in the Äspö groundwater. All water samples are presented. The ones which are of high quality have been given the error bar resulting from the 0.1 pH unit uncertainty in the measurements.

From the data in the figure it is evident that there is a slight oversaturation of calcite in almost all the sampled waters. The oversaturation is not correlated to depth. The calcite precipitation and dissolution is a fast reaction. Therefore one would have expected the water to be in equilibrium with calcite. Especially as the residence time of the Äspö groundwater is very long. The fact that the water samples are in general oversaturated is indicating that there is an on-going process which give rise to the calcite oversaturation. In view of the continuous mixing process described earlier this slight oversaturation, by a factor of two to three can be explained. The results from

the mixing of a high carbonate- low calcium water with a low carbonate- high calcium water can be described by the following principle:

high carbonate- low calcium	$[A][B]=[AB]$
low carbonate- high calcium	$[1/5A][5B]=[AB]$
mixing 1:1	$[3/5A][3B]=[9/5AB]$

i.e. an oversaturation by almost a factor of two. This simplified example assumes the two types of water have the same pH. At Äspö, the portion of the groundwater which has a low carbonate and a high calcium content also has a slightly higher pH. This causes an even higher oversaturation.

The fact that the water is oversaturated and that the mixing causes it has a major impact on the inflow to the HRL. The accelerated mixing caused by the inflow to the tunnel will result in high oversaturation followed by calcite precipitation in the conducting fractures. In time the inflow will decrease due to the sealing of the fractures by calcite precipitation. Also when Baltic sea water is mixed with the Äspö groundwater a slight oversaturation occurs.

Gas content - saturation

When the groundwater is pumped up from a packed off level in a borehole, the pressure is gradually lowered from e.g. 50 bar at 500 m depth to one bar at the ground surface. This major release of pressure is frequently accompanied by a de-gassing of the water. Obviously the water is oversaturated by dissolved gas with respect to atmospheric conditions.

The solubility of a gas is directly proportional to the partial pressure of the gas. The solubility of the gas increases linearly by increasing pressure. Therefore the deep groundwaters are oversaturated by dissolved gas only at atmospheric pressure, otherwise they are unsaturated. The de-gassing is a phenomenon which takes place because the water is subject to a major pressure drop. Gas samples which are isolated in situ pressure at the sampled depth have gas contents which are far from the solubility limit of the gas at that particular pressure. The deeper the water sample is taken, the further from the saturation of dissolved gas it is. Only very shallow samples, from depths < 100 m, are close to saturation. However, the total amount of dissolved gas increases with depth. This suggests that there is a source separate from the air in the atmosphere contributing to the dissolved gas content.

Redox conditions

The redox conditions of the Äspö groundwater are defined by the concentrations of iron and sulphide. The iron concentration ranges from 0.1 to 1 mg/l with five samples out of 22 with a concentration of less than 0.1 mg/l. One of the sampled waters has an iron concentration of 2.7 mg/l. The sulphide concentration of the water normally ranges from 0.05 to 1 mg/l with six samples having a concentration of less than 0.02 mg/l. Only one of the sampled sections has an extremely low concentration of both iron and sulphide, 0.027 mg/l and 0.01 mg/l respectively.

The highest iron concentration is related to the lowest pH, whereas the opposite correlation between low iron content and a high pH does not exist. The sulphide concentration shows no correlation to pH nor to the sulphate concentration.

The measured Eh values are very typical compared with other investigated Swedish groundwaters /Grenthe et al, 1991/. The values are in the interval -240 to -300 mV in the pH range of 7.9 to 8.3. The uranium concentrations are also low and the U-234/U-238 activity ratio is high which is in accord with the reducing character of the water.

3.3.8

Correlation to other methods and parameters

There seems to be a weak correlation between the Äspö diorite and a slight increase in the iron concentration of the water compared with the Småland granite.

Water-conducting sections of the boreholes which are considered to be part of the north-south fracture system NNW have given water with a higher tritium concentration than others. This is thought to be due to a recharge in this fracture system.

The correlation between the variation in salinity and the hydraulic head of the corresponding borehole sections gave the necessary background to evaluate the washing-out process of the saline water by the infiltrating fresh water.

3.3.9

Evaluation of the methods of investigation

The relevance of the chemical investigation methods concern the sampling and the analyses of the groundwater. In order to be useful the groundwater samples must be representative of the surroundings where it was sampled and the analyses must be made in a way to ensure that the composition of the water does not change.

The cooling-water used in the drilling operation is always tagged by a tracer, a dye called Uranine. In this way it is possible to identify the portion of drilling water in the groundwater samples. In most cases the highly conducting sections where $K > 10^{-6}$ m/s are severely contaminated by drilling water, due to the fact that large amounts are lost into the bedrock during drilling. In the investigations at Äspö two different activities were performed to avoid this situation namely:

- air-lift pumping during drilling
- sampling of the highly conducting sections in conjunction with the hydraulic pumping tests.

Air-lift pumping during the drilling operation is possible due to the fact that the uppermost 100 m of the borehole has been enlarged from 56 to 150 mm. The pumping mostly removes as large a volume as that used for the drilling, approximately 300 l/m.

Because of the very small amount of drilling water contamination, representative groundwater samples were obtained after much shorter pumping periods than earlier SKB investigations. Consequently, the total duration of the sampling campaign at a

section was reduced from (3 - 4) to (2 - 3) weeks. With more experience it might be possible to maximize the pumping period to two weeks. During drilling of the first 700 m of borehole KLX01 no pumping was done. The upper three sampled sections also contain a large amount of drilling water. When the borehole was deepened the drilling water was removed by air-lift pumping. A much lower content of drilling water was observed in the lower sampled sections (Table 3.26).

The sampling of sections with a hydraulic conductivity above 10^{-6} m/s is very time consuming because of the low capacity of the groundwater sampling pump. The pumping tests at Äspö were performed with a capacity which was two orders of magnitude larger than that of the chemical sampling pump. The three-day duration of the the pumping test was therefore sufficient to ensure representative water samples.

However this time was not sufficient to obtain stable readings on the Eh electrodes. Despite this drawback the combination of groundwater sampling and hydraulic pumping tests was successful.

The very simple survey of existing well water chemical data gave a rough estimate of the variation in the region. Together with the shallow percussion hole data and the surface water data it was possible to define the character and extent of the freshwater pillow at Äspö.

The multivariate analyses of the chemical data, together with the main geological and geohydrological data, turned out to be successful. Both classification and predictive modelling were used with good results. The basis for the predictions prior to the excavation was based on this work.

3.4 TRANSPORT OF SOLUTES

3.4.1 Purpose of the investigations

Both the geohydrological and the groundwater chemical investigations contribute to the understanding of the groundwater flow and turnover time. This knowledge forms the basis for understanding the transport potential on a site scale. Actual groundwater flow measurements in borehole sections sealed off by packers and tracer tests will give some of the quantitative data needed for transport calculations.

In the pre-investigation phase only the transport potential was examined.

3.4.2 Dilution and tracer tests

Scoping calculations of a radially converging traces experiment were based on the numerical groundwater flow model. The experiment has been performed on southern Äspö. The evaluation of the results is under way.

The objects of this first tracer experiment on Äspö were to check the conceptual and numerical models and provide a basis for the next tracer tests.

Dilution of a colour dye was used to determine the flow of groundwater through a borehole section. Two separate tubings end within the same packed off section, one just below the upper packer and the other one just above the lower packer in the permanently installed borehole equipment, see Figure 3.83. The tubings are connected to a circulation pump on the surface. The complete borehole equipment is described in more detail by Almén and Zellman /1991/.

The colour dye is added to the circulating water as a pulse which lasts for the same time as needed for the rotation of the system volume. Thus the concentration of the colour dye is evenly distributed. The pump continuously circulates the water in the closed system. The only change of the concentration is caused by the flow of groundwater through the borehole section.

The concentration of the dye is measured regularly. From the slope of the change in concentration it is possible to calculate the groundwater flow pass the borehole section.

Dilution tests have been performed in most of the core boreholes on Äspö. In many of them two different sections have been investigated. The results from the measurements are presented in Rhén, /1991b/.

According to dilution tests performed in 1989 and 1990 on Äspö results shown in Rhén /1991/ the groundwater level variations in typical conductive zones, cause a water flow in a borehole section limited by packers of 1-100 ml/min under undisturbed conditions (no pumping, no drainage to tunnels). Assuming good or rather good contact between the borehole and the conductive zone the flow in the typical zone becomes $1 \cdot 10^{-6}$ - $1 \cdot 10^{-8}$ m/s.

3.5

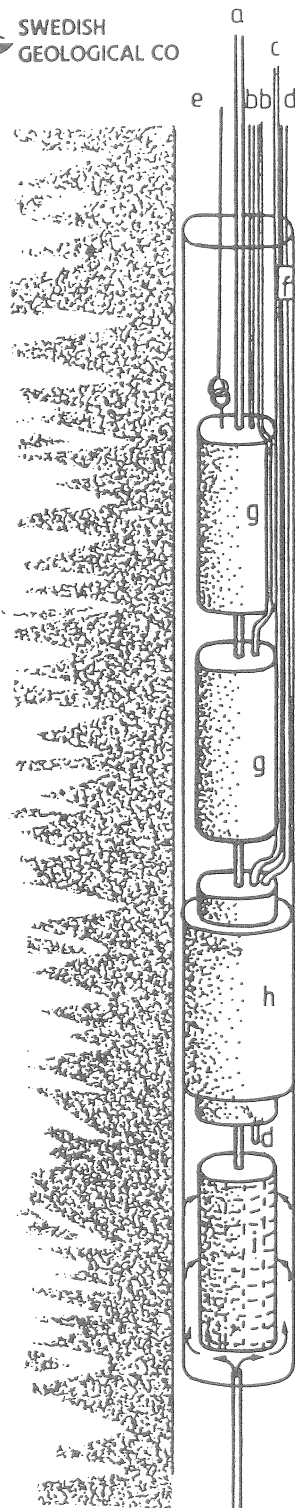
MECHANICAL STABILITY

Based on the results from rock stress measurements in three boreholes on Äspö, laboratory testing on core samples and geological pre-investigations a rock mechanics evaluation was performed for the Äspö HRL. /Stille and Olsson, 1990/.

3.5.1

Purpose of the investigation

The main purpose of the study was to make a rock mechanics evaluation based on the results from rock stress measurements in three boreholes on Äspö, perform laboratory testing on core samples and carry out the geological pre-investigations for the Äspö HRL. /Stille and Olsson, 1989/.



- a Inflow (to trace element unit)
- b Electrical cables to circulation pumps
- c Pressure support to PEM-packer
- d Ground water pressure tube
- e Wire
- f Pressure transducer
- g Circulation pump
- h PEM-packer
- i Filter (inlet)

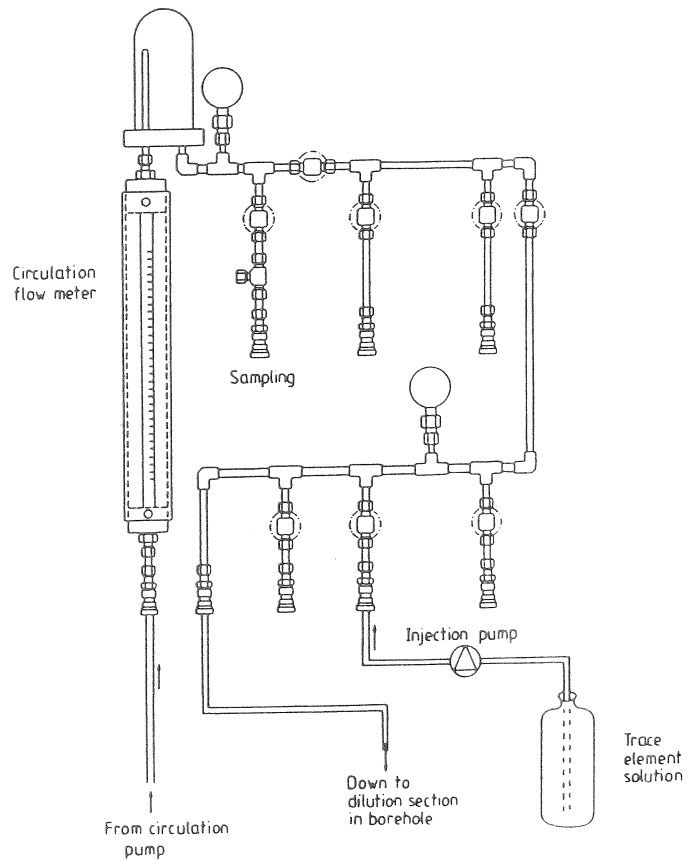


Figure 3.83. Schematic drawing of the borehole and surface compartments of the equipment used for the dilution tests at Äspö.

3.5.2

Rock stress measurements

Rock stress measurements were performed in boreholes KAS 02, KAS 03 and KAS 05 /Bjarnason et al, 1989/.

KAS 02 and KAS 05 are located in the Southern Block and KAS 03 in the Northern Block of Äspö.

KAS 03

The first measurements were performed by hydraulic fracturing in borehole KAS 03. The results for all levels are presented below (Table 3.29). The relations σ_h and σ_v have been calculated for each level. Mean values for the measured values at 550.9 m are 1.5 and 0.9. The maximum horizontal stress components are located in the sector N16°W to N65°W.

Table 3.29 Rock stress measurements in KAS 03

Vertical depth (m)	σ_v (MPa)	σ_h (MPa)	σ_{HII} (MPa)	$\frac{\sigma_h}{\sigma_v}$	$\frac{\sigma_{HII}}{\sigma_v}$
131.5	3.4	3.6	5.0	1.1	1.5
153.8	4.0	4.5	6.8	1.1	1.7
481.4	12.5	10.7	19.5	0.9	1.6
494.8	12.9	10.9	20.7	0.8	1.6
515.1	13.4	11.8	19.4	0.9	1.4
534.0	13.9	11.8	25.1	0.9	1.8
536.0	13.9	12.4	24.4	0.9	1.8
545.9	14.2	10.7	20.2	0.8	1.4
547.9	14.2	9.8	17.7	0.7	1.2
550.9	14.2	9.8	18.0	0.7	1.3
625.3	16.3	10.0	18.3	0.6	1.1
664.0	17.3	8.5	15.1	0.5	0.9
666.0	17.3	9.6	18.8	0.6	1.1
739.4	19.2	13.7	26.1	0.7	1.4
819.8	21.3	22.6	37.9	1.1	1.8
822.3	21.4	23.0	43.7	1.1	2.0
877.4	22.8	21.0	38.5	0.9	1.7
880.4	22.9	21.4	39.5	0.9	1.7
885.4	23.0	22.6	43.0	1.0	1.9
893.3	23.2	24.3	46.3	1.0	2.0
962.8	25.0	24.9	48.5	1.0	1.9

σ_v = presumed vertical stress, depth (m) x 0.0265 (MPa)

σ_h = minimum horizontal stress

σ_{HII} = maximum horizontal stress, calculated by the second breakdown method

KAS 05

The second set of measurements was made in borehole KAS 05 using the overcoring technique. Three measurements were made at level 195 m in medium-grained granite and four at level 355 m in diorite.

The stresses in the horizontal plane show a very obvious uniform pattern with maximum magnitude in the E-W direction and minimum magnitude in the N-S direction. Two of the values at the 355 m level show negative values, tensile stresses, for σ_h and low values for σ_H . These figures seem peculiar and may be caused by local residual stresses. The latter two values will not be considered in further calculations.

The mean value for all measured levels is 2.0 for σ_H/σ_v and 0.4 for σ_h/σ_v .

Table 3.30 Rock stress measurements in KAS 05

Vertical depth (m)	σ_v (MPa)	σ_h (MPa)	σ_H (MPa)	$\frac{\sigma_h}{\sigma_v}$	$\frac{\sigma_H}{\sigma_v}$
195.3	5.2	2.4	9.8	0.5	1.9
196.6	5.2	7.6	9.3	1.5	1.8
197.4	5.2	5.0	12.9	1.0	2.5
		Mean value	x = 1.0	x = 2.1	
355.0	9.4	1.9	17.0	0.2	1.8
355.9	(9.4	-2.6	10.3	-0.3	1.1)
356.8	(9.4	-0.6	10.6	-0.1	1.1)
357.7	9.4	2.3	17.7	0.2	1.9
		Mean value	x = 0.2	x = 1.8	

σ_v = presumed vertical stress, depth (m) x 0.0265 (MPa)

σ_h = minimum horizontal stress

σ_H = maximum horizontal stress

KAS 02

The third set of measurements was made in borehole KAS 02 by means of hydraulic fracturing. The results for all measured levels are presented below. Mean values for the ratios σ_H/σ_v and σ_h/σ_v relating to levels above 550 m were calculated to be 1.7 and 1.0. The largest horizontal stress components are located in the sector N12°W to N68°W.

Table 3.31 Rock stress measurements in KAS 02

Vertical depth (m)	σ_v (MPa)	σ_h (MPa)	σ_{HII} (MPa)	$\frac{\sigma_h}{\sigma_v}$	$\frac{\sigma_{HII}}{\sigma_v}$
113	2.9	4.7	6.0	1.6	2.0
158	4.1	5.9	10.2	1.4	2.5
229	5.9	5.5	10.3	0.9	1.7
233	6.1	5.2	10.3	0.9	1.7
243	6.3	5.4	9.5	0.9	1.5
250	6.5	5.9	10.9	0.9	1.7
280	7.3	5.2	9.1	0.7	1.3
339	8.8	5.7	10.2	0.6	1.2
364	9.5	6.6	10.7	0.7	1.1
381	9.9	6.8	12.3	0.7	1.2
390	10.1	7.0	12.8	0.7	1.3
426	11.1	8.8	17.2	0.8	1.6
495	12.9	13.7	22.9	1.1	1.8
504	13.1	16.0	27.8	1.2	2.1
515	13.4	12.6	23.5	0.9	1.8
547	14.2	19.0	35.1	1.3	2.5
585	15.2	23.9	43.9	1.6	2.9
625	16.2	23.0	41.4	1.5	2.5
661	17.2	22.4	39.9	1.3	2.3
718	18.7	24.4	42.5	1.3	2.3
737	19.2	21.0	40.5	1.1	2.1

Comments on measured rock stresses

The measurements in the three boreholes show rather similar results for both the ratio σ_h/σ_v (K_o) and the orientation of the largest horizontal stress component. The value K_o is of interest when evaluating deformations and possible rock burst in the tunnel.

As mentioned before, the measurements were made in the different blocks into which Äspö is divided from a structural geological point of view. However, the results do not indicate that different rock stress conditions tend to apply in different parts of the island. In KAS 02 horizontal stresses increase below the level 425 m. Diorite is the dominating rock type here. However, it has not been possible to correlate high rock stresses with diorite in any of the other boreholes in which rock stress measurements were performed. The only correlation that can be made with high rock stresses is that they occur at fairly great depth. In further discussions and calculations σ_h/σ_v is given the value 1.7. According to the rock stress measurements made, this value should be typical for the section between 300 and 550 m below the surface /Stille and Olsson, 1990/.

3.5.3

Laboratory tests on rock samples

As a complement to the rock stress measurements laboratory tests of rock samples were made. The laboratory tests were carried out according to methods suggested by ISRM. The uniaxial compressive strength (σ_c), Poisson's ratio (μ) and Young's modulus (E) were determined for the four dominating rock types. Controlled uniaxial compression tests were also performed to evaluate the brittleness of the rock. Finally, the joint characteristics were determined. All rock samples were taken from borehole KAS 02.

A summary of the results is presented below in Table 3.32.

Table 3.32 Rock strength parameters in KAS 02

	σ_c (MPa)		E (GPa)		μ	
	mean	range	mean	range	mean	range
Greenstone	118.8	72.9-167.7	52.4	31.7-74.2	0.25	0.24-0.26
Aplite	235.7	151.6-336.2	65.0	59.3-69.7	0.22	0.20-0.22
Diorite	183.5	164.5-216.9	59.8	53.6-65.2	0.23	0.20-0.25
Småland Granite	188.7	147.2-259.5	62.3	61.7-62.8	0.24	0.24

Brittleness of rock

The brittleness ratio has been determined from the controlled uniaxial compressive tests.

The brittleness ratio is defined as the ratio of the energy stored at failure load, divided by the total amount of energy consumed in the failure process. A ratio of less than 1 indicates a tough behaviour and a ratio higher than 1 a brittle behaviour, as described by Olofsson /1974/.

Brittle failure has been observed in all tested rock types from KAS 02.

Variations in the brittleness ratio have been observed in all rock types, ranging from low to high brittleness. The highest brittleness ratio was observed in the greenstone. The fine-grained granite has proved to be somewhat less brittle than the other rock types.

Strength of joints

Both steep and gently-dipping joints have been tested in the laboratory. The steep joints are named ST 1, ST 2, ST 3, ST 5 and ST 6, and the gently-dipping joints ST 8, ST 9, ST 10, ST 11 and ST 12. To describe the joints, Barton /1982/ developed a classification system in which the joints are given a value according to their roughness. This value is called the JRC, Joint Roughness Coefficient. When evaluating the laboratory tests on small samples, results were scaled according to Barton's system so that they are valid for larger blocks.

The steep joints proved to have a JRC value of more than 8, which implies smooth, undulating joints.

The gently dipping joints can be divided into two categories. One group of joints with a JRC value of more than 8 and one group with a JRC value of around 3. A JRC value of around 3 implies smooth planar joints.

The friction angle of the steep joints is in the range 47° - 63° , and that of the gently dipping joints in the range 37° - 65° .

3.5.4

Classification of the rock mass

The rock mass classification was based on the pre-investigations performed in the area and the conceptual model that has been established. Core logs from holes in the vicinity of the underground development and the structural conceptual model have been of particular interest.

The purpose of the classification is to divide the rock mass into representative groups in which the rock mechanics characteristics are different. There are a number of different classification systems in use around the world. The Geomechanics Classification proposed by Bieniawski and the Q-system proposed by Barton, Lien and Lunde are the two most commonly used classification systems /Hoek - Brown, 1980/.

For this classification the system proposed by Bieniawski has been applied. This system employs five parameters describing the rock mass and is more simple to use when the classification is based on pre-investigation data. If any parameter is missing, it is possible to estimate the value of the missing parameter. The system proposed by Barton et al. is more complex and operates with more parameters.

In the Geomechanics Classification System the parameters describing the rock mass are allocated points according to a proposed scale. The rock mass is described by parameters for strength of rock material, RQD-value, spacing of discontinuities, conditions of discontinuities and the inflow of water to the underground development.

The sum of all points allocated to the different parameters describes the rock mass in the form of a value called the RMR-value (Rock Mass Rating). Finally the RMR-value is adjusted for the joint orientation.

The RMR-value varies between 0 and 100 and in general terms the different RMR-values are often described as follows:

<u>RMR</u>	<u>Description</u>
100-81	Very good rock
80-61	Good rock
60-41	Fair rock
40-21	Poor rock
<20	Very poor rock

3.5.5

Stability

The stability of the underground openings will depend on a number of factors. Both geometrical factors, such as size and shape of the opening, as well as structural and rock mechanics conditions, will influence the stability.

The opening will have an area of approximately 25 m². This is a moderate size which does not normally cause significant stability problems in Scandinavian rock.

Laboratory tests previously presented proved that the strengths of both rock and joints are normal for this type of rock, in which stability problems are not usually expected.

The dominating fracture pattern has an east-west orientation with a steep dip of 70-90° from the horizontal plane. However, gently dipping joints have also been observed.

The RMR system does not take into consideration the initial rock stress conditions. The relationship between the maximum horizontal stress and the vertical stress, K_0 has been stated to be around 1.7. The orientation of the maximum horizontal stress has been measured and found to be E-W or N40°W.

Both the magnitude and orientation of the measured horizontal stresses will be favourable for the stability. The measured stress orientation, with the maximum horizontal stress almost perpendicular to the first 1475 m of the access ramp gives the best possible conditions for the creation of a stable arch.

Both the expected stress conditions and joint orientation will be very favourable for the development of a stable arch without any major support measures being required. With the given rock mechanics conditions and the moderate tunnel area, the stability in the decline and ramp will generally be very good and potential problems limited to specific areas.

Support measures will be related to the structural conditions and the rock quality. If gently dipping joints with reduced friction occur in the roof, it may be necessary to install untensioned grouted rock bolts to achieve a favourable arching effect. If the excavations encounter areas with fractured to highly fractured rock with reduced strength and joint friction, it may be necessary to apply shotcrete to create an artificial arch that assists the surrounding rock, so that a rock arch can be formed.

3.5.6

Failure of intact rock

Since the underground facilities will be located at a very considerable depth, an analysis of the possible risk of spalling activity is motivated. Spalling usually occurs at great depth where rock stresses are high, but may even be observed at lesser depths under certain conditions. Rock stress problems with frequent failure of intact rock are very difficult to foresee with any degree of certainty. This forecast includes a discussion on the conditions for spalling that will be present.

Spalling, or rock burst when the intensity is great, is an explosive-like failure in virgin rock and is due to a number of factors, such as:

- high stresses in the rock
- residual stresses
- anisotropic stress conditions
- mechanical properties of the rock (structure, compressive strength, brittleness)
- fracture pattern in the rock.

To enable an evaluation of spalling and rock burst activity to be made, some empirical relationships have been presented. Hoek and Brown /1980/ have worked out a relationship between the compressive strength of the rock and the vertical stresses caused by the overburden.

At Äspö, however, rock stress measurements confirmed the fact that the horizontal stresses are 1.7 times higher than the vertical stresses. Therefore the diagram will be used for the horizontal stresses, calculated as $1.7 \times \text{depth (m)} \times 0.0265 \text{ (MPa)}$.

According to Hoek and Brown's diagram, rock burst will not occur in Småland granite, fine-grained granite or diorite. Minor spalling may occur in the greenstone at depths greater than 400 m.

Russenes /1974/ has worked out another empirical method that compares the point-load index with the tangential stresses around the opening. When the compressive strength is known, the point-load index can, according to Hoek and Brown, be calculated as:

$$I_s = \frac{\sigma(c)}{(14 + 0.175D)}$$

where $\sigma(c)$	= compressive strength (MPa)
D	= diameter of the core (mm)
I_s	= pointload index (MPa)

The point-load index for the rock at Äspö is calculated to be:

Småland granite	$I_s = 6.9 - 12.2 \text{ MPa}$
Fine-grained granite	$I_s = 7.1 - 15.8 \text{ MPa}$
Greenstone	$I_s = 3.4 - 7.9 \text{ MPa}$
Äspö diorite	$I_s = 7.7 - 10.2 \text{ MPa}$

The maximum tangential stresses in a horseshoe-shaped tunnel are estimated at:

$$\sigma_t, \text{ max} = \sigma_v \times (A \times K_o - 1)$$

Where K_o is the ratio between σ_H and σ_v and A is a constant depending on the shape of the tunnel, here 3.2.

The tangential stresses at a depth of 300 m will be approximately 35 MPa and at a depth of 500 m, 60 MPa.

If calculations are performed for the different rock types at the levels at which they are expected to occur, Russenes' diagram gives:

Depth:	270 m Greenstone	some spalling
	310 m Greenstone	some to moderate spalling
	400 m Greenstone	moderate spalling
	420 m Sm. granite	some spalling
	500 m Äspö diorite	some spalling

According to Russenes, spalling may be expected at 250-300 m in the greenstone. The intensity will be higher at a greater depth.

Between 400 and 500 m some spalling may occur in the Småland granite and diorite.

Russenes' figure is more conservative than Hoek and Brown's and thus, according to his judgement, there is a risk that spalling will occur at a shallower depth and with greater intensity. The discussion presented here has so far concerned the stress conditions in the rock in relation to its compressive strength. However, the brittleness of the rock may also affect the intensity of the rock burst activity. As mentioned before, brittle behaviour has been observed in the tested rock material from Äspö, KAS 02. However, the degree of brittleness observed does not give any indication that failure in the rock will be increased by brittle rock. The rock stress measurements at Äspö show that horizontal stresses of a maximum of 10 MPa will occur at a depth of 300 m and 30 MPa at a depth of 500 m. The stresses in the rock material under consideration are of sufficient magnitude for spalling to develop. Taking into account the expected distribution of rock types, the intensity of spalling will be low. However, if greenstone should occur unexpectedly at a greater depth than predicted, the intensity could be severe. The rock stress measurements carried out showed a uniform distribution of the recorded values and must be considered as typical for the area. However, variations in the stress field at greater depth would drastically change the conditions for rock burst. A K_o value of 2.5 could give severe spalling in all rock types below 300 m.

3.5.7

Structural conditions and future loads

Several long faults with varying orientations intersect Äspö. Most of them dip steeply. The distance between these weakness zones is small in relation to their length.

The zones have been reactivated in various ways during different geological epochs in connection with the formation of mountain chains or superposition of sediments and ice caps. The fact that the zones have been activated at one time is in itself proof that they may be potential movement zones.

The rock in the zones is of much poorer quality and consequently the strength is lower than in the surrounding bedrock.

The orientation and stability of the zones imply a limitation of the size and/or orientation of the stress conditions that could be present today.

The current stress conditions are regional in character, i.e. the stresses may vary considerably from point to point, but are relatively constant when regarded as an average value over greater lengths of about 100-1000 m.

Future loads which may cause changes in the current stress field and thereby generate greater displacements will have an effect on large areas e.g. glaciation, land upheaval and plate tectonics. The load surface will be considerably larger than the distance between existing weakness zones.

It is not possible today to judge the direction of future loads.

Due to the fact that the load surface is considerably larger than the distance between existing zones and that the zones have less stability than the surrounding rock, it is probable that future displacement will be triggered in existing zones.

Since there are several zones with varying orientations on Äspö, the strength of one or more zones in each load direction will be so low that it will rupture. Failure and also displacements will therefore be concentrated in the existing zones. Thus, failure in the surrounding rock mass will be impossible due to its higher strength.

In zones with the same or a similar orientation, the zone with the lowest strength will rupture.

3.5.8

Potential movements

Minor changes in the present stress field, with increased maximum horizontal stress or decreased minimum horizontal stress or rotation, will be sufficient to cause movements in existing zones. It is, however, not possible to predict today the direction of the loads that will affect Äspö in the future and generate movements. Future loads will affect areas much larger than Äspö. The local structure on Äspö is thus of subordinate size, i.e. the entire regional area will be subjected to the same load both as to magnitude and direction. All large zones extending over greater areas are thus potential movement zones. Displacements will occur in the zone with the lowest strength and the least favourable orientation in relation to the actual load.

4**CONCEPTUAL MODELS****Description of geological structures and units and their properties**

In the description of the geological conceptual model of the Äspö HRL site area the bedrock is divided into a number of rock mass units (RMU). This classification is mainly based on petrographic parameters. The rock mass units are bordered or intersected by "fracture zones". SKB has identified a need to clarify the nomenclature especially for "fracture zone" and related topics.

The nomenclature in this report follows the "Guidelines for use of nomenclature on fracture, fracture zones and other topics /Bäckblom, 1989/. According to this guideline the designation "fracture zone" is only used if geological field evidence supports the assumption that "the intensity of natural fractures in a zone is at least two times higher than the mean fracture intensity in the surrounding rock".

A fracture zone is a three-dimensional feature. Certainty as to its extent and direction can only be obtained after investigations or measurements at several points. To define a "level of reliability" the three separate definitions "possible", "probable" and "certain" are used with increasing level of confidence. In this report the term "major fracture zone" is used for a feature with a width of more than about 5 m and an extent of several hundred metres.

Features less than about 5 m wide and with a more restricted extent are called "minor fracture zones".

4.1**MAJOR FRACTURE ZONES - SITE SCALE**

One of the main tasks in the characterization of the Äspö HRL rock mass is to predict which of the geological structures will have the most important rock- mechanic and hydraulic significance.

Of a great many structures mapped on Äspö the fracture zones now presented in Figure 4.1 are regarded as the most important for the geological-geohydrological modelling work. The most important characteristics of these are summarized in Table 4.1.

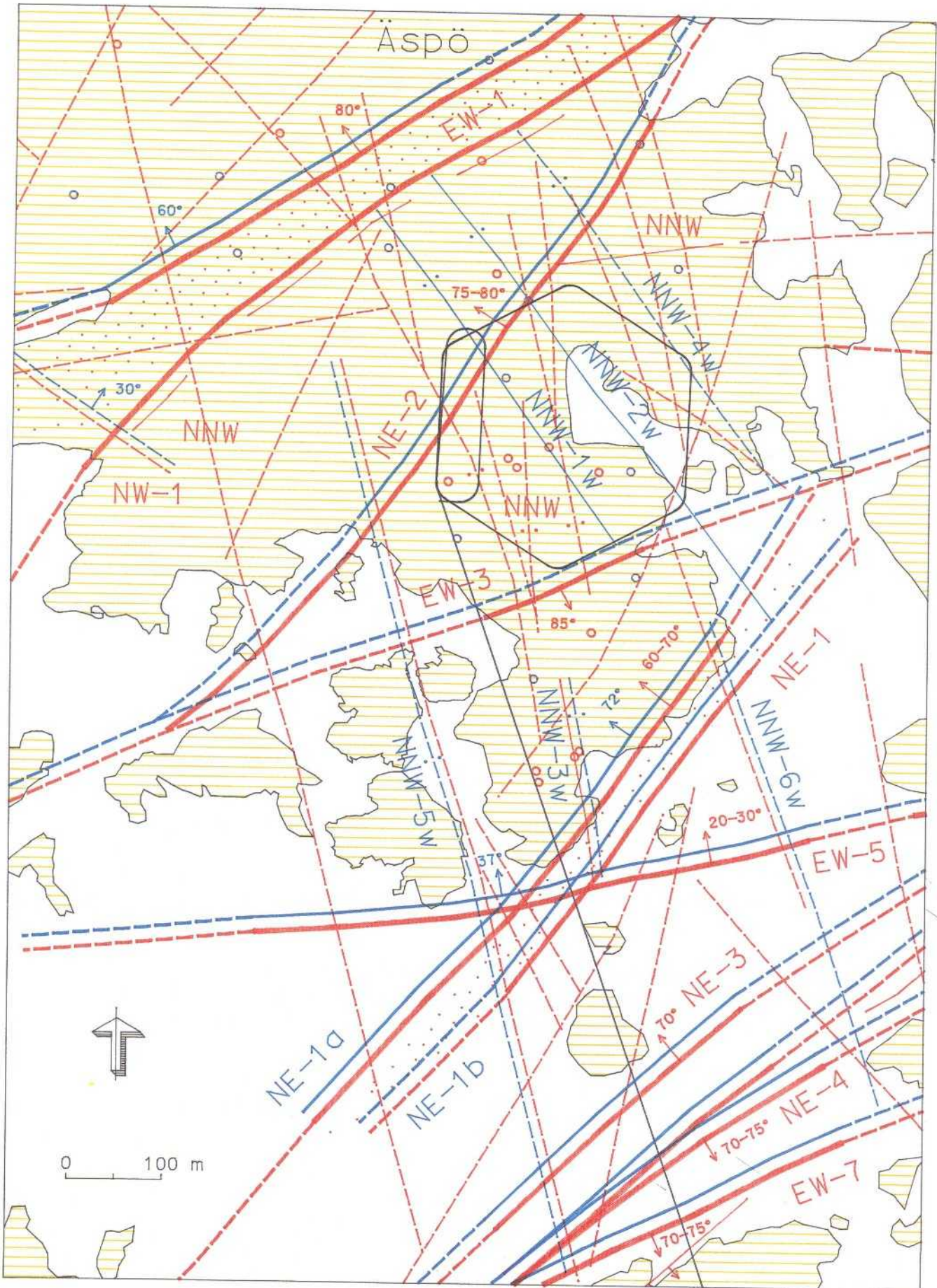


Figure 4.1 Äspö Hard Rock Laboratory - Structural model of the target area. For legend see Figure 3.16.

Table 4.1 Major Fracture Zones in the Äspö - Hälö area

Fracture zone	Orientation (O) Estimated width (W) Extent at surface (E)	Topographical identification (T) Geophysical identification (G)	Borehole identification			Reliability
			Geological	Geohydrological Interference test:(P) Injection test:(I) Airlift test:(A) Spinner survey:(S)	Groundwater chemistry	
EW-1	O:ENE (NE)/ ~ 80°NW W:50-100 m E:600-700 m	T:Very distinct G:Evident (magnetic, seismic and electric)	KAS04: c. 55-70, 115, 175- 190 m KAS12: c. 10-70 m HAS01, 05, 18, 19 and 20: Increased fracturing - alteration	EW-1 _w KAS04: 0-185 (P) EW-1 _w KAS03: 349-373 (S) 455-475 (S) 610-622 (S) 691-694 (S)	KAS04: 226-235 334-343	"Certain"
NE-2	O:NE/75°NW- ~ 85°SE W:5-10 m E:500-600 m	T:Faint G:Evident (magnetic and electric)	KAS04: c. 430 m KAS08: c. 40-60 m KAS12: c. 270-300 m KAS13: c. 370-410 m HAS16: c. 20-80 m	KAS04: 388-436 (S) KAS12: 240-325 (S)	KAS04: 440-481 KAS12: 303-380	NE-2 is estimated to be mostly "certain"
NNW	O:NNW/80°W- 80°E W:c. 1-3 m E:200-400 m (en échelon)	T:Faint-distinct G:No ambiguous indication	KAS13: c. 60, 160, 210, 260 m	NNW-1 _w KAS06: 208-234 (S) KAS07: 50-80 (RQD,P) NNW-2 _w KAS06: 447-450 (S) KAS08: 183-186 (S) KAS16: 0-120 (P) NNW KAS13: 161,169 (S) 211,214 (S)	KAS06: 204-277 439-602 KAS13: 104-211	The different sub- zones are estimated to be "possible or probable"
EW-3	O:ENE/85°S W:10-15 m E:c. 200 m	T:Distinct G:Evident (magnetic, electric and seismic)	KAS06: c. 60-70 m KAS07: c. 420 m	KAS07: 383-451 (I)	No indications	"Certain"

Table 4.1, Continuation

Fracture zone	Orientation (O) Estimated width (W) Extent at surface (E)	Topographical identification (T) Geophysical identification (G)	Borehole identification			Reliability
			Geological	Geohydrological Interference test:(P) Injection test:(I) Airlift test:(A) Spinner survey:(S)	Groundwater chemistry	
NE-1	O: ~ NE/50-60°NW W:c. 50 m E:400-600 m?	T:The fracture zone NE-1 is assumed to surface in the sea c. 50-100 m south of Äspö. G:Evident (seismic and magnetic)	<u>KAS09</u> : c. 100-150 m <u>KAS14</u> : c. 100-125 m <u>KAS11</u> : c. 150-175 m <u>KBH02</u> : c. 310-400 m <u>KAS08</u> : c. 570-600 m <u>KAS07</u> : c. 520-550 m	<u>KAS09</u> : 110-148 (S) <u>KAS14</u> : 110-160 (S) <u>(KBH02</u> : 408-760 (A)) <u>KAS08</u> : 555-601 (S) <u>KAS07</u> : 508-604 (S) <u>KAS02</u> : 803-920 (S)	<u>KAS14</u> : 105-212 <u>KAS07</u> : 462-604	"Certain"
EW-5	O: ~ ENE/20-30°NNW W:c. 100 m? E:400-600 m?	T:EW-5 is assumed to surface in the sea c. 50-100 m south of Äspö. G:Seismic reflection?	<u>KAS09,11,14</u> : c. 10-60 m <u>KAS04</u> : c. 330 m <u>KAS02</u> : c. 120-130,c. 275 m <u>KAS05</u> : c. 100-115,c. 210-220 m <u>KAS06</u> : c. 60-70 m <u>HAS13,14</u> : c. 50-60 m	<u>KAS02</u> : 309-343 (S) <u>KAS05</u> : 274-383 (I) 362-365 (I) <u>KAS06</u> : 312,351-354 (S) 362-365 (S) <u>KAS07</u> : 222-224 (S) 235-246 (S) <u>KAS09</u> : 50-100 (RQD,P) 50-100 (RQD,P) <u>KAS11</u> : 50-100 (RQD,P) <u>KAS14</u> : 50-100 (RQD,P)	<u>KAS07</u> : 212-304 <u>KAS06</u> : 389-406	"Possible"
EW-X	O: ~ ENE/20-30°NNW W:c. 100 m? E:400-600 m?	T:Assumed to surface in Hälö and in the sea north of Hälö G:-	<u>KAS02</u> : c. 400, 490 m <u>KAS05</u> : c. 400, 480 m <u>KAS09</u> : c. 140-160,250 m <u>KAS11</u> : c. 160-180,250 m <u>KAS14</u> : c. 150-200 m		<u>KAS09</u> : 306-447	"Possible"

4.1.1

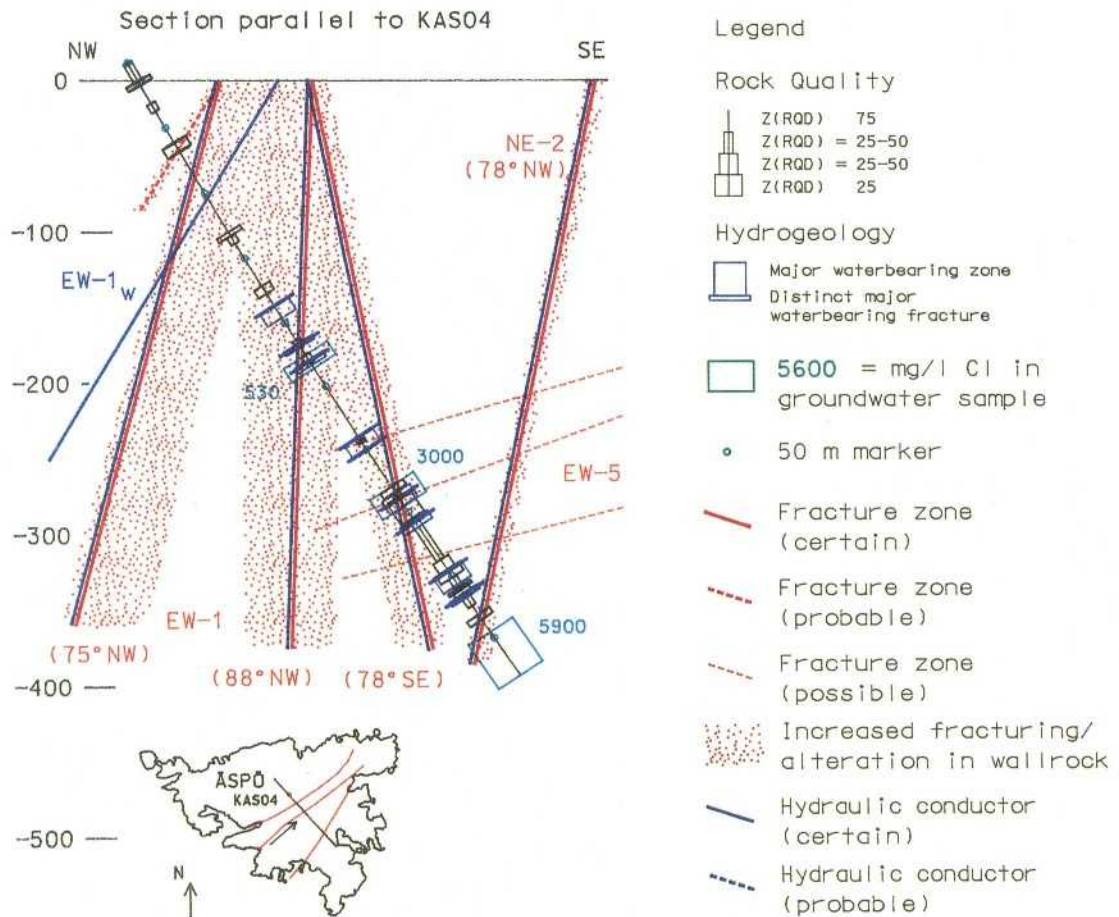
Fracture zone EW-1

Figure 4.2 Fracture zone EW-1

Geological evidence:

The fracture zone EW-1 is very well documented topographically (50-100 m wide depression in the ground extending many hundred metres), geophysically (low-magnetic and low resistivity zone 200-300 m wide), geologically (outcrops in trenches with mylonites and crushed sections) and in boreholes (mylonites and many highly fractured and altered sections in drilling cores). Indicated by VSP and radar. Fracture zone EW-1 can be regarded as the northern part of the about 300 m wide low-magnetic zone (Åspö shear zone), trending NE, which divides Åspö into two main blocks. EW-1 includes ENE as well as NE trending elements, mostly dipping steeply to the north. Initially the zone was characterized by early ductile-semiductile deformation. Local development of mylonites and epidotic shear zones controlled the orientation of later brittle deformation in the form of increased fracturing and brecciation. Hydrothermal alteration (oxidation of magnetite to hematite and red-staining of fractures) and formation of different fracture filling minerals very likely had an important sealing effect on the main part of the zone. The most conductive parts of EW-1 seem to coincide with some narrow highly fractured sections or single

open fractures which are probably not connected along the entire zone.

EW-1 should be regarded as a complex zone composed of some highly fractured (crushed), more or less mineralogically altered, metre wide sections, separated by slabs of Småland granite (less fractured but hydrothermally altered) and up to metre wide mylonites (more or less fractured).

EW-1 is judged to be "certain" according to the nomenclature on fracture zones /Bäckblom et al., 1990/.

Geohydrological evidence:

There are indications of a structure here called EW-1_w, striking approximately ENE with a dip of 60°N. Pumping of the hydraulic structures at 349-373, 455-473, 610-622 and 691-694 in KAS02 indicates an ENE striking structure, which intersects KAS04 at section 0-185 m (D6). There may well be several ENE structures, causing the responses, but here it is assumed that the responses can be explained by a single structure parallel to EW-1 and with a dip of 60°N. The pumping test in HAS20 also indicates a good hydraulic contact with the northern part of Äspö, probably because of EW-1_w.

Transmissivity is estimated at $T = 2.0 \cdot 10^{-5} \text{ m}^2/\text{s}$./Rhén, 1988, Nilsson L, 1989/.

The extent and transmissivity of the zone to the east are not known. Transmissivity is assumed here to be $1 \cdot 10^{-6} \text{ m}^2/\text{s}$ approximately 100 m east of KAS04.

The central part of EW-1 has a low conductivity, which hydraulically separates the northern part of Äspö from the southern part. This assessment is certain.

Geohydrochemical evidence:

The salinity of groundwater sampled within EW-1 was lower than expected from the depth dependence of the salinity at Äspö. Two separate intervals of about 200 and 300 m depth in KAS 04 gave chloride contents of 530 and 3000 mg/l respectively. Based on the sampling depth, chloride concentrations of 3000 and 4000 (+/- 1000) mg/l would have been expected. This deviation indicates that there is an inflow of fresh water in the upper part of the zone causing the saline/freshwater mixing to occur deeper in fracture zone EW-1 than in the surrounding rock. However, it should also be noted that despite the indicated inflow there is no high tritium content in the groundwater samples. The groundwater has a clearly reducing character as shown by Eh-measurement and sulphide analysis.

4.1.2

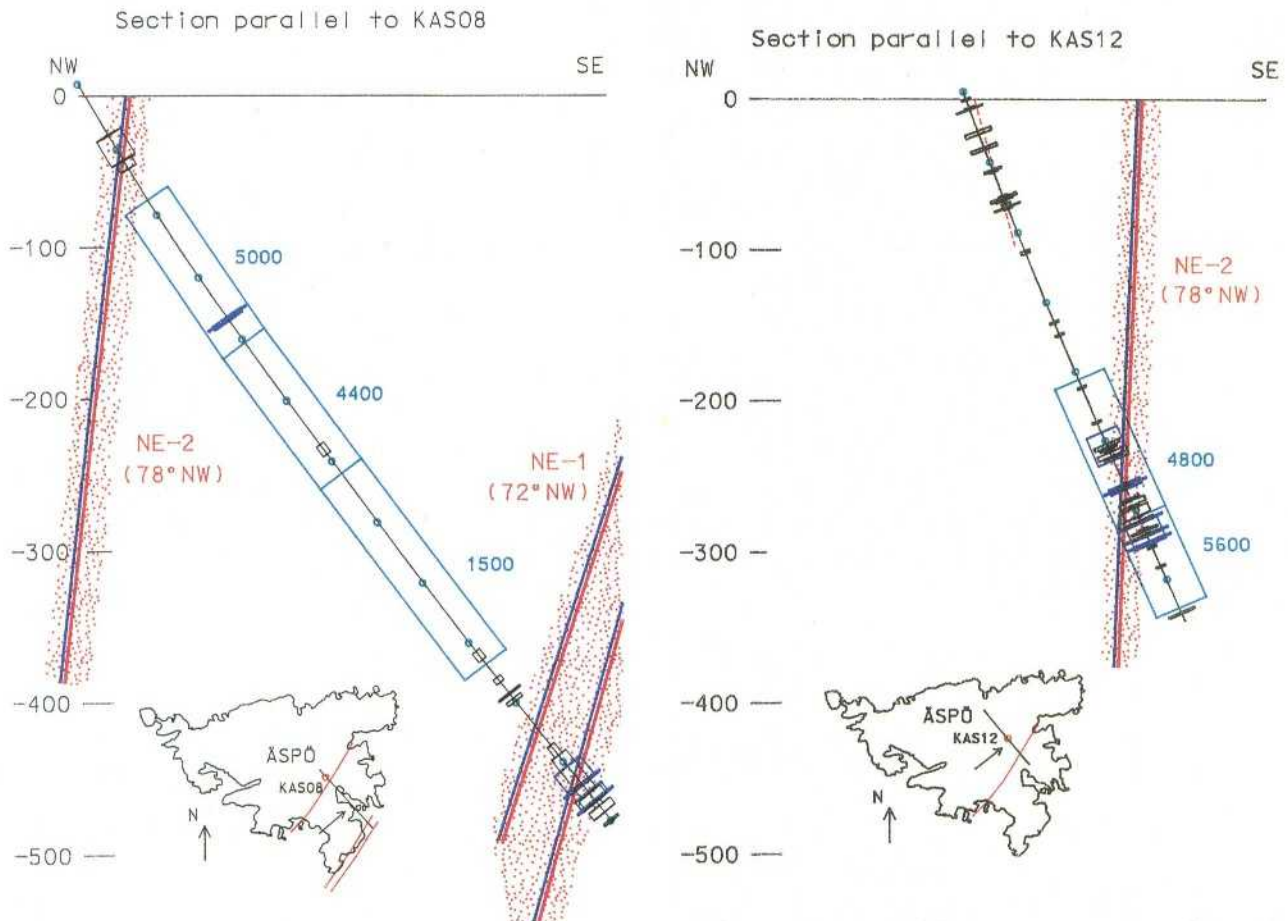
Fracture zone NE-2

Figure 4.3 Fracture zone NE-2 (see also Figure 4.8)

Geology:

Fracture zone NE-2 is only locally developed and rather faintly topographically indicated. NE-2 is indicated geophysically to some extent (low-magnetic and decreased resistivity along almost the entire zone). Geological indications are found in the SW-part of zone NE-2 (intense fracturing and altering of outcrops in the trench). Borehole indications in the form of crushed and highly altered sections are found in drilling cores as well as VSP and borehole radar indications.

Fracture zone NE-2 trending NE/ENE can be regarded as the southern part of the main Äspö shear zone. NE-2 is expected to follow a somewhat winding course. The brittle deformation of this zone is probably greatly influenced by the former ductile shearing and mylonitization. Hydrothermal alteration and formation of different generations of fillings in the fractures probably had a sealing effect on parts of the zone. The dip of NE-2 seems to change from steeply northwards in the NE to steeply southeast in the SW part of the zone.

The zone NE-2 seems to be only moderately hydraulically conductive.

The zone is judged to be "probable" - some northeastern parts of NE-2 also "certain".

Geohydrological evidence:

NE-2_w is a structure striking NE with dip 78°NW. According to the geological information NE-2_w may not be very conductive.

The estimated transmissivity and the probable range of the transmissivity for NE-2 are:

$$T = 0.4 \cdot 10^{-5} \text{ m}^2/\text{s}.$$

$$0.2 \cdot 10^{-5} < T < 1 \cdot 10^{-5} \text{ m}^2/\text{s}$$

Geohydrochemical evidence:

Groundwater sampled from NE-2 shows a slightly higher salinity than expected from the depth dependence: 4800 and 5900 mg/l (± 1000) at depths of 300 and 400 m respectively in KAS12 and KAS 04. This indicates that a slight discharge of groundwater through NE-2 might occur.

4.1.3

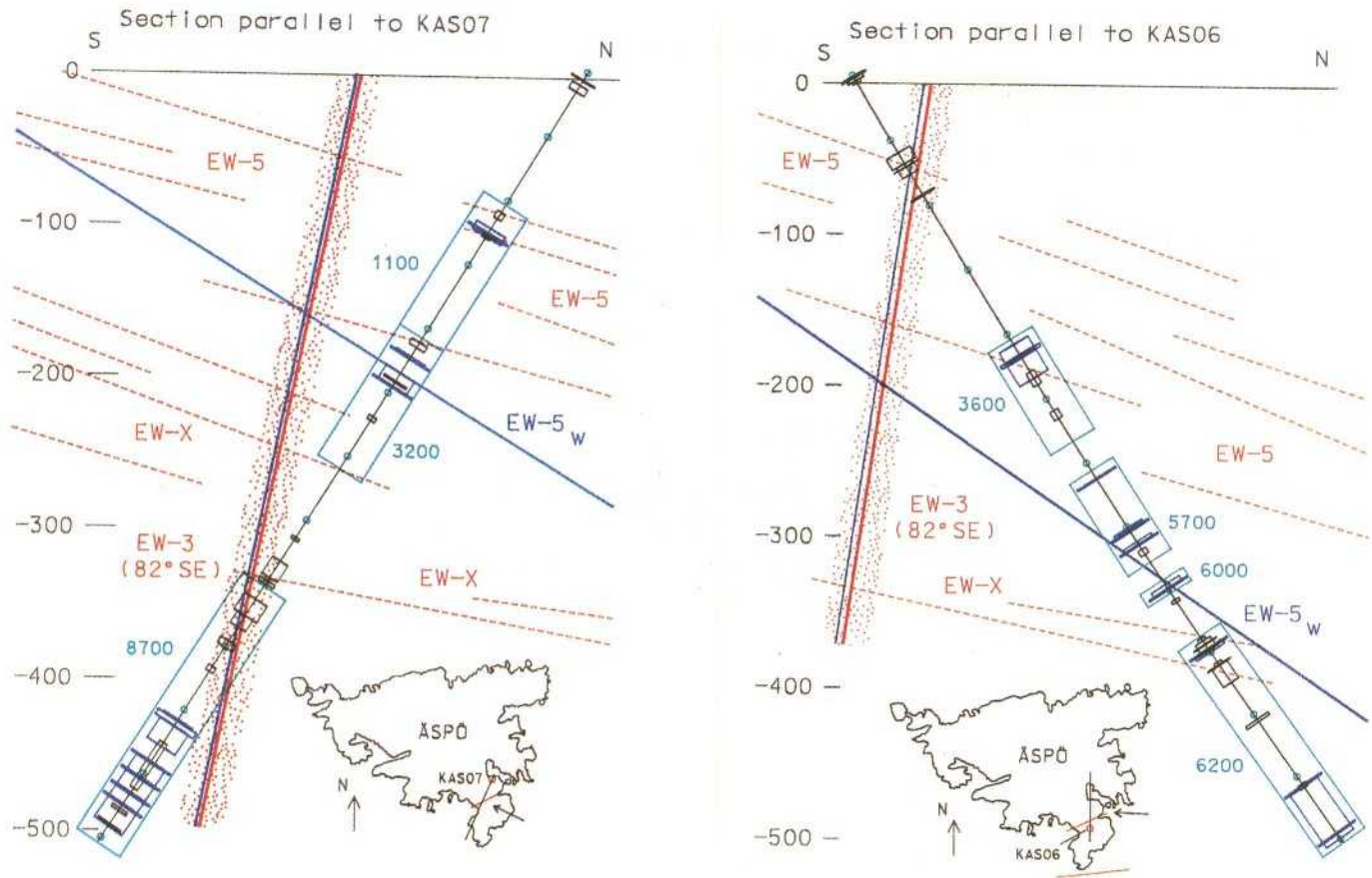
Fracture zone EW-3

Figure 4.4 Fracture zone EW-3

Geological evidence:

Fracture zone EW-3 is very well documented topographically (approximately ten metre wide depression extending c. E-W across the island with distinct scarps), geophysically (low magnetic and low resistivity zone), geologically (outcrops in trench with intense fracturing) and in boreholes (highly fractured and altered sections in drilling cores and VSP indications).

Zone EW-3 probably dips c.85° southwards.

According to drill-core observations the zone has developed in a very heterogeneous bedrock comprising rather thin sheets of Småland granite - greenstone - a fine-grained granite.

Hydrothermal alteration seems to have affected most of the rocks in the zone (clay to some extent). Conductive sections are probably rare and mostly coincide with open fractures along the contacts with the surrounding fresh rock.

EW-3 is judged to be "certain".

Geohydrological evidence:

EW-3_w is a structure with an EW strike and a dip of 82°SE. On a geological basis the transmissivity of the structure is expected to be low.

The estimated transmissivity and probable range of the transmissivity for EW-3_w are

$$T = 0.05 \cdot 10^{-5}$$

$$0.01 \cdot 10^{-5} < T < 0.1 \cdot 10^{-5} \text{ m}^2/\text{s}$$

Hydraulically, EW-3_w is probably of minor importance.

Geochemical evidence:

No specific groundwater representing EW-3 has been sampled.

4.1.4

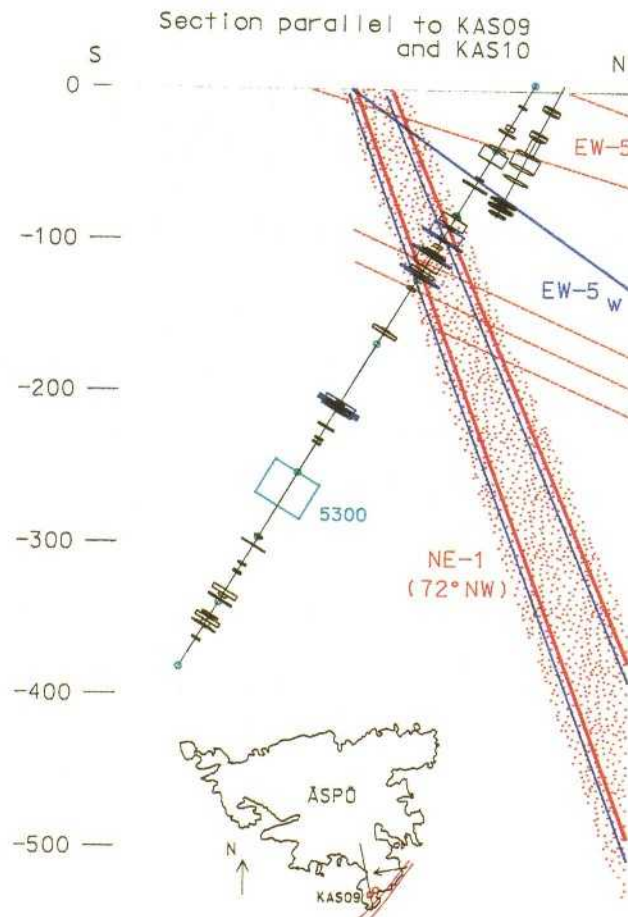
Fracture zones NE-1 and EW-5

Figure 4.5 Fracture zone NE-1 (see also Figure 4.3)

Geological evidence:

Fracture zones NE-1 and EW-5 are assumed to surface in the sea c. 50-100 metres south of Äspö.

Zone NE-1, trending c. NE and dipping c. 60°-70° northward - according to borehole investigations - is estimated to be complex with both more steeply dipping and gently dipping elements.

The zone is well documented in several core boreholes as a series of several metres wide, highly fractured and in part mineralogically altered sub-zones. Some of these sub-zones are probably connected with some of the NW-NE-trending zones and perhaps also EW-5. They seem to be very important as hydraulic conductors.

Fracture zone NE-1 is judged to be "certain".

Zone EW-5 is assumed to dip gently (20°-30°) to NNW and appears to be associated with a thrust trending c. ENE, observed on land c. 300 m east of southern Äspö. EW-5 probably comprises a series of more or less parallel fractures, partly open with stepped offsets in the dip direction. This means that the most significant hydraulic pathways will run parallel to the strike of the zone. The different steps of EW-5 - which seem to be poorly hydraulically connected for the most part - are probably intersected by the narrow NNW-NNE trending fracture zones, which are judged to be highly permeable.

Talbot et al, 1989, discuss the possibility of several gently dipping fracture zones parallel to EW-5 with a centreline vertical spacing of about 90-133 m.

The fracture EW-5 is judged to be "possible".

Geohydrological evidence:

EW-5_w

EW-5_w is an EW striking structure with an approximate dip of 37°N. Geologically the zone is probably very complex. According to the pumping tests the estimated transmissivity and probable range of the transmissivity for EW-5_w are

$$T = 2 \cdot 10^{-5} \text{ m}^2/\text{s}$$

$$1 \cdot 10^{-5} < T < 4 \cdot 10^{-5} \text{ m}^2/\text{s}$$

EW-5_w is believed to terminate at the south part of EW-1. EW-5_w has not been identified in KAS08 and its extent to the east is therefore thought to the end before KAS08.

NE-1a_w and NE-1b_w

NE-1a_w is a very conductive NE-striking structure with a dip of 72° NW.

The pumping tests on the southern part of Äspö indicate several conductive structures, one of which is NE-1a_w. There are probably several conductive structures south of NE-1a_w, whose properties and position cannot be identified properly. Some of these structures, properties and positions are discussed under NE-3_w, NE-4_w, EW-7_w and NNW 5-6_w.

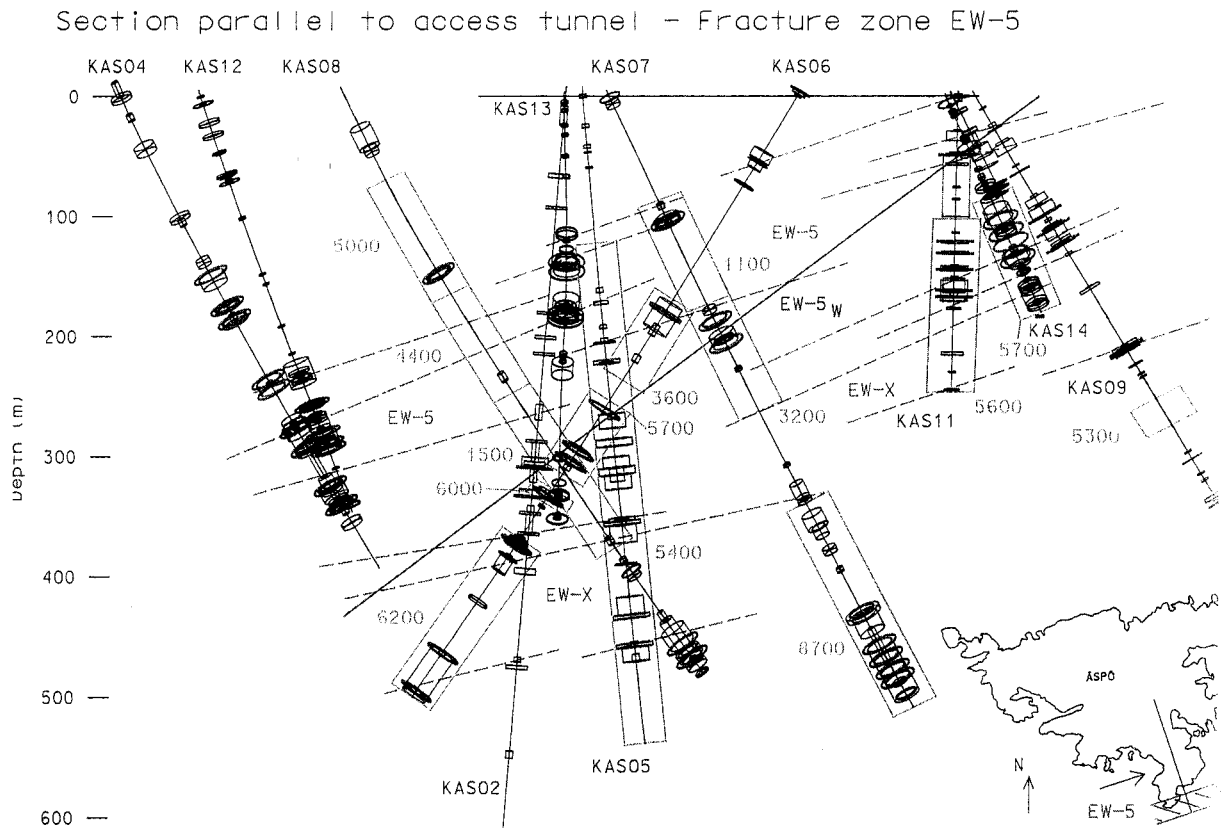


Figure 4.6 Fracture zone EW-5 (see also Figure 4.4)

Another structure that may be present is a structure intersecting KAS09 at section 245-252 m with $T = 4.2 \cdot 10^{-4} \text{ m}^2/\text{s}$. This structure may be parallel to or nearly parallel to NE-1a_w and is here called NE-1b_w.

There is evidence of a good hydraulic contact with some of the boreholes on Ävrö which indicates that there may be very conductive structures striking more or less N-S. The transmissivity estimated from pumping tests for NE-1a_w is probably overestimated due to this.

The tests in KAS07 indicate a lower transmissivity for NE-1a_w than other tests show. It is believed that the transmissivity decreases with depth. The higher transmissivity in KAS08 may be explained by NNW-2_w.

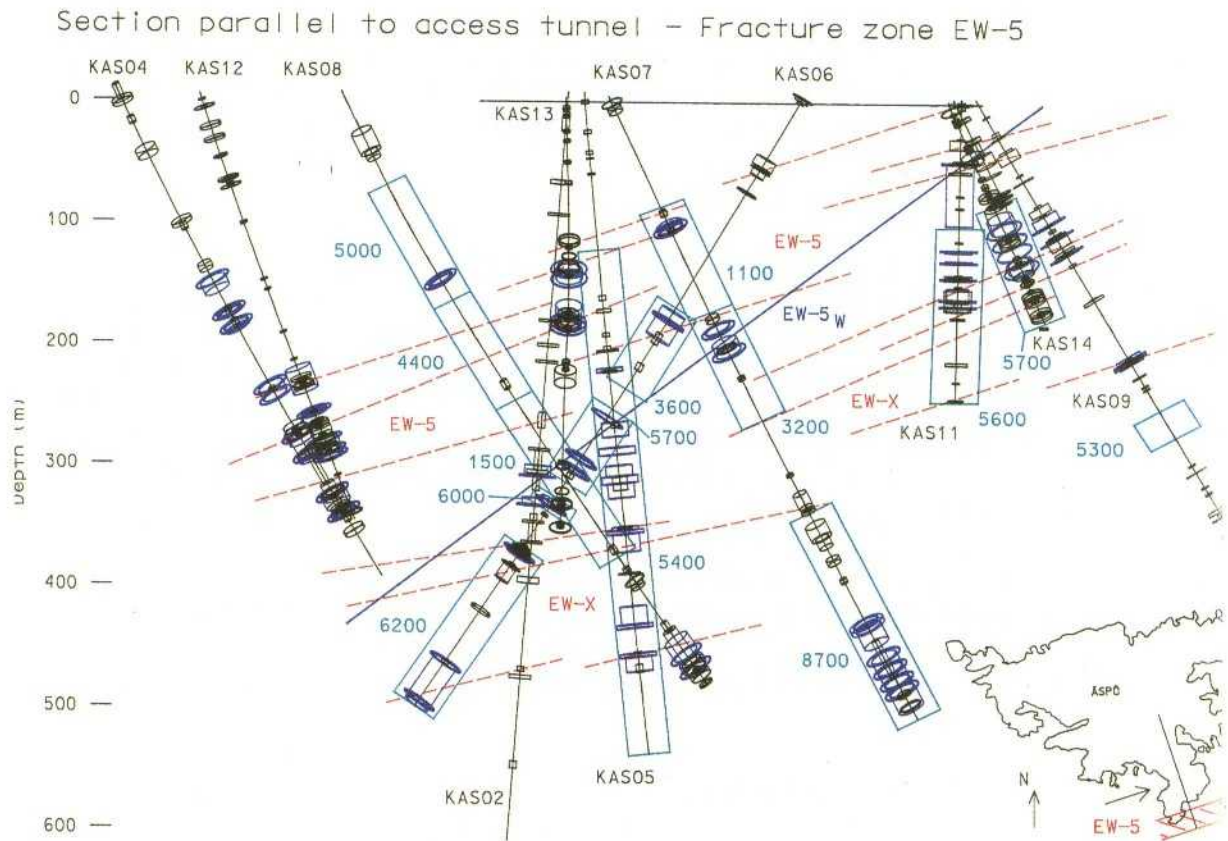


Figure 4.6 Fracture zone EW-5 (see also Figure 4.4)

Another structure that may be present is a structure intersecting KAS09 at section 245-252 m with $T = 4.2 \cdot 10^{-4} \text{ m}^2/\text{s}$. This structure may be parallel to or nearly parallel to NE-1a_w and is here called NE-1b_w.

There is evidence of a good hydraulic contact with some of the boreholes on Ävrö which indicates that there may be very conductive structures striking more or less N-S. The transmissivity estimated from pumping tests for NE-1a_w is probably overestimated due to this.

The tests in KAS07 indicate a lower transmissivity for NE-1a_w than other tests show. It is believed that the transmissivity decreases with depth. The higher transmissivity in KAS08 may be explained by NNW-2_w.

4.1.5

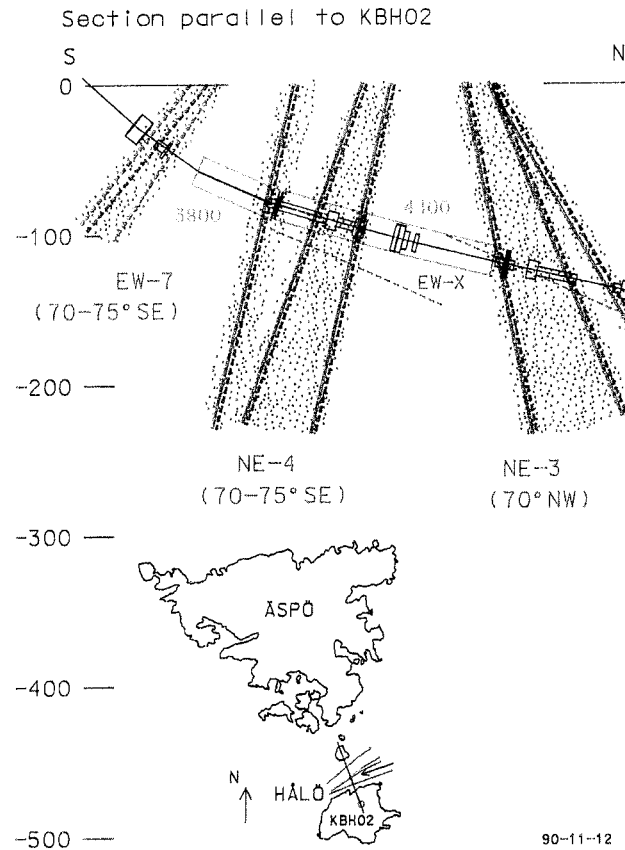
The fracture zone system EW-7, NE-3 and NE-4

Figure 4.7 Fracture zone system EW-7, NE-3 and NE-4

Geological evidence:

This zone system, which anastomoses in ENE-NE and regarded to have a regional extent, is geophysically well indicated as a broad band in the strait immediately north of Hålö.

NE-3 and NE-4 are probably composed of a number of one to a few metres wide sub-zones alternating with slabs of less fractured and altered rock. NE-3 seems to be associated with several dikes of fine-grained granite and some mylonites in the Småland granite. Some open fractures (narrow fracture zones) in NE-3 and NE-4 are assumed to be highly conductive. There are also indications of N-S trending narrow fracture zones, probably hydraulically connecting the NE-1/EW-5 system with NE-3/NE-4.

NE-3 and NE-4 are judged to be "certain".

EW-7 comprises three almost parallel sub-zones of which the dip especially of the southernmost is very uncertain but probably moderately-low to the south. Each sub-zone is probably composed of two or three up to several metres wide fractured and altered sections interveining more solid rock. Conductive sections are estimated to be associated mainly with dikes of fine-grained granite.

EW-7 is judged to be "probable".

Geohydrological evidence:

North of Hålö there are complex EW or NE striking structures. The dip of NE-3_w is approximately 70° NW, NE-4_w vertical and EW-7_w, 65°-80° SE.

Neither spinner survey nor packer tests have been performed in KBH02 and therefore the information on where these structures intersect KBH02 is very uncertain. RQD is used below to indicate where NE-3_w, NE-4_w and EW-7_w possibly intersect KBH02 and KAS09. NE-3_w may intersect KAS09, according to the estimated dip of NE-3.

The transmissivities are estimated to be

$$\text{NE-3}_{\text{w}}: T = 3 \cdot 10^{-5} \text{ m}^2/\text{s}$$

$$\text{NE-4}_{\text{w}}: T = 3.5 \cdot 10^{-4} \text{ m}^2/\text{s}$$

$$\text{EW-7}_{\text{w}}: T = 1.4 \cdot 10^{-4} \text{ m}^2/\text{s}$$

The structures are judged to be "probable", hydraulically speaking.

Geohydrochemical evidence:

The chloride content of the groundwater from NE-3 and NE-4 is in the range 2800 - 4400 mg/l. The carbonate content is 200 - 250 mg/l. No samples from EW-7 have been analysed. The high chloride content and carbonate concentration clearly show the different signature of the water from fracture zones covered by the sea.

4.1.6

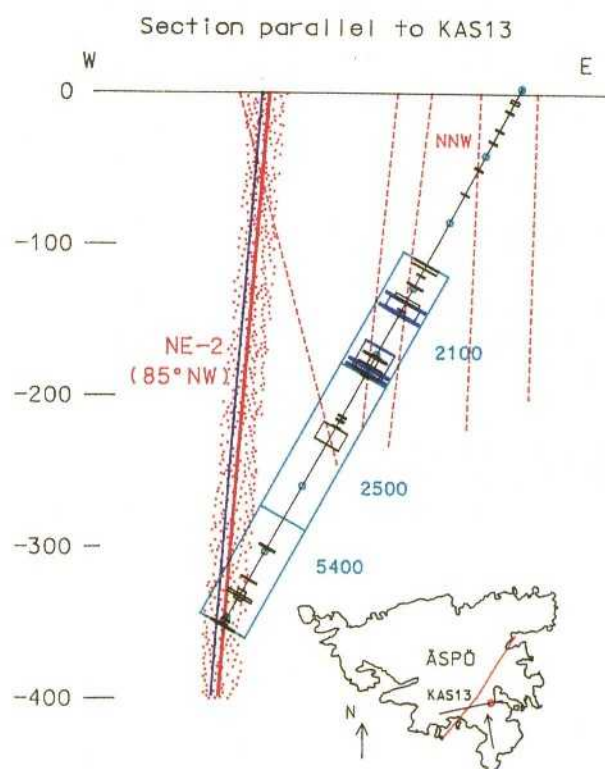
The fracture zone system NNW

Figure 4.8 Fracture zone system NNW

Geological evidence:

A great number of approximately north-striking fractures and narrow (dm - a few metres wide) fracture zones have been mapped on outcrops in Åspö. More or less extensive, they seem to anastomose in an en-échelon pattern across the island.

Only a few of them are topographically significant but normally too narrow to be geophysically unambiguously indicated. VSP and borehole information support the notion of steep, mostly easterly dips. All these fractures and fracture zones are described under the designation "NNW".

The hydraulic conductivity is assumed to reach a maximum parallel to the steep dilational direction (σ') in this zone. The axes of common intersection of fractures in the almost vertical north-trending zones and the low-dipping zone EW-5 are probably also of great importance as hydraulic conductors.

The different sub-zones in the system NNW are judged to be "possible-probable".

Geohydrological evidence:

Several pumping tests indicated that conductive structures striking N or NNW are likely to be present. From a geological and geophysical point of view these structures are difficult to find and they are judged to be single fractures, which are open due to the stress field.

NNW-1_w

The strike of NNW-1_w is about NNW with a vertical dip and NW-1 may intersect HAS05 and HAS17.

The transmissivity and probable range of the transmissivity for NNW-1_w are estimated to be

$$T = 1.5 \cdot 10^{-5} \text{ m}^2/\text{s}$$

$$0.5 \cdot 10^{-5} < T < 2 \cdot 10^{-5} \text{ m}^2/\text{s}$$

NNW-1_w is believed to terminate at the south part of EW-1 and at EW-3 to the south. NNW-1_w is an important hydraulic structure judged to be certain, but its position is uncertain.

NNW-2_w

Several pumping tests indicated that there may be a conductive structure with a strike of N or NNW somewhere around KAS08. Here it is assumed that the strike is NNW and the dip is vertical, as NNW-1_w.

The high transmissivity in KAS08 447-601 is probably a combination of NE-1_w and NNW-2_w. The estimated transmissivity and range of transmissivity of NNW-2_w are

$$T = 4 \cdot 10^{-5} \text{ m}^2/\text{s}$$

$$2 \cdot 10^{-5} < T < 6 \cdot 10^{-5} \text{ m}^2/\text{s}$$

NNW-2_w is believed to end towards the south part of EW-1 and to the south towards NE-1. NNW-2_w is an important hydraulic structure judged to be certain but its position is uncertain.

NW-3_w

NNW-3_w is a NNW striking structure with a vertical dip. Its properties and dip are uncertain but pumping tests in HAS13 indicated a transmissivity of $2.5 \cdot 10^{-4} \text{ m}^2/\text{s}$ and pumping tests in KAS08, 11, 14 and KBH02 indicated a good contact with HAS13. It is probably NE-1 that is seen in the tests. It is not possible to estimate the transmissivity in NNW-3_w from hydraulic tests. Its position is estimated on the basis of geophysical indications of the zone.

The transmissivity and range of the transmissivity are estimated to be

$$T = 2 \cdot 10^{-5}$$

$$0.5 \cdot 10^{-5} < T < 5 \cdot 10^{-5} \text{ m}^2/\text{s}$$

The estimation of T is very uncertain. NNW-3_w probably terminates near HAS13 to the north and at NE-1 to the south.

NNW-3_w is judged to be possible.

NNW-4_w

If the position of NNW-2_w is correct there is probably a structure striking N-S or NNW east of NNW-2_w since HAS18 shows good contact in pumping tests in KAS09, 14 and KBH02. Probably NNW-2 cannot explain the good contact. The transmissivity is unknown but is assumed here to be of the same order of magnitude as NNW-2, that is

$$T = 4 \cdot 10^{-5}$$

$$2 \cdot 10^{-5} < T < 6 \cdot 10^{-5} \text{ m}^2/\text{s}$$

NNW-4_w probably ends towards the south part of EW-1 to the north and towards NE-1 to the south.

NNW-4_w is judged to be possible.

NNW-5_w, NNW-6_w

Pumping tests in KAS09, 11 and 14 showed good contact with HAV2, 7 and 8 and the structures EW-5_w, EW-7_w, NE-1_w, NE-3_w and NE-4_w cannot explain the responses. There are probably one or several N-S or NNW conductive structures crossing these structures. There are also indications from a pumping test in KAS13 that there is probably a N-S or NNW structure west of KAS13 and HAS04. Based on geophysical indications two structures, NNW-5 and NNW-6, have been chosen. The transmissivity and range of the transmissivity for NNW-5 and NNW-6 are estimated to be

$$T = 5 \cdot 10^{-5} \text{ m}^2/\text{s}$$

$$1 \cdot 10^{-5} < T < 1 \cdot 10^{-4} \text{ m}^2/\text{s}$$

The estimation is naturally very uncertain. NNW-5_w is assumed to terminate about 150 m north of NE-2 and against NE-4_w. NNW-6_w is assumed to stop against NE-1 and against EW-7_w.

NNW-5_w and NNW-6_w are judged to be possible.

Geohydrochemical evidence:

The NNW fracture system carries fresh water into the rock mass. The salinity there is therefore lower than in the surrounding rocks and in zones of corresponding depth. These assumptions are verified by the sampling of KAS 13. The tritium concentration in the uppermost and lowermost sections of KAS 06 indicates a recharge of surface water.

4.1.7**The fracture zone system NW-1**

NW-1_w is a NW striking structure with an approximate dip of 30°N. It is believed to intersect KAS03 at 197-221 and 249 m and the pressure response is measured in section C5, 107-252 m. NW-1 is not believed to extend south of EW-1.

The transmissivity of the structure is estimated to be $T = 0.7 \cdot 10^{-5} \text{ m}^2/\text{s}$ /Rhén, 1989, Nilsson, 1989 a/.

NW-1_w is judged to be probable.

4.2

ROCK MASS UNITS — SITE SCALE

Based on the pre-investigations the site area can be described in a number of rock mass units (RMU).

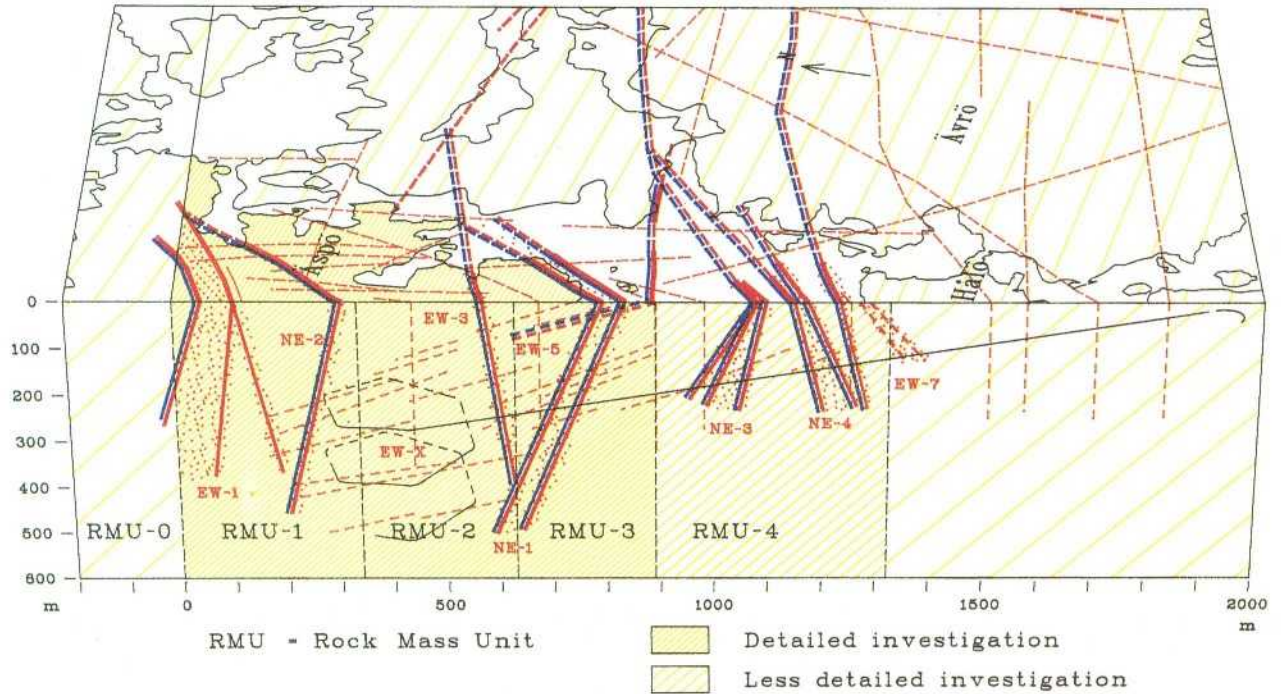


Figure 4.9 Rock mass units in the target area

General geohydrological characteristics:

The hydraulic conductivity is log-normally distributed and the geometric mean of the hydraulic conductivity is approximately constant with depth. The standard deviation (S_{LogK}) does however decrease with depth according to Table 4.2. Both the geometric mean value and the standard deviation are dependent on the test scale. (Tables 4.2 and 4.3.)

The conductivities in chapter 4 are all given for the test scale 3 m. If tests are performed on another scale the hydraulic conductivity values have to be converted to the 3 m scale if the values are to be compared.

4.2.1

RMU-0

Geohydrological characteristics:

RMU-0 is bordered to the south by fracture zone EW-1 and to the north by the strait north of Äspö.

The NW part of Äspö, RMU-0, is more conductive than the south part. The estimated geometric mean of the hydraulic conductivity for RMU-0 is

$$K_g^3 = 7.9 \cdot 10^{-10} \text{ m/s}$$

Table 4.2 Estimated standard deviation for LogK for the scale 3, 10, 20, 50 or 100 m

Vertical depth (m)	3m	10m	S_{LogK} 20m	50m	100m
0	2.17	1.39	1.13	0.44	0.65
200	2.0	1.26	0.83	0.70	0.61
400	1.74	1.13	0.74	0.61	0.52
600	1.52	0.96	0.65	0.62	0.48
800	1.26	0.83	0.52	0.43	0.39
> 800	1.26	0.83	0.52	0.43	0.39

Table 4.3 Estimated scale conversion factor (TF) for the geometric mean value of the hydraulic conductivity from the 3 m scale (K_g^3) to 10 m, 20 m, 40 m and 80 m scale

Scale (m)	CF (-)
10	3.46
20	7.05
40	14.4
80	29.5

4.2.2

RMU-1

Geological characteristics:

RMU-1 is bordered to the north by fracture zone EW-1 and to the south by zone NE-2.

The predominating rock type in RMU-1 is the reddish grey, medium grained porphyritic granite-granodiorite-monzodiorite (Småland granite) with megacrysts of red microcline.

Fine-grained metavolcanics (metadacite-metaandesite) and greenstone (metabasalt) constitute a particularly large part of the rock mass in outcrops and core boreholes in RMU-1. A variety of greenstone which is more coarse-grained and dike-shaped is found in the area.

The metavolcanic rocks are very often intruded by a fine-grained granite which also seems to be more frequent in this unit than in other parts of the site area. The fine-grained granite occurs both as well defined dikes and more irregular veins intersecting the older rocks. The dikes in RMU-1 are up to 25 m wide, usually striking c. NE. The fine-grained granite is often strongly deformed and fractured. A few pegmatitic segregations occur in this granite.

From the structural point of view RMU-1 coincides very well with the so-called "Äspö shear zone" and especially NE striking mylonites are very common. The mylonites here tend to be significantly wider (2-3 m) and occur more frequently than elsewhere on Äspö, where small scale mylonitic shearplanes less than about one cm thick and up to a few metres long, almost ubiquitous in orientation, are the norm.

Fracturing is more intense in all the rocks in RMU-1 than elsewhere on Äspö. The fractures are also denser and shorter with mean spacing from 0.50 m to 1.80 m. The dominant orientation of the fractures are c. N 60° E, N - S and NW. The most common fracture fillings are calcite and chlorite. Red-stained fractures are very frequent in the Småland granite. A low-dipping (20°-40° S) fracture zone (EW-5) is believed to intersect RMU-1 at a depth of c. 300-400 m.

Steeply dipping NNW-NNE trending fracture zones - mostly narrow - are judged to be of particular hydraulic importance.

Geohydrological characteristics:

The geometric mean of the hydraulic conductivity of RMU-01 is estimated to be

$$K_g^3 = 3.2 \cdot 10^{-10} \text{ m/s}$$

4.2.3

RMU-2

Geological characteristics:

RMU-2 comprises the rock mass between NE-2 and EW-3.

The dominant rock type in this unit is a granite-granodiorite (Småland granite) grading locally at increasing depth (300-500m) into more basic varieties such as quartz monzodiorite-diorite (Äspö diorite). A more reddish variety of the Småland granite with smaller and more sparsely scattered microcline megacrysts (Ävrö granite) has been found in this area. Greenstone in form of lenses, xenoliths and dikes (veins) of fine-grained granite are estimated to make up c. 8-10% each of the rock mass. Cm-wide mylonites and epidotic shears trending N or NE are common in the Småland granite. The fine-grained greenstone is often intensely cracked and intruded by fine-grained granite in an irregular pattern.

The dominant orientation of fractures is c. N 55° W and NE. The mean spacing in the NW direction is 0.80 m but up to 2.0 m in the NE direction. The most common fracture fillings are calcite and chlorite. Persistent, NNW-NNE-trending red-stained fractures - sometimes open - occur in the Småland granite. Fracture zones EW-5 and NE-1 are estimated to cut into RMU-2 at a depth of c. 200-300 m and c. 400-500 m, respectively.

Narrow, NNW-NNE trending fracture zones, mostly steeply dipping, are assumed to be at least partly connected to EW-5 and then provide important hydraulic pathways.

Geohydrological characteristics:

The geometric mean of the hydraulic conductivity of RMU-02 is estimated to be

$$K_g^3 = 1.0 \cdot 10^{-10} \text{ m/s}$$

4.2.4

RMU-3

Geological characteristics:

RMU-3 comprises the rock mass between EW-3 and NE-1 (EW-5).

A granodioritic variety of the Småland granite is the dominant rock type, especially in the southern part of this unit. Fine-grained granite in the form of dikes and irregular veins is estimated to make up c. 15-20% of the total rock mass while greenstone and other metavolcanics seem to be rarer (less than 3%). Narrow mylonites and epidotic shearplanes are also common in this unit.

The dominant orientation of the fractures is c. N 55° W and c. N-S. Low-dipping fractures (20°-40° S) are most frequent at the southern end of Äspö. The most common fracture fillings are calcite and chlorite. Locally prehnite is also common. Red-stained - sometimes open - fractures trending NNW-NNE occur in the Småland granite. Fracture zones EW-5 and NE-1 are believed to cut into RMU-3 at a depth of c. 0-150 m and 0-400 m respectively. Also in RMU-3 narrow NNW-NNE trending fracture zones are believed to be of great importance hydraulically.

Geohydrological characteristics:

The geometric mean of the hydraulic conductivity of RMU-03 is estimated to be

$$K_g^3 = 1.0 \cdot 10^{-10} \text{ m/s}$$

4.2.5

RMU-4

Geological characteristics:

RMU-4 comprises the rock mass between the southern part of Äspö (NE-1, EW-5) and the northern part of Hälö.

Småland granite is the dominant rock type in RMU-4, most often with rather closely spaced larger megacrysts. Especially in the northern part the true granitic variety, Ärvö granite, may occur. Locally, the Småland granite grades gradually into more basic rock types (monzodiorite-quartzdiorite).

Diorite/gabbro in irregular masses and fine-grained greenstone in metre-wide dikes and xenoliths are estimated to make up less than 3% of the rock mass.

Fine-grained granite, red to greyish red, intruding the older rocks in the form of smaller irregular veins and 0.5-5 m wide dikes, may constitute c. 15 % of the rock mass.

The dominant orientation of the fractures is judged to be c. N 60°-70° W, c. N-S and N 70°-80° E. The most common fracture fillings are calcite, chlorite and Fe-oxyhydroxides.

Geohydrological characteristics:

Only a few air-lift tests were performed in RMU 4, so K_g^3 is not definitely known but is probably equal to or greater than RMU 2-3, since parts of RMU 4 are highly fractured.

4.3

GEOLOGICAL UNITS - BLOCK SCALE, 50 M

The rock mass description on the 50 m scale in this chapter should only be regarded as an approximate model of rock distribution and dominant orientation of structures based on information from surface mapping geophysics and core drilling.

General geohydrological character:

The correlation ranges for an average value of a 3-m section is commonly less than 6 m for the logarithmic hydraulic conductivity series and about 10 m for the fracture frequency series.

The linear correlation between the average logarithmic hydraulic conductivity and the number of open coated fractures is weak but significant. The number of coated fractures only explains a small part of the variation in hydraulic conductivity.

Hematite and iron oxide are often found in fractures with a relatively high hydraulic conductivity. The fractures within the hydraulically conductive zones are also often coated with chlorite, calcite and epidote.

The expected distances between 3-m sections with hydraulic conductivities of an order of magnitude greater than $10^9 / 10^7 / 10^5$ m/s are on the order of 3-9 m / 6-16 m / 45- 130 m respectively.

4.3.1

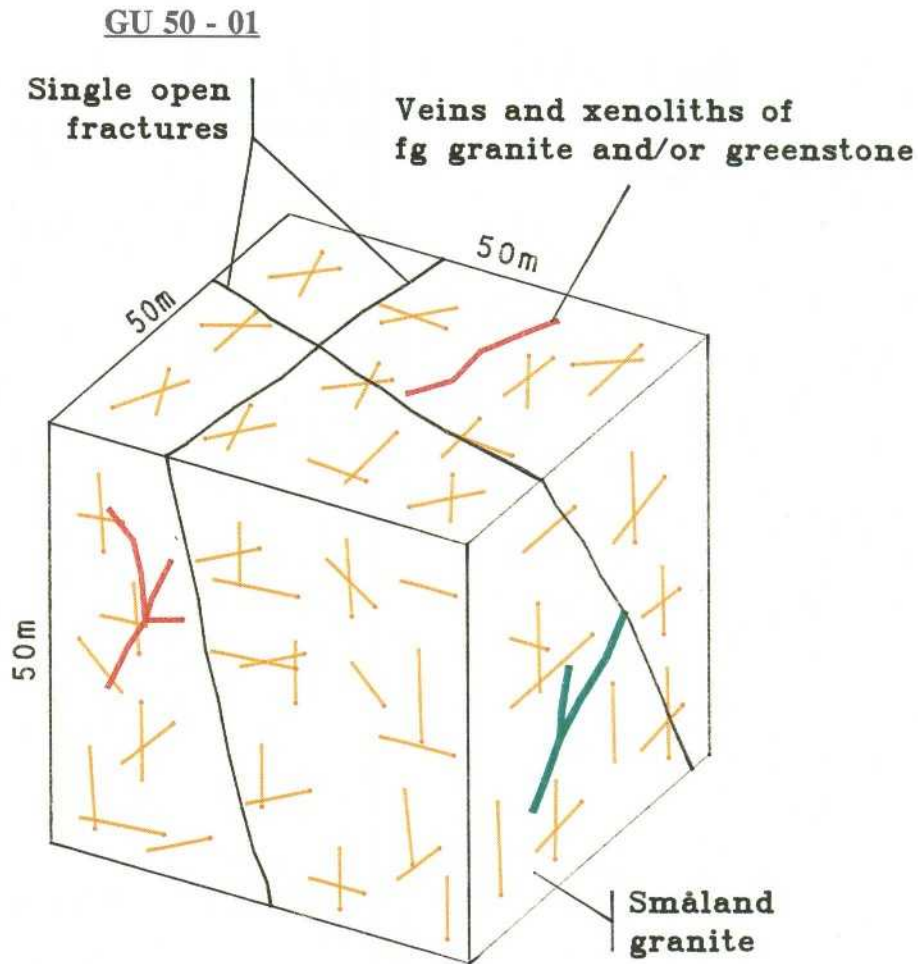


Figure 4.10 Geological unit GU 50-01.

Geological character:

This is an example of the rock type which is judged to be the most frequent, especially in the upper part of the site. This rock, which is called Småland granite, can as a rule be petrographically classified as granite or granodiorite. The foliation of the rock varies in intensity from weak to distinct and the main direction from NE to ENE. Veins of fine-grained granite and greenstone xenoliths are common. On average 1-3 mainly NNW-NNE trending single open fractures of high hydraulic conductivity are estimated to occur per 50 m.

Geohydrological character:

The single open fractures occur primarily in the brittle rock units of Småland granite and fine-grained granite. Typical for them is the fact that they are identified solely by hydraulic methods i.e. spinner surveys and packer tests. They are probably of limited extent compared to the major fracture zones and in many cases they are linked to the major fracture zones.

The geometric mean and standard deviation of the hydraulic conductivity of a 3-m section in Småland granite are estimated to be

$$K_g^3 = 1.2 \cdot 10^{-10} \text{ m/s} \quad S_{\log K}^3 = 2.04$$

4.3.2

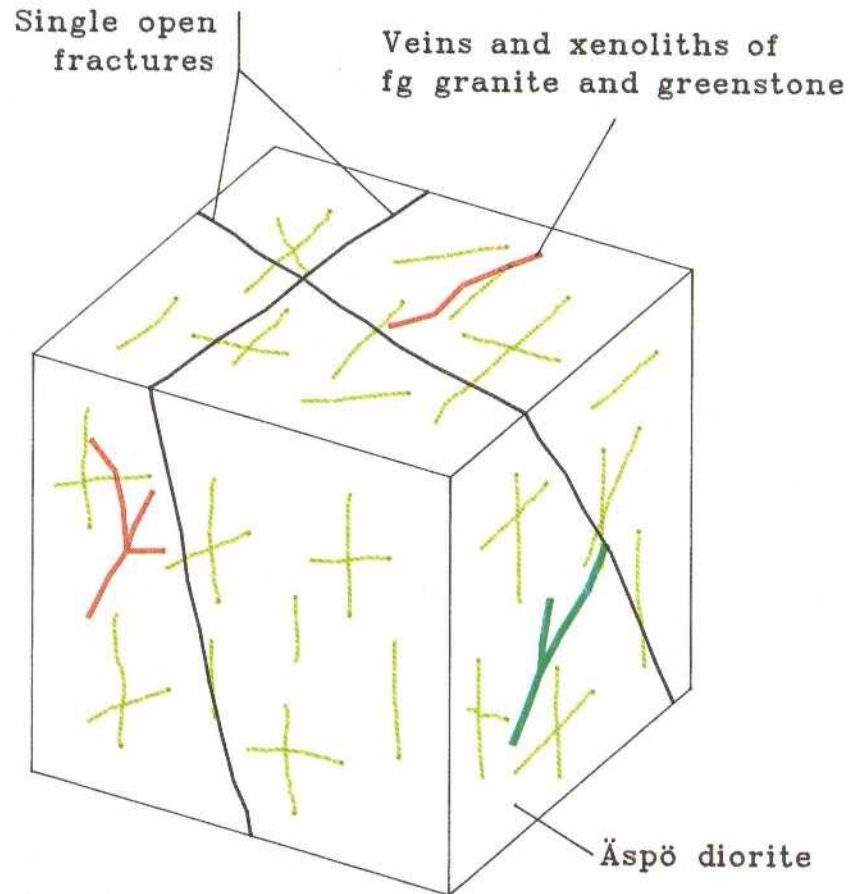


Figure 4.11 Geological unit GU 50-02

Geological character:

This is an example of a more basic variety of the Småland granite which according to borehole investigations seems to be especially common at lower levels on the site. This rock, which grades petrographically from granodiorite - monzodiorite - diorite, is called "Äspö diorite". Single open fractures are estimated to be somewhat less frequent than in 50 - 01.

Geohydrological character:

Single open fractures may also be found in the Äspö diorite and their general appearance is the same as for 50-01.

The hydraulic conductivity of the Äspö diorite is estimated to be

$$K_g^3 = 5.2 \cdot 10^{-11} \text{ m/s} \quad S_{\log K}^3 = 1.80$$

Geohydrochemical character:

Due to the more basic rock type containing easily weathered iron-rich minerals the iron content of groundwater is expected to be somewhat higher than that of the groundwater in the more acidic Småland granite 50-01.

4.3.3

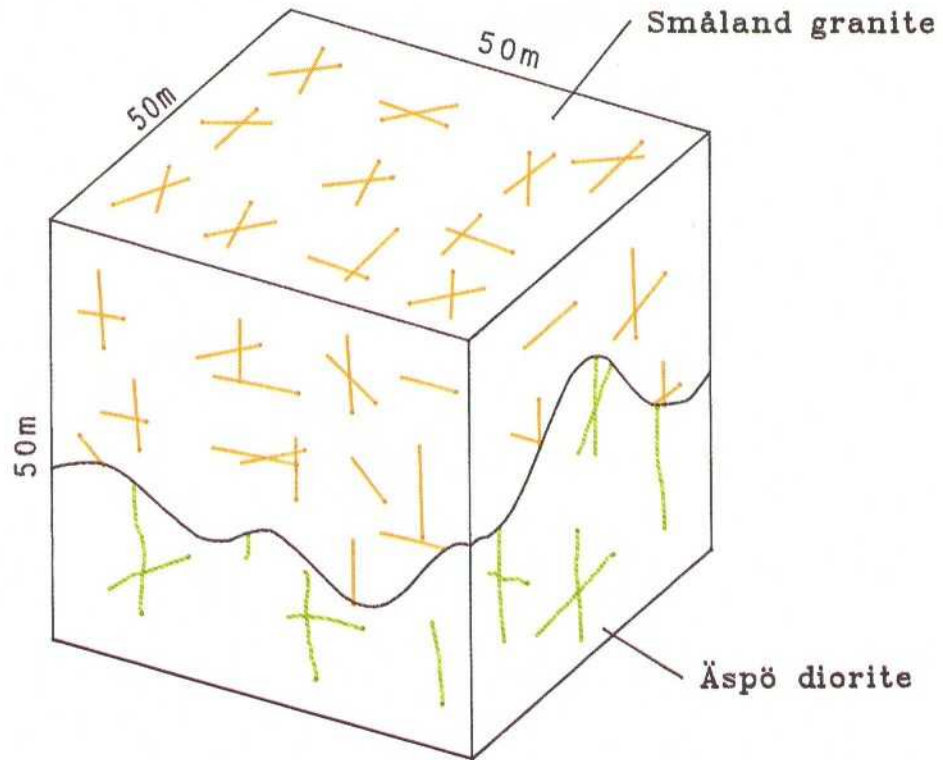
GU 50 - 03

Figure 4.12 Geological unit GU 50-03

Geological character:

This example illustrates the typical irregular and often diffuse contact between the granite and more basic rocks as a result of magma mixing. This mixing process often had a reinforcing effect on the bedrock, resulting in rather low hydraulic conductivity.

Geohydrological character:

The hydraulic conductivity of these blocks is expected to be low. The hydraulic conductivity around the contact between the Småland granite and the Äspö diorite is estimated to be

$$K_g^3 = 10^{-10} \text{ m/s}, \quad S_{\log K}^3 = 2.1$$

4.3.4

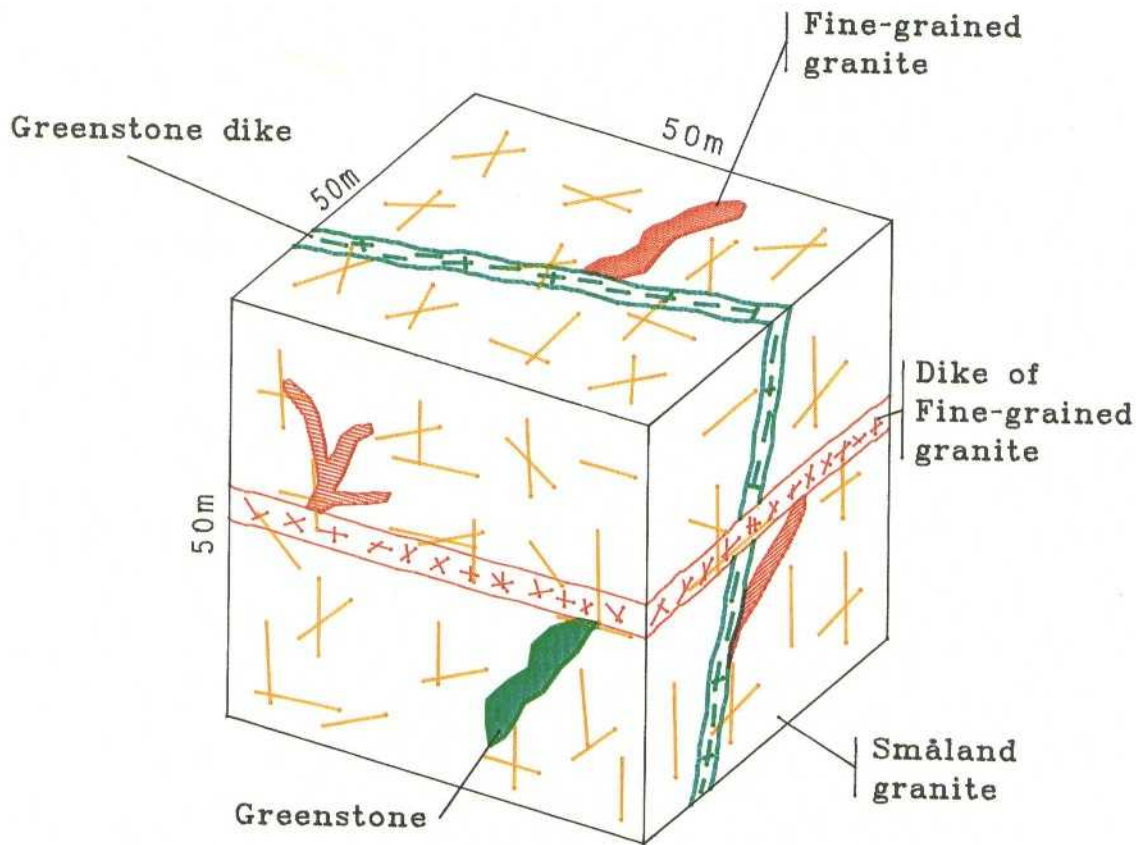
GU 50 - 04

Figure 4.13 Geological unit GU 50-04

Geological character:

This is an example of Småland granite with inclusions of thin sheets of several metres wide mostly ENE striking dike-shaped, grey-black coloured rock normally called greenstone. This rock is often highly fractured, but rather low-conductive except for the contacts with the wall rock, which may be open.

The rock mass described is extensively intruded by a younger fine-grained granite in form of NE-ENE striking dikes or irregular masses. The dikes specially are very often highly fractured or crushed and water-bearing.

Geohydrological character:

Dikes of fine-grained granite and greenstone in Småland granite are frequently associated with a higher hydraulic conductivity. Single open fractures are often found in the dikes or in the rock mass close to the dikes.

The hydraulic conductivity of the dikes and the rock mass close to the dikes is estimated to be

$$K_g^3 = 8 \cdot 10^{-9} \text{ m/s}, S_{\log K}^3 = 2.2$$

4.3.5

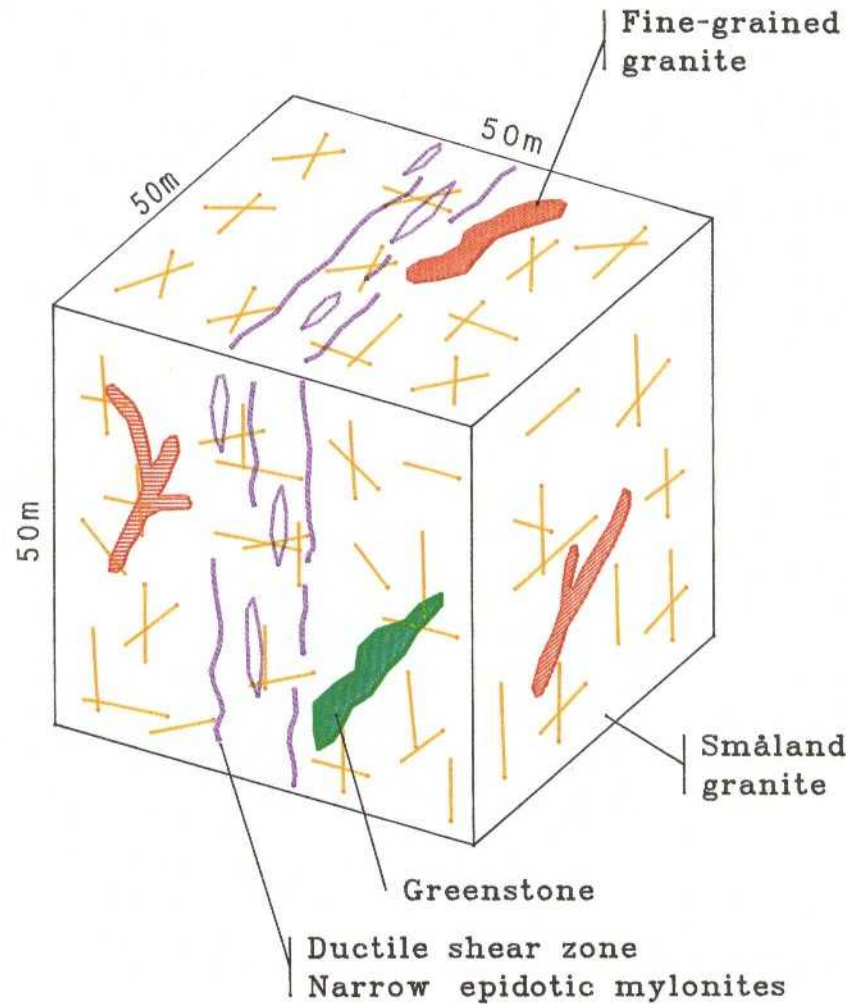
GU 50 - 05

Figure 4.14 Geological unit GU 50-05

Geological character:

Structures resulting from different intensities of ductile deformation are present in the bedrock in all degrees, from distinct foliation in the NE-ENE direction to more or less intense shearing and sometimes mylonitization. Narrow 5-10 cm wide ENE, NE and N-S striking shear zones and up to metre-wide mylonites are common in the Småland granite. Later brittle deformation (fracturing) and mineralogical alteration are very often associated with the ductile structures described.

Geohydrological character:

Ductile structures in fractured Småland granite probably have a higher hydraulic conductivity than the surrounding rock mass, but generally lower than fracture zones, (GU50-6). The range of the hydraulic conductivity and standard deviation are estimated to be

$$K_g^3 = 10^{-8} - 10^{-10} \text{ m/s}, S_{\log K}^3 = 1.5$$

4.3.6

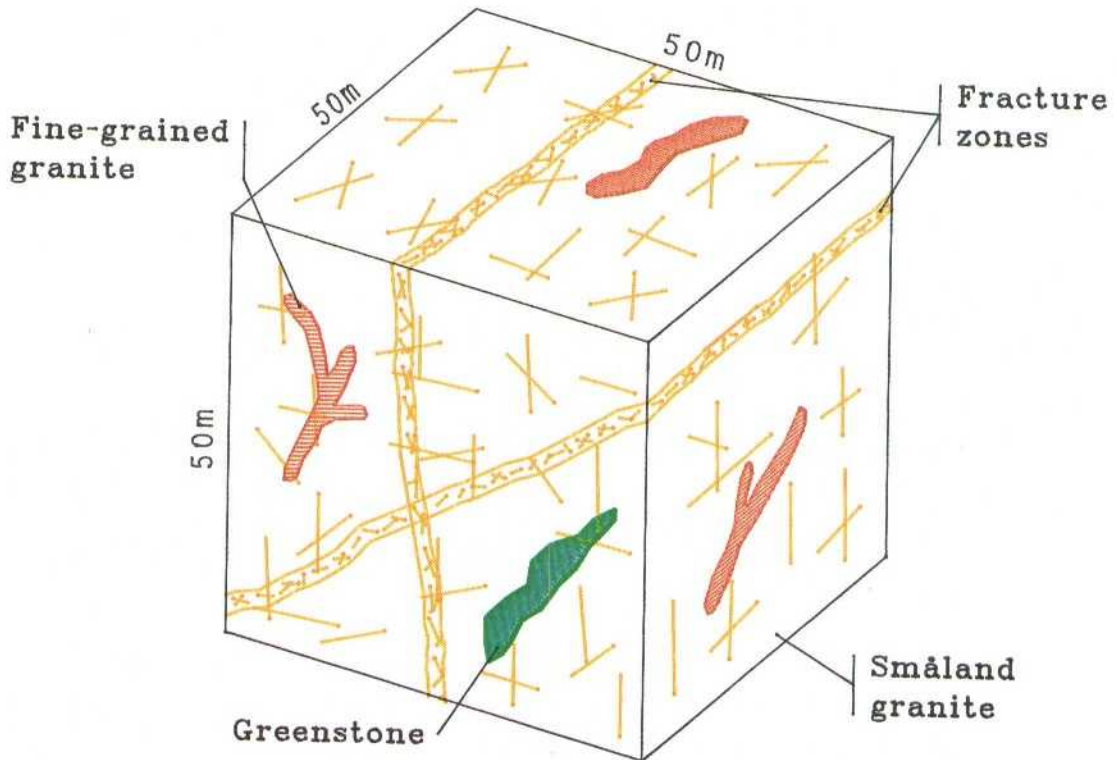
GU 50 - 06

Figure 4.15 Geological unit GU 50-06

Geological character:

Fracture zones which are too narrow (one around one metre wide or less) to be definitely located and characterized by means of general investigation methods are estimated on the basis of borehole information to occur at an average frequency of 2 - 3 per 50 m in Småland granite (granodiorite). The rock in these zones is normally highly fractured, more or less altered and hydraulic conductive.

Geohydrological character:

Fracture zones in Småland granite are not always but generally more conductive than the surrounding rock.

The hydraulic conductivity and standard deviation for zones with an RQD approximately 50 or less are estimated to be

$$K_g^3 = 10^{-8} \text{ m/s}, S_{\log K}^3 = 1.5$$

4.3.7

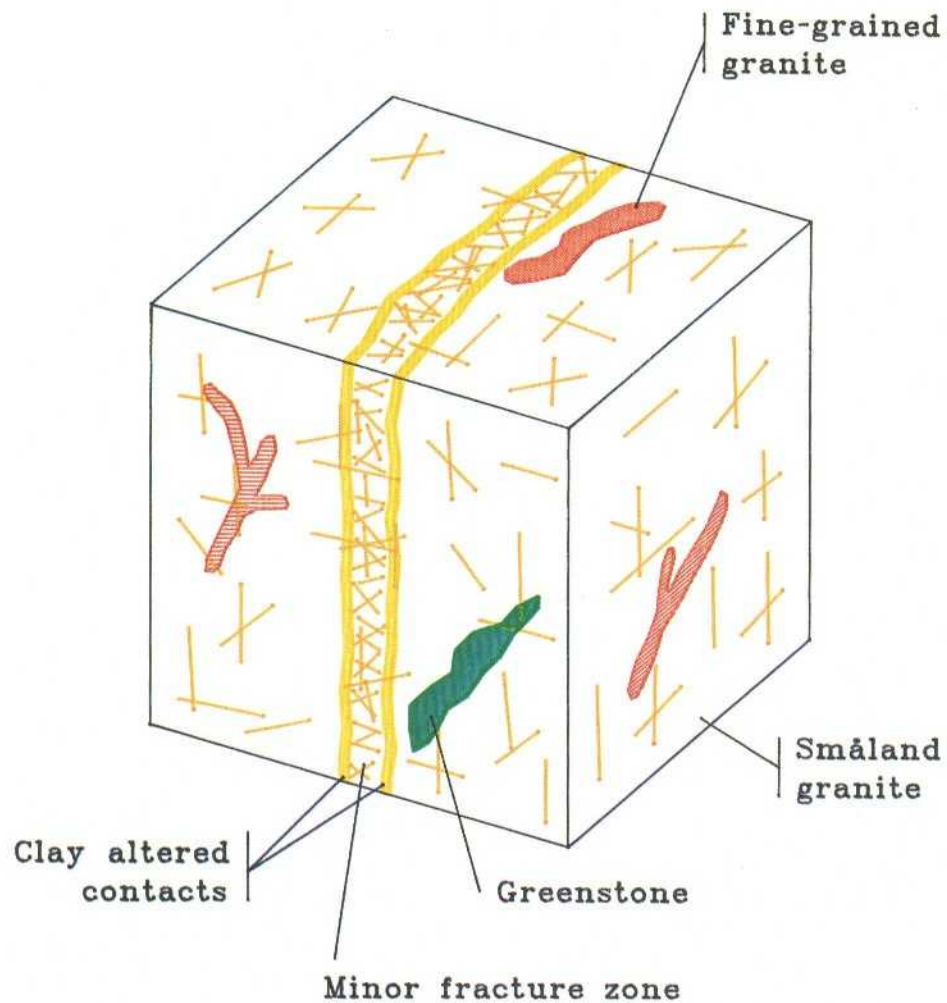
GU 50 - 07

Figure 4.16 Geological unit GU 50-07.

Geological character:

This is an example of a minor fracture zone of a more complex nature in Småland granite. Parts of the zone - mainly the contacts - are in this case estimated to be less permeable due to increased alteration and clay-filling than the central part of the zone with more open fractures.

Geohydrological character:

Minor fracture zones in Småland granite with some clay filling are estimated to have a lower conductivity than the fracture zone in GU 50-06.

$$K_g^3 <= 10^{-8} \text{ m/s}, S_{\log K}^3 = 1.5$$

4.3.8

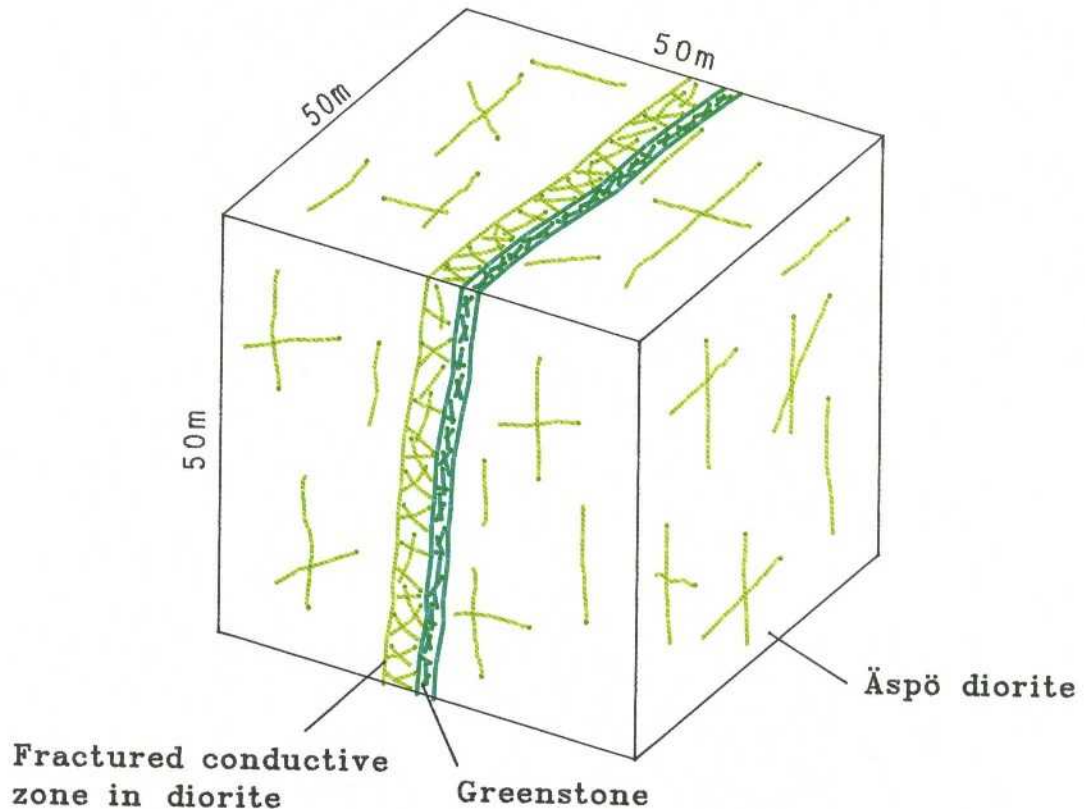
GU 50 - 08

Figure 4.17 Geological unit GU 50-08

Geological character:

Minor fracture zones in the more basic rock types are normally estimated to be less permeable than zones of the same kind in Småland granite, due to less persistent and irregular fractures. Fracture zones in greenstone are often more or less sealed due to intense alteration and clay-filling.

Geohydrological character:

Minor fracture zones in Äspö diorite have a lower conductivity than minor fracture zones in Småland granite. Fracture zones with an RQD of approximately 50 or less have a hydraulic conductivity of

$$K_G^3 = 10^{-9} \text{ m/s}, S_{\log K}^3 = 1.5$$

4.3.9

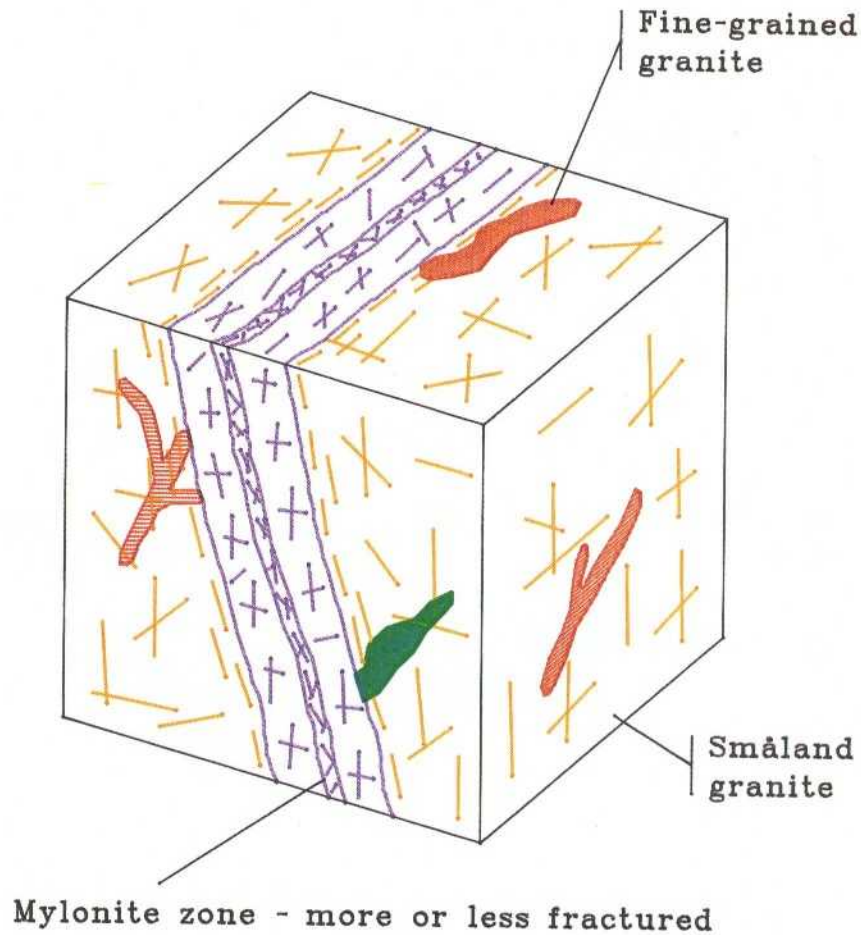
GU 50 - 09

Figure 4.18 Geological unit GU 50-09

Geological character:

This is an example of a mylonite zone in Småland granite with greater or lesser fracturing.

Hydraulic conductivity: Low - medium.

Geohydrological character:

The hydraulic injection tests in mylonitic parts of the boreholes show that the hydraulic conductivity is low. The estimated hydraulic conductivity and standard deviation are

$$K_g^3 = 10^{-10} \text{ m/s}, S_{\log K}^3 = 2.2$$

4.3.10

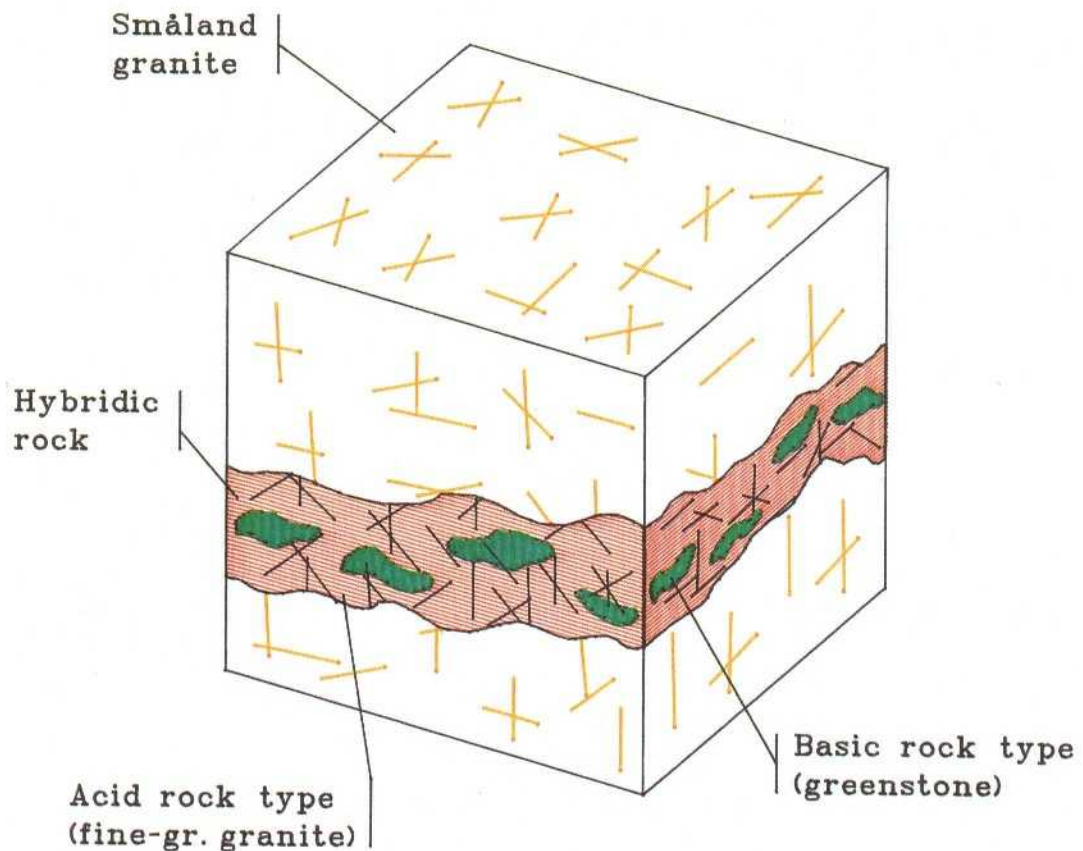
GU 50 - 10

Figure 4.19 Geological unit GU 50-10

Geological character:**Hybrid rock**

Some parts of the basic rocks - especially the fine-grained greenstones - are rather heterogeneous and seem to be affected by younger granitoids (mainly the fine-grained granite). This has resulted in hybrid rocks, difficult to classify. Irregular and winding foliation is often typical of this rock. The hybrid rock in Småland granite is often a complex mixture of a fine-grained granite and a fine-grained basic rock type. The hybrid rock is normally more fractured than the Småland granite and is therefore probably more conductive.

Estimated hydraulic conductivity: Low - medium.

4.4 GEOLOGICAL UNITS — DETAILED SCALE, 5 M

Rock mass description on the 5 m scale should be regarded as more or less homogeneous example of the different main rock types - only faintly tectonically affected.

4.4.1 GU 5 - 01

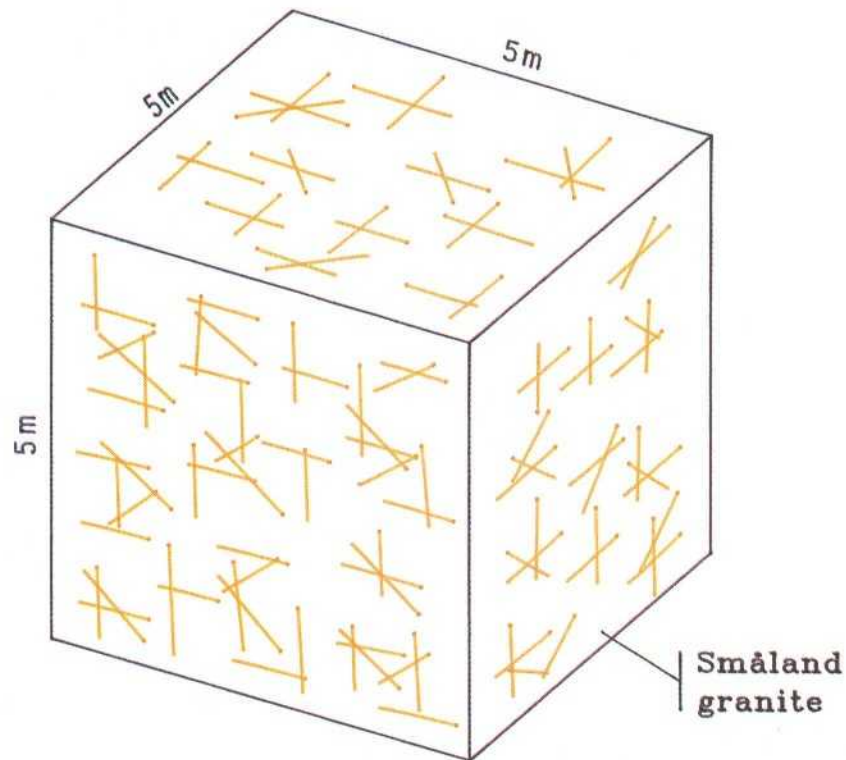


Figure 4.20 Geological unit GU 5-01

Homogeneous "Småland granite", petrographically granite-granodiorite, only faintly tectonically affected, is judged to be one of the most frequent rock types, especially in the upper levels, between the fracture zones on the site.

The Småland granite has a low-moderate hydraulic conductivity. Increased conductivity is caused by fracture zones of varying intensity and dikes and veins of fine-grained granite and greenstones.

The geometric mean and standard deviation of the hydraulic conductivity of Småland granite are estimated to be

$$K_g^3 = 1.2 \cdot 10^{-10} \text{ m/s}, \quad S_{\log K}^3 = 2.0$$

From inside a tunnel the granite appears dry to moderately wet. Inflows and drops of moisture occur as point flows along horizontal fractures and fracture intersections.

4.4.2

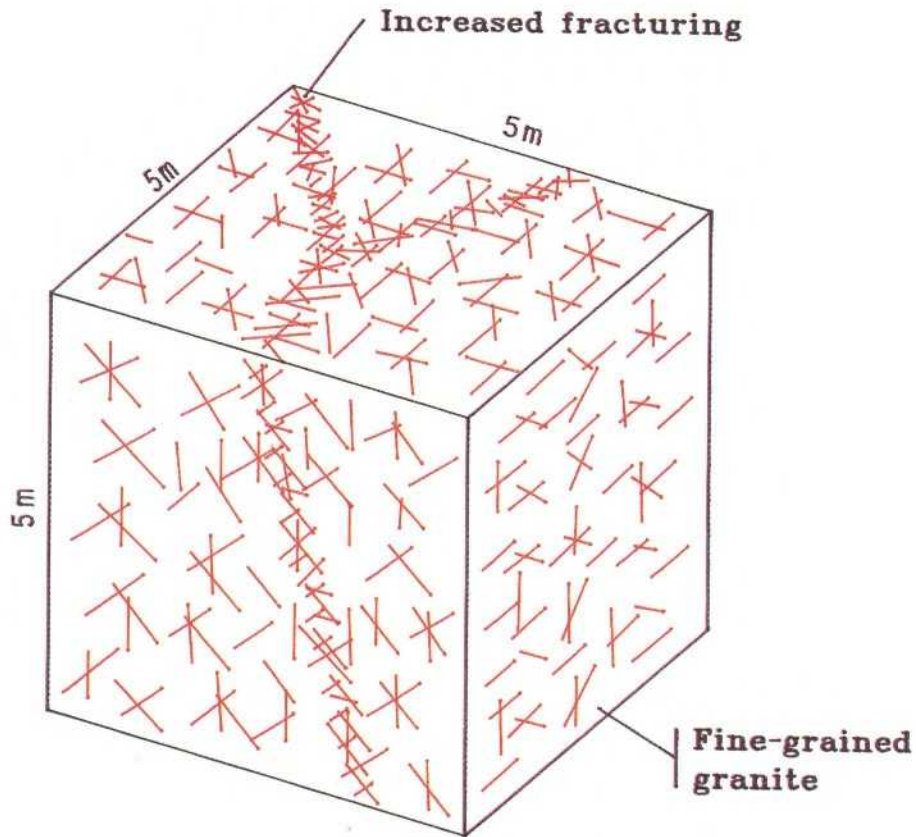
GU 5 - 02

Figure 4.21 Geological unit GU 5-02

Homogeneous "Fine-grained granite", normally more intensely fractured than the Småland granite and the Äspö diorite, is judged to occur rather rarely in masses wider than 5 m, between the fracture zones.

The fine-grained granite occurs as major dikes and veins in the Småland granite and the Äspö diorite. The fine-grained granite is generally the most permeable rock unit on Äspö, along with the Småland granite.

The geometric mean and standard deviation of the hydraulic conductivity for fine-grained granite are estimated to be

$$K_g^3 = 7.9 \cdot 10^{-10} \text{ m/s}, \quad S_{\log K}^3 = 2.1$$

The fine-grained granite appears from inside a tunnel as areas with a somewhat greater fracture frequency and also greater water inflow. The parts of the rocks close to other rock types are particularly fractured and permeable.

4.4.3

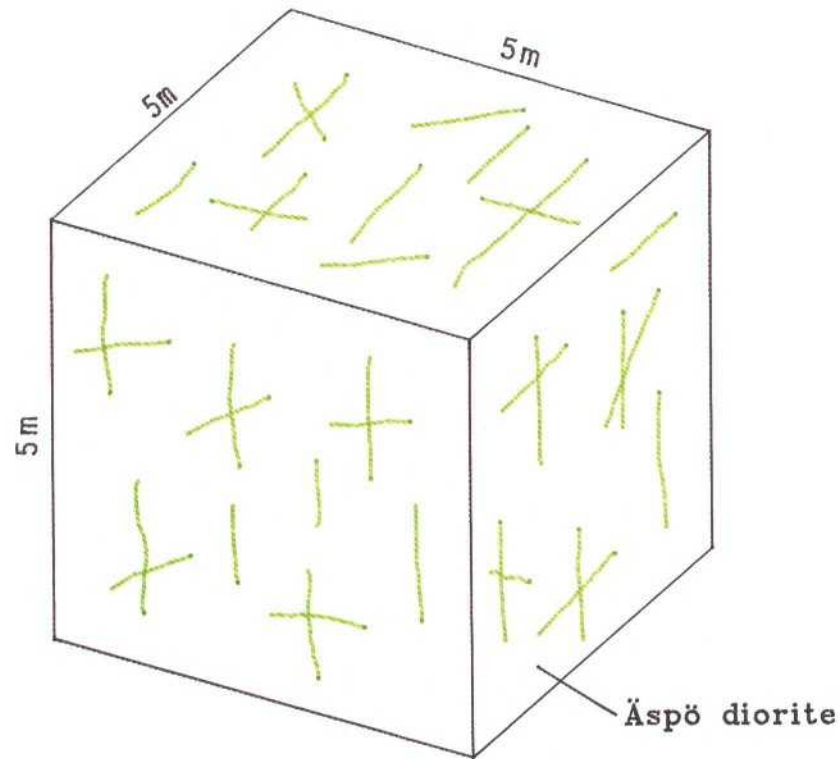
GU 5 - 03

Figure 4.22 Geological unit GU 5-03

Homogeneous "Äspö diorite", petrographically granodiorite-diorite, only faintly tectonically affected, is judged to be one of the most frequent rock types, especially at lower levels, between the fracture zones on the site.

Hydraulic conductivity: Low.

The Äspö diorite normally has a low hydraulic conductivity. Some dikes and sills of fine-grained granite occur within the diorite, which may be more hydraulically conductive.

The geometric mean and standard deviation of the hydraulic conductivity of Äspö diorite are estimated to be

$$K_g^3 = 5.2 \cdot 10^{-11} \text{ m/s}, S_{\log K}^3 = 1.8$$

From inside a tunnel the Äspö diorite appears dry. Some inflows and drops may occur at boundaries with other rocks.

4.4.4

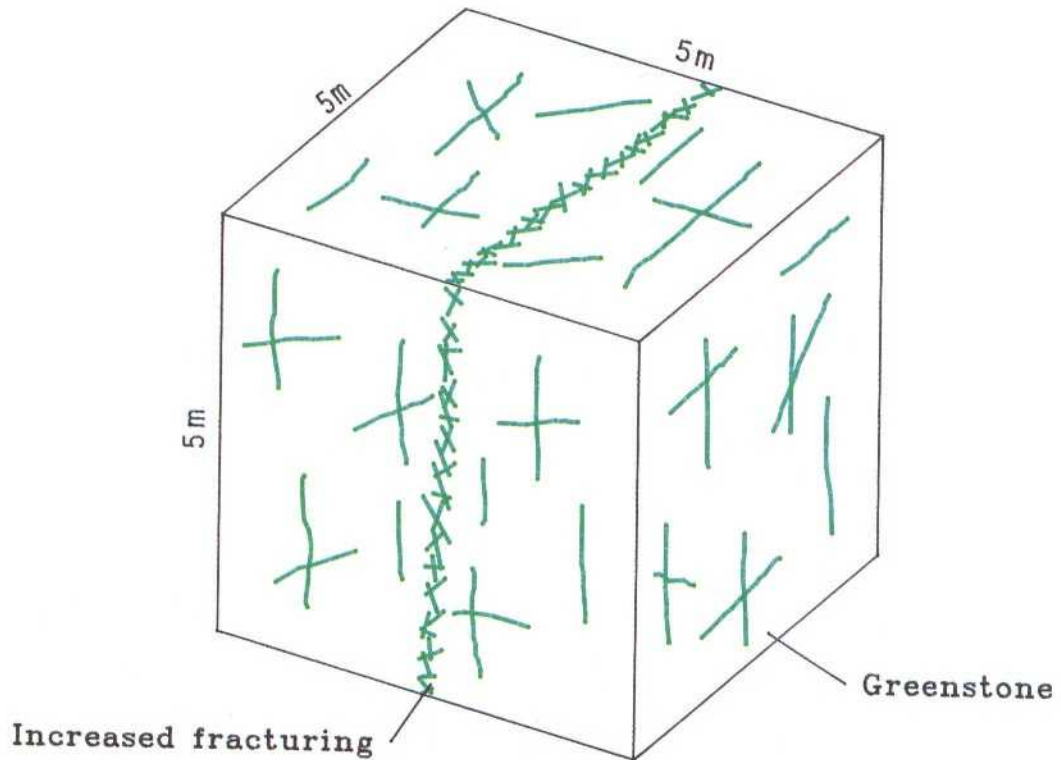
GU 5 - 04

Figure 4.23 Geological unit GU 5-04

The more or less homogeneous basic rock type described as Greenstone is petrographically a metadacite-metabasalt or in some cases a gabbro. This rock type is widely distributed in the form of ENE striking lenses or thin sheets but is judged to be more infrequent in masses more than 5 m wide on the site.

Hydraulic conductivity: Low.

Greenstone (basic volcanite) normally has a low hydraulic conductivity except in contact zones with the wall rock, which may be more permeable.

The geometric mean and standard deviation of the hydraulic conductivity of greenstone are estimated to be

$$K_g^3 = 5.2 \cdot 10^{-11} \text{ m/s}, S_{\log K}^3 = 1.8$$

5

GROUNDWATER FLOW MODEL OF SOUTHERN ÄSPÖ

One purpose of the geohydrological investigations has been to test our ability to make predictions of the groundwater flow based on information from the pre-investigations. The first test was of predictions of a pumping test (LPT1) reported in chapter 3.2 and the second of calculations of the groundwater flow during the construction of the HRL. The basis for the groundwater flow model of the HRL is presented in this chapter. The input data for the numerical simulations, based on the conceptual model, HRL layout pumping tests etc, are presented in Rhén/1991 a,b/. The model, the calibrations etc are presented in detail in Svensson /1991/ and the results of the calculations are presented in Gustafson et al /1991/ and Rhén (ed) et al /1991d/.

Due to the heterogeneous nature of the medium and the different boundary conditions, analytical equations cannot be used to solve the groundwater flow, so a numerical model has been used. The code used is PHOENICS /Spalding, 1981/.

5.1

THE TRANSFORMATION OF THE CONCEPTUAL MODEL TO THE NUMERICAL MODEL

The numerical model is generally a simplification of the conceptual model since it is not possible, at least with a reasonable effort, to build a model as detailed and complex as the conceptual model. This chapter summarizes the transformation (and simplification) of the conceptual model to the numerical model.

Boundaries

In the horizontal plane, the model covers an area of 1920 x 1500 m, with a vertical depth of 1290 m. (See figure 5.1.)

Upper boundary

The infiltration rate under natural conditions on Äspö is estimated by calibration and is assumed to be constant during the excavation of the HRL. The wetlands by the sea are assumed to have the same water level as the sea. The level of the sea is assumed to be constant with $z=0$ m (Äspö coordinate system). A wetland area between KAS04 and KAS12 is assumed to have a constant head of +2.5 m both under natural conditions and during the construction of the Äspö Hard Rock Laboratory. The infiltration rate will probably increase as the water table decreases due to leakage into the tunnel system. The relationship between the infiltration rate and the water table at Äspö is not yet fully understood but the constant head of the wetland between KAS04 and KAS12 probably gives a more realistic draw-down for the predictions.

Lower boundary

The flow across the lower boundary is zero.

Side boundaries

The salinity is 0.7‰ at the sea surface and increases linearly at the side boundaries to 1.8‰ at a level of 1300 m below the sea surface. The pressure at the boundaries is hydrostatic. The conductive structures reach the boundaries but the cells close to the boundary have a hydraulic conductivity of $1 \cdot 10^{-7}$ m/s

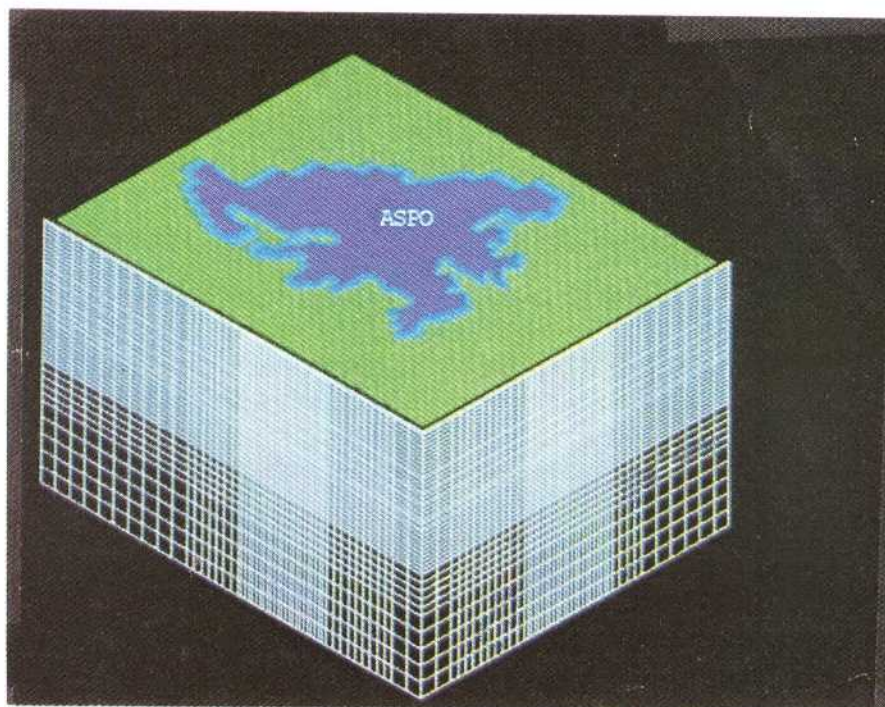


Figure 5.1 Model area with the contours of Äspö /Svensson, 1991/

Hydraulic conductivity of the rock mass between the conductive structures

The median value of the hydraulic conductivity for each RMU has been used to generate the values for each cell, assuming a log-normal distribution of the hydraulic conductivity.

The mean value of $\log K$ has been scaled according to the cell size. The standard deviation of $\log K$ has been estimated from the level of the cell and the value has also been scaled according to the cell size. This is in accordance with the conceptual model.

Transmissivity of the conductive structures

The conductive structures shown in Figure 3.2.36 have been superimposed on the rock mass with the stochastically distributed hydraulic conductivity. The hydraulic conductivity of all cell walls in the model that are intersected by a conductive structure is calculated from the transmissivity of the structure, the trace length of the structure on the cell wall and the stochastic hydraulic conductivity. The transmissivity of each structure was as in the conceptual model prior to the calibration (Chapter 4). The positions of all structures in the numerical model are as shown in Figure 3.57, except for the following structures.

- NE-2 has been rotated 5° clockwise around the intersection point between NE-2 and EW-3 so that NE-2 intersects the bottom of KAS12. NE-2 also continues to the model boundary on the west.
- NNW-5 ends towards NE-3.

5.2

CALIBRATION EXERCISES

The computer model is a mathematical realization of a conceptual model within a defined computer code. To begin with, a model close to the preliminary conceptual model is used. In order to test the model and to improve it, the calibration is run.

In order to determine the properties of the structural elements, tests and observations are made in the field. This gives sets of responses from the real system that can be matched to the calculation results. The agreement between the responses and the results can be measured by, for instance, the mean error and its variance. A common strategy for calibration is to minimize these measures by adjusting the model parameters. If this is done systematically the term inverse modelling may be used.

When agreement between the model results and the system responses is deemed to be sufficiently good, the model is said to be calibrated against a certain set of data. Furthermore, the accuracy of the calibrated model, as shown by comparison between measured and calculated variables, is an indication of the expected accuracy of predictions made with the calibrated model.

5.2.1

Calibration of the HRL model

In the case of the groundwater flow model of Äspö, the model has been calibrated by interference tests in KAS06 (Nos. 1 and 4), KAS07, KAS12, KAS13 and KAS14. Furthermore, the model has also been calibrated against the natural water table. The calibration of the model gave the results below.

Upper boundary

The infiltration rate was estimated to be 3 mm/year.

Hydraulic conductivity of the rock mass between the structures

The uppermost layer of the cells covering Äspö, cell height 20 m, has a minimum conductivity of $3 \cdot 10^{-10}$ m/s. This adjustment of the conductivities was necessary because unreasonably high hydraulic heads were generated in cells which had extremely low conductivities.

Transmissivity of the conductive structures

The transmissivities of some of the conductive structures have been adjusted as a result of the calibration, see table 5.2.1.

Table 5.2.1 Adjustment of transmissivities of conductive structures

Structure	previous T m ² /s	new T m ² /s	Comment
NE-1 and NE-12	$4 \cdot 10^{-4}$	$1.5 \cdot 10^{-4}$	z=0-300 m
NNW2	$4 \cdot 10^{-5}$	$8 \cdot 10^{-5}$	
NNW-5 and NNW-6	$5 \cdot 10^{-5}$	$2 \cdot 10^{-5}$	

NNW-1, NNW-2 and NNW-4 were also ended about 20 m south of what is shown in Figure 3.2.36. This was done because the hydraulic contact between the southern part and the northern part in the numerical model was too good, and the shortening of the NNW structures to the north decreased the hydraulic contact.

Salinity

The salinity in the borehole sections in the numerical model was compared to the measured values, and it was found that the vertical salinity distribution agreed fairly well.

Mean error and accuracy of the calibration examples

The mean error and accuracy of the final calibration model have been calculated for all calibration examples mentioned above and the results are shown in Table 5.2.2.

Table 5.2.2 Comparison of measured and calculated draw-downs. (Definitions of n, ds, and Ds are found in Chapter 3.2). (1) (2) (3) are different realizations of the stochastic distribution of the hydraulic conductivity of the rock mass.

Test		n	ds (m)	Ds (m)
KAS06-1		66	0.084	1.64
KAS06-4		66	-0.024	0.366
KAS07	(1)	69	0.388	2.17
"	(2)	69	0.370	2.20
"	(3)	69	0.282	2.26
KAS12		68	0.121	0.830
KAS13		65	-27.2	111.0
"	*	65	-0.69	6.9
KAS14		89	0.139	0.923

* An extra fracture parallel to NE-2 crossing KAS13 was included in the model.

As can be seen in Table 5.2.2. the mean error (ds) and accuracy (Ds) are rather small except for the test in KAS13. This is because it has not been possible to identify, and include in the conceptual model, any important structure (with strike and dip) crossing or close to KAS13. The deviations between measured and calculated draw-downs are greatest close to KAS13. A test with a new structure parallel to NE-2 crossing KAS13 showed that ds and Ds would decrease (see Table 5.2.2), but it was decided that this structure should not be included in the model because it had not been possible to identify the structure in the pre-investigations.

If the draw-downs are studied in detail it is found that there are a few borehole sections where there are great deviations and they have a particularly great influence on the value of Ds. In these parts of the model, the numerical, and possibly also the conceptual model, is less accurate than on the rest of Äspö.

For the calibration case KAS07, three realizations of the stochastic distribution of the hydraulic conductivity were made to see how different ones would affect the pressure response. As can be seen in Table 5.2.2, no major difference between ds and Ds was found, as can be expected, because the conductive structures are the main flow paths and they are treated as deterministic. Looking at individual borehole sections it can be concluded that the difference between different realizations can be up to several decimetres but is generally less. In this test the measured maximum draw-down in the well was 58 m, and in many of the observation sections the draw-down was greater than 1 m.

The natural groundwater flow conditions

The numerical model was also calibrated against the undisturbed water level on Äspö, and the water level calculated by means of the final numerical model is shown in Figure 5.2.

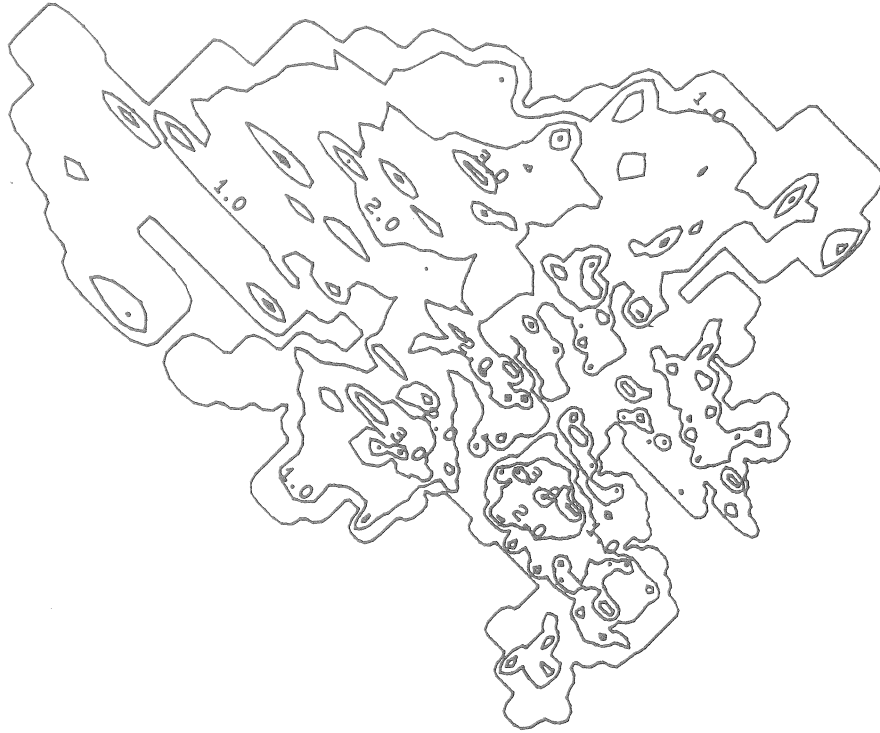


Figure 5.2 The water table under undisturbed conditions /Svensson, 1991/.

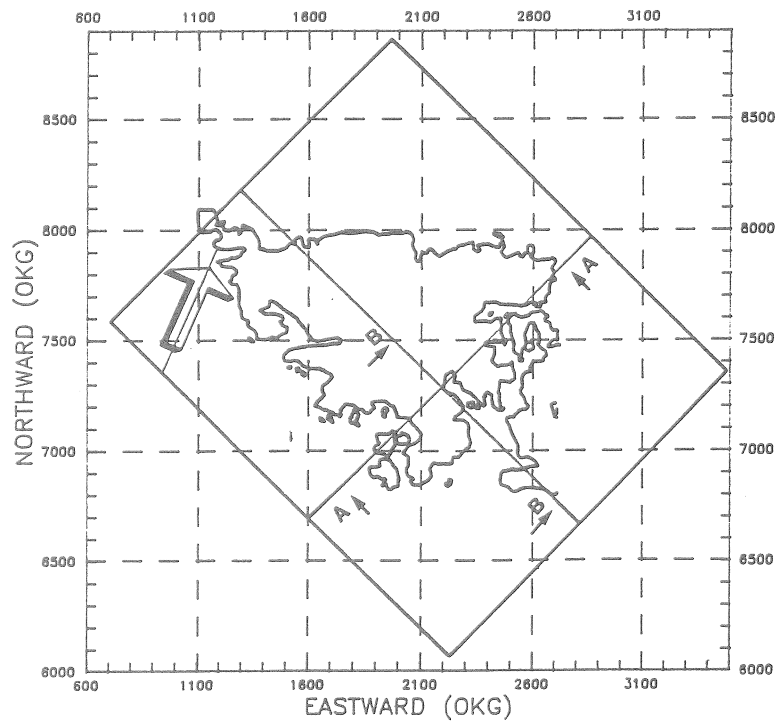


Figure 5.3 Äspö with the vertical sections A and B.

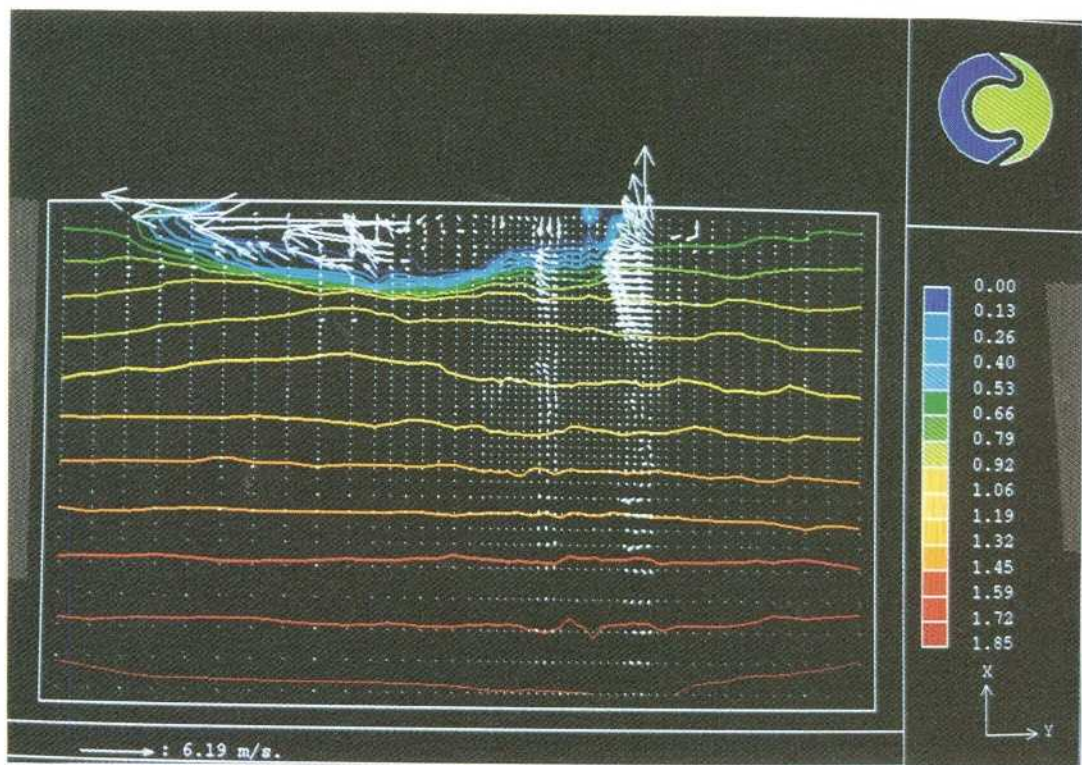
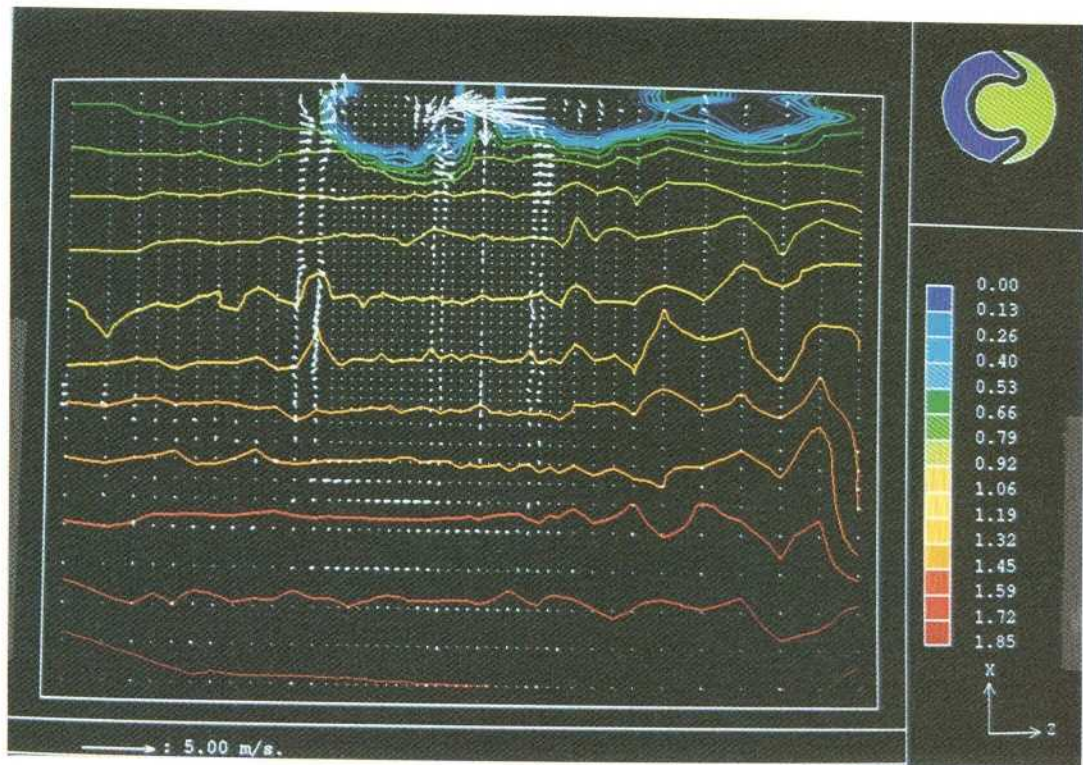


Figure 5.4 The salinity field and the water fluxes are shown for section A (above) and B (below), see figure 5.2.2. Salinity is given in ‰ and the flux vector shall be multiplied by 10^{-10} to give fluxes in m/s. The length scale is approximately 1 cm = 163 m. /Svensson, 1991/.

5.3

MODEL FOR PREDICTIONS OF THE HRL

The hydraulic resistance around the tunnel, here called the skin, is assumed to be 0 or 10 and all simulations are performed with the skin either 0 or 10. The definition of how the skin is included in the numerical model is shown in Svensson /1991/ and Liedholm /1991;26/.

The leakage from the conductive zones into the tunnel has been limited to a maximum of approximately $3 \cdot 10^{-3}$ m³/s. Fracture zones which give greater leakage than this figure will probably be grouted, so the skin for each conductive structure has been calibrated to reduce the calculated leakage into the tunnel from each conductive structure to less than $3 \cdot 10^{-3}$ m³/s. Following the tunnel from the model boundary, tunnel section 850 m to final depth, the skin for the structures has been estimated by calibration (see Table 5.3.1).

Table 5.3.1 Skin for the structures in the numerical model that intersect the tunnel

Structure	Skin (-)
NE-4	120
NE1	80
NE-1,2	80
EW-5	20
NNW-2	30
NNW-4	30
NNW-2	30
NNW-2	60
NNW-1	30
EW-5	20
NNW-1	30
NNW-2	80
NNW-4	30
NNW-2	80
NNW-1	50
NNW-1	30
EW-5 (shaft)	20

References

- Almén K, Zellman O. 1991. Äspö Hard Rock Laboratory. Field investigation methodology and instruments used in the pre-investigation phase, 1986-1990. SKB TR 91-21.
- Axelsson C, Jonsson E-K, Geier J, Dershowitz W. 1990. Discrete fracture modelling. SKB PR 25-89-21.
- Axelsson C L. 1987. Generic modelling of the SKB rock laboratory. SKB PR 25-87-12.
- Barmen G, Stanfors R. 1988. Ground level geophysical measurements on the island of Äspö. PR 25-88-16.
- Barmen G, Dahlin T. 1989. Ground level geophysical measurements on the islands of Äspö and Hälö in October 1989. SKB PR 25-89-22.
- Barton N, Bandis S. 1982. Effects of block size on the shear behaviour of jointed rock. 23rd U.S. Symposium on rock mechanics. Berkeley, California.
- Bjarnason B, Klasson H, Leijon B, Strindell L, Öhman T. 1989. Rock stress measurements in boreholes KAS02, KAS03 and KAS05 on Äspö. SKB PR 25-89-17.
- Bäckblom G. 1989. Guidelines for use of nomenclature on fractures, fracture zones and other topics. SKB TPM 25-89-007.
- Bäckblom G, Gustafson G, Stanfors R, Wikberg P. 1990. A synopsis of predictions before the construction of the Äspö Hard Rock Laboratory and the process of their validation. SKB PR 25-90-14.
- Carlsten S. 1989. Results from borehole radar measurements in KAS05-08 on Äspö. Interpretation of fracture zones by including radar measurements from KAS02 and KAS04. SKB PR 25-89-10.
- Carlsten S. 1990. Borehole radar measurements at Äspö boreholes KAS09-14. SKB PR 25-90-05.
- Cosma C, Heikkinen P, Keskinen J, Korhonen R. 1990. VSP-survey including 3-d interpretation on Äspö, Sweden, borehole KAS07. SKB PR 25-90-07.

Ericsson L O. 1987. Fracture mapping on outcrops.
SKB PR 25-87-05.

Ericsson L O. 1988. Fracture mapping study on Äspö island.
SKB PR 25-88-10.

Fridh B, Strähle A. 1989. Orientation of selected drillcore sections from the boreholes KAS05 and KAS06 Äspö, Sweden. A Televiwer investigation in small diameter boreholes.
PR 25-89-08.

Gentzschein B, Nilsson G, Stenberg L. 1987. Preliminary investigations of fracture zones at Ävrö - Results of investigations performed July -86 - May -87.
SKB PR 25-87-16.

Grenthe I, Stumm W, Laaksoharju M, Nilsson A-C, Wikberg P. 1991. Redox potentials and redox reactions in deep groundwater systems.
(Submitted to Chemical Geology.)

Grundfelt B, Liedholm M, Lindbom B, Rhén I. 1990. Predictive groundwater flow modelling of a long time pumping test (LPT 1) on Äspö.
SKB PR 25-90-04.

Gustafson G, Stanfors R, Wikberg P. 1988. Swedish Hard Rock Laboratory, First evaluation of pre-investigations 1986-87 and target area characterization.
SKB TR 88-16.

Gustafson G, Stanfors R, Wikberg P. 1989a. Swedish Hard Rock Laboratory Evaluation of 1988 year pre-investigations and description of the target area, the island of Äspö.
SKB TR 89-16

Gustafson G, Liedholm M, Lindbom B, Lundblad K. 1989b. Groundwater flow calculations on a regional scale at the Swedish Hard Rock Laboratory.
SKB PR 25-88-17.

Gustafson G, Liedholm M, Rhén I, Stanfors R, Wikberg P. 1991. Äspö Hard Rock Laboratory. Predictions prior to excavation and the process of their validation.
SKB TR 91-23.

Hemström B, Svensson U. 1988. The penetration of sea water into a fresh-water aquifer, a numerical study.
SKB PR 25-88-02.

Herbert A W, Jackson C P. 1987. Coupled groundwater flow and solute transport with fluid density strongly dependent upon concentration.
Water Resour Res, Vol 23, No 10.

Hoek E, Brown E T. 1980. "Underground Excavations in Rock".
Institute of Mining and Metallurgy, London.

- Juhlin C. 1990. Evaluation of Reprocessed Seismic Reflection Data from Äspö.
PR 25-90-02.
- Kornfält K-A, Wikman H. 1987a. Description to the map of solid rocks around Simpevarp.
SKB PR 25-87-02.
- Kornfält K-A, Wikman H. 1987b. Description to the map (No 4) of solid rocks of 3 small areas around Simpevarp.
SKB PR 25-87-02a.
- Kornfält K-A, Wikman H. 1988. The rocks of the Äspö island. Description to the detailed maps of solid rocks including maps of 3 uncovered trenches.
SKB PR 25-88-12.
- Laaksoharju M. 1988. Shallow groundwater chemistry at Laxemar, Äspö and Ävrö.
SKB PR 25-88-04.
- Laaksoharju M, Nilsson A-C. 1989. Models of groundwater composition and of hydraulic conditions based on chemometrical and chemical analysis of deep groundwater at Äspö and Laxemar.
SKB PR 25-89-04.
- Laaksoharju M. 1990. Measured and predicted groundwater chemistry on Äspö.
SKB PR 25-90-13.
- Liedholm M. 1987a. Regional Well Data Analysis.
SKB PR 25-87-07.
- Liedholm M. 1987b. Regional Well Water Chemistry.
SKB PR 25-87-08.
- Liedholm M. 1989. Combined evaluation of Geological, Hydrogeological and Geophysical information 1.
SKB PR 25-89-03.
- Liedholm M (ed). 1991a. General geological, hydrogeological and hydrochemical information. Technical notes 1-17.
SKB PR 25-90-16a.
- Liedholm M (ed) 1991b. General geological, hydrogeological and hydrochemical information. Technical notes 18-32.
SKB PR 25-90-16b.
- Lindahl H. 1989. Framtagning av översiktligt underlag för bedömning av förutsättningarna för grundvattenbildning i Äspö-området.
SKB TPM 25-89-008.
- Lindén A. 1988. Radon and Radium Concentrations in ground- and surface water in the Simpevarp area.
SKB PR 25-88-08.

Munier R, Riad L, Tullborg E-L, Wikman H, Kornfält K-A. 1988. Detailed investigation of drillcores KAS02, KAS03 and KAS04 on Äspö island and KLX01 at Laxemar.
SKB PR 25-88-11.

Munier R. 1989. Brittle tectonics on Äspö, SE Sweden.
SKB PR 25-89-15.

Mörner N-A. 1989. Postglacial faults and fractures on Äspö.
SKB PR 25-89-24.

Nilsson A-C. 1989. Chemical characterization of deep groundwater on Äspö 1989.
SKB PR 25-89-14.

Nilsson L. 1987. Hydraulic tests on Ävrö and Äspö.
SKB PR 25-87-11.

Nilsson L. 1988. Hydraulic tests. Pumping tests at Laxemar.
PR 25-87-11b.

Nilsson L. 1989. Hydraulic tests at Äspö and Laxemar.
SKB PR 25-88-14.

Nilsson L. 1990. Hydraulic tests on Äspö KAS05-KAS08, HAS13-HAS17
Evaluation.
SKB PR 25-89-20.

Nisca D. 1987a. Aerogeophysical interpretation.
SKB PR 25-87-04.

Nisca D. 1987b. Aeromagnetic Interpretation 6G Vimmerby, 6H Kråkelund NW, SW.
SKB PR 25-87-23.

Nisca D. 1988. Geophysical laboratory measurements on core samples from KLX01
Laxemar and KAS02 Äspö.
SKB PR 25-88-06.

Nisca D, Triumf C-A. 1989. Detailed geomagnetic and geoelectric mapping of Äspö.
SKB PR 25-89-01.

Niva B, Gabriel G. 1988. Borehole radar measurements at Äspö and Laxemar.
Boreholes KAS02, KAS03, KAS04, KLX01, HAS02, HAS03 and HAV07.
SKB PR 25-88-03.

Nyberg G, Jöhnsson S, Ekman L. 1991. Groundwater level program. Report for the
period 1987-1989.
SKB PR 25-90-18.

Nylund B. 1987. Regional gravity survey of the Simpevarp area.
SKB PR 25-87-20.

Olofsson T. 1974. Bergarters brottskaraktistik - Klassificeringssystem för sprödhet. BeFo:s Bergmekanikdag, 1974 (in Swedish).

Palmqvist K, Olsson T. 1991. SKN:s granskning av förundersökningarna inför byggandet av Äspölaboratoriet. SKN Rapport 42 (in Swedish).

Ploug C, Klitten K. 1989. Shallow reflection seismic profiles from Äspö, Sweden. SKB PR 25-89-02.

Rhén I. 1987. Compilation of geohydrological data. SKB PR 25-87-10.

Rhén I. 1989. Transient interference tests on Äspö 1988. SKB PR 25-88-13.

Rhén I. 1990. Transient interference tests on Äspö 1989 in KAS06, HAS13 and KAS07. Evaluation. SKB PR 25-90-09.

Rhén I (ed). 1991a. Information for numerical modelling 1990. General information. SKB PR 25-90-17a.

Rhén I (ed). 1991b. Information for numerical modelling 1990. Calibration cases. SKB PR 25-90-17b.

Rhén I, Forsmark T, Nilsson L. 1991c. Hydraulic tests on Äspö, Bockholmen and Laxemar, 1990, in KAS09, KAS11-14, HAS18-20, KBH01-02 and KLX01. Evaluation. SKB PR 25-91-01.

Rhén I (ed), Gustafson G, Gustafsson E, Svensson U, Wikberg P. 1991d. Prediction prior to excavation of the Äspö Hard Rock Laboratory. Supplement. SKB PR 25-91-02.

Russenes B. 1974. Bergslagsanalyse for tunneler i dalsider. NTH, Geol. Inst., Trondheim, 1974.

Rydström H, Gereben L. 1989. Seismic refraction survey on Äspö and Hälö. SKB PR 25-89-18.

Rydström H, Gereben L. 1989. Regional geological study seismic refraction survey. SKB PR 25-89-23.

Sandberg E, Forslund O, Olsson O. 1989. Ground surface radar measurements on Äspö. SKB PR 25-89-12.

Sehlstedt S, Triumf C-A. 1988. Interpretation of geophysical logging data from KAS 02 - KAS04 and HAS08 - HAS12 at Äspö and KLX01 at Laxemar. PR 25-88-15.

Sehlstedt S, Strähle A. 1989. Geological core mapping and geophysical bore hole logging in the boreholes KAS05-KAS08 on Äspö. SKB PR 25-89-09.

- Sehlstedt S, Strähle A, Triumf C-A. 1990. Geological core mapping and geophysical bore hole logging in the boreholes KBH02, KAS11-KAS14 and HAS18-HAS20 on Äspö.
SKB PR 25-90-06.
- Sehlstedt S, Strähle A. 1991. Identification of water conductive oriented fractures in the boreholes, KAS 02 and KAS 06.
SKB PR 25-91-XX (in prep).
- Spalding D B. 1981. A general-purpose computer program for multi-dimensional one- and two phase flow.
Math and Comp in Simulation, XIII, pp 267-276.
- Stanfors R. 1989. Översiktlig beskrivning av berggrunden i Simpevarpsområdet 1989.
SKB TPM 25-89-003 (in Swedish).
- Stanfors R, Erlström M, Markström I. 1991. Äspö Hard Rock Laboratory. Overview of the investigations 1986-1990.
SKB TR 91-20.
- Stenberg L, Sehlstedt S. 1989. Geophysical profile measurements on interpreted regional aeromagnetic lineaments in the Simpevarp area.
SKB PR 25-89-13.
- Stille H, Olsson P. 1989. First evaluation of rock mechanics.
SKB PR 25-89-07.
- Stille H, Olsson P. 1990. Evaluation of rock mechanics.
SKB PR 25-90-08.
- Strähle A. 1989. Drill core investigation in the Äspö area, Oskarshamn, Sweden.
SKB PR 25-88-07.
- Sundin S. 1988. Seismic refraction investigation at Äspö.
PR 25-87-15.
- Svensson T. 1987. Hydrological conditions in the Simpevarp area.
SKB PR 25-87-09.
- Svensson U. 1988. Numerical simulations of seawater intrusion in fractured porous media.
SKB PR 25-88-09.
- Svensson U. 1990a. The island of Äspö. Numerical calculations of natural and forced groundwater circulation.
SKB PR 25-90-03.
- Svensson U. 1990b. Numerical prediction of tracer trajectories during a pump test.
SKB PR 25-90-10.
- Svensson U. 1990c. Preliminary calculations of ambient and disturbed groundwater flow at Äspö.
SKB PR 25-90-11.

- Svensson U, 1991. Groundwater flow at Äspö and changes due to excavation of the laboratory.
PR 25-91-03.
- Talbot C, Riad L, Munier R. 1988. Structures and tectonic history of Äspö SE Sweden.
SKB PR 25-88-05.
- Talbot C, Munier R. 1989. Fault and fracture zones on Äspö.
SKB PR 25-89-11.
- Talbot C. 1990. Some clarification of the tectonics of Äspö and its surroundings.
SKB PR 25-90-15.
- Thunvik R, Braester C. 1989. Preliminary calculation of the flow conditions at prospective study site for the Swedish Hard Rock Laboratory.
SKB PR 25-89-05.
- Tirén S, Beckholmen M. 1987. Structural analysis of contoured maps, Äspö and Ävrö SE Sweden.
SKB PR 25-87-22.
- Tirén S, Beckholmen M, Isaksson H. 1987. Structural analysis of digital terrain models, Simpevarp area, SE Sweden. Method study EBBA 11.
SKB PR 25-87-21.
- Triumf C-A, Sehlstedt S. 1989. Magnetic measurements over Bornholmsfjärden between Äspö and Hälö.
SKB PR 25-89-19.
- Tullborg E-L. 1989. Fracture fillings in the drillcores KAS05-KAS08, SE Sweden.
SKB PR 25-89-16.
- Tullborg E-L, Wallin B, Landström O. 1991. Hydrogeochemical studies of fracture minerals from water conducting fractures and deep groundwaters at Äspö.
SKB PR 25-90-01.
- Voss C I, Souza W R. 1987. Variable density flow and solute transport simulation of regional aquifers containing a narrow freshwater-saltwater transition zone. *Water Resour Res*, Vol 23, No 10, pp 1851-1866.
- Wallin B. 1990. Carbon Oxygen and Sulfur isotope signatures for groundwater classification at Laxemar, SE Sweden.
SKB PR 25-90-12.
- Wikberg P, Axelsen K, Fredlund F. 1987. Deep groundwater chemistry.
SKB TR 87-07.
- Wikström A. 1989. General geological-tectonic study of the Simpevarp area with special attention to the Äspö island.
SKB PR 25-89-06.

List of SKB reports

Annual Reports

1977-78

TR 121

KBS Technical Reports 1 – 120

Summaries

Stockholm, May 1979

1979

TR 79-28

The KBS Annual Report 1979

KBS Technical Reports 79-01 – 79-27

Summaries

Stockholm, March 1980

1980

TR 80-26

The KBS Annual Report 1980

KBS Technical Reports 80-01 – 80-25

Summaries

Stockholm, March 1981

1981

TR 81-17

The KBS Annual Report 1981

KBS Technical Reports 81-01 – 81-16

Summaries

Stockholm, April 1982

1982

TR 82-28

The KBS Annual Report 1982

KBS Technical Reports 82-01 – 82-27

Summaries

Stockholm, July 1983

1983

TR 83-77

The KBS Annual Report 1983

KBS Technical Reports 83-01 – 83-76

Summaries

Stockholm, June 1984

1984

TR 85-01

Annual Research and Development Report 1984

Including Summaries of Technical Reports Issued during 1984. (Technical Reports 84-01 – 84-19)

Stockholm, June 1985

1985

TR 85-20

Annual Research and Development Report 1985

Including Summaries of Technical Reports Issued during 1985. (Technical Reports 85-01 – 85-19)

Stockholm, May 1986

1986

TR 86-31

SKB Annual Report 1986

Including Summaries of Technical Reports Issued during 1986

Stockholm, May 1987

1987

TR 87-33

SKB Annual Report 1987

Including Summaries of Technical Reports Issued during 1987

Stockholm, May 1988

1988

TR 88-32

SKB Annual Report 1988

Including Summaries of Technical Reports Issued during 1988

Stockholm, May 1989

1989

TR 89-40

SKB Annual Report 1989

Including Summaries of Technical Reports Issued during 1989

Stockholm, May 1990

Technical Reports

List of SKB Technical Reports 1991

TR 91-01

Description of geological data in SKB's database GEOTAB Version 2

Stefan Sehlstedt, Tomas Stark

SGAB, Luleå

January 1991

TR 91-02

Description of geophysical data in SKB database GEOTAB Version 2

Stefan Sehlstedt

SGAB, Luleå

January 1991

TR 91-03

1. The application of PIE techniques to the study of the corrosion of spent oxide fuel in deep-rock ground waters 2. Spent fuel degradation

R S Forsyth

Studsvik Nuclear

January 1991

TR 91-04

Plutonium solubilities

I Puigdomènech¹, J Bruno²

¹Environmental Services, Studsvik Nuclear,
Nyköping, Sweden

²MBT Tecnología Ambiental, CENT, Cerdanyola,
Spain

February 1991

TR 91-05

**Description of tracer data in the SKB
database GEOTAB**

SGAB, Luleå

April, 1991

TR 91-06

**Description of background data in the SKB
database GEOTAB**

Version 2

Ebbe Eriksson, Stefan Sehlstedt

SGAB, Luleå

March 1991

TR 91-07

**Description of hydrogeological data in the
SKB's database GEOTAB**

Version 2

Margareta Gerlach¹, Bengt Gentzschlein²

¹SGAB, Luleå

²SGAB, Uppsala

April 1991

TR 91-08

**Overview of geologic and geohydrologic
conditions at the Finnsjön site and its
surroundings**

Kaj Ahlbom¹, Sven Tirén²

¹Conterra AB

²Sveriges Geologiska AB

January 1991

TR 91-09

**Long term sampling and measuring
program. Joint report for 1987, 1988 and
1989. Within the project: Fallout studies in
the Gideå and Finnsjö areas after the
Chernobyl accident in 1986**

Thomas Ittner

SGAB, Uppsala

December 1990

TR 91-10

**Sealing of rock joints by induced calcite
precipitation. A case study from Bergeforsen
hydro power plant**

Eva Hakami¹, Anders Ekstav², Ulf Qvarfort²

¹Vattenfall HydroPower AB

²Golder Geosystem AB

January 1991

TR 91-11

**Impact from the disturbed zone on nuclide
migration – a radioactive waste repository
study**

Akke Bengtsson¹, Bertil Grundfelt¹,

Anders Markström¹, Anders Rasmuson²

¹KEMAKTA Konsult AB

²Chalmers Institute of Technology

January 1991

TR 91-12

**Numerical groundwater flow calculations at
the Finnsjön site**

Björn Lindbom, Anders Boghammar,

Hans Lindberg, Jan Bjelkås

KEMAKTA Consultants Co, Stockholm

February 1991

TR 91-13

**Discrete fracture modelling of the Finnsjön
rock mass**

Phase 1 feasibility study

J E Geier, C-L Axelsson

Golder Geosystem AB, Uppsala

March 1991

TR 91-14

Channel widths

Kai Palmqvist, Marianne Lindström

BERGAB-Berggeologiska Undersökningar AB

February 1991

TR 91-15

**Uraninite alteration in an oxidizing
environment and its relevance to the
disposal of spent nuclear fuel**

Robert Finch, Rodney Ewing

Department of Geology, University of New Mexico

December 1990

TR 91-16

**Porosity, sorption and diffusivity data
compiled for the SKB 91 study**

Fredrik Brandberg, Kristina Skagius

Kemakta Consultants Co, Stockholm

April 1991

TR 91-17

**Seismically deformed sediments in the
Lansjärv area, Northern Sweden**

Robert Lagerbäck

May 1991

TR 91-18

**Numerical inversion of Laplace
transforms using integration and
convergence acceleration**

Sven-Åke Gustafson

Rogaland University, Stavanger, Norway

May 1991

TR 91-19

**NEAR21 - A near field radionuclide
migration code for use with the
PROPER package**

Sven Norman¹, Nils Kjellbert²

¹Starprog AB

²SKB AB

April 1991

TR 91-20

**Äspö Hard Rock Laboratory.
Overview of the investigations
1986-1990**

R Stanfors, M Erlström, I Markström

June 1991

TR 91-21

**Äspö Hard Rock Laboratory.
Field investigation methodology
and instruments used in the
pre-investigation phase, 1986-1990**

K-E Almén, O Zellman

June 1991